COMPARTMENTAL ORGANIZATION IN EMBRYONIC STRIATAL GRAFTS AND IN THE DEVELOPING STRIATUM

by

FU-CHIN LIU

B.S., Psychology, National Taiwan University
(1985)

SUBMITTED TO THE DEPARTMENT OF BRAIN AND COGNITIVE SCIENCES IN PARTIAL FULFILLMENT OF THE REQUIREMENTS FOR THE DEGREE OF

DOCTOR OF PHILOSOPHY
IN NEUROSCIENCE

at the

MASSACHUSETTS INSTITUTE OF TECHNOLOGY

September 1991

Signature of Author_____
Department of Brain and Cognitive Sciences
June 25, 1991

Certified by_____
Dr. Ann M. Graybiel
Thesis Supervisor

Accepted by_____
Dr. Emilio Bizzi
Chairman, Department of Brain and Cognitive Sciences

Compartmental organization
in embryonic striatal grafts and
in the developing striatum

by

Fu-Chin Liu
Submitted to the Department of Brain and Cognitive Sciences
on June 25, 1991 in partial fulfillment of the
requirements for the degree of Ph.D.

Abstract

Embryonic striatal grafts implanted into excitotoxin-damaged adult striatum express a striking compartmental organization in which patches of neurochemical substances (P regions) are embedded in substance-poor non-patch surrounds (NP regions). The nature of this modular organization was studied by histochemistry, immunocytochemistry and autoradiography. Neurons with phenotype resembling normal mature striatal neurons were found in the P regions. These include large choline acetyltransferase (ChAT)-positive, acetylcholinesterase (AChE)-positive neurons, and medium-sized calbindin-D_{28K}-positive neurons, met-enkephalin-positive neurons, somatostatin-positive neurons and dopamine- and adenosine 3':5'-monophosphate-regulated phosphoprotein (DARPP-32)-positive neurons. By contrast, neurons that were not similar to normal mature striatal neurons, namely, medium-to-large multipolar calbindin-D_{28K}-positive and somatostatin-positive neurons with well stained dendrites, medium-sized ChAT-positive neurons and small met-enkephalin-positive cells, were present in the NP regions. Accordingly, the modular organization of striatal grafts may reflect an admixture of heterogeneous types of tissues with P regions representing striatal tissue and NP regions representing non-striatal and/or immature striatal tissue.

The extent of reconstruction of histochemical compartmentation that occurs in the normal mammalian striatum was also evaluated in striatal grafts by using patches of μ opiate receptors and medium-sized calbindin-D_{28K}-positive neurons as markers for striosomes and extrastriosomal matrix, respectively. Many medium-sized calbindin-positive neurons but few strong patches of [^{3}H]naloxone binding were present in the P zones of striatal grafts. These results suggest that the P regions of striatal grafts at least contain the matrix tissue.

Furthermore, there was an anatomical reconstitution of cholinergic and dopaminergic systems in the P zones of striatal grafts. The markers for cellular components of these two systems, including ChAT, AChE, [^{3}H]hemicholinium binding for high affinity choline uptake sites, [^{3}H]pirenzepine binding for M1 receptor sites, tyrosine hydroxylase (TH), [^{3}H]mazindol binding for dopamine uptake sites, [^{3}H]SCH23390 binding for dopamine D1 receptor sites and [^{3}H]sulpiride binding for

dopamine D2 receptor sites, were all primarily concentrated in the P regions. The preferential expression of these cellular elements in the P zones provides an anatomical basis for restoration of functional interactions between cholinergic and dopaminergic systems in striatal grafts.

The migratory capability of striatal grafted neurons and host neurons in the graft milieu was studied by prior exposure the donor tissue and the host striatum, respectively, to [^{3}H]thymidine. In experiments in which pulse-labeled donor tissue was placed in non-radioactive host striatum, no labeled donor neurons were found in the host striatum. In experiments in which non-radioactive donor tissue was implanted into the host striatum labeled with [^{3}H]thymidine, few labeled neurons were found in the cores of the grafts, and, at most, a few labeled neurons were present at the margins of the grafts. These findings suggest that there is no extensive mutual migration between the donor and host neurons in embryonic striatal graft placed in neurodegenerated adult striatum. These results strongly suggest that the P zones of striatal grafts are not derived from host striatal tissue.

The fact that TH-positive fibers were primarily concentrated in the P zones suggested that these afferents might influence the development of modular organization. This possibility was assessed by implanting striatal grafts into host striatum dopamine-depleted by prior injection of 6-hydroxydopamine (6-OHDA) into the ipsilateral medial forebrain bundle. The 6-OHDA lesions in the host resulted in disappearance of TH-rich patches in the grafts. The formation of P and NP modules in the grafts was not blocked by lack of dopaminergic innervation. The destruction of TH-containing afferents, however, resulted in less crisp pattern of AChE staining, and the AChE-rich P zones also tended to be smaller. Moreover, enhanced met-enkephalin immunostaining was observed in many met-enkephalin-rich P zones of the denervated grafts. These findings first, demonstrate that the TH-containing afferents of striatal grafts are predominantly derived from the host; and second, show that these afferents are not obligatorily required for sorting out populations of cells to form P regions and NP regions in striatal grafts. The apparent up-regulation of met-enkephalin staining in the grafts was highly reminiscent of the enkephalinergic up-regulation that occurs in the normal striatum deprived of nigrostriatal dopaminergic inputs. This result suggests that the capacity for regulation of enkephalinergic system by TH-containing afferents is likely to be restored in striatal grafts reinnervated by host mesostriatal fibers.

Further functional integration between striatal grafts and host brain was tested at the signal-transduction level by using the paradigm of induction of the immediate-early gene c-*fos* by dopamine indirect agonist, cocaine. Clusters of neurons immunoreactive for Fos (the protein product of c-*fos*)-like antigen were preferentially induced in AChE/TH-rich P regions of striatal grafts in hosts challenged with cocaine. The induction of Fos-like immunoreactivity in striatal grafts, like that in the hosts and normal rats, was greatly reduced by pretreatment of D1 antagonist, SCH23390. These findings suggest that the cellular signaling pathway leading to the expression of Fos-like protein by cocaine is functionally reconstituted in the P zones of striatal grafts.

As an adjunct to these transplantation studies, the development of calbindin-D_{28K} expression in the striatum was examined. Compartmentation of the developing striatum

was identified by using the dopamine islands as marker for the developing striosomes. The expression of calbindin-D_{28K} in medium-sized striatal neurons followed a ventromedial to dorsolateral gradient during development. Calbindin-D_{28K} was consistently expressed by the medium-sized neurons outside the TH-positive dopamine islands. Thus, calbindin-D_{28K} was selectively expressed in the extrastriosomal matrix throughout development.

In addition, three transient calbindin-D_{28K}-positive systems were identified in the ganglionic eminence and the developing striatum. They were multipolar calbindin-D_{28K}-immunoreactive cells, calbindin-D_{28K}-positive neuropil patches that corresponded to the dopamine islands, and radial calbindin-D_{28K}-immunoreactive processes stretching from the ventricular zone across the developing striatal proper to the external capsule. These three systems were primarily distributed in the dorsal caudoputamen from embryonic day 20 to postnatal day 15. They were anatomically related such that a few multipolar calbindin-D_{28K}-positive cells were associated with calbindin-D_{28K}-positive neuropil patches and with calbindin-D_{28K}-positive processes. The calbindin-D_{28K}-positive patches were also intermingled with calbindin-D_{28K}-positive processes. The close topographic relationship among these three developmental regulated calbindin-positive systems suggests that intriguing interactions may occur among them during striatal development.

In conclusion, the present work suggests that the cells in the P regions of embryonic striatal grafts probably follow the normal program of striatal development to express striatal phenotype, and this process equips them with appropriate molecular and cellular constituents which in turn enable the cells to respond to dopaminergic regulation in a similar way to normal striatal cells. Furthermore, the finding of cells uncharacteristic of mature striatum in the NP regions raises an important issue of how these NP cells affect the developmental and functional interactions between striatal grafts and the host brain. Finally, understanding the nature of the interactions among the P and NP regions of embryonic striatal grafts and the host brain will not only shed light on the fundamentals of development and regeneration of striatum, but also on the design of potential grafting therapies for neurodegenerative disorders related to the striatal system.

Thesis Supervisor: Dr. Ann M. Graybiel
Title: Professor of Neuroanatomy

Table of Contents

Chapter 1

INTRODUCTION

One of the most important issues in neurobiology is how neural tissue develops from rather simple neuroblasts into a highly complicated adult nervous system. Building up such an intriguing system is certainly as sophisticated as operating the system itself. Many experimental strategies have been applied to investigate this interesting and important aspect of neurobiology. Among them, neural transplantation has long been regarded as an alternative approach to studying neural development *in vivo*. As the complexity of neural architecture is built upon spatiotemporal axes, the common parameters for grafting experiments usually involve the manipulation of the source and age of the donor tissue as well as those of the host tissue. Thus, different combinations of homotopic/heterotopic and isochronic/heterochronic grafting have been used to investigate different aspects of neural development and regeneration such as neural tissue induction, neuronal commitment, migration, differentiation, neurite outgrowth and neurotrophic factors (e.g. Spemann and Mangold, 1924; LeDouarin and Teillet, 1974; Björklund et al., 1983; Nieto-Sampedro et al., 1984; Aguyao, 1985; McConnell, 1988; Schnell and Schwab, 1990; Barbe and Levitt, 1991; Yamada et al., 1991; Eisen, 1991). It is the capability of manipulating the spatiotemporal variables of neural development that makes transplantation a suitable and powerful tool for deciphering neural developmental.

On the practical side, neural transplantation has opened a potential clinical

avenue for treating neurological disorders (Backlund et al., 1985; Lindvall et al., 1987; Madrazo et al., 1987; Goetz et al., 1989; Lindvall et al., 1990; Freed et al., 1990a). In the last two decades, intracerebral transplantation techniques have been developed with the specific aim to provide a neuronal replacement therapy for neurodegenerative disorders such as Parkinson's disease, Huntington's disease and Alzheimer's disease (for review, see Freed, 1983; Björklund and Stenevi, 1984; Gage and Björklund, 1986; Björklund et al., 1987; Dunnett, 1990; Freed et al., 1990b; Gage and Fisher, 1991). Within the past few years, animal studies of intracranial grafting have advanced to clinical trials in treating Parkinson's disease with different degrees of success (Backlund et al., 1985; Lindvall et al., 1987; Madrazo et al., 1987; Goetz et al., 1989; Lindvall et al., 1990; Freed et al., 1990a). More recently, with advances in recombinant DNA techniques in molecular biology, grafting genetically engineered cells releasing neurotransmitter precursors, neurotransmitters or neurotrophic factors into the neurodegenerative regions of host brains has become possible (Gage et al., 1987; Rosenberg et al., 1988; Wolff et al., 1989; Horellou et al., 1990; Stromberg et al., 1990). The grafting experiment is further becoming a rigorous paradigm for characterizing the differentiation capacity of immortalized cell lines. These lines, derived from neuronal and/or glial precursor cells *in vivo* may provide potentially unlimited sources of donor cells for transplantation therapy and avoid the ethical issue of using embryonic tissue for donor tissue (for reviews, see Cepko, 1988; McKay, 1989).

Embryonic striatal transplantation as a potential clinical therapy for Huntington's disease

Huntington's disease, a progressive neurodegenerative disease primarily affecting the striatum, is inherited through an autosomal dominant gene (Martin, 1984, Wexler et al., 1991). Although genetic studies using recombinant DNA technique have localized the genetic deficit in human chromosome 4 (Gusella et al., 1983), it may still be years before a practical clinical therapy can be developed. Unlike Parkinson's disease, in which the etiology mainly involves the degeneration of neurons that synthesize a common neurotransmitter, dopamine, Huntington's disease involves degeneration of a broad profile of different neurons in the striatum and probably in the cortex having different transmitter characteristics, making it difficult to develop replacement therapies with pharmacological agents (Lange et al., 1976; Martin, 1984; Kowall et al., 1987; DiFiglia, 1990; Wexler et al., 1991).

As an alternative, neuronal transplantation offers a potential therapy for Huntington's disease. Neuronal degeneration of the striatum induced by excitotoxin has been used as an animal model for Huntington's disease (Coyle and Schwarcz, 1976; McGeer and McGeer, 1976). Transplanting cell-suspensions or solid explants of donor tissue prepared from embryonic striatal primordia into the excitotoxin-damaged adult striatum has been a focus of intensive study for the past few years (for review, see Björklund et al., 1987). Such embryonic striatal grafts have been shown to survive transplantation into the striatum of adult rats. The grafted cells have the capability to express a variety of neurotransmitter-associated substances, and to establish synaptic

contacts with different regions of the host brain (Deckel et al., 1983; Isacson et al., 1984, 1987; McAllister et al. 1985; Deckel et al., 1986, 1988; Sanberg et al., 1986, 1989; Pritzel et al., 1986; Walker et al., 1987; Graybiel et al., 1987a, 1989; Deckel et al., 1988a, b; Clarke et al., 1988; DiFiglia et al., 1988; Roberts and DiFiglia 1988; Giordano et al., 1988; Wictorin et al., 1988, 1989a, b, c, 1990; Wictorin and Björklund 1989; Xu et al., 1989; Sirinathsinghji et al., 1990; Mayer et al., 1990; Helm et al., 1991; Liu et al., 1990a, b, 1991). Behavioral studies have also indicated that varying but considerable degrees of behavioral recovery occur in animals bearing striatal grafts (Deckel et al., 1983, 1986, 1988; Sanberg et al., 1986, 1989; Isacson et al., 1986; Giordano et al., 1988; Dunnett et al., 1988).

Histochemical compartmentation in the mature striatum

It is now well established that the striatum consists of at least two neurochemical compartments, striosomes and extrastriosomal matrix. Striosomes ("striatal bodies") were first defined in cross-sections through the adult cat, monkey and human striatum as patches expressing low acetylcholinesterase (AChE) activity embedded in AChE-rich surrounds (extrastriosomal matrix) (Graybiel and Ragsdale, 1978). Subsequent work in several laboratories has established that these two compartments can be distinguished not only on the basis of expression of different levels of neurochemical substances in each compartment, including neurotransmitters, neuropeptides and their precursor mRNAs, neurotransmitter uptake sites and receptor binding sites, but also on the basis of the different patterns of connectivity of these two compartments with other brain

regions (for review, see Graybiel and Ragsdale, 1983; Graybiel, 1990). Recent studies further indicate that striosomal and matrix cells have different genomic responsiveness to dopaminergic stimulation (Paul et al., 1990; Grimes et al., 1990; Graybiel et al., 1990a). Although the physiological function of the compartmentation of the striatum is still unknown, the projections from limbic brain regions such as the prefrontal cortex, the insular cortex and the amygdala primarily to the striosomes and from non-limbic regions such as the sensory and motor cortex to the extrastriosomal matrix suggest that the striosomes and matrix may participate in different aspects of striatal function.

Histochemical compartmentation in the developing striatum

This macroscopic compartmentation is also reflected in the striatum during development. It has been shown that striosomes are ontogenic units in the developing striatum because striosomal and matrix cells have different birthdates and developmental schedules. Striosomal cells are born earlier than most cells in the matrix, and they differentiate and project to their target region (the substantia nigra) earlier than cells in the matrix do (Graybiel and Hickey, 1982; Graybiel, 1984a, 1984b; Fishell and van der Kooy, 1987, 1989; Foster et al., 1987; Graybiel and Newman-Gage, 1987; van der Kooy and Fishell, 1987; van der Kooy et al., 1987; Voorn et al., 1988; Newman-Gage and Graybiel, 1988).

A striking marker for the developing compartments in the perinatal striatum is a modular distribution of AChE in which patches containing high AChE activity are embedded in AChE-poor surrounds (Butcher and Hodge, 1976; Graybiel et al., 1981).

The AChE-rich patches have been demonstrated to correspond to the immature striosomes*. Thus, in contrast to mature striosomes, which contain low AChE activity, immature striosomes in the developing striatum contain high AChE activity.

Developing AChE-rich striosomes contain a high density of dopaminergic nigrostriatal fibers ("dopamine islands") and of μ opiate receptor binding sites (Olson et al., 1972; Tennyson et al., 1972; Graybiel et al., 1981; Kent et al., 1982; Moon Edley and Herkenham, 1984; Murrin and Ferrer, 1984; van der Kooy, 1984; Graybiel, 1984a). Other neurochemical markers in the developing striatum have also been shown to be primarily expressed in patchy distributions during prenatal and early postnatal periods, namely, high affinity dopamine uptake sites, dopamine D1 and D2 receptor binding sites, dopamine- and adenosine 3':5'-monophosphate-regulated phosphoprotein (DARPP-32), high affinity choline uptake sites, muscarinic M1 and M2 receptor sites, synaptic vesicle-associated protein recognized by SV48 antibody, type II calcium/calmodulin-dependent protein kinase and tachykinin (Foster et al., 1987; Lowenstein et al., 1987, 1989; Newman-Gage and Graybiel, 1988; Voorn et al., 1988; Murrin and Zeng, 1989; Happe and Murrin, 1989; Nastuk and Graybiel, 1989; Boylan et al., 1990; Zahm et al., 1990). Some of these patch systems have been confirmed as forerunners of striosomes in the adult striatum.

*The AChE-rich staining of immature striosomes occurs in all species studied. In most species, mature striosomes are AChE poor. In rat and other rodents, however, the AChE stain is not a reliable marker for striosomes. Although it has been reported that mature striosomes (patches) in adult rats contain low AChE-activity (Herkenham and Pert, 1981), the AChE staining (Geneser-Jensen and Blackstad, 1971; Graybiel and Ragsdale, 1978) used in the experiments of this thesis (and in many laboratories) does not show a pronounced heterogeneous pattern throughout the adult rat striatum. Only a few patches containing AChE activity lower than their surrounds in the medial and ventral striatum are detected.

Compartmental organization in embryonic striatal grafts

The most prominent feature of embryonic striatal grafts is that the grafts develop a compartmental organization in which some neurochemical substance-rich patches are embedded in surrounds containing less of the corresponding substances. These neurochemical substances include AChE, choline acetyltransferase, tyrosine hydroxylase (TH), DARPP-32, enkephalin and substance P, dopamine D1 and D2 receptor binding sites, high affinity dopamine uptake sites, high affinity choline uptake sites, muscarinic M1 receptor binding sites, and μ opiate receptor binding sites (Pritzel et al., 1986; Isacson et al., 1987; Walker et al., 1987; Sanberg et al., 1987; Graybiel et al., 1987a, 1989; Clarke et al., 1988; Wictorin et al., 1989c; Mayer et al., 1990; Liu et al., 1990b). All these substances are neurochemical constituents of the normal adult striatum. Of particular interest is that the distributions of these different neurochemically identified patches in the grafts have been shown largely coincident with one another.

The close anatomical alignment of patches of high AChE activity, high density of TH-positive fibers and strong μ opiate receptor binding in embryonic striatal grafts (Isacson et al., 1987; Graybiel et al., 1987a) are reminiscent of the compartmentation in the immature striatum as described above. This led Isacson et al. (1987) to suggest the interesting possibility that the modular organization in such embryonic striatal grafts may represent an immature compartmentalized organization, in which the striatum is rebuilt but developmentally arrested in the graft environment. The implication of this hypothesis is that embryonic striatal grafts have the capacity to develop the immature compartmental ordering of normal striatum, but some factors that are important for

promoting the process of maturation of the striatal compartmentation are lacking in the graft milieu. Thus, embryonic striatal grafting would serve as a model system to study the factors influencing maturation of striatal compartmentation during development.

Because of this potential value of embryonic striatal grafts for studying striatal compartmentation during development and their potential application in clinical therapy for Huntington's disease, the first part of the work presented in this thesis (Chapters 2-6) is aimed at reevaluating the developmental status of compartmentation and its neurochemical correlates in embryonic striatal grafts.

Embryonic striatal transplantation was carried out according to a protocol modified from Isacson et al. (1984). For the host rats, neuronal degeneration was induced in the striatum by injecting the excitotoxin, ibotenic acid, into the right caudoputamen. Seven to eight days later, embryonic day 14-16 donor rat tissue was dissected from the lateral ganglionic eminence, identified as the striatal primordium (Smart and Sturrock, 1979; Lammers et al., 1980; Fentress et al., 1981). Cell-suspensions prepared from the dissected tissue were injected bilaterally into the caudoputamen at the center of the ibotenate-induced lesion, and, on the contralateral side, into a corresponding site in the intact caudoputamen. In some rats, grafting was performed only unilaterally, on the ibotenate-damaged side. The grafted rats were allowed to survive for 2-17 months. Brain tissues were processed for histochemistry, immunocytochemistry and autoradiography.

Developmental expression of calbindin-D_{28K} in the ganglionic eminence and the developing striatum

The second part of the work presented in this thesis (Chapters 7 and 8) is concerned with the expression of calbindin-D_{28K}, a calcium binding protein, in the developing striatum. The goal of this study was twofold: first, although calbindin-D_{28K} is known to be selectively expressed by medium-sized striatal matrix neurons of adult rats (Gerfen et al., 1985), its developmental distribution with respect to the striatal compartmentation was not documented. An attempt to use calbindin-D_{28K} as a marker for studying the status of embryonic striatal grafts required characterization of the time of expression and the compartmental distribution of calbindin-D_{28K} in the developing striatum. Moreover, the neurochemical development of the striatal matrix had not been well investigated despite many studies of the development of striosomes. If the calbindin-D_{28K} were consistently a matrix marker during development, this would then provide a marker with which to study how the matrix develops.

Chapter 2

The nature of compartmental organization in embryonic striatal grafts

ABSTRACT

Embryonic striatal grafts display a striking modularity of composition. With acetylcholinesterase (AChE) histochemistry, the tissue of such grafts can be divided into regions with strong AChE staining of the neuropil and regions in which AChE staining of the neuropil is weak. In the experiments reported here we reexamined the nature of this modularity. Striatal grafts were made by injecting dissociated cells of E15 ganglionic eminence into the striatum of adult rats which 7 days before had received intrastriatal deposits of ibotenic acid. Some donors had been exposed to [^{3}H]thymidine at E11-E15. After 9-17 month survivals, the anatomical organization of the grafts was studied by histochemistry, immunohistochemistry and autoradiography.

In every graft, the AChE-rich regions formed patches (P regions) in a larger AChE-poor surround (NP regions). Neurons labelled with [^{3}H]thymidine appeared both in P and in NP regions, suggesting that donor cells were distributed in each type of region and that neither type of tissue, P or NP, was composed exclusively of host tissue. In the AChE-rich P regions, markers characteristic of normal perinatal and mature rat striatum were expressed by medium-sized cells: calcium binding protein (calbindin-D_{28K})-

This chapter is modified from the paper, "Intrastriatal grafts derived from fetal striatal primordia. I. Phenotypy and modular organization by Graybiel, A.M., F.-C. Liu, and S.B. Dunnett", published in J. Neurosci. (1989) 9:3250-3271 with permission from the authors.

immunostaining, met-enkephalin (mENK)-immunostaining, and, more rarely, somatostatin (SOM)-immunostaining. In the NP regions, however, medium-sized cells expressing calbindin- and mENK-immunostaining were very rare, and there was an abundance of neuronal types not normally found in normal mature striatal tissue. These included (a) large multipolar calbindin-positive neurons with well ramified densely stained dendrites, (b) large SOM-positive neurons with prominent dendritic trees, and (c) mENK-positive cells smaller than typical striatal medium-sized mENK-immunoreactive neurons. In Nissl stains, the AChE-rich P regions resembled the normal striatum of mature animals, whereas the AChE-poor NP regions did not.

These findings suggest that the P regions of embryonic striatal grafts achieve a phenotypy similar to that of normal striatum at maturity and during much of postnatal development. The dominant expression of perikaryal calbindin-like immunoreactivity in the P regions further suggests that these zones have a high proportion of tissue resembling striatal matrix. By contrast, expression of marker antigens in the NP zones of the grafts suggests that these zones are predominantly composed of nonstriatal tissue or that they have the phenotypy of immature striatum intermixed with some nonstriatal cells. We conclude that although some striosome-matrix compartmentalization may be reconstituted within P zones, the modular organization of embryonic striatal grafts may principally reflect an atypical compartmentalization of different tissue types.

INTRODUCTION

Embryonic striatal grafts provide a potentially powerful experimental system for studying the determinants of neurotransmitter-specific neural development. Several research groups have demonstrated that cells derived from the embryonic ganglionic eminence survive transplantation to the striatum of the adult rat, and express a variety of neurotransmitter- and receptor-related markers characteristic of normal striatal tissue (Pritzel et al., 1986; Isacson et al., 1984, 1985, 1987; Walker et al., 1987; Deckel and Robinson, 1987; Sanberg et al., 1987; Graybiel et al., 1987a; Clarke et al., 1988; Roberts and DiFiglia, 1988). In the most systematic study so far, Isacson et al. (1987) have shown that such grafts develop a compartmentalized organization in which markers for neurotransmitter-related compounds are arranged in macroscopic patches visible in sections through the grafts. These authors found that acetylcholinesterase (AChE) staining, a variety of neuropeptide-immunoreactive neurons, fibers immunoreactive for tyrosine hydroxylase (TH) and for met-enkephalin-like peptide (mENK), and ligand binding for dopamine D2, muscarinic cholinergic and opiate receptors all showed a patchy distribution within the grafts. Most remarkably, a substantial overlap was observed among the patches detected by the different markers.

Compartmentalization of transmitter-related markers is now well characterized in the normal striatum (see, e.g. Graybiel and Ragsdale, 1983; Graybiel, 1986, 1989; Gerfen, 1984; Gerfen et al., 1985, 1987a, 1987b). In particular, the correspondence of zones detectable in AChE stains with patches observed with markers for mENK and substance P (SP)-like peptides, TH and various receptor-related ligands is a landmark

feature of the striosomal system of the striatum. In the immature striatum, future striosomes express high AChE activity and TH-like immunoreactivity (Butcher and Hodge, 1976; Graybiel et al., 1981). By contrast, the striosomes at maturity show relatively weaker AChE staining and TH-like immunoreactivity than the matrix in which they lie embedded (Graybiel and Ragsdale, 1978; Graybiel et al., 1987b; Ferrante and Kowall, 1987).

As pointed out by Isacson et al. (1987), the staining characteristics of embryonic striatal grafts more closely resemble those of immature striatum than those of mature striatum: they have AChE-rich, TH-rich patches in a weakly staining or unstained surround. This led Isacson et al. (1987) to suggest that the tissue of the grafts, lacking normal environmental cues, might have established compartmental order but have maintained the immature form of this compartmentalization. The possibility that striatal grafts exhibit such an arrested development would have important implications for understanding what molecular cues are involved in the initiation and subsequent maturation of compartmentalization in the striatum. Immature characteristics of the grafts would also raise new questions about how the grafts exert their functional influence on host behavior (Björklund et al., 1987). There is, however, a major problem in evaluating the developmental status of the graft tissue. Many of the transmitter-related markers that were first employed to identify mature and immature striosomes in the cat and primate do not unambiguously identify these compartments in the striatum of the rat. In this species, mature striosomes cannot always be clearly identified either by heterogeneity of AChE activity (as was originally employed to define striosomes in other

species), or on the basis of other markers such as low TH-like immunoreactivity in the striosomal neuropil (see, Butcher, 1983; Hökfelt et al., 1984; Fallon and Loughlin, 1987). Indeed, individual markers are not always secure identifiers of striosomes even in primates and cats because of regional differences in their expression in different parts of the striatum (Graybiel and Ragsdale, 1983; Besson et al., 1988b) Accordingly, in the striatal grafts, the patches rich in AChE activity and in TH-like, mENK-like and SP-like immunostaining, surrounded by another compartment poor in all these markers, need not necessarily be immature striosomes embedded in immature matrix tissue.

In the experiments reported here, we set out to reexamine the compartmental organization of embryonic striatal grafts in an effort to determine (a) whether both the AChE-rich regions and the AChE-poor regions of the grafts are composed of donor tissue; (b) whether both the AChE-rich and the AChE-poor regions are striatal tissue; and (c) whether the AChE-rich regions, if striatal, more closely resemble striosomes, matrix or both.

METHODS

Host animals

Surgeries were performed on 20 adult Sprague-Dawley rats (Charles River Laboratories, Inc.) deeply anaesthetized with Nembutal or Chloropent and mounted in a Kopf stereotaxic apparatus. In all of the rats, lesions were made in the right caudoputamen by stereotaxic injection of the neurotoxin, ibotenic acid. Each rat received six deposits of 0.2 µl of 10µg/µl ibotenic acid (Sigma) in 0.1 M phosphate buffer, pH=7.4, at the following sites: A=0.2 mm, L=2.2 mm and =3.7 mm, and A=1.7 mm, L=2.5 mm, V=4.0 mm and 5.5 mm with A measured from bregma, L from the midline, and V from the dura mater, the nose bar being set -2.3 mm below the interaural line. Each aliquot was delivered over 2-3 min from a 10 µl Hamilton syringe connected to a Harvard microdrive pump. One of these animals served as a control for the effects of ibotenic acid in the caudoputamen. The remaining 19 served as hosts for embryonic striatal grafts.

Transplantation

Donor tissues were obtained from striatal primordia dissected from fetuses at embryonic day (E) 15 (crown-rump length 12-15 mm). Donor fetuses had been exposed to [^{3}H]thymidine at one embryonic day (E11, E12, E13, E14 or E15) by intraperitoneal injection of 1 mCi [^{3}H]thymidine (78.8 Ci/mmol, New England Nuclear) into the pregnant mothers. The dissected embryonic tissue was stored briefly in a solution containing 0.6% glucose and 0.9% saline at room temperature, then incubated for 20 min at 37°C in 0.1% trypsin (Sigma, crude type II) dissolved in the glucose-saline medium,

rinsed four times with fresh glucose-saline solution, and mechanically dissociated by repeated gentle pipetting with a fire-polished Pasteur pipette. Alliquots of the resulting stock suspension were loaded into the injection syringe just before the injection protocol began. Several rats received injections of the same stock suspension. The final suspensions contained cells from approximately 3 dissected specimens per 10 µl of medium. Seven to eight days after the ibotenic acid injections, 9 rats received unilateral right side (one died after the surgery) and 10 rats bilateral striatal cell suspension grafts at the following coordinates: A=0.9 mm, L=±3.0 mm and V=4.7 mm. The hemispheres without lesions also received unilateral grafts at the same coordinates; these will be described in a separate account. Three microliters of the cell suspension were injected at each site over a 3-5 min (or, in 1 rat, 30 min) period. After the injection, a 5 min period was allowed for diffusion before slow retraction of the needle. Calculations based on those by Isacson (1987) suggests that this procedure yield a total of approximately 405 x 10^3 donor cells injected per hemisphere (estimated 150 x 10^3 cells/µl cell suspension, x 90% *in vitro* survival rate, x 3 µl injected).

Tissue processing. Nine to 17 months after grafting, the host animals were deeply anaesthetized and all but one were perfused transcardially with 500 ml of 4% paraformaldehyde in 0.1 M phosphate buffer containing 5% sucrose and 0.9% saline (pH 7.4). Brains were postfixed at 4°C for 2-4 hr in the same fixative and then immersed overnight in a solution of 20% sucrose and 0.9 % saline made up in 0.1 M phosphate buffer. In the single exceptional case, the brain was removed from the deeply anaesthetized host and was rapidly frozen in pulverized dry ice in preparation for ligand

binding (see below). All perfused brains were cut in the coronal plane at 30 μm on a freezing microtome. Sections were prepared for histochemistry, immunohistochemistry or ligand binding in serial sequences permitting comparisons among adjacent sections processed for different markers. All sections through the grafts were processed.

Immunohistochemistry and acetylcholinesterase histochemistry

For mENK, calcium binding protein (calbindin-$D_{28\,or\,CaBP}$; Baimbridge et al., 1982; Gerfen et al., 1985), somatostatin (SOM), glial fibrillary acidic protein (GFAP), epidermal growth factor (EGF) and laminin immunohistochemistry, sections pretreated with methanolic H_2O_2, Triton X-100 and normal goat serum were processed by the peroxidase-antiperoxidase method as described elsewhere (Graybiel, 1984a; Graybiel and Chesselet, 1984). Dilutions of the antisera were: 1:1000 for mENK and 1:600 for SOM (1-28) antisera (both kindly provided by Dr.R.P. Elde); 1:500-1:1000 for calbindin antisera (kindly donated by Dr.C.R. Gerfen and Dr. P.C.Emson); 1:500 for GFAP (Boehringer Mannheim, West Germany); 1:1000 for laminin (Gibco laboratories); and 1:800 for EGF (kindly donated by Dr.J.H. Fallon). The primary incubation times for all antisera were 2-3 days at 4°C. For EGF immunohistochemistry, some sections were processed in the laboratory of Dr. Fallon (Fallon et al., 1984). References to immunostaining (e.g. "mENK-like") refer only to immunoreactivity detected with the particular antisera specified.

Acetylcholinesterase histochemistry was carried out according to a slightly modified Geneser-Jensen and Blackstad method (Geneser-Jensen and Blackstad, 1971) in which the sections were developed in potassium ferricyanide (Graybiel and Ragsdale,

1978). In some cases, selected sections were stained with cresylecht violet.

Receptor autoradiography

Sections from 4 perfused brains and 1 unperfused brain were incubated in 2.5 nM [^{3}H]naloxone (New England Nuclear) and processed for opiate receptor binding by film-autoradiography as described by Herkenham and Pert (1982) with slight modifications (Besson et al., 1988a). Autoradiographic exposures (Amersham Hyperfilm) were for 10-12 weeks. Following autoradiography, sections were stained for AChE.

Thymidine autoradiography

Sections were mounted, defatted and dipped in Kodak NTB-2 emulsion [diluted 1:1 in distilled water containing 0.1% detergent (Dreft)], and developed as described elsewhere (Graybiel, 1984a) in Kodak D-19 after exposure times for 2-4 months. All autoradiographic sections were stained with cresylecht violet.

Analysis

Sections were examined with light- and dark-field optics and elements of interest in individual sections were charted with a computerized plotting system or with the aid of a macroprojector. Charts of serially adjoining sections were aligned by reference to vascular landmarks. For charting of [^{3}H]thymidine-labelled neurons, ca. 20 grains per nucleus was taken as the threshold for considering the cell labelled. For estimates of cell diameters, the longest axis of the cell was taken; when possible, measurements were made through the plane of the nucleus.


A
B
LV
NP
P
AC
CP
C
D
P
NP

Figure 2-1: Serially adjoining sections through an embryonic striatal graft illustrating in A, AChE-rich P and AChE-poor NP compartments in the graft visible with acetylthiocholinesterase histochemistry; and in B, the heterogeneous cellular architecture of the grafts visible with Nissl stains. Scale bar for A and B, shown in B, indicates 1 mm. Case RSG2-21, post graft survival time 13 months. AChE-poor fiber bundles form a ring around the graft separating it from the thin rim of host striatal tissue (CP) that survived the ibotenic acid lesion placed there 7 days before injection of the embryonic cell suspension. Arrows in A and B point to the thin zone of small, intensely stained cells (presumably glia) separating an AChE-rich P region from neighboring AChE-poor NP tissue. This region is shown at higher magnification in C, with arrow as fiducial marker pointing to same site as arrows in A and B. D illustrates normal striatal tissue of the contralateral host's striatum. Scale bar for C and B, shown in D, indicates 100 μm. Comparison of C and D shows that neuronal phenotypes in P regions resemble those of the host's striatum, whereas those in NP regions do not. LV-lateral ventricle; AC-anterior commissure.

RESULTS

AChE histochemistry and Nissl staining

The control brain containing an ibotenic acid lesion without graft confirmed that massive striatal damage was inflicted by the ibotenic acid injections (Coyle and Schwarcz, 1976; Köhler and Schwarcz, 1983; Walker et al., 1987; Isacson et al., 1987). In each brain containing a graft, the tissue of the transplant formed a distinctly delimited zone lying within the part of the host striatum that remained in the wake of the ibotenic acid-induced lesion. AChE staining in all of the grafts had the typically patchy appearance already reported by Isacson et al. (1985, 1987) and Walker et al. (1987). An example is shown in Fig. 2-1A. Within the graft, zones of high AChE activity [here called "patch" (P) regions] lay embedded in surrounding tissue [here called "nonpatch" (NP) regions] in which the AChE activity was much weaker. The sizes of the grafts and the proportion of the grafts taken up by the intensely AChE-positive patches differed from brain to brain. These variations and other characteristics of the AChE staining will be discussed in a separate account.

Sections stained for Nissl substance (Fig. 2-1B) showed that the transplanted tissue was composed of neurons and small intensely stained cells (presumably glia). Cellular clusters of varying size appeared within each graft. When adjoining Nissl-stained and AChE-stained sections were compared, it became apparent that some of the cellular clusters were in register with AChE-rich P regions whereas others were not (Figs. 2-1A, B). Typical examples of each type are shown at high magnification in Fig. 2-1C. The AChE-rich P region corresponds to a zone containing predominantly medium-sized

neurons (ca. 10-16 μm diameter), a few large neurons (ca. 25 μm diameter) and some small glial cells. The sizes and relative proportions of medium and large diameter cells in this cluster are similar to those of the normal host striatum (Fig. 2-1D). This P cell-cluster was particular clearly delimited from the remainder of the graft tissue by a cell-poor margin.

In contrast to the AChE-rich P regions, the AChE-poor NP regions had a highly heterogeneous in cellular composition that did not resemble striatal tissue of the normal adult rat. (Figs. 2-1B, C). The aggregate of NP cells shown at high magnification in Fig. 2-1C contains a mixed population of neurons ca. 13-31 μm in diameter, many of them larger than striatal medium spiny cells (average diameter ca. 14 μm ,see Fig. 2-1D). As sometimes occurred elsewhere, this NP zone was separated from the adjoining P region by a thin wall of small (presumably glial) cells. Otherwise it blended into adjoining parts of the NP zone without abrupt borders. Elsewhere in the NP tissue there were zones containing even larger neurons and other zones containing smaller neurons.

Laminin immunostaining

To assess the vascular structure of the graft we employed an antiserum against laminin, a glycoprotein in the basement membranes of blood vessels (Eriksdotter-Nillson et al., 1986). Interestingly, prominent laminin-positive blood vessels were found in rings encircling some of the grafts. Laminin-positive vessels of varying diameters appeared within the transplant. However, neither neurons nor neuropil in the P and the NP regions contained detectable laminin-like immunoreactivity.

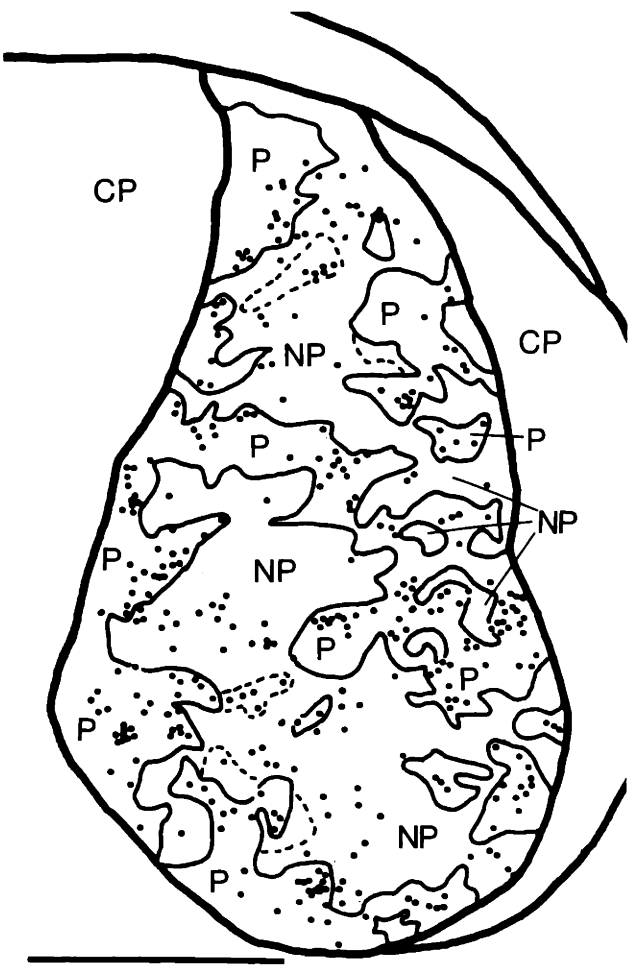
CP
P
P
CP
NP
P
P
NP
P
NP
P
P
P
P
NP
P


A
B
C
C
D

Figure 2-2: Chart illustrating the distribution of [^{3}H]thymidine-labelled neurons (black dots) present in a section processed for autoradiography. Case RSG2-33, post-graft survival time 9 months. The donor tissue was exposed to [^{3}H]thymidine at E15. Solid outlines indicate borders of the AChE-rich P regions visible in a serially adjoining section stained for AChE. Dotted lines indicate borders of weakly stained zones. Note that [^{3}H]thymidine-labelled neurons are present both in P and in NP regions of the graft, but they do not appear in the surrounding striatal tissue of the host (CP). Scale bar indicates 1 mm.

Figure 2-3: Serially adjoining sections through embryonic striatal graft stained for GFAP-like immunoreactivity (A) and for AChE activity (B). From RSG2-32, post-graft survival time 12 months. The three arrowheads in A and in B mark corresponding locations. Note that many GFAP-immunoreactive cells border AChE-rich P regions, but that these cells also occur elsewhere in NP tissue and within P regions. Scale bar for A and B, shown in A, indicates 1 mm. Zone marked by brackets in A and labelled C is illustrated at higher magnification in panel C. Compare with field of GFAP-positive cells in normal striatum on the contralateral side of the host's brain, shown in D.. Scale bar for C and D, shown in C, indicates 100 μm.

Donor origin of labelled neurons in patch and nonpatch regions

[^{3}H]thymidine neuronography was used to test whether the modular expression of striatal markers was the result of a strict separation of labelled graft and unlabelled host tissue. We exposed donor animals to [^{3}H]thymidine at times (E11-E15) known to coincide with the first half of neurogenesis in the rat's striatum and, in the resulting grafts, plotted the distribution of labelled neurons relative to the AChE-positive P regions.

Labelled neurons were strictly confined to the graft tissue and did not appear in the host striatum. Few neurons were labelled with E11 and E12 exposures. Many more labelled neurons were present in the transplants from donor animals exposed at E13-E15. The disposition of [^{3}H]thymidine labelled neurons in a graft derived from E15 donor tissue is shown in Fig. 2-2. Labelled neurons appeared both in the P and in the NP regions in this graft and in all others studied.

Glial and pallidal markers in the graft tissue

Given that the NP regions of the grafts did not express the typically high levels of AChE characteristic of mature striatal tissue, it was important to check whether these AChE-poor NP zones contained high proportions of nonstriatal or even nonneural tissue. We began by staining sections from 3 cases for GFAP-like immunoreactivity to identify the distribution of astrocytes (Bignami et al., 1972). As shown in Fig. 2-3A, in addition to the many GFAP-positive cells at the borders of the implants, GFAP-immunoreactive cells were distributed throughout the grafts. The immunoreactive cells had the typically

multipolar appearance of astrocytes and appeared similar to the GFAP-positive cells of the host striatum (Figs. 2-3C, D). Particularly high densities of GFAP-immunoreactive cells sometimes occurred at the borders between AChE-rich P and AChE-poor NP regions, but many also appeared within subfields of the P and NP regions (see Figs. 2-3A, B). No singular relationship was found between the distribution of GFAP-positive cells and the locations of NP or P regions within the grafts.

We next tested the possibility that the grafts might contain pallidal tissue derived from pallidal progenitor cells included in the dissection of striatal primordia (Walker et al., 1987; DiFiglia et al., 1988). Sections from 4 cases were immunostained with an antiserum to EGF which binds to fibers in mature pallidal tissue and tissue of the pallidal "type" located in the mature substantia nigra and olfactory tubercle but does not bind in the striatum (Fallon et al., 1984). EGF-like immunoreactivity was not detectable either in the AChE-rich P regions or in the AChE-poor NP regions of the grafts despite being present in the host pallidum in the same brains (Fig. 2-4). We also stained for calbindin-like immunoreactivity to test whether the grafts contained large calbindin-positive neurons that resembled calbindin-positive neurons found in the caudal part of the host pallidum. As described in the next section, many such neurons were found in the grafts.

Striatal markers expressed in the graft tissue

Taken together, the results of the Nissl, GFAP and EGF staining showed that the P regions of the grafts are not islands of nerve cells embedded in an NP surround made up of noncellular or glial tissue. The next issue we addressed was whether both P and


CP

Figure 2-4: Cross section through host brain stained for EGF-like immunoreactivity. From case RSG2-24, post-graft survival 17 months. On right, borders of the graft are indicated by arrowheads. A rim of striatal tissue of the host (CP) remains, separated from the graft by fiber bundles. Single arrowhead on left indicates dorsal part of graft introduced into this side (without a prior injection of ibotenic acid). At arrow on left, dense EGF-like immunoreactivity marks the globus pallidus. On the right, the ibotenic acid injection apparently resulted in loss of pallidal neuropil of the host at the transverse level illustrated, but farther caudally EGF-positive pallidal neuropil was present on this side. Note that the grafts do not express EGF-like immunoreactivity. Scale bar indicates 1 mm.


A
B
CP
E
G
*
*
E
F
G
H


C
G
*
J
K
L


D

Figure 2-5: Serially adjacent sections stained for AChE activity (A), calbindin-like immunoreactivity (B) and mENK-like immunoreactivity (C) to illustrate large graft in case RSG2-32, post-graft survival 12 months. Asterisks indicate one of the AChE-rich P regions in the graft. D, overlay drawing of patterns in sections shown in A and C, illustrating schematically the overlap of the AChE-rich P regions in A (pale stipple) and the clusters of calbindin-positive medium-sized neurons visible in B (dark stipple). Note that nearly every cluster of calbindin-positive medium-sized neurons is within an AChE-rich P region. Dashed lines indicate zones of weak AChE staining; fine lines indicate borders of blood vessels. Scale bar for A-D, shown in panel C, 1 mm. E-L, photomicrographs illustrating calbindin-positive cells (E-J) and mENK-positive cells (K, L). Scale bar for E-L, shown in H, indicates 100 μm. E, G, and K illustrate fields indicated by brackets with corresponding letters in low-power photographs of B and C. Bracketed field in C marked 6 is shown at higher magnification in Fig. 2-6. Arrowhead in A points to edge of mENK-positive zone shown in the bracketed region (at arrowhead) in C. E, clustered calbindin-immunoreactive medium-sized neurons in P region. Compare with similar neurons of the host's striatum, shown in F. G, medium- and large-sized multipolar calbindin-positive neurons with well-stained dendrites found in NP region of the graft. Compare with the similar calbindin-positive neurons found in the host's basolateral amygdala (H) and caudal pallidum (I), and with neurons with similar morphology but smaller size found in the ventrolateral cortex of the host (J). K, mENK-immunoreactive medium-sized neurons in an AChE-rich P region. These mENK positive neurons resemble those of the host striatum (examples shown in L).

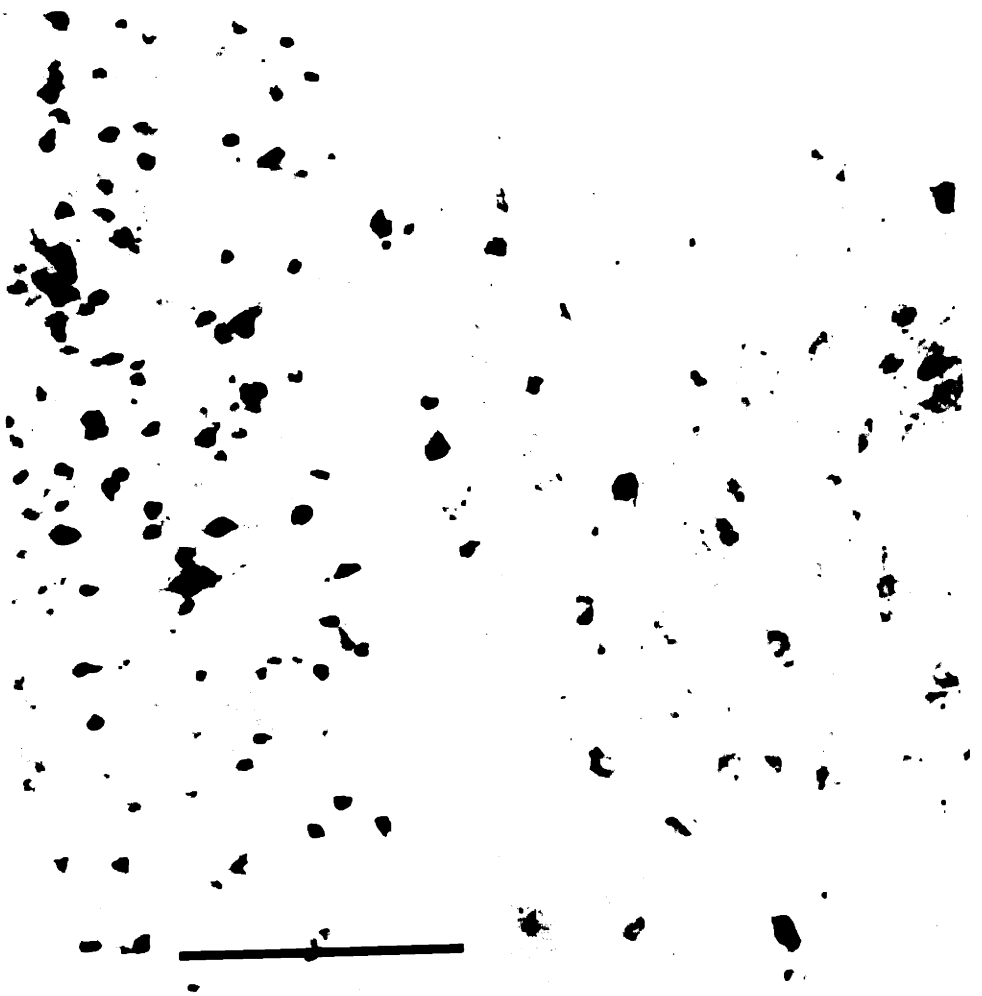

Figure 2-6: Enlargement of bracketed region marked 6 in Fig. 2-5C, shown to illustrate small mENK-positive neurons in an NP zone (left side of field). Some typical medium-sized mENK-positive neurons appear in the right side of the field, which lies in an AChE-rich P region. Scale bar, 100 μm.

NP regions contained striatal tissue. There is no known molecular marker specific for all striatal neurons and only striatal neurons. Immunostaining for a calcium binding protein, calbindin-D_{28K} (calbindin), however, is characteristic of medium-sized neurons of the extrastriosomal matrix in a large part of the mature striatum (Gerfen et al., 1985) and also in a large part of the immature striatum (Liu and Graybiel, 1991b), and mENK-like immunoreactivity is also characteristic of a large proportion of striatal neurons (Graybiel and Chesselet, 1984a, 1984b; Besson et al., 1986, 1988). We employed each of these markers.

Immunostaining for calbindin-like immunoreactivity

Immunostaining for calbindin was carried out in 14 rats. The two calbindin antisera employed yielded similar patterns of immunostaining. In the host striatum, the calbindin antibodies stained medium-sized neurons and neuropil except in the dorsolateral and lateral parts of the caudoputamen and in small gaps shown by Gerfen et al. (1985) to correspond to [^{3}H]naloxone-positive patches (striosomes). In the graft tissue, calbindin-like staining was highly heterogeneous (Fig. 2-5B), and appeared in regions corresponding to both P and NP zones identified in adjacent sections stained for AChE (Fig. 2-5A). The character of the elements stained in the P and NP compartments differed sharply from one another. In the AChE-rich P regions, nearly all of the calbindin-positive neurons were medium-sized (ca. 10-16um diameter) and appeared similar to those in the host striatum (Figs. 2-5E, F). The cell bodies were stained but dendrites were rarely visible. When dendritic segments were detected, they

were short and thin. These medium-sized calbindin-positive neurons and the associated neuropil tended to form distinct aggregates within the grafts. Clusters of calbindin-positive medium-sized neurons appeared only within P regions. Some were coextensive with the P regions, whereas others appeared only within subfields of the P regions (see below and Figs. 2-5D and 2-9). Certain clusters of medium-sized calbindin-positive neurons were surrounded by a very pale ring, so that they formed distinct isolated patches (see Fig. 2-5B). For other clusters, sometimes within the same graft, there was a gradient of calbindin-like immunoreactivity in the neuropil extending with diminished intensity into immediately adjoining NP regions. In all of the sections stained for calbindin-like immunoreactivity from the 14 rats, only four large (ca. 19-25 μm diameter) calbindin-immunoreactive neurons were found in P regions. Two of these cells resembled in size and shape the very rare medium-large (ca. 19 μm diameter) calbindin-positive cells that were found in the ventral and ventrolateral parts of the caudoputamen of the hosts.

In the AChE-poor NP regions of the grafts, medium-sized calbindin-positive cells with a morphology similar to those of the P regions were extremely rare. However, multipolar calbindin-positive neurons with well-stained dendrites were prominently scattered through the NP tissue (Figs. 2-5B, G). These neurons comprised a mixed population of large to medium-sized cells (ca. 13-31 μm diameter, a few up to 38 μm) cells with dendrites extending for considerable distances from the cell body and sometimes branching extensively. Spines were not detected on the dendrites. To distinguish these cells from the medium-sized calbindin-positive neurons in the P regions,

we will call them the "multipolar calbindin-positive neurons".

These multipolar calbindin-positive neurons and associated calbindin-positive neuropil appeared to form subfields within the NP zones of some grafts. In other grafts, the multipolar calbindin-positive neurons were scattered through most of the NP tissue, and the calbindin-positive neuropil in the NP zones was also diffusely distributed. Occasionally, well-stained processes of such multipolar calbindin-positive neurons in NP regions extended into the margins of patches of calbindin-positive medium-sized neurons in adjoining P regions.

Almost no calbindin-positive multipolar neurons comparable to those in the NP regions of the grafts were present in the striatum of the hosts. However, calbindin-positive neurons with similar shapes and sizes were present in the caudal pole of the host's pallidum (ca. 13-31 μm diameter, Fig. 2-5I) and in the basolateral nucleus of the amygdala (ca. 14-31 μm diameter, Fig. 2-5H). Calbindin-positive neurons with similarly well-stained dendrites but smaller size (ca. 12-31 μm diameter, most ca. 19 μm, a few up to ca. 25-31 μm) were always found in the perirhinal cortex that lies ventrolateral to the caudoputamen (Fig. 2-5J).

In addition to NP regions rich in calbindin-positive multipolar neurons, there were fields within the NP regions of the grafts in which such neurons were absent and in which little calbindin-like immunoreactivity appeared in the neuropil. Thus, at least three types of tissue were identified in the transplants based on the calbindin-immunostaining: (1) tissue rich in medium-sized calbindin-positive neurons without well-stained dendrites (occurring in P regions); (2) tissue containing multipolar often very large calbindin-

positive neurons with prominent dendritic arbors (occurring in NP zones); and (3) tissue containing few neurons of either category (occurring both in P and in NP zones).

Just as the restriction of multipolar calbindin-positive cells with well-stained dendrites to NP regions was nearly absolute, the localization of clusters of medium-sized calbindin-positive cells within P regions was also the rule with only 3 exceptions observed in NP regions of 3 sections (from 2 brains) out of 23 sections (from 7 brains) in which AChE-stained sections serially adjoining calbindin-stained sections were available. The first was a cluster in NP containing calbindin-positive neuropil and also a few medium-sized calbindin-positive neurons. The second was an NP zone with one large calbindin-immunoreactive cell but also some medium-sized calbindin-positive neurons. The third was a calbindin-positive patch rich in medium-sized immunostained neurons similar to those in the P regions, but for which there was no AChE-positive correspondent in the adjoining section.

Immunostaining for mENK-like immunoreactivity

Like the calbindin-positive medium-sized neurons in the grafts, mENK-positive medium-sized neurons were mainly confined to P regions (Fig. 2-5A, C). In such regions, both neuropil and medium-sized cell bodies were immunostained (Fig. 2-5K). The medium-sized mENK positive neurons were similar to those of the normal host striatum (Fig. 2-5L). They tended to aggregate in clusters, but the clusters varied in the intensity of mENK-like immunoreactivity they expressed.

Although mENK-like immunostaining in NP regions was generally much weaker than that in P regions, the immunostaining was quite heterogenous, and some mENK-

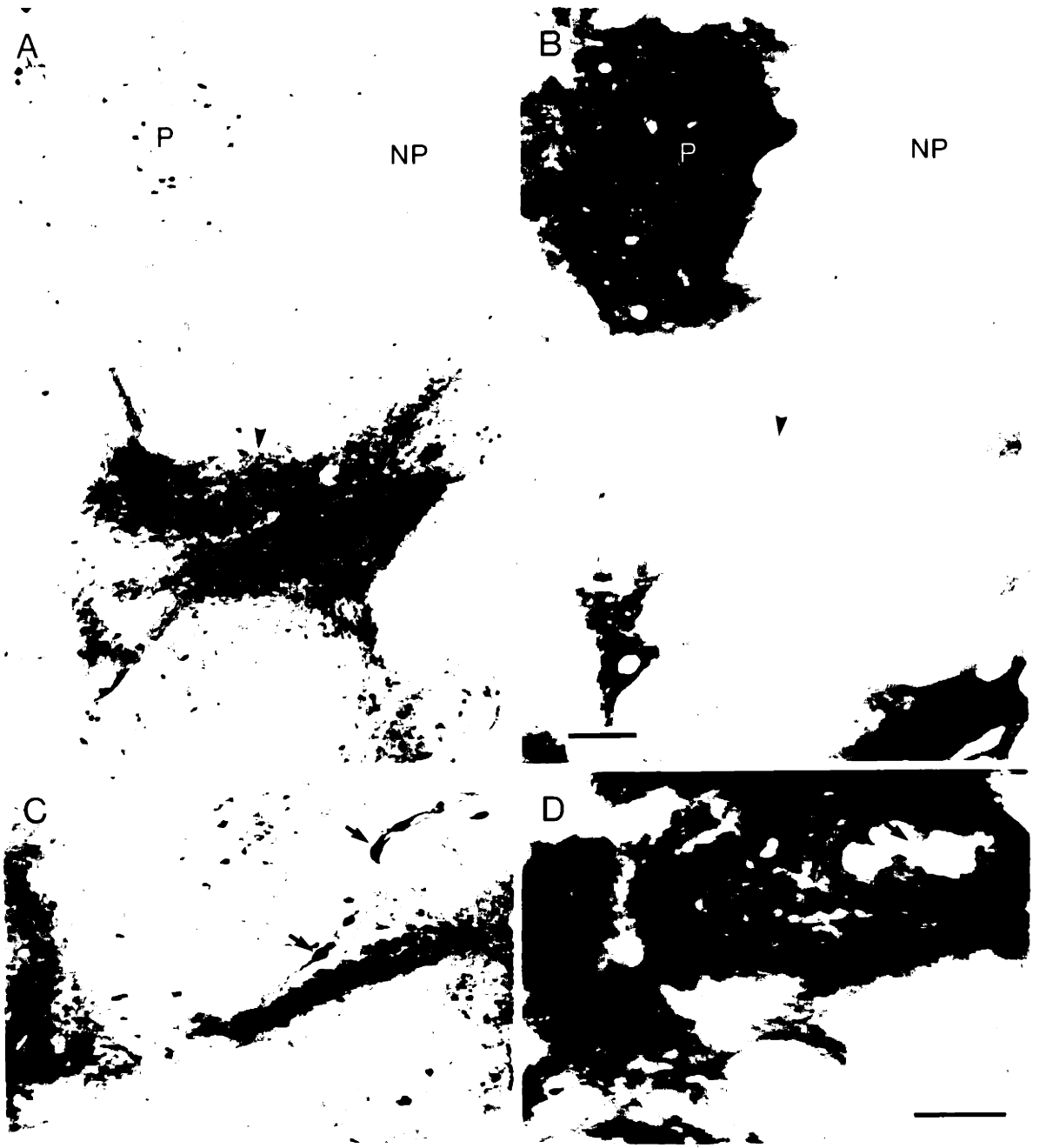
A
P
NP
B
P
NP
C
D

Figure 2-7: Photomicrographs of corresponding fields from serially adjacent sections through graft tissue in case RSG2-23, post-graft survival 15 months, illustrating patterns of mENK-like immunoreactivity (A) in relation to distribution of AChE-activity (B). Medium-sized mENK-positive cells appear in P region (P) along with weakly immunoreactive neuropil. Zone of dense mENK-positive neuropil appears at arrowhead in A in a nearby part of the NP tissue. Arrowhead in B denotes corresponding site in AChE-stained section. Scale bar for A and B, shown in B, indicates 100 μm. C and D, corresponding fields from serially adjacent sections from same case as in A and B stained for mENK-like immunoreactivity (C) and for AChE activity (D). Note, at arrows in C, 3 immunoreactive neurons slightly larger than the typical mENK-positive medium-sized neurons of the host striatum. They are in an AChE-rich P region (see corresponding arrows in D). Note streaks of strongly mENK-positive neuropil at the borders of the P region. Scale bar for C and D, shown in D, indicates 100 μm.

positive regions appeared within NP tissue. Some NP zones contained many small mENK-positive cells (ca. 6-10 μm), often packed together closely (see Figs. 2-5C and 2-6). Occasionally a patch of highly mENK-immunoreactive neuropil appeared in an NP region (Figs. 2-7A, B), sometimes in association with a few heavily stained medium-sized mENK-positive neurons.

A few of the intensely mENK-immunoreactive neurons in the graft had diameters slightly to considerably larger than mENK-positive medium-sized neurons of the normal host striatum (ca. 18-31 μm diameter versus ca. 13-15 μm diameter in our sample). These mENK-positive neurons had well-stained dendrites that lacked the densely spiny character of the mENK-positive neurons of normal striatum. The largest of the group (ca. 31 μm diameter) was about the same size and shape as the cholinergic interneurons of the rat's striatum. These mENK-positive neurons were nearly all associated with zones of neuropil expressing intense mENK-like immunoreactivity (Fig. 2-7C). Thus, patches of intensely mENK-positive neuropil occurred both in P zones (Figs. 2-7C, D) and in NP zones. Interestingly, some of the mENK-rich NP zones had detectable, though weak, AChE activity (see Figs. 2-5A, C). Patches of mENK-positive neuropil in register with zones of relatively weak AChE activity normally occur in the ventral caudoputamen of the rat at rostral levels (see Figs. 2-11B, C).

Immunostaining for SOM-like immunoreactivity

Many large and medium-sized SOM-positive neurons (ca. 13-31 μm diameter, a few up to ca. 38-44 μm) were located in the NP regions of the transplants (Figs. 2-8A-C).


A
B
C
D
E
F

Figure 2-8: Serially adjoining sections from case RSG2-17, post-graft survival 11 months, stained for SOM-like immunoreactivity (A) and AChE activity (B); scale bar for A and B, shown in A, indicates 0.5 mm. Arrowheads in A and B point to locations of 2 P regions. Note that many medium to large SOM-positive neurons with prominent dendrites are distributed through the AChE-poor NP regions but do not occur in the P regions. Brackets in A marked C indicate location of field shown at higher magnification in panel C. Similar types of SOM-positive neurons present in the ventrolateral cortex of the host are shown in D. E illustrates bracketed region in A (marked by letter E) showing a single medium-sized SOM-positive cell at the margins of the P region in this field (location is indicated by the arrow in B). F, a field of SOM-positive neurons from the normal contralateral striatum of host. Scale bar for C-F, shown in F, indicates 100 μm.

By contrast, few SOM-positive neurons appeared within the AChE-rich P regions (Fig. 2-8E), and these were similar in size to the SOM-positive neurons of the normal host striatum (Fig. 2-8F). The large SOM-positive neurons in the NP regions (Fig. 2-8C) were larger than the SOM-positive neurons of the normal host striatum (Fig. 2-8F). Medium to large SOM-positive neurons (ca. 13-34 μm diameter) were common in the cortex of the host brains, especially ventrolaterally (Fig. 2-8D), but none were as large as the largest SOM-positive neurons in the NP regions of the grafts.

Expression of markers for striosomal and matrical tissue in the AChE-rich P regions of the grafts

Calbindin-like and mENK-like immunoreactivities are normally expressed by medium-sized neurons of the striatal matrix at maturity, and during much of the postnatal development, and either are not expressed normally by striosomal neurons (calbindin, Gerfen et al., 1985, 1987b; Liu and Graybiel, 1991b) or are less consistently and intensely expressed by striosomal neurons (mENK, Graybiel and Chesselet, 1984; Besson et al., 1986, 1988b). Neither calbindin-like immunoreactivity nor mENK-like immunoreactivity is a secure indicator that a striatal neuron is matrical, however, because calbindin-positive neurons are absent altogether in the dorsolateral striatum, and mENK-immunoreactivity is detectable in some striosomal neurons. Nevertheless, the combination of the two markers within a given zone of the graft would strongly suggest that the zone corresponds to matrix tissue, or at least to tissue expressing markers characteristic of matrix tissue at maturity and during much of postnatal development.

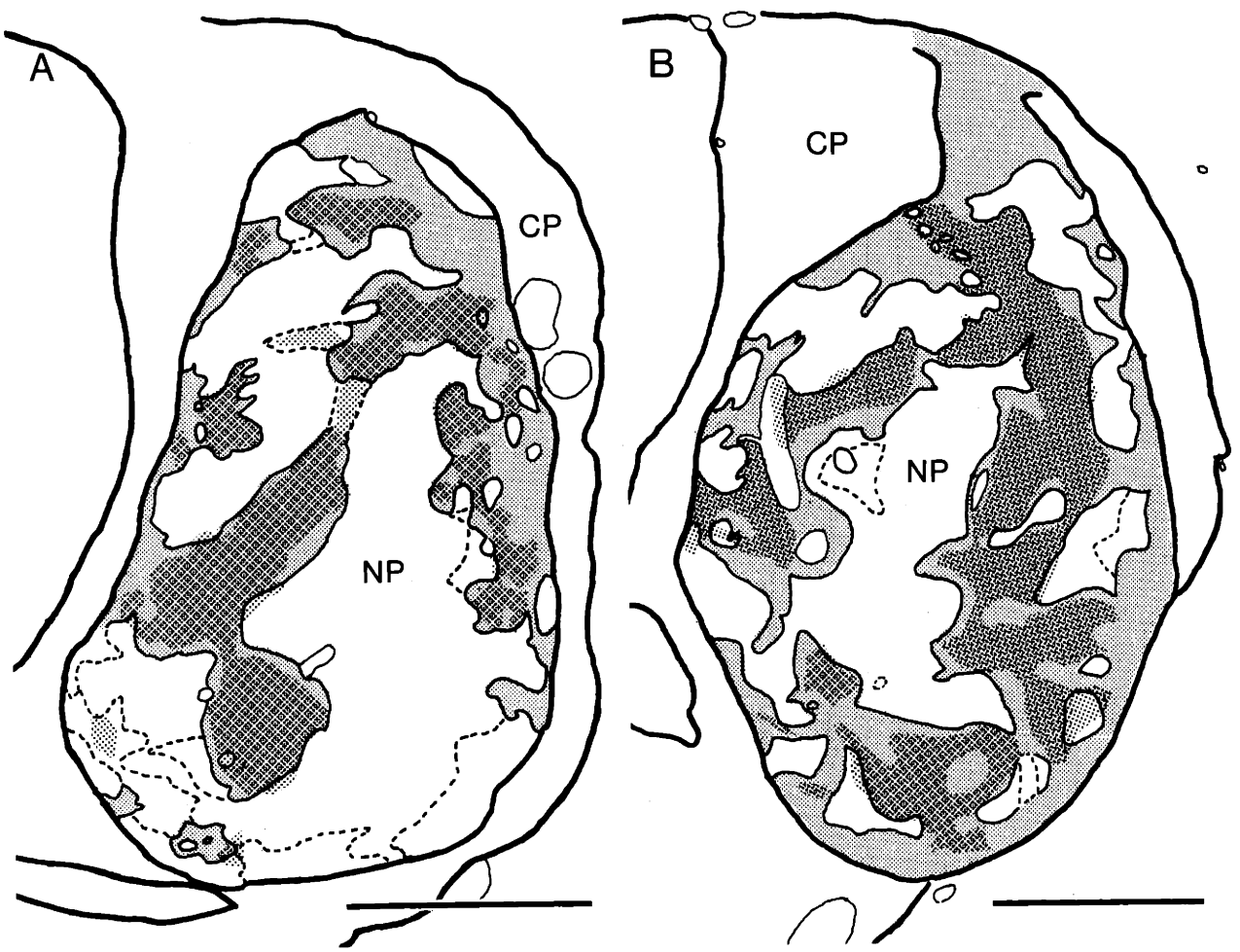
A
CP
NP
B
CP
NP

Figure 2-9: Schematic overlay drawings illustrating relative distributions of the AChE-rich P regions (light stipple) and the clusters of calbindin-positive medium-sized neurons (dark stipple) observed in serially adjoining sections from 2 different cases (A, RSG2-21, post-graft survival 13 months; B, RSG2-32, post-graft survival 12 months). Note that for some P regions, the calbindin-positive cell clusters and AChE-rich zones share nearly the same space. For other P regions, the patches of calbindin-positive medium-sized neurons form subfields within the AChE-rich P regions. Fine lines indicate borders of blood vessels; dashed lines indicate zones of weak AChE activity. Scale bars indicate 1 mm.

The best marker for putative striosomes in the mature rat's striatum and in the developing rat's striatum after about P2-P3 is ligand binding for mu opioid receptors (Herkenham and Pert, 1981; van der Kooy, 1984; Moon Edley and Herkenham, 1984). To determine whether the AChE-rich P regions of the grafts contained markers of striosomal tissue or of matrical tissue, or both, we therefore carried out detailed serial-section comparisons of the patterns of immunostaining for calbindin-like and mENK-like immunoreactivity in relation to the distribution of AChE staining, and compared these to the distribution of binding sites for [^{3}H]naloxone, a marker for mu opioid receptors. Typical findings are illustrated in Figs. 2-5A-D and Figs. 2-9 to 2-11.

Nearly every patch of medium-sized calbindin-positive cells and mENK-positive cells clearly fell within an AChE-positive P region identified in serial sections, and for the most part the calbindin-positive medium-cell clusters and mENK-positive medium-cell clusters were in close serial-section alignment. For some P regions, the size, shape, and location of the clusters of medium-sized cells seen with the calbindin and mENK antisera were nearly identical to those of the AChE-positive regions (see Fig. 2-9A). In other instances, however, the P regions were larger than the calbindin-positive or mENK-positive medium-sized cell patches they overlapped with, even when the zones of AChE staining and of calbindin or mENK staining shared some borders (Figs. 2-5D, 2-9). Thus some AChE-positive P regions of the grafts corresponded to zones of high calbindin-like and mENK-like immunoreactivity, whereas other P regions contained subfields expressing these striatal matrix markers and subfields lacking them. We found no instances in which the calbindin-positive or mENK-positive medium-sized cell clusters were larger than the

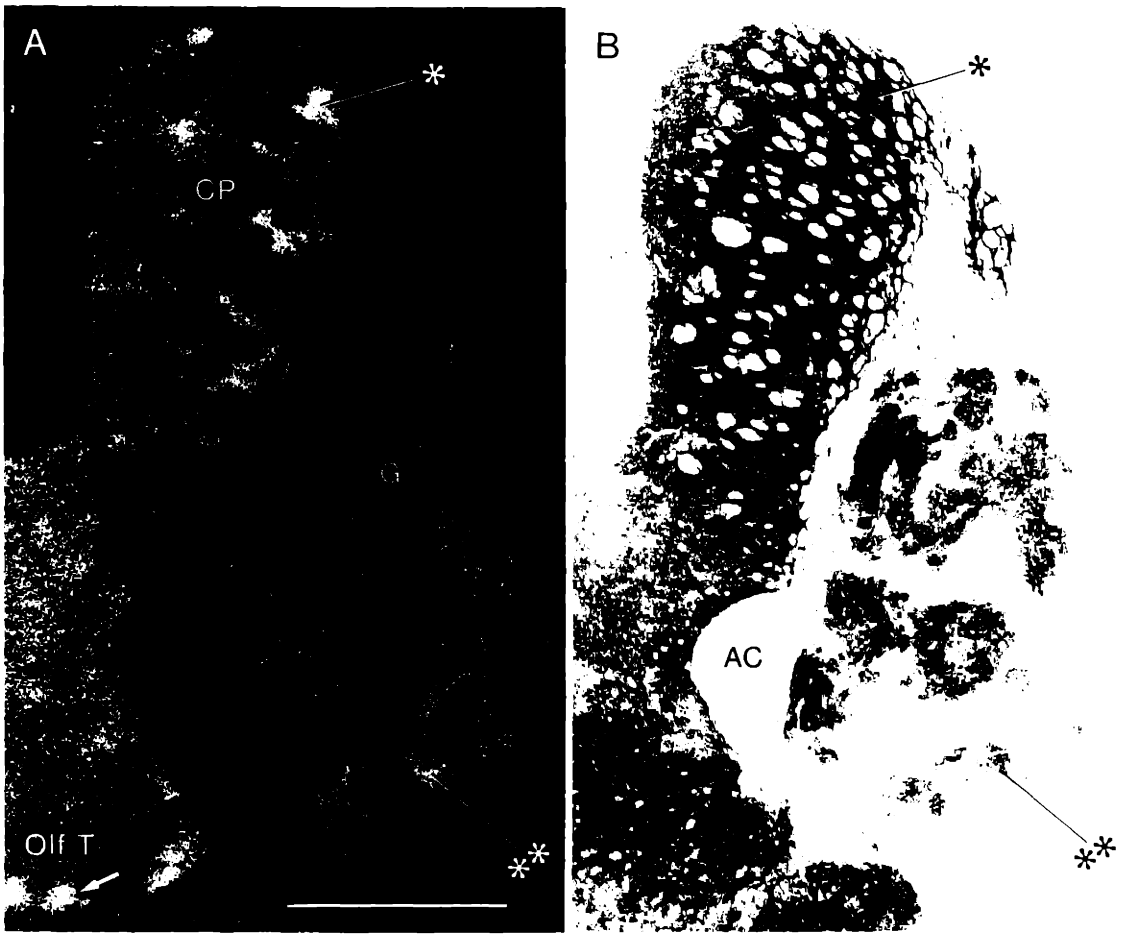
A
*
CP
Olf T
**
B
*
AC
**

Figure 2-10: Photograph of film autoradiogram illustrating [^{3}H]naloxone binding in host striatum (CP) and in adjacent tissue of embryonic striatal graft (G) in case RSG2-34, post-graft survival 12 months, processed fresh-frozen. B: adjacent section stained for AChE to illustrate locations of P and NP regions in the graft. Asterisk in A indicates one of the patches of dense [^{3}H]naloxone binding (putative striosomes) in host striatum. Asterisk in B marks same site in AChE-stained section; note that the patch is not identifiable as AChE-poor zone. Arrow in A marks dense patch of [^{3}H]naloxone binding in olfactory tubercle of host. In the graft, only 1 crisp zone of heightened [^{3}H]naloxone binding is visible (double asterisks). As shown by matching double asterisks in B, it is in a P region. AC-anterior commissure. Scale bar for A and B, shown in A, indicates 1 mm.

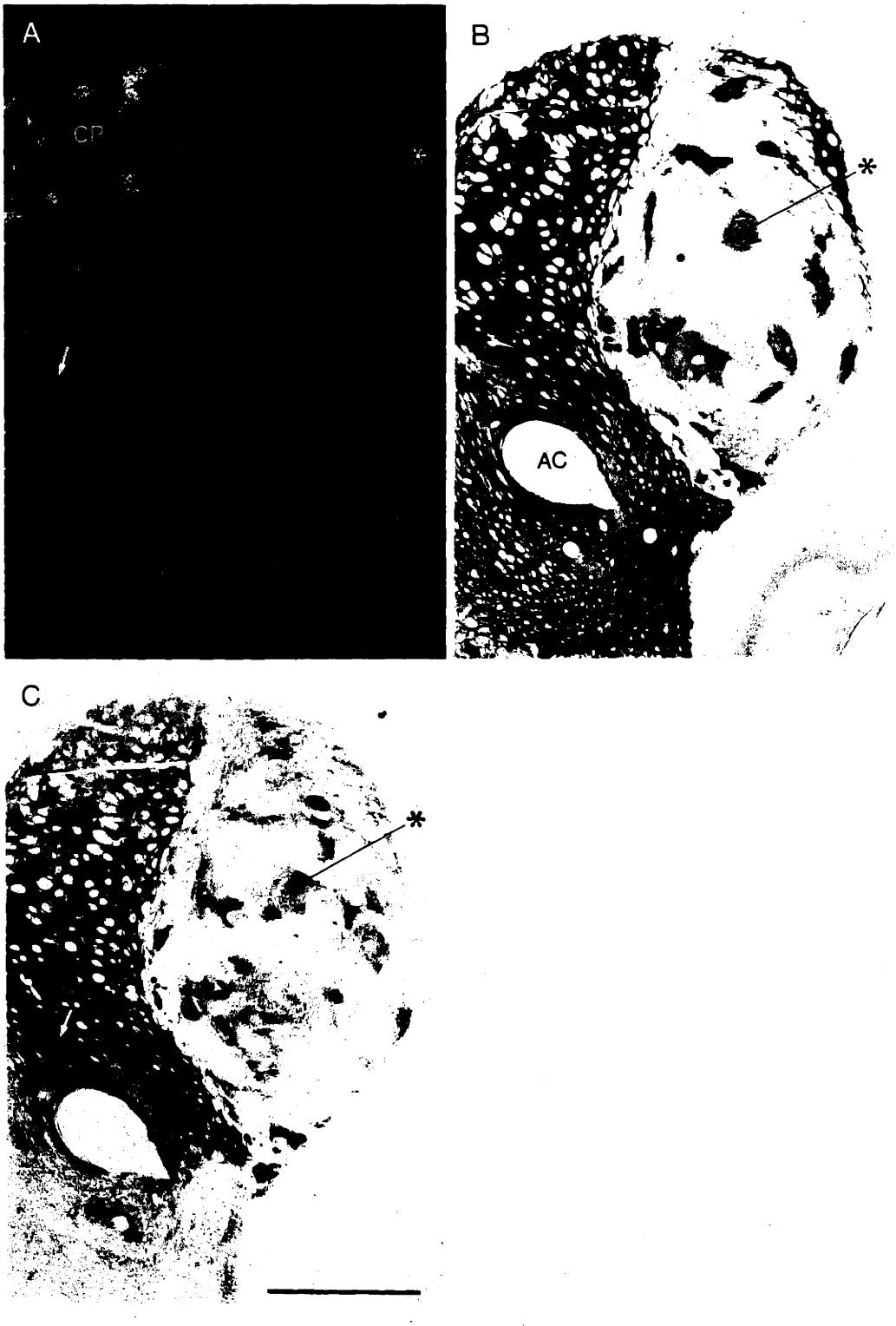
A
CP
B
AC
*
C
*

Figure 2-11: Patterns of (A) [^{3}H]naloxone binding in film autoradiogram, (B) AChE activity and (C) mENK-like immunoreactivity in graft tissue of case RSG2-30, post-graft survival 16 months. A: patches of [^{3}H]naloxone binding are visible in host's striatum (CP) but not in graft. B: slight heterogeneity of AChE activity visible in host's striatum (including ventral AChE-poor zone at arrow), and typical AChE-rich P zones (example at asterisk) embedded in fields of AChE-poor NP tissue in the graft. C: heterogeneity of mENK immunostaining in host's striatum, including patch of mENK-rich neuropil at arrow matching AChE-poor zone at arrow in B. In graft, zones of high and low mENK immunoreactivity occur, including mENK-rich zone at asterisk corresponding to P zone marked by asterisk in B. AC-anterior commissure. Scale bar for A-C, shown in C indicates 1 mm.

corresponding AChE-positive P zones.

In all 5 brains in which sections were processed for [^{3}H]naloxone binding, typical opiate receptor patches appeared in the host striatum. However, in only 1 of the grafts was [^{3}H]naloxone binding above background levels. In this graft (Fig. 2-10), the one fresh-frozen specimen, much of the binding was diffuse. Even where the binding was not uniform, it lacked the crisp modularity of [^{3}H]naloxone binding characteristic of the normal striatum of the adult rat. Only one small patch of intense binding, visible in films of several closely spaced sections, and a few regions of slightly heightened binding were present. The patch of most intense binding was in a P region, but the other regions of heightened binding were in NP zones (compare Figs. 2-10A and B). Some zones of especially impoverished binding appeared in the graft, both in P and in NP regions. In the normal adult striatum, such zones occur in the matrix (see Fig. 2-10A).

The four remaining perfused brains had normal patterns of [^{3}H]naloxone binding in the host tissue but almost no [^{3}H]naloxone binding in the grafts (see Fig. 2-11A). The grafts contained patches of opioid peptide (mENK-like) immunoreactivity (Fig. 2-11C), and the patches of medium-sized mENK-positive cells fell within AChE-rich P regions (Figs. 2-11B, C). In all of the grafts, donor cells had been exposed to [^{3}H]thymidine, but at the exposure times used for the [^{3}H]naloxone binding, [^{3}H]thymidine labeling did not interfere with interpretation of the sparse autoradiographic labeling visible in the films (cf. Nastuk and Graybiel, 1985). The low levels of grain in the graft tissue were similar to those in nearby nonstriatal gray matter.

DISCUSSION

The observations reported here confirm the presence of a macroscopic modular architecture in embryonic striatal grafts and a remarkable phenotypic resemblance of many neuronal constituents in the grafts to neuronal constituents found in normal postnatal and mature striatum (Pritzel et al., 1986; Isacson et al., 1984, 1985, 1987; Walker et al., 1987; Deckel and Robinson, 1987; Sanberg et al., 1987; Graybiel et al., 1987a; Clarke et al., 1988; Roberts and DiFiglia, 1988; DiFiglia et al., 1988). The phenotypic resemblance inferred from the markers screened does not necessarily imply identity; but does suggest that at the cellular level many antigens characteristics expressed by neurons in the grafts were like those expressed by neurons in normal striatal tissue. Unexpectedly, however, our experiments raise the possibility that the compartmental architecture of the grafts may be quite different from that seen in the normal striatum. Our results suggest that the AChE-rich patches in embryonic striatal grafts may represent islands of striatal tissue surrounded by cells lacking the phenotypy of mature striatum, and that at least part of the tissue of these islands, rather than being striosomal, might actually be matrical in type. The phenotypy of the AChE-poor NP zones was not definitively determined, but the evidence suggests that these may be comprised of nonstriatal tissue or, perhaps, of an admixture of tissue resembling immature striatal tissue and some nonstriatal cells. The experiments did not resolve the question of whether the tissues of the P and NP regions were mature or immature in phenotypy. As discussed below, however, the evidence tends to favor a degree of maturation for at least the P regions of near or greater than the immediate perinatal stage.

Donor-cell distributions

The results of the [^{3}H]thymidine experiments argue against the hypothesis that the modular arrangement of P and NP zones in the grafts reflects the separation of compartments made up exclusively of host and of donor tissue, respectively. Some donor cells, marked by [^{3}H]thymidine, appeared both in the AChE-rich P and in the AChE-poor NP compartments. The absence of labelled neurons in the adjacent host tissue agrees with the report of McAllister et al. (1987), and suggests that large numbers of grafted cells were not incorporated into the adjacent host tissues, or if they were initially, that they did not survive. Because cells of host origin were not experimentally labelled, we can not exclude the possibility that some cells in the grafts were actually derived from the host, or that part or even most of the patchiness of the grafts resulted from segregation of donor tissue from host tissue.

If there were an mixture of host and donor tissue in the grafts, it seems reasonable to suppose that it would be the P zones, not the NP zones, that were derived from the host. Almost certainly it would be mainly striatal tissue of the host that would become mixed with donor tissue at the time of grafting, and it is the P regions that most resemble the host's striatal tissue. Any such host neurons in the grafts would have had to survive the toxic effects of the ibotenic acid injections (Isacson et al., 1987; Walker et al., 1987; Coyle and Schwarcz, 1976; Köhler and Schwarcz, 1983), which we confirmed in the control non-graft animal. It should be noted that Isacson et al. (1987) observed AChE-rich regions embedded in AChE-poor tissue in transplants placed outside of the striatum, for example, in the substantia nigra and globus pallidus.

The E13-E15 [^{3}H]thymidine exposure times were within the window of peak neurogenesis for neurons destined to inhabit striosomes (van der Kooy and Fishell, 1987). As the donor tissues were taken at E15, they could not be exposed during the reported window of peak neurogenesis for cells of the matrix, E18-E20 (van der Kooy and Fishell, 1987). This schedule of neurogenesis suggests that many if not most of the heavily labelled neurons would have been striosomal progenitors, but there is overlap between the birthdates of striosomal and matrical cell-populations. Accordingly, the labelled neurons in the grafts could not be identified unequivocally as being either of striosome or matrix type despite the E13-E15 exposure times. Many neurons of the cerebral cortex (and other forebrain regions) are also born during the E13-E15 time period, including many neurons in tissue ventral and lateral to the striatum (e.g. van der Kooy and Fishell, 1987). Some of these neurons may derive from the ganglionic eminence (see below). Consequently, neurons in the grafts labelled with [^{3}H]thymidine could not be identified positively as striatal.

Nature of the AChE-rich P regions

The present study, taken together with previous reports (Pritzel et al., 1986; Isacson et al., 1987; Walker et al., 1987), leaves little doubt that the AChE-rich P regions comprise striatal tissue. With only one exception ([^{3}H]naloxone) discussed below, every marker we employed to detect transmitter-related compounds enriched in normal mature striatal tissue had a heightened representation in the P regions relative to the NP regions of the grafts. Conversely, neuronal types uncharacteristic of normal mature striatum

were absent or nearly absent from the P regions but were present in NP tissue.

In our analysis of the AChE-rich P regions, we found two main patterns. Some clusters of medium-sized calbindin-positive neurons were coextensive with AChE-rich tissue defining the P regions. Calbindin is selectively expressed in medium-sized matrix neurons at maturity and, as discussed below, available evidence suggests that this antigen is also expressed in the matrix developmentally, during the early postnatal period. Clearly, for calbindin-like immunoreactivity as for other markers used in this study, we cannot be sure that the expression of the marker would be identical in the transplants and in normal striatum of any age. Nevertheless, this evidence is compatible with the view that some P regions were mainly matrical.

For other P regions, the calbindin immunostaining of medium-sized neurons was limited to subregions of the AChE-rich P zones. This evidence suggests that some P regions were composed of more than one type of striatal tissue, matrix (calbindin-positive) tissue and calbindin-negative tissue that either was dorsolateral or lateral striatum (not normally calbindin-positive), or was striosomal in nature, or did not, through incomplete development or other causes, express a full repertoire of antigens characteristic of mature striatal neurons. We stress that a few calbindin-immunoreactive neurons may occur in striosomes in the normal striatum and that the presence of a few calbindin-negative neurons in matrix has nor been excluded (Gerfen et al., 1985; present observations). In the one case in which mENK immunostaining was available in sections immediately adjacent to those stained for calbindin-like immunoreactivity, the clusters of mENK-positive medium-sized neurons overlapped the calbindin-positive medium-sized

cell clusters but sometimes were larger (although still within the AChE-rich P regions). This correlative evidence suggests that at least some of the neurons in the calbindin-negative parts of the P regions may have more closely resembled striosomal neurons than dorsolateral matrix neurons, because medium-sized neurons in the dorsolateral mature matrix do express mENK-like immunoreactivity, whereas not all calbindin-negative striosomes are rich in strongly mENK-immunoreactive neurons.

Opioid receptor-related ligand binding was only rarely aggregated into strongly labelled patches in the grafts, even though intensely labelled [^{3}H]naloxone-positive patches (striosomes) could be detected in the immediately adjacent host striatum. Thus, although characteristics matrix markers were absent in parts of certain P zones, the [^{3}H]naloxone binding did not provide evidence for dense concentrations of striosomal tissue in these subfields. The strongest binding observed in graft tissue was in the unperfused brain, but in the perfused brains there was intense [^{3}H]naloxone binding in host tissue adjoining the grafts having very little detectable binding. It therefore seems unlikely that the low binding from a technical problem. Conceivably, striosomal cells in the P regions had down-regulated receptor numbers or were mixed with larger matrix-cell populations in numbers too small to detect. The limited development of patches of dense [^{3}H]naloxone binding observed is directly comparable to the findings of Lanca et al. (1986). Isacson et al. (1987) observed [^{3}H]diprenorphine-positive patches within their series of grafts, but these were clearly smaller than the AChE-positive patches. These investigators also found other characteristic constituents of striosomes in the AChE-positive patches, such as mENK-positive fibers and SP-positive cell bodies, further

suggesting that AChE-rich regions of embryonic striatal grafts can also contain striosomal tissue.

The sparseness of patches of dense [^{3}H]naloxone binding observed in the present graft preparations may reflect a selective cell death occurred in grafted striosomal cell population. Fishell and van der Kooy (1987b) have reported that striosomal cells projecting to the substantia nigra preferentially survive the cell death period during striatal development. Given that retrograde tract-tracing studies have shown that limited number of striatal grafted cells project to the host substantia nigra (Pritzel et al., 1986; Wictorin et al., 1989b; Zhou et al., 1989), it is possible that the inability of the grafts to establish the full normal extent of efferent connections with the substantia nigra, either because of the long distance between the striatum and substantia nigra, or the lack axon-outgrowth directing factors in the graft environment, results in poor survival of grafted striosomal cells. A further implication of this hypothesis is that the substantia nigra may provide some retrograde-transported neurotrophic factors for developing striosomal cells. These unknown trophic factors could be developmental regulated and down-regulated in the mature host.

The apparent predominance of matrical markers in the P regions in the present series of grafts is interesting given the larger proportion of striosomal than matrical tissue that should have been present in donor the striatal anlage at the time of dissection (E15). However, a larger fraction of progenitors of matrical cells should have been present in the germinal epithelium at the time of dissection (van der Kooy and Fishell, 1987), and these could have survived and developed preferentially. When all the findings

so far available are considered together, it seems likely that markers characteristic of both striosomes and matrix can be concentrated in the AChE-rich P zones of striatal grafts, but that their relative proportions may vary depend on slight differences in the methods of dissection and of tissue preparation.

Nature of the AChE-poor NP regions

One of the most clear-cut findings of the present study was the presence in the NP regions of many large multipolar calbindin-positive neurons and SOM-positive neurons that were unlike any found in the host striatum, but that resembled neurons found elsewhere in the host's forebrain. We did not test for cellular colocalization of the calbindin and SOM antigens. Even if the two antibodies singled out the same populations of cells, however, the findings with each argue strongly that neuronal types not found in mature striatum were widely distributed in the AChE-poor NP regions. Neurons larger than those of the normal striatum have been observed previously in striatal grafts prepared both from embryonic (DiFiglia et al., 1988) and from neonatal striatal tissue (McGeer et al., 1984). Walker et al. (1987), DiFiglia et al. (1988) and Roberts and DiFiglia (1988) have also noted other morphological characteristics of embryonic striatal grafts that differ from those of normal striatum. Unfortunately, it is not clear whether the unusual characteristics they observed were associated with cells of what we here call P regions and consider striatal in nature, or were characteristic of NP regions.

The large multipolar calbindin-positive neurons found in the present series of

grafts closely resembled those of the caudal (but not rostral) pallidum, the basolateral amygdala and the ventrolateral cortex of the hosts. The possibility of pallidal contamination of embryonic striatal grafts has been discussed in several previous reports (Walker et al., 1987; Isacson et al., 1987; DiFiglia et al., 1988). Our own evidence based on calbindin immunohistochemistry make this an attractive possibility at least for caudal pallidal tissue. The results of EGF-like immunohistochemistry suggest that the neuropil of the graft tissue did not express the EGF-like staining typical of normal mature pallidum (Fallon et al., 1984), but because EGF-like immunoreactivity is confined to pallidal neuropil, we could not judge perikarya. The basolateral nucleus of the amygdala is rich in AChE activity, unlike the NP regions. Because most of the AChE in the basolateral nucleus is thought to be contained in afferent fibers (Emson et al., 1979), however, this does not necessarily detract from the possibility that the multipolar calbindin-positive neurons of the grafts represented amygdaloid neurons. The diameters of some of the multipolar calbindin-positive neurons in the NP regions were larger than those of calbindin-positive neurons in the cortex, but their appearance was otherwise reminiscent of the multipolar calbindin-positive cells of the ventrolateral cortex of the hosts.

The SOM-positive cells of the NP regions similarly resembled SOM-positive neurons in the host cortex, both ventrally and elsewhere, again except that some of the SOM-positive neurons in the grafts were larger than those in the cortex. Interestingly, the distribution of neurons in the grafts expressing cholinergic markers (Graybiel et al. 1987a; Liu et al., 1990b) suggests that the large neurons of the NP regions are not

cholinergic: most large choline acetyltransferase-positive and AChE-positive neurons lie in P regions.

A reasonable explanation for the occurrence in the grafts of neurons similar to those of the caudal pallidum, basolateral amygdala and cortical plate is that cells destined to have these phenotypys were included within the tissue dissected to prepare the "striatal" cell suspensions. The pallidum and basolateral amygdala both physically adjoin the striatum ventrolaterally, and the ventrolateral cortex lies just beyond these tissues. An attractive hypothesis suggested by our findings is that some of the progenitor cells giving rise to these tissues may lie in the ganglionic eminence and migrate out through the striatal anlage (see below). An alternative interpretation is that such neuronal constituents, though uncharacteristic of mature striatum, may normally appear in immature striatum, and that the grafts, as suggested by Isacson et al., (1987), may have the phenotypy of immature striatum. In fact, as discussed in the following section, in a developmental study of calbindin in the striatum (Liu and Graybiel, 1991a), we have observed large calbindin-positive neurons with widely ramified dendritic arbors in the perinatal striatum, but have not observed large multipolar SOM-positive cells similar to those of NP regions.

A third possibility to be considered is that under the abnormal conditions of the transplant's environment, some striatal progenitor cells (or other progenitor cells) could have been transformed into neurons with characteristics not found normally in the striatum. Whether the large multipolar calbindin-positive and SOM-positive cells represented immature or transformed striatal neurons or other neurons, there remains

the question of why, in the grafts, they were commonly found in NP regions but almost never found in immediately adjoining P regions.

The large multipolar calbindin-positive and SOM-positive cells were not the only cells in the NP regions that were unlike host striatal neurons. In sections stained for mENK-like immunoreactivity, we also found NP zones containing groups of mENK-positive cells that were smaller than medium-spiny striatal neurons. However, judging by the small size of these mENK-positive cells, they may be astrocytes, as cultured astrocytes derived from the developing cortex and striatum have been shown to contain proenkephain mRNA and ENK peptides (Shinoda et al., 1989).

In summary, 3 types of cells with phenotypy unlike that of cells in host striatum were detected in NP (but almost never in P) regions of the grafts. The AChE-poor NP regions did not, however, express high levels of transmitter-related compounds typical of mature striatum and, according to available evidence, of much of striatum during postnatal development.

Developmental status of the grafts

A natural interpretation of the compartmentalization of embryonic striatal grafts, given their appearance in AChE-stained sections, is that the AChE-rich zones are immature striosomes embedded in immature matrix tissue (Isacson et al., 1987). As first noted by Isacson et al. (1987), a number of characteristics of the grafts in addition to their AChE-positive patches could also be taken to suggest their immaturity. Here, as well, we found such characteristics: there were patches of mENK-like immunoreactivity

coincident with AChE staining (Graybiel et al., 1981); there was diffuse mu opioid receptor-related binding in the grafts (Kent et al., 1982; Moon Edley and Herkenham, 1984; van der Kooy 1984; Lanca et al., 1986); and E13-labeled [^{3}H]thymidine-positive neurons were relatively diffusely distributed through the grafts (van der Kooy and Fishell, 1987). Other evidence, however, highlights the difficulty of determining with certainty the developmental status of the graft tissue. Nearly all available markers for identifying the striosomal and matrix compartments undergo pronounced developmental shifts in expression occurring at different times in different striatal regions, and their expression tends to be graded across development and across compartments. For some markers, there are special problems in making inferences from species to species. For example, in the newborn rat, as in other neonatal mammals, AChE is expressed more strongly in the neuropil of future striosomes than in the neuropil of future matrix, but at adulthood, when the relative staining densities of the striosomes and matrix are reversed in most other mammalian species, not all "striosomes" as identified by mu opioid ligand binding in the rat are obviously more weakly stained for AChE than the surrounding "matrix", even with optimal staining. Therefore, in a novel tissue preparation, such as an embryonic striatal graft, an AChE-positive patch in a paler surround is not necessarily an immature striosome. It could equally be a patch of either mature striosome or mature matrix tissue. Moreover, during the progressive expression of AChE activity in the striatum (of the rat and other species) there are dorsoventral and mediolateral gradients in expression, so that even in a single section not all sites of future striosomes (as identified with another marker) have enhanced AChE staining relative to future

matrix. Therefore, a zone of weak AChE staining might conceivably represent immature striosomal tissue rather than immature matrix tissue.

Despite these limitations, the combinations of markers we screened, and information about the TH immunostaining and catecholaminergic fluorescence in the grafts (Isacson et al., 1987; Pritzel et al., 1986; Graybiel et al., 1987a; Liu et al., 1990b), taken together with information about marker expression in perinatal striatum (Specht et al., 1981a, 1981b; Voorn et al., 1988; Shiosaka et al., 1982; Armstrong et al., 1987) suggest certain bounds for the maturational development of striatal tissue with marker profiles similar to tissue in the striatal transplants.

The P regions

Calbindin-like immunoreactivity is first expressed in medium-sized striatal neurons by E20 (Liu and Graybiel, 1991b). If the grafts were arrested at an early stage of development, then judging from the medium-sized perikaryal calbindin immunostaining, the developmental stage would probably be at least perinatal for the calbindin-positive part of the P regions. The calbindin antigen is expressed along a ventrocaudal to dorsomedial gradient during the perinatal period (Liu and Graybiel, 1991b), whereas strong AChE staining is expressed dorsolaterally. In fact, in the early postnatal period, calbindin-positive medium-sized cells appear only ventrocaudally, whereas AChE-positive patches appear mainly dorsally. Thus, an AChE-positive, calbindin-positive patch (typical P zone) should indicate a maturational stage advance enough for the two markers to overlap. For most of the caudoputamen (all but its caudal part) this would be a stage later than P3 and for some parts later than P7.

The appearance of mENK-immunoreactivity and SOM-immunoreactivity in medium-sized neurons in the P regions supports the suggestion based on calbindin immunostaining that the P zones are at least at a perinatal level of development. The expression of perikaryal mENK-like immunoreactivity in medium-sized striatal neurons follows a ventrocaudal to dorsomedial developmental gradient of expression and becomes detectable throughout the striatum only postnatally. According to Shiosaka et al. (1982), SOM-like immunoreactivity is first expressed in striatal neurons at E19, and typical SOM-immunoreactive neurons become more prominent postnatally (Shiosaka et al., 1982; Liu et al., unpublished observations).

By a P2-P3 stage of striatal development the grafts should have had intense mu opioid ligand binding in parts comparable to striosomes, and weak binding in parts comparable to matrix (Kent et al., 1982; Moon Edley and Herkenham, 1984). The weak binding in P zones would be compatible with these zones as being like either early postnatal or more mature matrix. If the paucity of [^{3}H]naloxone binding is interpreted as meaning that the P zones were immature, they could not be less mature in phenotypy than the stage indicated by the calbindin-like immunoreactivity of medium-sized neurons in these zones.

The NP regions

The present findings confirm Isacson et al.'s (1987) demonstration of low expression of a number of neurotransmitter-related markers in what here are called the NP regions of the grafts. We detected minimal mENK-like and calbindin-like

immunostaining of medium-sized neurons, low AChE-staining, and as just noted, little mu opioid receptor ligand binding. As we will describe in the second paper of this series, we also found little TH-like immunoreactivity in the NP zones, in agreement with the observations of Isacson et al. (1987; see also Pritzel et al., 1986 and Graybiel et al., 1987a); and we found relative few AChE-positive neurons in the NP zones though there were many in P regions (Liu et al., 1990b). As first emphasized by Isacson et al. (1987), such characteristics make it unlikely that the NP zones are striosomal, but instead suggest, especially because these zones lie around marker-rich patches (P zones) that the NP zones may have the phenotypy of immature matrix. If the NP regions are considered to be at the same developmental level as the P zones they adjoin, however, then certain of their characteristics are inconsistent with the model of these NP zones as immature matrix.

First, in normal striatal development, as soon as patches of heightened AChE staining and TH immunostaining become prominent, there is also considerable, though much weaker, AChE activity and TH-like immunoreactivity in the matrix around the patches (Butcher and Hodge, 1976; Graybiel, 1984a). This was not the case in the NP zones, most of which had low AChE staining and very little TH immunostaining. In fact, by the developmental stage indicated by the presence of calbindin-positive medium-sized cells in the P regions (perinatal or later), TH-like immunoreactivity in the rat's striatum is quite considerable in the matrix at all anteroposterior levels and AChE activity is appreciable in the dorsolateral matrix at most anteroposterior levels (Liu et al., unpublished observations).

Second, as noted above, perikaryal calbindin-like immunoreactivity in medium-sized neurons is expressed perinatally; and evidence from serial section comparisons of P3 calbindin-like and TH-like striatal immunostaining (Liu and Graybiel, 1991b) suggests that the calbindin antigen is already preferentially matrical (and not preferentially striosomal). The lack of calbindin-like immunostaining in medium-sized perikarya in the NP zones would thus mean (1) that the NP zones are at a phenotypic developmental stage earlier than that of first expression of calbindin antigen, (2) that they have the phenotypy of dorsal caudoputamen arrested at early perinatal ages before dorsal calbindin expression, or (3) that the NP zones represent exclusively dorsolateral caudoputamen of any age. The first alternative is not in accord with the age predicted by the calbindin-positive zones in the same grafts, and the second and third do not fit the low AChE activity, especially the near absence of TH-like immunoreactivity in the NP zones.

Third, in the normal developing striatum, AChE-positive neurons are not confined to the AChE-positive patches. They appear also in the matrix containing the AChE-positive patches (Graybiel et al., 1981; Nastuk and Graybiel, 1985). In the grafts, such neurons were mainly confined to P zones and were comparatively rare in NP zones (Graybiel et al., 1987a; Liu et al., 1990b).

Fourth, in the neonatal rat, mENK-like immunoreactivity in medium-sized neural perikarya tends to be stronger in matrical neurons than in striosomal neurons and tends to follow regional gradients similar to those of medium-sized perikaryal calbindin-like immunoreactivity. The lack of mENK-like immunostaining in medium-sized neurons in

NP regions adjoining P zones with such immunostaining is inconsistent with the NP zones as immature matrix if the P and NP zones are considered to be at the same developmental stage from the same part of the striatum.

In the perinatal (E20-P15) rat's striatum, there is a transient calbindin-positive population of large multipolar striatal neurons (Liu and Graybiel, 1991a). Clearly, these could contribute to the population of large multipolar calbindin-positive neurons in the NP regions of the grafts. Some of these multipolar striatal neurons are clustered, and appear to lie mainly in dorsolateral parts of the perinatal striatum where calbindin-like antigen is not yet expressed in medium-sized neurons. In fact, at perinatal period, there is minimal overlap between the fields with large and with medium-sized calbindin-positive neurons. The association of NP zones having large calbindin-positive neurons with P zones having medium-sized calbindin-stained cells would thus once again suggest a compartmental mixture of ventrocaudal and rostrodorsal striatal counterparts if NP as well as P zones are striatal; that is, the P zones would correspond to ventrocaudal caudoputamen and the NP zones would correspond to rostrodorsal striatum.

It is not known whether the larger calbindin-positive neurons in the neonates transiently express calbindin-like antigen or are a transient population. In a recent study of calbindin expression in the ganglionic eminence and the developing striatum, we have found that at E15, the age of the donor tissue dissected for the present study, there are many multipolar calbindin-immunoreactive neurons transiently piled up in the ventrolateral part of the lateral ganglionic eminence in which the striatal and cortical anlagen are fused (Liu and Graybiel, 1991a; see also Figs. 7-1C and 7-2F in chapter 7).

At subsequent ages, similar calbindin-positive neurons are found in the ventrolateral cortical anlage. Although our dissection of striatal primordia for donor tissue is aimed at dissecting primarily the dorsal part of the lateral ganglionic eminence, it is possible and even likely that the dissection extends ventrally enough to include this population of multipolar calbindin-positive neurons. Despite the unknown nature of these multipolar calbindin-positive neurons, our observations raise the possibility that they could be nonstriatal cells either migrating radially through the striatal primordium or migrating tangentially from the lateral cortical primordium during early development (Bayer, 1990; Austin and Cepko, 1990). In fact, by using Rat.401 antibody to nestin (a new class of intermediate filament protein, see Lendahl et al., 1990) as a marker for radial glial cells (Hockfield and McKay, 1985; Frederiksen and McKay, 1988), we have found that at rostral levels of E16 rat forebrain, nestin-positive radial glial fibers stretch from the ventricular zone through the subventricular zone to the striatal anlage, and some fibers seem to extend further into the lateral and ventral cortical anlage. At caudal levels, nestin-positive radial glial fibers extend through the striatal anlage toward the basal forebrain regions (Liu et al., unpublished observations). This is, in part, in accord with the recent report by Edwards et al. (1990) who have studied the distribution of the radial glial in the developing mouse forebrain with antibody RG2. Because radial glial cells are thought to guide the migrating neurons during development (Rakic, 1971, 1972, 1988), it is possible that during early development some nonstriatal cells may migrate along the radial glial fibers in the striatal anlage en route to destinations such as the cortex and nuclei in the basal forebrain. Interestingly, some large multipolar calbindin-positive

neurons appear in the white matter of the ventral corona radiata in the perinatal period, and there are many large multipolar calbindin-positive cells in the ventrolateral cortex.

In summary, most of the evidence obtained suggests that combinations of region-specific attributes of immature striatum are not faithfully replicated in the grafts when P and NP zones are considered together as having the same maturational status. The evidence favors P zones as containing considerable amounts of matrix-like tissue. The findings are not conclusive with respect to the maturity of the NP zones, but are compatible with these zones as containing nonstriatal tissue or immature striatal tissue with some intermixed nonstriatal neurons. Given that TH-containing afferents do innervate the grafts, the near lack of TH-like immunoreactivity in the NP zones suggests that they would, if striatal, resemble very immature striatum.

It is important to stress that nearly all of our comparisons with immature striatum are so far limited to postnatal stages and that positive identifiers of the level of maturity for most striatal cell types are not yet available. It also is not clear that the degree of development of adjoining P and NP zones in the grafts is equivalent. In fact, based on the reduced density of spines on Golgi-impregnated medium-sized neurons in the grafts, McAllister et al. (1985) concluded that the grafted neurons are relatively immature. By contrast, DiFiglia et al. (1988) reported that the neuronal organization of such grafts appears mature by 5-6 weeks after transplantation. Finally, it is not certain that cells of the P and NP zones would in all aspects mimic, in the graft environment, normal patterns of expression of the markers screened. The issue of the maturational status of the grafts may be further complicated by cross-tissue inductive effects. For example, if

the NP regions contained cortical, pallidal or basolateral amygdaloid cells, these nonstriatal cells may have stimulated the maturation of striatal cells in the P regions. The cortex, pallidum and basolateral amygdala all project to the striatum, and the pallidum is a major target of striatal efferents. Experiments with organotypic tissue cultures of striatum suggest that striatal neurons need to be co-cultured with cortical explants in order to develop spines and mature axospinous synaptic inputs (Whetsell et al., 1979). Nonstriatal cells of the transplants, ingrowing TH-containing or other afferents, or efferent connections made by the grafts could exert comparable inductive influences (Pritzel et al., 1986; Lanca et al., 1986; Graybiel et al., 1987a; Isacson et al., 1987; Wictorin et al., 1987, 1988; Rutherford et al., 1987; Clarke et al., 1988; Xu et al., 1988). Afferent regulation of neurotransmitter and receptor expression is well known for the striatum (see, eg., Young et al., 1986; Eghbali et al., 1987).

Factors underlying modularity in the grafts

A major implication of these and previous experiments on embryonic striatal grafts is that the modular design of these grafts may reflect a sorting out of cells of different types in what here are called the P and NP regions of the grafts. This would be so even if the P zones mainly represented host striatum and the NP zones contained most of the donor cells (see above). The protocol for preparation of the grafts yields suspensions of predominantly single cells with a few cell clumps (Liu et al., unpublished observation). Thus, cells of similar types appear to have reaggregated, presumably by virtue of cell-specific adhesion molecules expressed on their surfaces. The aggregation

could have occurred during the interval between preparation of the suspensions and their injections (a matter of minutes) or *in situ* in the grafts. Aggregation of neurons and substantial neuronal migration between aggregates has been observed in striatal cell cultures (Surmeier et al., 1987). The compartmentalization of the grafts also may have been influenced by subsequent ingrowth of afferent fibers attracting particular subsets of the transplanted cells to themselves, or repelling others. However, modularity of embryonic striatal grafts has been observed also in intraocular striatal graft preparations where no graft-host connections form (Johnston et al., 1987).

Different interpretations of the modularity of embryonic striatal grafts bear directly on what factors may be responsible for the architecture. If the grafts are composed of striatal tissue arrested at an immature stage of development, this would mean that the grafts can reconstitute the macroscopic morphological characteristics of normal neostriatal compartmentalization, but that cues for maturation of the compartments are missing or inadequate. This would be a situation analogous to the effects of certain mutations in invertebrates (Horvitz et al., 1983).

Our own experiments do not favor reconstitution of normal striosome-matrix modularity by P-NP compartmentalization, even at an arrested stage of development, because the P zones seem more like matrix than like striosomes. The findings are, however, consistent with other types of compartmentalization of striatal tissues arrested at immature stages. For example, the patchiness of the grafts could reflect a segregation of tissue resembling immature dorsal striatal districts in NP zones and tissue resembling immature ventral striatal districts of the same developmental stage in P zones.

Alternatively, the P and NP zones might both represent immature striatum but be at different developmental stages. If this were true, it could be argued, for example, that TH-positive fibers innervate P but not NP zones because the P zones are mature enough to trigger or to receive the ingrowth, but that the NP zones are not.

Another possibility is that the modularity of the grafts might reflect a compartmentalization of striatal and nonstriatal types of tissue. According to this hypothesis, many biochemical and morphological characteristics of the normal adult rat's striatum may be duplicated in the P regions of the graft tissue, even some matrix-striosome-like modularity, but the NP regions may primarily comprise nonstriatal tissue. This possibility would suggest that the formation of compartments resulted from a separation of cells of fundamentally different tissue types. If makes no specific prediction about the level of maturation of the different compartments other than to suggest that they need not be similar. Indeed, if the P and NP tissues are fundamentally different, they might be responsive to different maturational cues or respond differently to signals for which they share receptivity.

Functional implications

The behavioral tests on which striatal grafts have been found to induce recovery from deficits induced by striatal lesions include spontaneous locomotor activity, amphetamine- and apomorphine-induced rotation, skilled paw-reaching and delayed alternation learning in T-mazes (Deckel et al., 1986; Isacson et al., 1986; Sanberg et al., 1986; Dunnett et al., 1988). For some of these tests, it may simply be necessary for the

grafted cells to exert a diffuse regulatory influence over host targets, such as the globus pallidus, without the requirement that the grafted neurons receive normal afferent innervation from the host. However, for the grafts to influence behavior in other test situations, such regulatory control from afferent systems of the host is probably essential. It would therefore be a necessary condition for graft-induced behavioral recovery from striatal lesions that particular populations of afferent fibers establish connections with the appropriate subpopulations of neurons within the grafts, and that these "striatal replacement neurons" in turn establish appropriate efferent connections within the host brain.

Afferent connections from host midbrain and forebrain do innervate striatal grafts (see above). There apparently is a reinstatement of normal nigrostriatal connectivity within the P regions of the grafts (Pritzel et al., 1986; Isacson et al., 1987; Graybiel et al., 1987a; Clarke et al., 1988). Moreover, at least some of these innervated graft neurons can be retrogradely labelled by injection of HRP into the globus pallidus (Clarke and Dunnett, unpublished observations) and can induce increases in release of gamma aminobutyric acid (GABA) in the globus pallidus of the host (Sirinathsinghji et al., 1988). Accordingly, certain trans-striatal circuits do appear to run specifically through the P regions of the grafts. Although the P regions take up a small proportion of total graft volume, the grafts are themselves extremely large so that this proportion may be sufficient to meet some functional demands.

If there were considerable nonstriatal tissue in the NP regions, this might account for the lack of appreciable innervation of NP zones by TH-containing afferents (Pritzel

et al., 1986; Isacson et al., 1987; Graybiel et al., 1987a). For these (or other) ingrowing fibers normally innervating striatal tissue, terminal ramifications might be inhibited while the fibers are in an NP zone, but be promoted in P zones. This reconstitution of normal connectivity could be crucial for behavioral recovery. On the other hand, a considerable amount of nonstriatal tissue (or developmentally arrested striatal tissue) in the graft could be functionally deleterious, not just by occupying space that striatal neurons otherwise could grow in, but also by providing a framework for an aberrant pattern of connections that might compete with the appropriate reconstitution of striatal circuitry. Behavioral studies have yielded little evidence for severe abnormal functioning of the grafts, but the functional recovery so far detected has been only partial even for simple tests.

From the practical point of view, the most important aspect of our findings is that they stress the need, in future work with graft tissue, to obtain selective sets of donor neurons with methods that do not compromise the viability or developmental potential of the cells. Only then may it be possible to obtain a full repertoire of behavioral recovery.

Chapter 3

Reconstitution of Cholinergic and Dopaminergic Systems in embryonic striatal grafts

ABSTRACT

Reconstitution of striatal cholinergic and dopaminergic systems was studied in intrastriatal grafts derived from embryonic day 15 rat striatal primordia and implanted into adult host rats in which unilateral ibotenic acid lesions had previously been made in the striatum. Histochemical, immunohistochemical and ligand binding autoradiographic techniques were applied to analyze different constituents of these two systems and to study their locations relative to each other in grafts allowed to grow for 9-17 months following transplantation.

For the cholinergic system, a modular organization was found in the striatal grafts with stains for choline acetyltransferase and acetylcholinesterase, respectively the synthetic and degradative enzymes for cholinergic neurons; by autoradiographic [^{3}H]hemicholinium binding, specific for high affinity choline uptake sites associated with cholinergic terminals; and by autoradiographic [^{3}H]pirenzepine binding, selective for M1 receptors. For the dopaminergic system, a comparable modular organization was found in the grafts by immunostaining for tyrosine hydroxylase, the catecholamine synthetic

This chapter is modified from the paper, "Liu, F.-C., A.M. Graybiel, S.B. Dunnett, and R.W. Baughman (1990) Intrastriatal grafts derived from fetal striatal primordia: II. Reconstitution of cholinergic and dopaminergic systems. J. Comp. Neurol. 295:1-14", with permission from the authors.

enzyme; by autoradiographic [^{3}H]mazindol binding for dopamine uptake sites; and by [^{3}H]SCH23390 binding for dopamine D1 receptors and [^{3}H]sulpiride binding for dopamine D2 receptors. The results indicate that the distributions of the cholinergic and dopaminergic markers in striatal grafts are in close anatomical register.

These markers for intracellular and membrane-associated components of the cholinergic and dopaminergic systems were preferentially localized in the acetylcholinesterase-rich patches of the grafts in which cortical and thalamic fibers have also been found in striatal grafts, and in which output neurons projecting to the pallidum are located. This anatomical correlation suggests that the substrates for cholinergic-dopaminergic interactions typical of the normal striatum may be reinstated in the grafts both in relation to efferent neurons establishing connections with the host brain that are typical of normal striatofugal connections, and in relation to major afferent fiber systems from the host brain originating in regions known to project densely to the normal striatum. Accordingly, the cholinergic and dopaminergic systems in such grafts may regulate the functional influence of the grafts on the behavior of host animals.

INTRODUCTION

Intrastriatal grafts derived from rodent embryonic striatal primordia have become a major focus for study of reconstruction of striatal tissue damaged by treatment with excitotoxins (Björklund et al., 1987). These experiments explore the limits of repair in an animal model for Huntington's disease, and also open new approaches to analyze cell-cell interactions in neuronal tissue. It is now well known that many neuronal types characteristic of the normal rat's striatum are present in striatal grafts. These include neurons expressing acetylcholinesterase (AChE), gamma-aminobutyric acid (GABA), enkephalin, substance P, cholecystokinin, neuropeptide Y, somatostatin, NADPH-diaphorase, calbindin-D_{28k}, and dopamine- and adenosine 3':5'-monophosphate-regulated phosphoprotein (DARPP-32) (Sanberg et al., 1986; Sanberg et al., 1987; Walker et al., 1987; Isacson et al., 1987; Graybiel et al., 1987a; Roberts and DiFiglia, 1988; Liu et al., 1988; Wictorin et al., 1989c; Graybiel et al., 1989).

In the normal striatum, cholinergic neurons are thought to exert important regulatory control over the neural processing (Lehmann and Langer, 1983). With the aid of choline acetyltransferase (ChAT) immunocytochemistry, the cholinergic neurons have been demonstrated to be the large aspiny interneurons in the striatum (Eckenstein and Sofroniew, 1983; Bolam et al., 1984; Phelps et al., 1985). Anatomically, these large ChAT-immunoreactive neurons are rare (Phelps et al., 1985), but they have long sparsely branching aspiny dendrites that can be traced for long distances (about 1 mm). Thus they could serve to integrate information within extensive regions of the striatum. As the cholinergic neurons synapse on the medium spiny projection neurons of the striatum

(Izzo and Bolam, 1988), the information integrated by the cholinergic interneurons could in turn influence the outputs of the striatum.

The existence of functionally important interactions between cholinergic interneurons and dopamine-containing afferents in the striatum was suggested over two decades ago (McGeer et al., 1961; Barbeau, 1962). Clinical and pharmacological studies pointed to a "balance" between striatal dopaminergic and cholinergic systems (for review, see Lehmann and Langer, 1983). One type of clinical evidence is that a variety of anticholinergic drugs ameliorate some of the symptoms associated with the deficiency of striatal dopamine in parkinsonian disorders (McGeer et al., 1961; Barbeau, 1962; Duvoisin, 1967). Similarly, it was suggested that interactions between dopamine-containing afferents and cholinergic neurons of the striatum are important for normal motor function (Duvoisin, 1967; Aquilonius and Sjöström, 1971). It has since been shown that the release of acetylcholine in the striatum can be inhibited by stimulation of dopaminergic receptors both *in vitro* and *in vivo*, and that acetylcholine can facilitate the release of striatal dopamine *in vitro* and *in vivo* (for review, see Chesselet, 1984). This dopaminergic-cholinergic balance is now seen as part of a more complicated interplay of neurotransmitter systems in the striatum. For example, the release of acetylcholine from cholinergic neurons in the striatum has been shown to be modulated by different neurotransmitters including dopamine, serotonin, glutamate and GABA (Lehmann and Langer, 1983; Jackson et al., 1988; Lehmann and Scatton, 1982; Stoof et al., 1979).

Ultrastructural evidence indicates that some dopaminergic (TH-containing) terminals, presumably arising from the substantia nigra, form synapses on cholinergic

neurons in the striatum (Kubota et al., 1987b; Chang, 1987), although such contacts appear to be rare (Freund et al., 1984). Besides such direct connections, both dopaminergic and cholinergic terminals form synapses on striatal efferent neurons (Kubota et al., 1986a, 1986b, 1987a; Izzo and Bolam, 1988; Pickel and Chan, 1990) and apparently have similar spatial patterns of contact on these neurons (Izzo and Bolam, 1988). Therefore, both appear to be in a position to regulate the output of the striatum and may have some similarities in effect. Given all of this evidence, the reconstitution of cholinergic and dopaminergic systems should be a prerequisite for functional recovery in animals bearing striatal lesions and intrastriatal grafts.

We and others have previously reported that striatal grafts derived from embryonic striatal primordia exhibit a modular organization as shown by sections stained for AChE, a marker for cholinergic neuropil in normal striatum at maturity (Sanberg et al., 1986; Walker et al., 1987; Isacson et al., 1987; Graybiel et al., 1987a, 1989; Liu et al., 1988). The grafts are characterized by patches of high AChE activity embedded in an AChE-poor surround. The relative proportions of the AChE-rich patches (P regions) and surrounding AChE-poor non-patch (NP) regions vary from graft to graft, but nearly always the NP zones appear as the surround, the P zones as modules within the NP regions. The P regions of such striatal grafts have many characteristics of the normal postnatal and adult rat's striatum. The surrounding NP regions of the grafts, however, not only contain low AChE activity but also lack most other striatal markers and they contain features not found in normal striatal tissue, at least at adulthood. The NP regions thus appear to represent predominantly nonstriatal tissue, though they may also

contain intermixed nonstriatal and immature striatal tissue (Liu et al., 1988; Graybiel et al., 1989).

In the present study, we have asked whether the normal constituents of the cholinergic and dopaminergic systems of the striatum can be reconstructed in such striatal grafts, and whether they were found both in P and NP regions or predominantly in the P regions thought to represent striatum. We examined the anatomical distributions in the striatal grafts of cellular components of the cholinergic system with markers for the synthetic cholinergic enzyme ChAT, high affinity choline uptake sites associated with cholinergic terminals (Vickroy et al., 1985; Rhodes et al., 1987; Beckenstein and Wooten, 1989) and muscarinic M1 receptor sites (Nastuk and Graybiel, 1988). In parallel we studied cellular components of the dopaminergic system with anatomical markers for the synthetic enzyme tyrosine hydroxylase (TH), high affinity dopamine uptake sites (Javitch et al., 1985; O'Dell and Marshall, 1988), and dopamine D1 and D2 receptor sites (Gehlert and Wamsley, 1985; Boyson et al., 1986; Richfield et al., 1987; Beckstead et al., 1988; Besson et al., 1988). For each graft we analyzed the distributions of these markers both in relation to the distribution of AChE staining for identification of P and NP zones, and in relation to each other. The results indicate that all of these cholinergic and dopaminergic components are preferentially localized in the P regions of the grafts, suggesting that these are the principal sites in which the cholinergic-dopaminergic balance characteristic of striatal tissue may be reestablished. Some of these results have been reported in abstract form (Graybiel et al., 1987a; Liu et al., 1988).

METHODS

Transplantation

Twenty six 200-300 g Sprague-Dawley rats (Charles River Laboratories, Inc.) were used in the present experiments. Some of these animals served as subjects for our first study in which a detailed description of the lesion and transplantation procedure is given (Graybiel et al., 1989).

In an initial surgery, ibotenic acid was injected under stereotaxic guidance into six sites in the central part of the right caudoputamen of rats deeply anaesthetized with Chloropent or Nembutal. At each site, 0.2 µl of 10 µg/µl ibotenic acid (Sigma) dissolved in 0.1 M phosphate buffer (pH 7.4) was injected over a 2-3 min period. Seven to eight days later, transplantation was carried out in all but one animal which served as a control for evaluation of the appearance of the striatum exposed to ibotenic acid but not subjected to grafting. Embryonic striatal cell suspensions serving as donor tissue were prepared from striatal primordia dissected from fetuses at embryonic day (E) 15 (crown-rump length 12-15 mm). Tissue was briefly stored in a 0.6% glucose-saline solution (room temperature), incubated for 20 min at 37°C in glucose-saline medium containing 0.1% trypsin (Sigma, crude type II), washed (x 4, 0.6% glucose-saline), and triturated with a fire-polished Pasteur pipette. This dissociation procedure yielded about 3 dissected striatal primordia per 10 µl of the final cell suspension. With a stereotaxically guided 10 µl syringe, 3 µl of the cell suspension were injected over a 3-5 min period (or, for 1 rat, 30 min period) into the caudoputamen of deeply anesthetized rats, either bilaterally at matched stereotaxic coordinate sites (16 rats) or unilaterally on the right

side (9 rats). The coordinate sites were chosen to correspond to the center of the region previously injected with ibotenic acid on the right side. The injection needle was left in place for 5 min following deposition of the aliquot.

Tissue preparation

All but 2 rats were perfused transcardially under deep Nembutal anaesthesia after 9-17 month survival times. Perfusion solutions were (a) 4% paraformaldehyde in 0.1 M phosphate buffer containing 5% sucrose and 0.9% saline (500 ml, pH 7.4), or (b), for ChAT immunohistochemistry, 4% paraformaldehyde and 15% saturated picric acid in 0.1 M sodium phosphate buffer (300 ml, pH 7.2). Following 2-4 hr postfixation in the same fixative at 4°C, brains were washed in 0.1 M phosphate buffer containing 20% sucrose and 0.9 % saline. For ligand binding (see below), 2 brains were removed from terminally anaesthetized animals and rapidly frozen in powdered dry ice. All brains were cut in the coronal plane. Perfused brains were cut at 30 μm on a freezing microtome; unperfused brains were cut at 15 μm on a cryostat. Alternating sets of consecutive sections were processed for histochemistry, immunohistochemistry or ligand binding.

Histochemistry and Immunohistochemistry

Acetylcholinesterase staining was carried out with acetylthiocholine iodide as substrate and ethopropazine as pseudocholinesterase inhibitor by a slightly modified Geneser-Jensen and Blackstad (1971) method (Graybiel and Ragsdale, 1978). The incubation times were 90-120 min except for some control experiments in which prolonged (12-24 hr) incubations were allowed.

For ChAT immunostaining, sections were pretreated with three 1 hr rinses in 0.1

M Tris buffer containing 150 mM NaCl (TBS, pH 7.4) to which 10% rabbit serum, 2% bovine serum albumin and 0.5% Triton X-100 were added (incubation buffer). The sections were incubated at room temperature overnight in primary incubation solution containing 1:1,000 mouse polyclonal antiserum against rat ChAT (prepared by Dr. R.W. Baughman) or rat monoclonal antibodies against porcine ChAT (kindly donated by Dr. F. Eckenstein or purchased from Boehringer Mannheim, West Germany) in incubation buffer. Sections were then taken through the following steps with four 5 min intervening rinses in TBS: (1) goat anti-mouse IgG (ICN ImmunoBiologicals) or goat anti-rat IgG (Sternberger-Meyer) 1:50 in incubation buffer with 0.2% Triton X-100, 1 hr; (2) mouse or rat peroxidase-antiperoxidase (Sternberger-Meyer) 1:50 in incubation buffer with 0.2% Triton X-100, 1 hr; (3) repetitions of steps (1) and (2); (4) 0.01% H_2O_2 and 0.5 mg/ml diaminobenzidine in 0.1 M phosphate buffer.

For TH immunostaining, sections were pretreated in steps with 10% methanol-3% H_2O_2, 0.1% Triton X-100, and 1:30 normal goat serum and then were incubated in primary antiserum (Eugene Tech., 1:240) and processed by the peroxidase-antiperoxidase method of Sternberger (1979) as described elsewhere (Graybiel, 1984a).

Ligand binding autoradiography

For dopamine D1 receptor site binding, sections were incubated in 50 mM Tris-HCl buffer (pH 7.4) containing 2.5 nM [^{3}H]SCH23390 (77 Ci/mmol, Amersham) and 10 μM sulpiride at room temperature for 1 hr, then rinsed twice for 5 min in ice-cold buffer, quickly dipped in ice-cold distilled water, and dried under a stream of cool air (Besson et al., 1988). Nonspecific binding was determined by adding 1 μM unlabelled SCH23390

to the incubation buffer.

For dopamine D2 receptor site binding, sections were incubated in 50 mM Tris-HCl buffer (pH 7.4) containing 20 nM [^{3}H]sulpiride (60 Ci/mmol, New England Nuclear) and 0.01% ascorbic acid at room temperature for 45 min, then rinsed twice for 2.5 min in ice-cold buffer and dipped once into ice-cold distilled water (Gehlert and Wamsley, 1985). To determine nonspecific binding, 1 μM unlabelled haloperidol was added into the incubation buffer.

Ligand binding for high affinity dopamine uptake sites was carried out by preincubating sections in 50 mM Tris buffer containing 120 mM NaCl and 5 mM KCl (pH 7.9) at 4°C for 5 min, then incubating them in Tris buffer containing 300 mM NaCl, 5 mM KCl, 15 nM [^{3}H]mazindol (15 Ci/mmol, New England Nuclear) and 0.3 μM desipramine, washing twice for 3 min in Tris buffer containing 300 mM NaCl and 5 mM KCl at 4°C, and then rinsing in distilled water at 4°C for 10 sec (O'Dell and Marshall, 1988; Javitch et al., 1985). Nonspecific binding was determined by adding 1 μM unlabelled mazindol or 30 μM benztropine to the incubation buffer.

For muscarinic M1 receptor ligand binding, sections were preincubated in 50 mM sodium phosphate ($NaHPO_4$) buffer (pH 7.4) containing 10 mM ethylenediaminetetraacetic acid (EDTA) and 0.1 mM N-ethylmaleimide at 4°C for 30 min, then incubated in buffer containing 1 mM EDTA and 10 nM [^{3}H]pirenzepine ([^{3}H]PZ) (85 Ci/mmol, New England Nuclear) at room temperature for 1 hr, rinsed 5 min in buffer at 4°C and twice for 1 min in distilled water at 4°C (Nastuk and Graybiel, 1988). Nonspecific binding was determined by adding 1 μM atropine to the incubation

buffer.

For high affinity choline uptake site binding, sections were incubated in 50 mM glycylglycine buffer (pH 7.8) containing 200 mM NaCl and 10 nM [^{3}H]hemicholinium ([^{3}H]HC-3) (145.8 Ci/mmol, New England Nuclear) at room temperature for 30 min, then rinsed twice for 2 min in ice-cold buffer and 10 sec in ice-cold distilled water (Rhodes et al., 1987). For nonspecific binding controls, 10 μM unlabelled HC-3 was added to the incubation buffer.

Exposure times for film autoradiography (Amersham Hyperfilm) were 1-2 weeks for [^{3}H]SCH23390 binding; 11.5-14 weeks for [^{3}H]sulpiride binding; 3-6 weeks for [^{3}H]mazindol binding; 1-2 weeks for [^{3}H]PZ binding; and 3-6 weeks for [^{3}H]HC-3 binding. Films were developed in Kodak D-19 at 20°C and then fixed in Kodak Rapid Fixer. To permit comparisons of autoradiographic binding patterns and AChE staining, many sections processed for binding were subsequently stained for AChE activity.

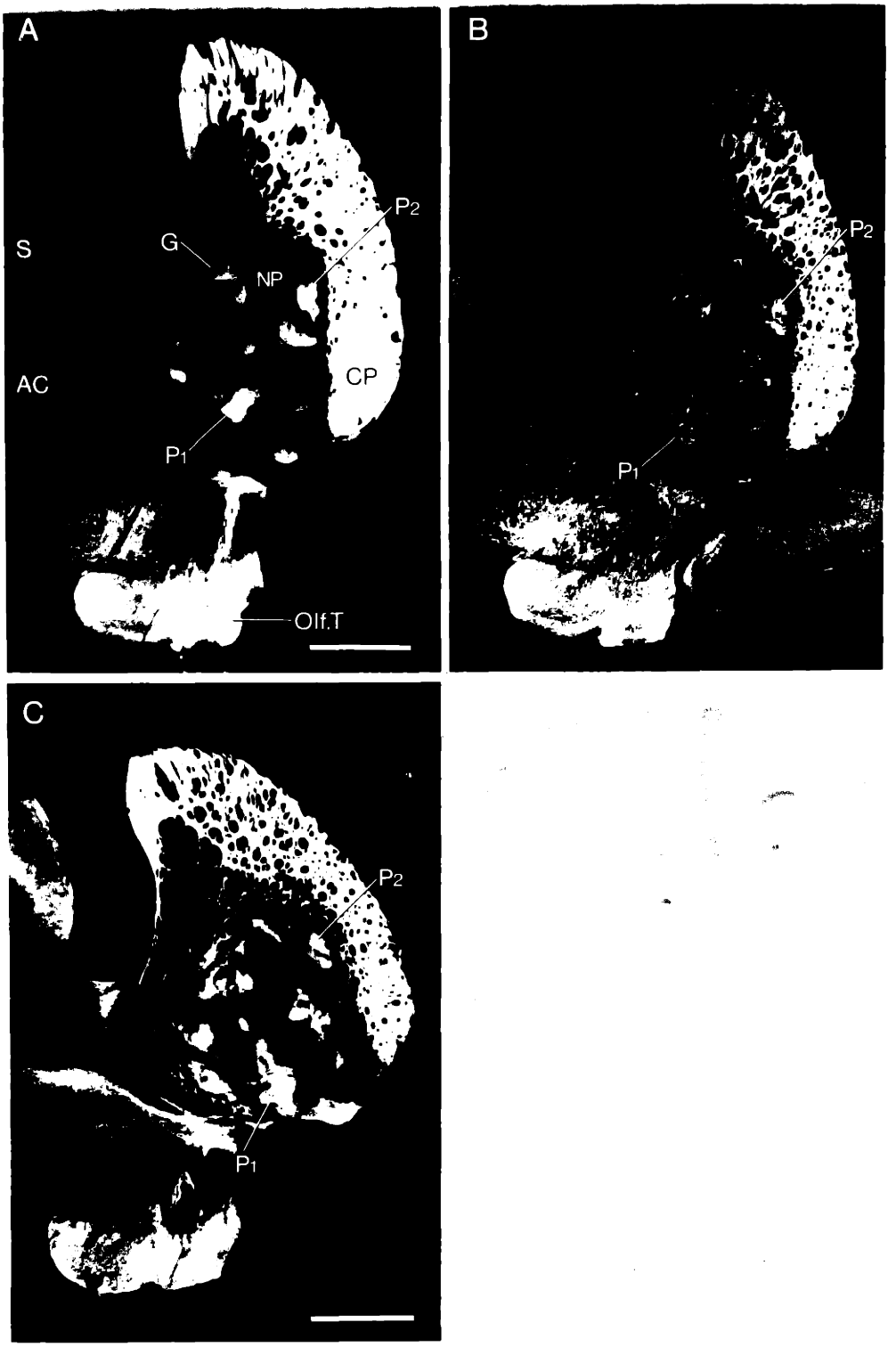
A
S
G
NP
P2
AC
CP
P1
Olf.T
B
P2
P1
C
P2
P1

Figure 3-1: Reverse contrast photomicrographs of serial sections showing the distribution of AChE staining (A), ChAT immunostaining (B) and TH immunostaining (C) in the embryonic striatal graft (G) of case RSG7. The graft is separated from the host's striatum by compacted fiber bundles. Internally, the graft tissue displays a modular chemoarchitecture in which patches of high AChE activity, ChAT-like immunoreactivity and TH-like immunoreactivity (P regions) are embedded in surrounds expressing low AChE, ChAT and TH staining (NP regions). The P regions identified by these three different staining methods were closely aligned with one another, as indicated by two examples, marked P1 and P2 in the three panels. The staining patterns in C appear rotated relative to those in A and B because there is a tear in the tissue below the graft. CP, caudoputamen of the host; S, septum; AC, anterior commissure; Olf.T, olfactory tubercle. Photographs in B and C were taken at the magnification; photograph in A was made at a slightly higher magnification to compensate for tissue shrinkage. Scale bars = 1 mm.

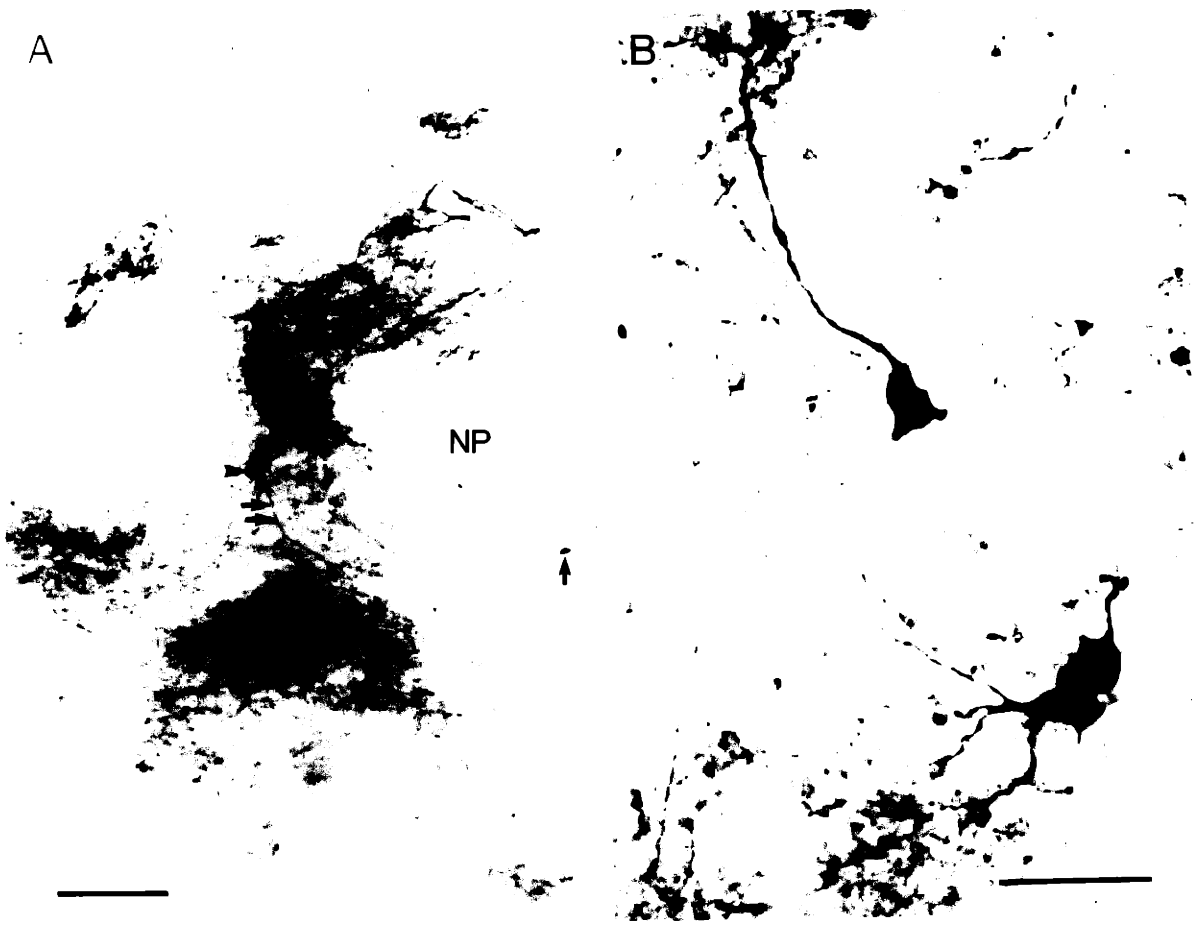
A
B
NP

Figure 3-2: Light-field photomicrographs of ChAT immunostaining in a section from an embryonic striatal graft (case RSG7). A shows three large ChAT-positive neurons associated with two P regions enriched in ChAT-immunoreactive neuropil. A ChAT-positive neuron at the edge of the upper P region (arrowhead) extends a single process (double arrows) up to the P region below it. Note that a small ChAT-positive neuron is present in the NP tissue (arrow). Scale bar = 100 μm. The photomicrograph in B shows at higher magnification a P region enriched in ChAT-immunoreactive neuropil and containing three large ChAT-immunoreactive neurons with infrequently branching aspiny dendrites. Scale bar = 50 μm.

RESULTS

Distribution of AChE activity

Regions of high AChE activity in the striatal grafts were confined to patches (P regions) that were surrounded by fields of low AChE activity (NP regions, see Fig. 3-1A). The differential staining of neuropil in the P and NP regions remained vivid even in sections incubated for prolonged periods, though the intensity of the staining in both P and NP regions was increased. In some of the grafts, it was possible to see AChE-positive neurons. The diameters of their perikarya (ca. 18-30 μm) were comparable to those of the large AChE-positive neurons in the normal rat's striatum. Nearly all of these large AChE-positive neurons were present in the AChE-rich P regions of the grafts, even in sections with the most prolonged incubation times. A few smaller, weakly stained AChE-positive cells did appear in the NP regions in the heavily stained material. These observations are fully compatible with previous descriptions of heterogeneous AChE-staining in striatal grafts (Sanberg et al., 1986; Sanberg et al., 1987; Walker et al., 1987; Isacson et al., 1987; Graybiel et al., 1987a; Liu et al., 1988; Graybiel et al., 1989).

Immunostaining for ChAT-like immunoreactivity

Consistent with previous biochemical evidence that ChAT activity is partially restored in the striatum of animals bearing striatal grafts (Isacson et al., 1985), ChAT immunostaining was detected in the striatal grafts. ChAT-immunoreactive cell bodies with well stained dendrites were found with both the mouse anti-rat ChAT and the rat anti porcine ChAT antisera. However, dense ChAT-immunoreactive neuropil was

detected in the grafts (and in the host's striatum) only with the mouse anti-rat ChAT antiserum. The ChAT-immunoreactive neuropil in the grafts was located in patches surrounded by regions with low or negligible immunostaining (Fig. 3-1B).

Within the patches of enriched ChAT-immunoreactive neuropil, large (ca. 18-30 μm diameter) ChAT-immunoreactive neurons with infrequently branching aspiny dendrites were often found. Their dendrites could be traced for long distances (up to ca. 140 μm) within the patches (Fig. 3-2). Occasionally, a single process could be traced from one patch to a neighboring patch or out into the ChAT-poor surround (Fig. 3-2A). These large ChAT-positive neurons had oval, triangular or multifaceted perikarya (Fig. 3-2B); their phenotypy and diameters (ca. 18-34 μm) were very similar to the ChAT-positive neurons in the host's striatum. The large ChAT-immunoreactive neurons in the grafts were almost entirely confined to the ChAT-positive patches, but occasionally occurred at the borders between the ChAT-positive patches and their ChAT-poor surrounds (Fig. 3-2A). A small number of medium-sized (ca. 12 μm diameter) lightly stained ChAT-immunoreactive neurons without well stained dendrites also appeared in the ChAT-positive patches.

In contrast to the near absence of large ChAT-positive neurons in ChAT-poor regions, a few small to medium-sized (ca. 7-14 μm diameter) ChAT-immunoreactive neurons were consistently found in these zones (Fig. 3-2A). They tended to be lightly stained and to have a bipolar shape because of their axially directed dendritic arbors. ChAT-immunoreactive neurons with similar phenotypy have been identified previously as bipolar interneurons in the rat neocortex (Eckenstein and Thoenen, 1983; Houser et


A
P
NP
B

Figure 3-3: Photomicrographs illustrating TH-immunoreactive neuropil (A) and neurons (B) in two embryonic striatal grafts (cases RSG2-25 and RSG2-28, respectively). A shows a P region (P) enriched in TH-immunoreactive neuropil, and an adjoining NP region (NP) with very low TH-like immunoreactivity. Note that the TH-immunoreactive neuropil of the P region ends abruptly to form a sharp border between the P and NP regions. Scale bar = 100 μm. B shows a TH-positive neuron with a small number of aspiny dendrites. One of the dendrites (arrowheads) can be traced vertically (=dorsally) for over 220 μm. Scale bar = 25 μm.

al., 1983; Eckenstein and Baughman, 1984), and they were found in the present experiments in the neocortex of the host animals, where they had ca. 8-14 μm diameters. No such neurons were observed in the host striatum. ChAT-positive patches and large and small-to-medium-sized ChAT-immunoreactive neurons appeared not only in the intrastriatal parts of the grafts, but also in the parts of the graft tissue that in some brains extended dorsally into the host neocortex.

Distribution of ChAT-positive patches in relation to AChE-positive P regions

When sections processed for ChAT immunostaining were compared to adjoining sections stained for AChE activity, the ChAT-positive patches were found to be aligned with and nearly coincident with the patches of high AChE activity in the grafts (see Figs. 3-1A, B). Thus, the AChE-rich P regions were the regions containing most of the ChAT-immunoreactive neuropil as well as the large and medium-sized ChAT-immunoreactive neurons of the grafts.

Immunostaining for TH-like immunoreactivity

In accord with previous catecholamine fluorescence and TH immunohistochemical studies (Pritzel et al., 1986; Isacson et al., 1987; Graybiel et al., 1987a; Clarke et al., 1988), neuropil enriched in TH-immunoreactivity was confined to patches embedded in surrounds containing little or no TH-like immunoreactivity (Fig. 3-1C). The distribution of TH-immunoreactive neuropil was not homogeneous throughout the grafts, in that some of the patches were larger than others. For some of the TH-positive patches that

lay close to the host's striatum, TH-immunoreactive fibers could be traced back to the internal capsule or to the host's caudoputamen. Furthermore, though most of the TH-positive neuropil was confined in patches (Fig. 3-3A), some coarse and fine TH-immunoreactive fibers ran through regions of low immunoreactivity from one TH-positive region to another. In some grafts, TH-positive patches formed a network by interconnecting with bridges of TH-immunoreactive neuropil. Patches of TH-like immunoreactivity were also observed in the parts of striatal grafts that in some brains lay within the cortex overlying the host's striatum. The density of TH-immunoreactive neuropil in these patches in the intracortical parts of the grafts was not as high as that in their counterparts in the parts of striatal grafts lying within the host striatum.

Scattered small to medium-sized TH-immunoreactive neurons (ca. 7-16 μm diameter) were regularly found within the grafts (Fig. 3-3B). The distribution of these TH-immunoreactive cells did not respect the boundaries of the patches of TH-immunoreactive neuropil; they appeared both in TH-positive patches and in their TH-poor surrounds. These TH-immunoreactive neurons did not have a uniform morphology. Some were bipolar, others were multipolar with well stained aspiny dendrites that could be traced for long distances (over 200 μm, see Fig. 3-3B), and yet others had stained perikarya but no visibly stained dendrites. No TH-immunoreactive neurons were found in either the striatum or the neocortex of the hosts. The patches of TH-positive neuropil could not have been entirely derived from these TH-immunoreactive neurons, because they represented a very small neuronal population in the grafts and were not particularly associated with the TH-rich patches.

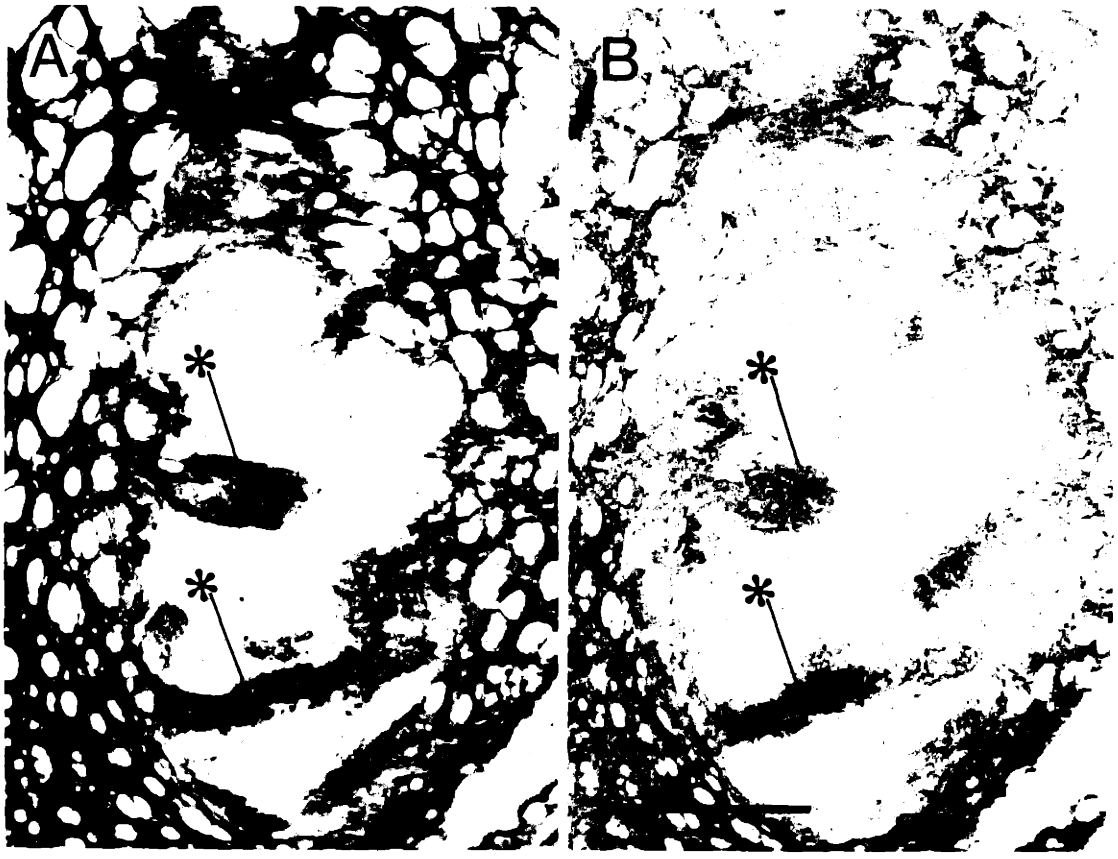
A
B

Figure 3-4: Light-field photomicrographs of adjoining sections showing the close alignment of patches of strong AChE staining (A) and TH immunostaining (B) found in an E15 striatal transplant that was placed into the intact left striatum of case RSG2-25. The asterisks indicate two such pairs of corresponding patches. Scale bar = 500 μm.

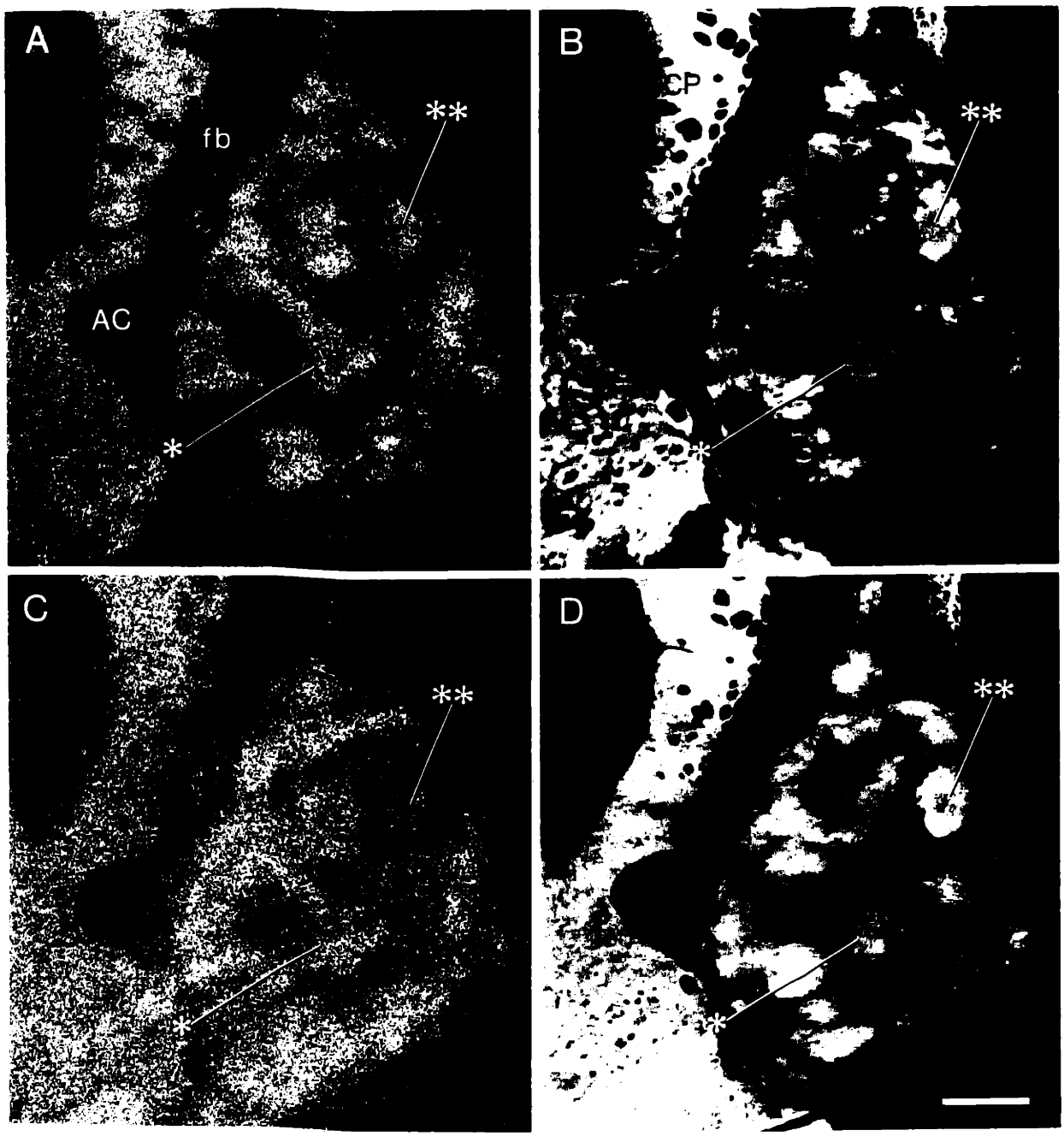
A
fb
**
AC
*
B
CP
**
*
C
**
*
D
**
*

Figure 3-5: Negative-image photomicrographs of film autoradiograms illustrating patterns of [^{3}H]SCH23390 binding for dopamine D1 receptors (A) and [^{3}H]sulpiride binding for dopamine D2 receptors (C) in an embryonic striatal graft (case RSG2-34). B and D respectively illustrate the same sections following autoradiography for AChE. The distributions of [^{3}H]SCH23390 binding and [^{3}H]sulpiride binding in the graft show obvious heterogeneities, and patches of strong [^{3}H]SCH23390 binding and [^{3}H]sulpiride binding are preferentially localized in the zones of high AChE activity (P regions). Two examples of such correspondence are indicated by the single and double asterisks. All photographs were taken at the same magnification. CP, caudoputamen; AC, anterior commissure; fb, compacted fiber bundles around graft. Scale bar = 500 μm.

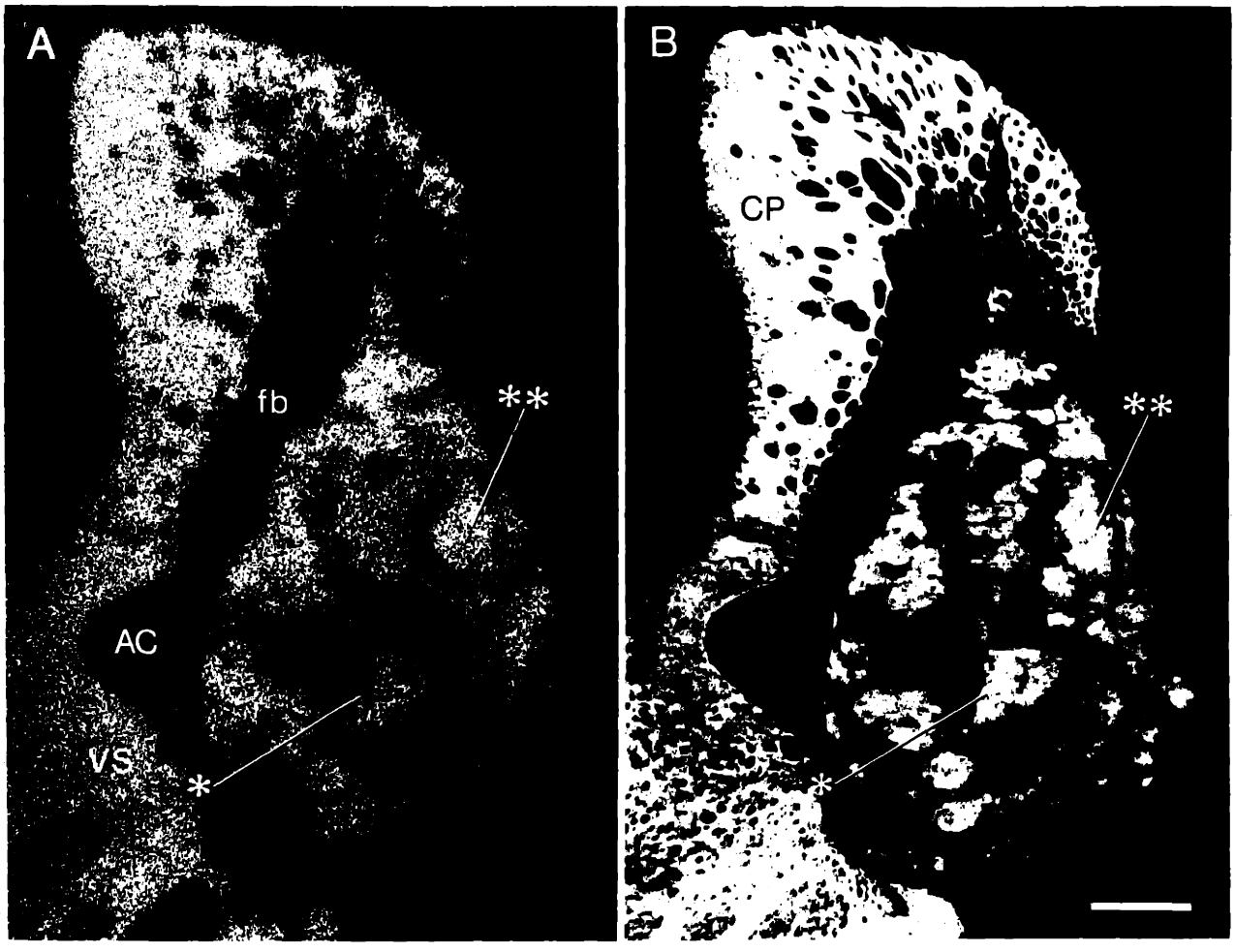
A
fb
**
AC
VS
*
B
CP
**
*

Figure 3-6: Comparison of the distribution of [^{3}H]mazindol autoradiographic binding for high affinity dopamine uptake sites (A) and the AChE staining developed from the same section following autoradiography (B) in an embryonic striatal graft (case RSG2-34). A highly inhomogeneous pattern of [^{3}H]mazindol binding appears in the graft. Nearly all patches of strong [^{3}H]mazindol binding occur in the AChE-rich P regions (examples shown by single and double asterisks). VS, ventral striatum; AC, anterior commissure; fb, fiber bundles around the graft. Photographs in A and B were taken at the same magnification. Scale bar = 500 μm.

Distribution of TH-positive patches in relation to AChE-positive P zones

Sections processed for TH-like immunoreactivity were compared to adjacent sections stained for AChE in 7 brains. In the 41 pairs of sections analyzed, the TH-positive and AChE-positive patches were aligned with each other in 32 pairs. The two sets of patches corresponded both in shape and in location (Figs. 3-1A, C). Thus, TH-positive fibers selectively innervated the P regions defined by high AChE activity. The remaining pairs of sections showed a partial correspondence in that some parts of the AChE-rich P regions did not have intensely TH-immunoreactive neuropil. However, there were no triplets of sections available for these regions with AChE-stained sections on either side of a TH-stained section, so that we could not judge whether the apparent mismatch represented true (partial) lack of correspondence or the end of a patch formation. The weak TH-positive patches in the intracortical parts of the grafts corresponded to zones of high AChE activity. The correspondence between TH-positive patches and AChE-rich P regions also occurred in the implants made in the contralateral intact striatum (Fig. 3-4A, B)

Patterns of [^{3}H]SCH23390, [^{3}H]sulpiride and [^{3}H]mazindol binding and their relation to the distribution of AChE activity

The distributions of [^{3}H]SCH23390 binding for dopamine D1 receptor sites and [^{3}H]sulpiride binding for dopamine D2 receptor sites were highly heterogeneous in the graft tissue (Figs. 3-5A, C). There were patches of strong [^{3}H]SCH23390 binding and [^{3}H]sulpiride binding in striatal grafts, and they occurred in the AChE-rich P regions

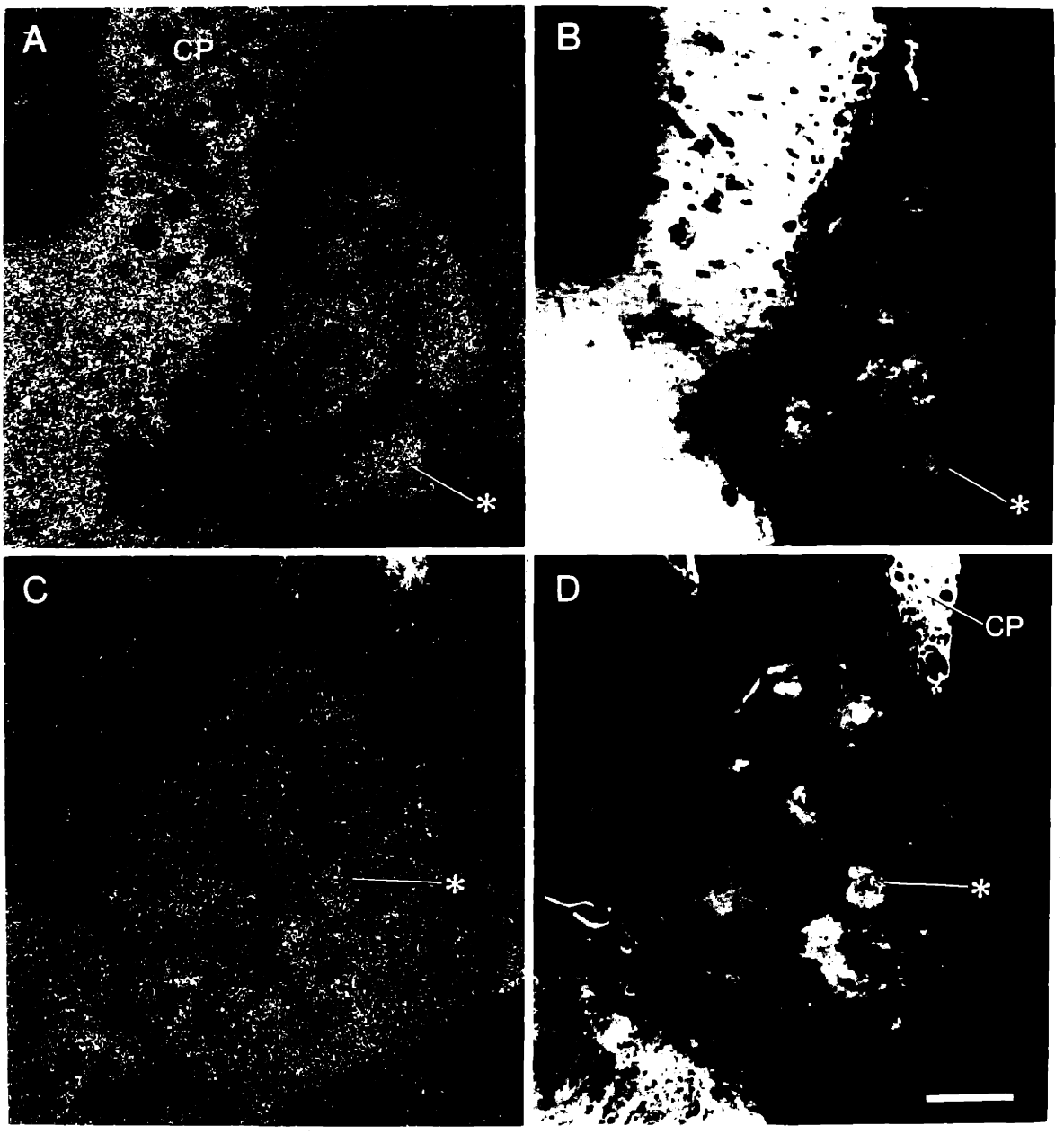
A
CP
*
B
*
C
*
D
CP
*

Figure 3-7: Photomicrographs of film autoradiograms showing patterns of [^{3}H]PZ binding for muscarinic M1 receptors (A) and [^{3}H]HC-3 binding for high affinity choline uptake sites (C) in the embryonic striatal graft of case RSG2-34. The photomicrographs in B and C illustrate AChE staining developed, respectively, in the same sections. Uneven distributions of [^{3}H]PZ binding and [^{3}H]HC-3 binding are present in the graft. Although the binding is somewhat diffuse, patches of enhanced [^{3}H]PZ binding and [^{3}H]HC-3 binding can be identified by reference to the vivid patchiness of the corresponding AChE staining. For both ligands, the zones of heightened binding are preferentially localized in the AChE-rich P regions. The asterisk indicates one such P region. CP, caudoputamen. All photographs were taken at the same magnification. Scale bar = 500 μm.

(Figs. 3-5B, D). Only a few zones of high AChE activity lacked corresponding patches of dense [^{3}H]SCH23390 or [^{3}H]sulpiride binding. The distribution of [^{3}H]mazindol binding for dopamine uptake sites in the striatal grafts also was patchy (Fig. 3-6A). Patches of strong [^{3}H]mazindol binding always occurred in correspondence with in AChE-rich P regions (Fig. 3-6B), but a few regions of high AChE activity lacked corresponding patches of strong [^{3}H]mazindol binding.

Patterns of [^{3}H]PZ and [^{3}H]HC-3 binding and their relation to the distribution of AChE activity

Binding of the M1-selective ligand [^{3}H]PZ in the grafts was uneven (Fig. 3-7A), and the zones of enhanced [^{3}H]PZ binding were localized in regions enriched in AChE activity (Fig. 3-7B). For some patches, the zones of heightened [^{3}H]PZ binding and the zones of high AChE activity seen in the same section were not exactly coextensive. In these instances, the zones of high [^{3}H]PZ binding were smaller, as though forming subfields within the patches of high AChE-activity. As with the other ligands, there were only a few regions of high AChE activity found which did not have enhanced [^{3}H]PZ binding in correspondence with them.

[^{3}H]HC-3 binding for high affinity choline uptake sites also was characterized by zones of higher and lower density, but the ligand binding overall tended to be diffuse (Fig. 3-7C). The regions of heightened [^{3}H]HC-3 binding, like the patches of binding seen with the other radioligands, were preferentially located in the regions enriched in AChE activity (Fig. 3-7D). A few regions of high AChE activity were found to lack

heightened [^{3}H]HC-3 binding.

Neither the [^{3}H]PZ nor the [^{3}H]HC-3 binding patterns were as crisp as those detected with the three dopamine-related ligands, even in nearby sections from the same brains. Of all the markers studied, [^{3}H]HC-3 had the least clearly delineated organization into zones of high and low binding. Similar patterns of correspondence between ligand binding and AChE staining were found in the grafts on the contralateral (non-ibotenic treated) side.

DISCUSSION

Cholinergic and dopaminergic markers in embryonic striatal grafts are preferentially expressed in the P regions

In agreement with previous findings (Isacson et al., 1985; Sanberg et al., 1986; Pritzel et al., 1986; Walker et al., 1987; Isacson et al., 1987; Graybiel et al., 1987a; Deckel et al., 1988a, b; Clarke et al., 1988; Liu et al., 1988; Graybiel et al., 1989), the observations presented here demonstrate that the cholinergic and dopaminergic systems exist in embryonic striatal grafts and display a modular organization. This modular organization was seen for the cholinergic system by histochemical staining for AChE, immunostaining for ChAT, autoradiographic [^{3}H]HC-3 binding for high affinity choline uptake sites and [^{3}H]PZ binding for M1 receptors. For the dopaminergic system, a comparable organization was seen by immunostaining for TH, autoradiographic [^{3}H]mazindol binding for high affinity dopamine uptake sites, [^{3}H]SCH23390 binding for dopamine D1 receptors and [^{3}H]sulpiride binding for dopamine D2 receptors.

The results from comparisons of adjacent sections processed for AChE staining and immunostaining for TH or ChAT, and from comparisons of autoradiographic ligand binding and AChE staining in the same sections, indicated that all of the markers were preferentially localized in AChE-rich P regions. Therefore, the cellular machinery of the cholinergic system, including the synthetic and degradative enzymes, high affinity choline uptake sites and receptor binding sites, as well as corresponding cellular elements of the dopaminergic system, were selectively concentrated in the P regions of striatal grafts. We infer from these observations that synthesis, release, and receptor activation for

acetylcholine and for dopamine all could take place in P regions.

In the first report of this series (Liu et al., 1988; Graybiel et al., 1989), we defined P regions in E15 embryonic striatal grafts as zones containing high AChE activity, and suggested that these AChE-rich P regions may be the main representatives of striatal tissue in such striatal grafts. We reached this conclusion because the P regions exhibit many characteristics of the normal postnatal and adult rat's striatum, whereas NP regions do not. The present findings are consistent with this suggestion because the cholinergic and dopaminergic markers that are all highly characteristic of the normal rat's striatum are all preferentially distributed in P regions. In the experiments reported here we did not investigate the possibility that P regions of the grafts were themselves divided into compartments that could correspond to the striosome/matrix (patch/matrix) compartments of normal striatum. This is because in the rodent striatum (in contrast to the striatum of cats and primates) most of the cholinergic and dopaminergic markers we employed do not consistently show pronounced differences in relative distribution in striosomes and extrastriosomal matrix at maturity (Graybiel and Ragsdale, 1979; Murrin and Ferrer, 1984; Loopuijt et al., 1987; Graybiel et al., 1989).

In related studies, with single or double retrograde tracing techniques, embryonic striatal grafts have been shown to receive nigrostriatal afferents from the host (Pritzel et al., 1986; Wictorin et al., 1988), in good accord with the findings from TH immunohistochemistry. Thus, the close alignment of cholinergic and dopaminergic markers in P regions offers an anatomical basis for possible physiological interactions between the nigrostriatal dopamine-containing system of the host and the striatal

cholinergic system of the donor graft tissue. This interaction is known to occur in at least two ways in the normal rat's striatum. First, acetylcholine-containing and dopamine-containing terminals share a characteristic mode of termination on the necks of dendritic spines of medium-spiny neurons (Freund et al., 1984; Izzo and Bolam, 1988; Pickel and Chan, 1990). These two inputs may thus have conjoint influences on other afferent inputs to their postsynaptic neurons. No double labelling experiments have yet been carried out to test for this pattern in embryonic striatal grafts, but Clarke et al. (1988) have found both TH-immunoreactive and other unlabelled terminals synapsing on the necks of spines of medium spiny neurons in such grafts. Second, cholinergic neurons have been reported to receive direct monosynaptic input from dopamine-containing axons in the normal rat's striatum (Kubota et al., 1987b; Chang, 1987). The nearly coextensive distributions of ChAT-like immunoreactivity and TH-like immunoreactivity described here suggest that the proximity necessary for contacts by TH-immunoreactive axons on cholinergic neurons exists in embryonic striatal grafts.

We found no suggestion of abnormal relations between ChAT-positive and TH-positive elements in the P regions of the grafts. By contrast, TH-positive fibers from intrastriatal transplants of embryonic nigral tissue have been reported to make highly abnormal, dense perisomal contacts with large striatal neurons of the host-- almost certainly mainly the cholinergic neurons (Freund et al., 1985). Such intrastriatal dopaminergic grafts have been shown to restore inhibitory control over cholinergic neurons of the host rat's striatum (Herman et al., 1988a).

The P regions are probably the zones where trans-graft information processing takes place

Embryonic striatal grafts are able to compensate for, and to decrease, the methamphetamine- or apomorphine-induced rotation in rats subjected to prior unilateral striatal excitotoxin lesions (Dunnett et al., 1988). Furthermore, peripheral administration of methamphetamine has been shown by *in vivo* dialysis to induce the release of GABA in the globus pallidus and the substantia nigra of host animals transplanted with striatal grafts (Sirinathsinghji et al., 1988). Methamphetamine is known to stimulate release of dopamine and to block dopamine uptake, and apomorphine is an agonist for dopamine D1 and D2 receptors. Both the behavioral and the dialysis experiments suggest that these dopaminergic agents influence outputs from the grafts to the host, though contributions of direct effects on dopamine receptor sites and release sites in the pallidum and substantia nigra cannot be excluded.

The presence of patches of [^{3}H]spiroperidol and [^{3}H]spiperone ligand binding selective for dopamine D2 receptors in embryonic striatal grafts has been reported earlier by Isacson et al. (1987) and Deckel et al. (1988b), respectively. In the present study, we confirmed these observations with [^{3}H]sulpiride binding for D2 receptors and, in addition, demonstrated that patches of [^{3}H]SCH23390 binding, selective for dopamine D1 receptors, were also present in striatal grafts. Our observations are in good accord with the findings of Wictorin et al. (1988b) who have shown that immunostaining for DARPP-32-- known to be localized in neurons possessing dopamine D1 receptors (Walaas and Greengard, 1984)--appears in a patchy distribution in striatal grafts. In the

present experiments, we showed that dopamine D1 and D2 receptor-related binding sites were concentrated in the P regions in which TH-immunoreactive fibers were ramified. It is probable, therefore, that the dopamine released from TH-positive terminals in the grafts would primarily act through dopamine receptors in the P regions, and that the effects of methamphetamine and apomorphine would similarly be mediated through neural circuits in the P regions.

Further evidence for the functional primacy of the regions we have designated as the P regions of the grafts comes from experiments suggesting that the efferent fibers connecting the grafts to the host brains mainly originate in these P regions. Grafted neurons labelled by retrograde tracer injections placed in the globus pallidus of the host form clusters aligned with patches of TH-like and DARPP-32-like immunoreactivity (Wictorin, 1988b, 1989). Thus, the capacity of the striatal grafts to affect the host's behavior (for example by reducing methamphetamine- or apomorphine-induced turning responses) may be mediated by actions through P regions in which the projection neurons of the grafts lie. These efferent neurons likely include the medium-sized calbindin-D_{28k}- and met-enkephalin-immunoreactive neurons that we have shown to be present in large numbers in P regions (Liu et al., 1988; Graybiel et al., 1989).

Our experiments also suggest that the information destined for the efferent neurons of the striatal grafts could be influenced by grafted neurons having the phenotypy of intrinsic interneurons of the striatum-- not only the aspiny cholinergic interneurons studied here, but also the somewhat smaller somatostatin-immunoreactive aspiny neurons that we also have identified in P regions (Graybiel et al., 1989). Aspiny

interneurons in the normal striatum, are thought to regulate the level of striatal output (Groves, 1983).

One interesting question raised by these findings is whether there are connections between the P and NP regions of the grafts. For instance, do P regions receive inputs from NP regions? Intragraft injections of the anterograde axonal tracer, Phaseolus vulgaris leucoagglutinin, have been shown to label axons arborizing extensively within the graft itself (Wictorin et. al., 1989), but the distribution of these labelled axons with respect to P and NP regions has not been determined. If the NP regions did project to the P regions, then given that both NP and P regions receive afferents from host cortical and thalamic regions that normally project to the striatum (Wictorin et al, 1988a, 1988b, Wictorin and Björklun, 1989), the P regions would probably be the essential foci within which afferent signals from the host converge and are regulated in the grafts, and within which decisions regarding outputs to the host are made.

This kind of integrated information processing occurring in the P regions may be responsible, at least partly, for the behavioral improvement following striatal lesions in the tasks such as rewarded alternation, maze learning and skilled paw reaching, which require complex sequential sensory-motor functioning in animals bearing striatal grafts (Deckel et al., 1986; Isacson et al., 1986; Dunnett et al., 1988). Interestingly, available evidence suggests that striatal grafts may succeed in establishing only sparse connections with the substantia nigra (Pritzel, et al., 1986; Wictorin et al., 1989). This deficit in efferent connectivity suggests that classes of behavior requiring direct striatonigral signaling-- perhaps those related to axial orientation-- may not fully recover.

Why do the NP regions in embryonic striatal grafts not strongly express markers for the cholinergic and dopaminergic systems?

In the first study of this series, we suggested that the NP regions in striatal grafts may represent nonstriatal tissue, or a mixture of nonstriatal cells with immature striatal tissue (Liu et al., 1988; Graybiel et al., 1989). Information from the present experiments is not sufficient to resolve this issue, but the findings favor the viewpoint that the NP regions may be predominantly nonstriatal.

First, ChAT-immunoreactive neurons reminiscent of the bipolar ChAT-immunoreactive interneurons in the neocortex were found almost exclusively in the NP regions of the grafts. At least 80% of the intrinsic bipolar ChAT-immunoreactive neurons in the neocortex have been found to co-express vasoactive intestinal polypeptide (Eckenstein and Baughman, 1984). It would be of interest to determine whether the ChAT-immunoreactive neurons in the NP regions also express this neuropeptide.

Second, TH-immunoreactive neurons were observed in the NP regions. TH-immunoreactive neurons are reported to be present transiently in the neocortex of early postnatal rats and mice (Berger et al., 1985; Satoh and Suzuki, 1988) and they occur in cultured embryonic cortical neurons (Iacovitti et al., 1987). TH-immunoreactive neurons have also been found in intracerebral grafts of embryonic neocortex (Park et al., 1986; Herman et al., 1988b; Liu et al., unpublished observations). It is therefore possible that TH-immunoreactive neurons in the NP regions were derived from neocortical progenitor cells present in the dissected donor tissue. Our evidence is not conclusive on this point, however, because a very small population of TH-immunoreactive neurons has been

reported to occur in the normal adult rat's striatum (Tashiro et al., 1989). Interestingly, some TH-immunoreactive neurons were observed in the P regions of the grafts, which we suggest to be comprised of striatal tissue.

Third, growing dopamine-containing neurons preferentially innervate striatal tissue both in tissue culture (Hemmendinger et al., 1981; Denis-Donini et al., 1983; Won et al., 1989) and in intracerebral transplantation preparations (Björklund et al., 1983). In the present experiments, TH-positive fibers showed a similar selectivity in preferentially innervating the P zones of the grafts. In fact, the NP regions received only scant innervation by TH-immunoreactive fibers, even parts of the NP tissue immediately beside richly innervated P regions. This sharpness of differential innervation suggests that the ingrowing TH-positive fibers of the host recognize the P zones as the principal striatal targets present in the grafts.

If the NP regions contain considerable amounts of cortical tissue, this could account for the apparent difference in the crispness of modular distribution of the dopaminergic and cholinergic ligand binding in the grafts. In the autoradiographic films, there was a much more pronounced contrast between cortical and striatal binding for the dopamine-related ligands than for the acetylcholine-related ligands. This argument could also apply to the finding by Isacson et al. (1987) that in embryonic striatal grafts there is a relatively homogenous distribution of [^{3}H]propylbenzilycholine mustard, which binds both M1 and M2 muscarinic subtypes.

Clearly, it is possible that abnormal phenotypic transitions in the expression of neurotransmitters take place in tissues derived from suspended cells implanted into a

neuron-depleted and glia-enriched environment such as the damaged host's striatum (Coyle and Schwarcz, 1976; Köhler and Schwarcz, 1983; Isacson et al., 1987). The patterns of neurotransmitter expression in striatal grafts must therefore be interpreted cautiously. Given these limitations, it is all the more remarkable that in the P regions of the grafts, there is an apparent reconstitution of a cholinergic interneuronal plexus and a host-derived catecholaminergic fiber plexus together with the enzymes, receptor sites and uptake sites necessary for active functioning of these two key systems of the normal striatum.

Chapter 4

Migratory capability of host striatal neurons in embryonic striatal graft environment

ABSTRACT

A fundamental issue in assessing the nature of embryonic striatal grafts is whether the resulting graft, which is usually surrounded by a ring of fibers and gliotic tissue, contains cells that migrated from the host striatum. In the present study, we placed striatal grafts into host brains whose striatal cells had been pulse-labeled with [^{3}H]thymidine to test for possible spatial interactions between host and donor cells in the zones of intrastriatal grafting. Four groups of host rats were pulse-labeled with [^{3}H]thymidine at embryonic days E12-E15 or E12 and E15-E18 or E12 and E16-E19 or E12 and E20-P1, and were allowed to reach maturity. One week prior to grafting, ibotenic acid-induced lesions were made unilaterally in the host striatum. At grafting, dissociated cells from E14-E16 rat striatal primordia were injected bilaterally into the host caudoputamen. Tissue was processed for autoradiography 8-16.5 months post-grafting.

Despite the presence of many intensely-labeled neurons in the host striatum of rats in all four groups, very few intensely-labeled neurons were found in the cores of grafts either in the ibotenate-treated or in the intact host striatum. A few weakly-labeled small cells appeared in the graft cores, and a few strongly- or weakly-labeled neurons

appeared at the margins of the graft zones. Some perivascular cells associated with blood vessels in the grafts were also weakly labeled, but the gliotic tissue surrounding the graft zones was not labeled.

These results suggest that very few striatal neurons migrate into the cores of graft zones, or that, if they do, such neurons do not survive. At most, a few surviving host striatal neurons have limited spatial interactions with donor cells at the margins of the grafts, both in the damaged and intact host striatal environment. These observations, combined with our previous finding that [^{3}H]thymidine-labeled cells derived from E15 striatal primordia do not appear in the host striatum, indicate that no extensive mutual migration between striatal donor neurons and host neurons occurs in the zones of grafting.

INTRODUCTION

Embryonic striatal transplantation, in which dissociated cells from embryonic striatal primordia are implanted into the excitotoxin-damaged adult striatum, has been studied for the past several years with the specific aim to develop a potential neuronal replacement therapy for striatal degeneration in Huntington's disease (for review, see Björklund et al., 1987). Besides this potential clinical application, embryonic striatal grafts may also offer an alternative approach to study the development of the striatum *in vivo*. Embryonic striatal grafts survive transplantation successfully, express a variety of neurotransmitter-associated substances characteristic of the normal striatum, and establish connections with specific regions of the host brains. Some of these connections have been demonstrated to have synaptic specialization (Deckel et al. 1983; Isacson et al. 1984; McAllister et al. 1985; Deckel et al. 1986, 1988a, 1988b; Sanberg et al. 1986, 1989; Pritzel et al. 1986; Isacson et al. 1987; Walker et al. 1987; Graybiel et al., 1987a; Clarke et al. 1988; Roberts and DiFiglia 1988; Giordano et al. 1988; Wictorin et al. 1988, 1989a, 1989b, 1989c, 1990a, 1990b; Wictorin and Björklund 1989; Xu et al. 1989; Graybiel et al. 1989; Sirinathsinghji et al. 1990; Mayer et al. 1990; Liu et al. 1988, 1990a, 1990b).

Of particular interest is that the grafts develop a modular organization in which patches rich in neurochemical substances typical of striatum (we have called these P regions) are embedded in their surrounds (non-patch, NP regions) with very low expression of these neurochemical substances. We have previously suggested that this modular organization may reflect segregated zones of striatal tissue and nonstriatal

and/or immature striatal tissue (Liu et al., 1988, 1990b; Graybiel et al., 1989).

To interpret such apparent admixtures of cell types in striatal grafts, it is essential to know whether the grafted cells and host cells interact in the graft environment by migrating among one another. In a previous study, we pulse-labeled donor cells with [^{3}H]thymidine at E11, E12, E13, E14 or E15 and studied the grafts at 9-17 months post-grafting (Graybiel et al., 1989). The [^{3}H]thymidine labeled neurons were confined to the grafts, suggesting that donor neurons had not migrated into host tissue or, if they had, they had not survived. This result did not exclude the possibility, however, that such grafts could contain neurons derived from the host striatum. Especially as the P regions of the grafts contain neurons resembling normal striatal neurons, it is possible that the P regions represent pockets of host striatal cells that had migrated into the transplants and aggregated together to form the P regions. To test this possibility, we pulse-labeled striatal cells of different groups of host rats by prior exposure to [^{3}H]thymidine at different embryonic ages at which striatal neurons are generated (Fentress et al., 1981; Bayer, 1984; Marchand and Lajoie, 1986), and then grafted non-radioactive donor tissue into the [^{3}H]thymidine-labeled striatum of these host rats. The results reported here have in part been summarized in abstract form elsewhere (Liu et al., 1990a).

METHODS

[^{3}H]thymidine labeling of host striatal neurons

Four Sprague-Dawley time-pregnant rats (Taconic Farm) were intraperitoneally injected daily with 1 ml of 5 mCi/ml [^{3}H]thymidine dissolved in 2% ethanol aqueous solution (84.2 Ci/mmol, New England Nuclear) at E12-E15 or E12 and E15-E18 or E12 and E16-E19 or E12 and E20-E22. The pups exposed at E20-E22 received further intraperitoneal injections of 0.1 ml [^{3}H]thymidine (0.1 mCi) at postnatal day (P) 0 (the day of birth) and P1. Three months after birth, the radioactively labeled rats served as host rats for grafting (E12-E15, n=6; E12 and E15-E18, n=3; E12 and E16-E19, n=3; E12 and E20-P1, n=4).

Transplantation

Striatal grafting was performed according to the procedure described elsewhere (Graybiel et al., 1989; Liu et al., 1990b). Cell-suspensions prepared from the dissected non-radioactive E14-E16 rat striatal primordia were bilaterally injected into the ibotenate-damaged striatum and the contralateral intact striatum. In some hosts, transplantation was done unilaterally either in the lesioned striatum or in the intact striatum.

Autoradiography and histochemistry

Eight to 16.5 months after grafting, the grafted rats were deeply anaesthetized with sodium pentobarbital and perfused transcardially with 4% paraformaldehyde in 0.1 M phosphate buffer containing 5% sucrose and 0.9% saline (pH 7.4). Brains were postfixed at 4°C for 2-4 hr in the same fixative, cryoprotected with 20% sucrose

containing 0.9 % NaCl in 0.1 M phosphate buffer, and cut in the coronal plane at 20-30 μm on a freezing microtome. Sections were mounted on slides, defatted and dipped in Kodak NTB-2 emulsion diluted 1:1 in distilled water containing 0.1% detergent (Dreft). Sections were developed in Kodak D-19 after exposure times for 1.5-2 months and were stained with cresylecht violet. Cells labeled with over 20 silver grains in autoradiographic sections were regarded as strongly-labeled. The adjacent sections were stained for acetylcholinesterase (AChE) (Geneser-Jensen and Blackstad, 1971; Graybiel and Ragsdale, 1978). Some of the grafted rats used in the present investigation are the subjects of another striatal graft study (Liu et al., 1991).

RESULTS

The structure of the transplanted tissue was studied with the aid of AChE and Nissl stains. In all four groups of rats, the striatal graft contained AChE-rich patch regions embedded in AChE-poor surrounds (see Figs. 4-1A, 2A, 3A). The grafted tissue in the ibotenate-induced degenerated striatum was usually surrounded by a gliotic ring and by fiber bundles at the graft margins.

The radioactively labeled cells were largely confined to the host tissue in all four groups of rats. Many intensely labeled neurons were distributed homogeneously throughout the host striatum labeled at E12 and E15-E18, E16-E19, or E20-P1. Clusters of labeled neurons were frequently present in the host striatum labeled at E12-E15 (van der Kooy and Fishell, 1987). In the grafts, very few intensely-labeled medium-sized neurons were found except at the graft margins. This was true both for grafts placed in the ibotenate-damaged striatum and for those (much smaller) grafts in the intact striatum (Figs. 4-1B, 2B, 3B). A few weakly-labeled cells were present in the graft cores. They were mainly small (ca. 4-8 μm) and were presumably glial and microglial cells. Some perivascular cells associated with blood vessels in the grafts were also weakly labeled. At the margins of the grafts as identified by the intensely Nissl stained gliotic tissue, a few strongly- or weakly-labeled medium-sized neurons appeared (Figs. 4-1B, 2B, 3B). The small (glial) cells in the gliotic ring surrounding the graft zones were not labeled.

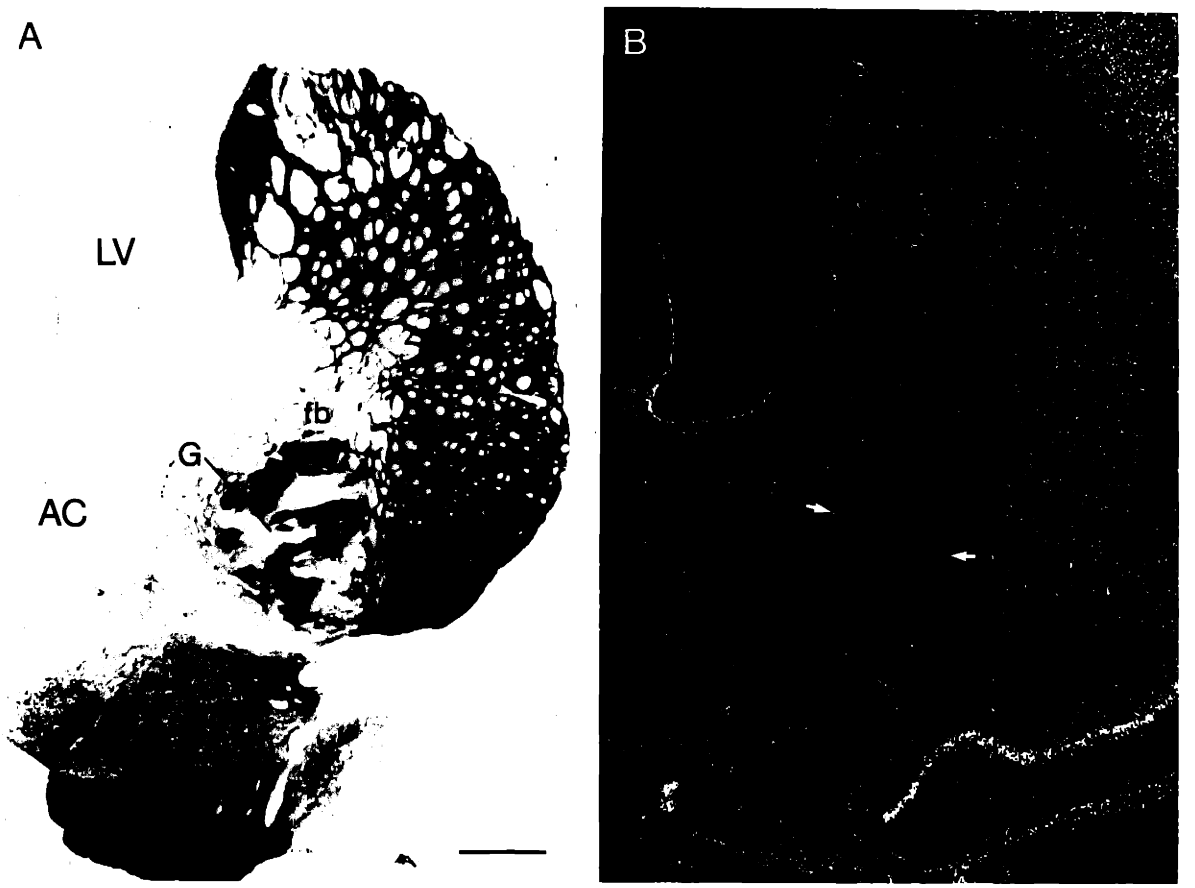
A
LV
fb
G
AC
B

Figure 4-1: Lightfield (A) and darkfield (B) photomicrographs of adjoining sections taken from an E15 striatal graft (case RSG4-15) implanted into the ibotenate-damaged host striatum that was previously exposed to [^{3}H]thymidine at E12 and E15-E18. A: photomicrograph of a section stained for AChE. AChE-poor fiber bundles (fb) form a ring around the graft separating it from the host striatal tissue (CP). The graft developed a typical modular organization in which patches of high AChE activity (P regions) are embedded in their AChE-poor surrounds (NP regions). The distribution of [^{3}H]thymidine-labeled cells in the graft zone and the host striatum is illustrated in adjoining section in B. Although there are many strongly-labeled neurons in the host striatum, few intensely-labeled neurons are found in the graft zone (arrows). No labeled neurons are found in the graft core in this section. LV, lateral ventricle; AC, anterior commissure. Scale bar = 500 μm.

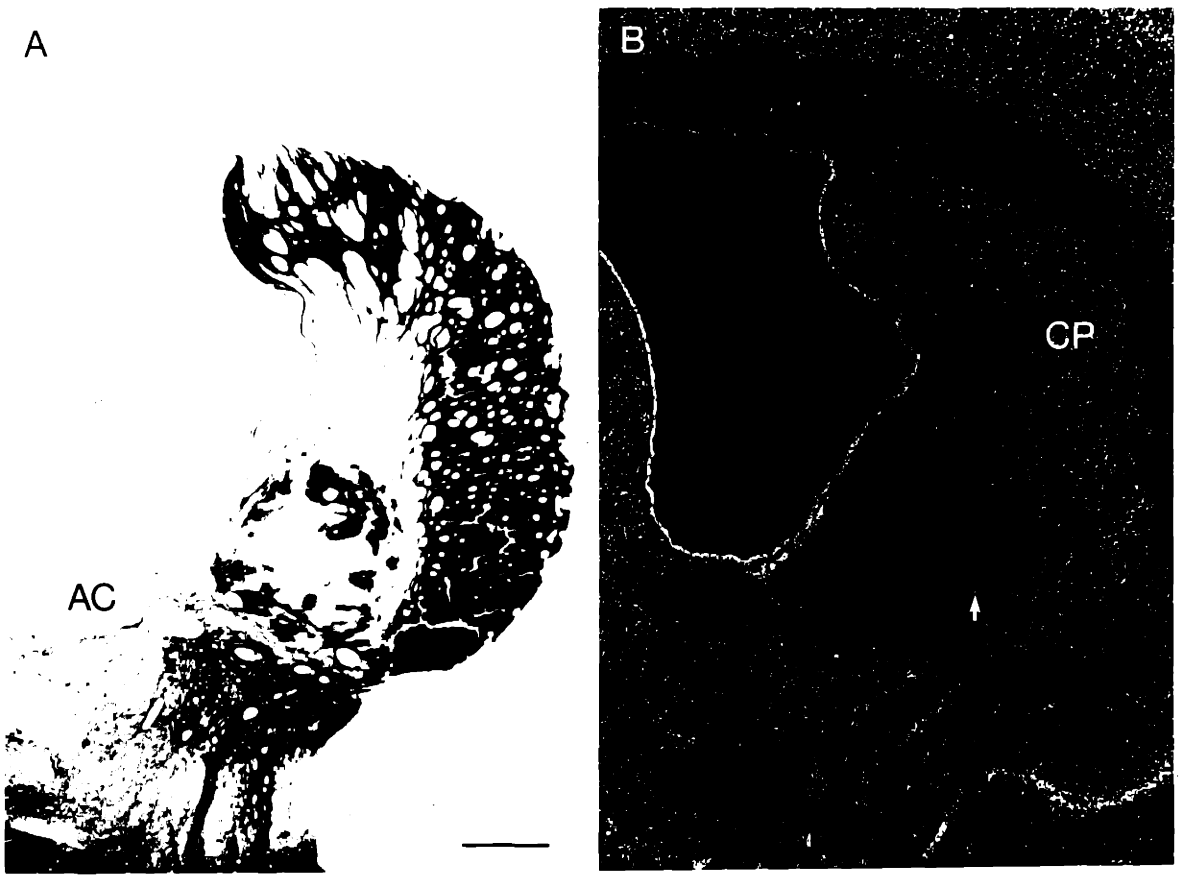
A
AC
B
CP

Figure 4-2: Photomicrographs of adjacent sections taken from an E15 graft (case RSG4-21) placed in the ibotenate-damaged host striatum that was labeled with [^{3}H]thymidine at E12 and E16-E19. Serial adjoining sections stained for AChE and processed for [^{3}H]thymidine autoradiography are shown in lightfield photomicrograph A and darkfield photomicrograph B, respectively. A similar modular organization as that in Fig. 1A is present in the graft. Note that most of the AChE-rich P regions in A are distributed at the margins of the graft. Only one strongly-labeled neuron (arrow) is present in the adjoining section B despite many intensely-labeled neurons appear in the host striatum. AC, anterior commissure. Scale bar = 500 μm.

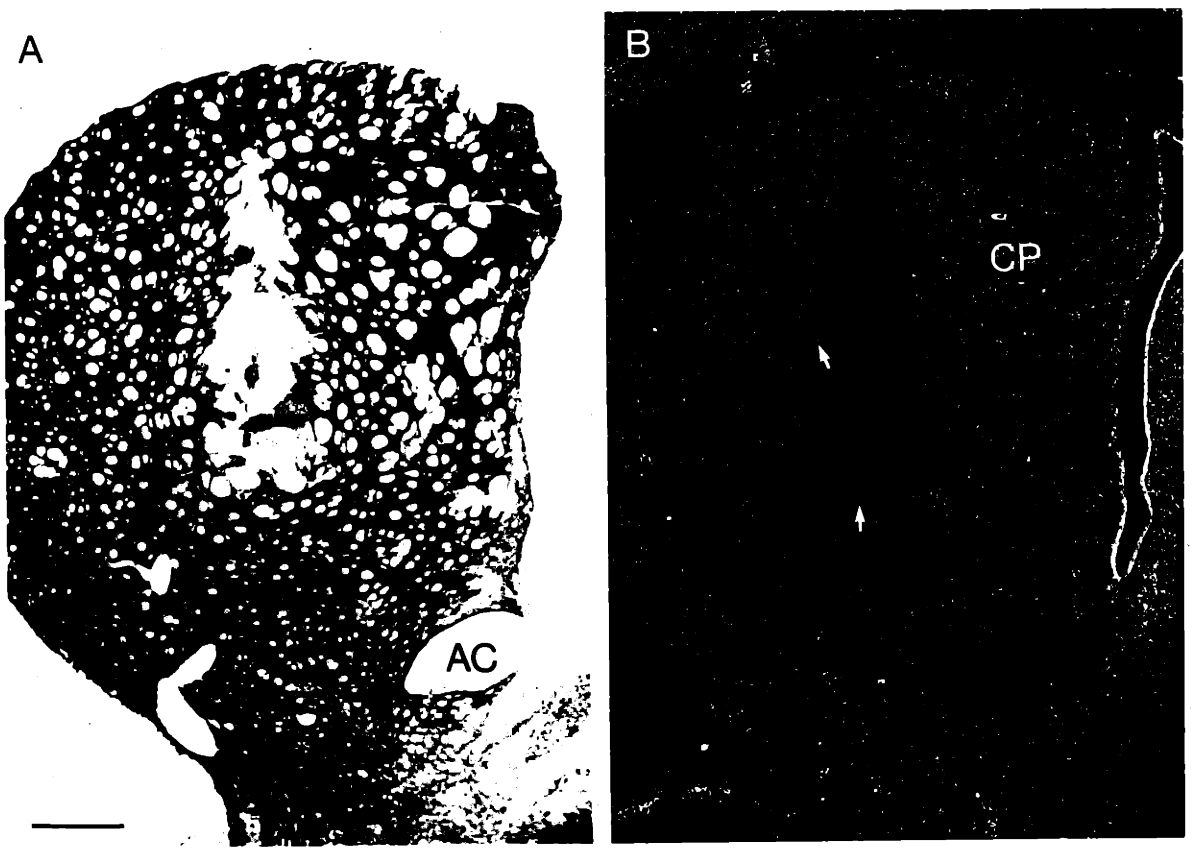
A
AC
B
CP

Figure 4-3: Lightfield (A) and darkfield (B) photomicrographs of adjacent sections taken from an E15 striatal graft (case RSG4-21) placed in the intact host striatum that was previously exposed to [^{3}H]thymidine at E12 and E16-E19. A: darkfield photomicrograph of a section processed for [^{3}H]thymidine autoradiography. B: The adjoining section stained for AChE illustrating a modular organization in the graft similar to that in the grafts implanted into the damaged striatum. No labeled neurons are found in the graft core. A few intensely-labeled neurons are found at the graft margins (arrows). Note that many strongly-labeled neurons are present in the host striatum (CP). AC, anterior commissure. Scale bar, 500 μm.

DISCUSSION

The rational of the present study was to label host striatal neurons with a permanent marker so that we could determine whether any eventually came incorporated into the grafts introduced into the host striatum. We labeled samples of host striatal neurons born from E12 to P1 by prior exposure different groups of host rats to [^{3}H]thymidine at different embryonic ages, thus covering the E12-P1 during which the vast majority of the striatal neurons are generated (Fentress et al., 1981; Bayer, 1984; Marchand and Lajoie, 1986). Remarkably, the results suggest that even when ibotenic acid lesions have been made to damage the host striatum prior to grafting, only very few striatal neurons of the host migrate into the cores of graft zones, or if host neurons do migrate into the graft zones, they do not survive. Thus, at most a few surviving host striatal neurons have limited spatial interactions with donor cells at the margins of the grafts, both in excitotoxin-damaged and intact host striatal environments. It should be noted, however, that the labeled neurons found at the margins of the graft zones may be surviving host neurons that remained in the same place, but appear to have migrated toward the margins of the graft because the graft tissue expanded to reach the surviving host striatum,

We and others have previously suggested that embryonic striatal grafts may contain heterogeneous tissue types (Isacson et al., 1987; DiFiglia et al., 1988; Wictorin et al., 1989c; Graybiel et al., 1989; Liu et al., 1988, 1990b). This mixture of inhomogeneous tissue is reflected by the modular neurochemical organization of the grafts as shown by AChE staining and by immunostaining and autoradiographic binding

for other transmitter-related markers. The modular organization of embryonic striatal grafts is typically characterized by patches of high AChE activity (P regions) embedded in their poor surrounds (NP regions). Our previous studies suggest that the AChE-rich P regions in striatal grafts probably represent striatal tissue, whereas the AChE-poor regions probably represent non-striatal tissue and/or immature striatal tissue (Liu et al., 1988, 1990b; Graybiel et al., 1989). As AChE-rich P zones are often distributed at the margins of the grafts (see Fig. 6-2A), and the afferents from the cortical and subcortical structures, particularly from the neocortex and the thalamus to the striatal grafts are concentrated at the margins of the grafts (Wictorin et al., 1988; Wictorin and Björklund, 1989), it was a reasonable possibility that AChE-rich P regions were in fact islands of host striatal tissue in a sea of donor tissue. Our present results clearly argue strongly against this possibility, as very few labeled neurons occurred in the cores of grafts and only a limited number of labeled neurons were found at the margins of the grafts. Such a small number of host striatal neurons cannot account for all the neurons in AChE-rich P zones.

A second goal of the experiments was to test the possibility that the cholinergic neurons in embryonic striatal grafts may be derived from the host striatum. This concern was prompted by the fact that injections of ibotenic acid into the striatum result extensive death of intrinsic medium-sized striatal neurons (Köhler and Schwarcz, 1983; Beal et al., 1986; Isacson et al., 1987; Daves and Roberts, 1987; Daves and Roberts, 1988), but have been reported to selectively spare the large, AChE-positive and choline acetyltransferase (ChAT)-immunoreactive cholinergic neurons in the striatum (Köhler and Schwarcz, 1983;

Daves and Roberts, 1987; Davies and Roberts, 1988). We and other groups have previously shown that large AChE-positive neurons are present in striatal grafts (Walker et al., 1987; Liu et al., 1990). We have further demonstrated immunocytochemically the existence in striatal grafts of ChAT-rich patches consisted of ChAT-immunoreactive neuropil and large ChAT-immunoreactive neurons. The ChAT-rich patches are in fact in close register with AChE-rich P regions (Graybiel et al., 1987a; Liu et al., 1990). Conceivably, then, it was possible that the AChE-positive and ChAT-positive neurons in the grafts were derived from host through the sparing of cholinergic neurons in the excitotoxin-damaged host striatum, and that these cholinergic neurons influenced the formation of P zones.

The cholinergic neurons in the normal striatum are well known to be large interneurons (Eckenstein and Sofroniew, 1983; Bolam et al., 1984; Phelps et al., 1985), and the majority of them are generated at E12 to E15 (Semba et al., 1988; Phelps et al., 1989). Because of this early birthdates, all host groups were exposed [^{3}H]thymidine at E12 as well as at later 3-4 day spans. Although there were labeled large cells in the striatum of host rats labeled with [^{3}H]thymidine from E12 to E15, we did not find labeled large cells in the graft zones. Nor did we find such neurons in grafts of the later-exposed hosts. Therefore, it is unlikely that the cholinergic neurons in embryonic striatal grafts are derived from the host striatum. Moreover, it is unlikely that host cholinergic neurons set up the P/NP modularity unless host cholinergic neurons first mingled with the grafted cells and then migrated away or died.

Despite the fact that the neurodegenerated striatum may provide sufficient

physical space and supporting environment for the process of migration, and grafted embryonic cells may carry diffusable developmental signals to trigger the migration of host neurons, our results suggest that these migrations do not occur or end in cell death or reverse migration. Lack of migration by the host cells may be accounted for by the fact that the host neurons at the time of grafting have a mature status in which their migratory machinery may no longer exist, and that the host neurons may also be spatially restricted by their input-output connections. Furthermore, the gliotic ring surrounding the graft zone may form a barrier for preventing the host neurons migrating into the graft.

In a previous study, we demonstrated that donor neurons pulse-labeled at E11, E12, E13, E14 or E15 from E15 striatal primordia do not migrate into the host striatum (Graybiel et al., 1989). Together with the present findings, these results indicate that there are no extensive migrations in either direction by striatal donor neurons and host neurons surviving the transplantation period in the zones of grafting. This cellular segregation of donor and host tissue in the neurodegenerated zones of the host striatum does not necessarily suggest that no functional interactions occur between the donor and the host striatal neurons as the anatomical connections between the donor and the host striatal neurons are built up. Learning more about whether such interactions occur is clearly a point of great interest.

In summary, we conclude that the modular organization of embryonic striatal grafts, in which P zones with striatal phenotype are embedded in NP zones with different phenotype, should not be attributed to the formation of host striatal islands in the grafts.

Instead, this modularity appears to be produced by segregation of different tissue types within the grafts.

Chapter 5

The influence of tyrosine hydroxylase-containing afferents on the development of modular organization in embryonic striatal grafts

ABSTRACT

One of the most prominent features of embryonic striatal grafts is that they develop a modular organization in which patches enriched in many transmitter substances characteristic of striatum (P regions) are embedded in surrounds (NP regions) expressing only low levels of these substances. Of particular interest is the fact that tyrosine hydroxylase (TH)-positive fibers grow into such grafts and specifically terminate in patches that are spatially aligned with P regions. This spatial correspondence suggests that the TH-containing fibers may be capable of regulating the development of cells in the P regions of striatal transplants. In the present study, striatal grafts derived from E15 striatal primordia were implanted into the host striatum previously treated with 6-hydroxydopamine (6-OHDA) to destroy TH-containing dopaminergic nigrostriatal afferents. Our goals were to determine 1) whether the TH-containing fibers in the grafts are derived from the dopaminergic nigrostriatal afferents of the host striatum; 2) whether, if so, the ingrowing TH-positive fibers from the host striatum are required for sorting out of different populations of grafted cells to form P regions and NP regions; and 3) whether such TH-containing fibers from the host regulate the development of

neurochemical phenotypes of grafted neurons.

Our results suggest that the majority of TH-positive fibers in striatal grafts are derived from the TH-containing afferents of the host striatum. The 6-OHDA lesions not only eliminated TH immunostaining in the host striatum, but it also resulted in disappearance of TH-positive patches in the grafts. There were, however, a few TH-positive neurons in the denervated grafts. Our findings also demonstrate that the development of modular organization in the grafts can occur in the absence of TH-containing afferents from the host. Patches containing acetylcholinesterase (AChE) activity, medium-sized calbindin-positive neurons, met-enkephalin-positive neurons and DARPP-32-positive neurons were still present in the denervated grafts. Given that the modular organization probably reflects an admixture of striatal tissue (P regions) and non-striatal tissue (NP regions), these observations suggest that the ingrowing TH-positive fibers from the host striatum are probably not obligatorily involved in sorting out of striatal from non-striatal cells during the formation of P regions in embryonic striatal grafts.

Despite the fact that dopaminergic denervation of the host striatum did not disrupt the expression of several neurochemical substances characteristic of striatum in the grafts placed in this dopamine-depleted environment, there were perceptible differences between the staining patterns of these grafts and grafts placed into dopamine-innervated striatum. In the dopamine-depleted environment, grafts developed AChE-rich P zones that tended to be less crisp than those in the grafts implanted into the host striatum without 6-OHDA lesions. Furthermore, an increase of met-enkephalin

immunostaining in the neuropil of met-enkephalin-positive patches was observed in the denervated grafts. As up-regulation of enkephalin is well known to occur in the dopamine-depleted mature striatum and was observed in the host striatum on the 6-OHDA lesioned side. These results suggest that TH-containing afferents from the host striatum may regulate expression of enkephalin in neurons of the P regions of striatal grafts in a similar way to that in the normal striatum. Thus, functional interactions between dopaminergic and enkephalinergic systems are likely to occur in the striatal circuits reconstructed by embryonic striatal grafts.

INTRODUCTION

The dopamine-containing nigrostriatal track probably is the first afferent system to innervate the developing striatum. The fibers of this tract start to innervate the striatal anlage as early as E14 in the rat (Specht et al., 1981; Moon Edley and Herkenham, 1984; Voorn et al., 1988), at which time only a small number of striatal cells have been born (Fentress et al., 1981; Bayer et al., 1984; Marchand and Lajoie, 1986). Besides reaching the striatal anlage, a few of the early arriving dopamine-containing fibers also invade the ganglionic eminence (Specht et al., 1981; Voorn et al., 1988; Newman-Gage and Graybiel, 1988), which is the presumptive striatal primordium (Smart and Sturrock, 1979). Such early innervation of the ganglionic eminence and the striatal anlage by TH-containing dopaminergic fibers raises the possibility that these dopaminergic fibers may regulate the development of striatal cells. For instance, they may support the survival of developing striatal neurons, or they may be involved in induction and/or maintenance of expression of neurochemical substances in developing striatal neurons. It has been shown in both the visual and somatosensory systems that denervation of target neurons during development can result in anterograde atrophic effects on target neurons (for review, see Purves and Lichtman, 1985; Oppenheim, 1991).

In the striatum, dopamine-containing nigrostriatal afferents exert control over striatal neuropeptides and also GABA (Vernier et al., 1988; Gale et al., 1988). Depletion of dopaminergic inputs to the adult striatum results in up- or down-regulation of neuropeptides and neuropeptide mRNAs (Hong et al., 1985; Young et al., 1986; Voorn et al., 1987; Merchant et al., 1988; Normand, et al., 1987, 1988; Weiss and

Chesselet, 1989; Walaas et al., 1989; Jiang, et al., 1990; Gerfen et al., 1991; see Graybiel, 1990 for review). In striatal tissue co-cultured with ventral mesencephalon, the activity of choline acetyltransferase (ChAT) and levels of substance P have also been shown to be increased (Kessler, 1986). But it is not known how dopamine-containing afferents affect striatal target neurons during development *in vivo*.

One strategy to approach this intriguing question is to destroy the dopaminergic inputs to the developing striatum by using the 6-hydroxydopamine (6-OHDA), a catecholaminergic neurotoxin. But injecting 6-OHDA into rat embryos as early as E13 not only presents a technical difficulty, but it also may cause morbidity in the rats. Embryonic striatal grafts may allow this technical limitation to be circumvented, and may thus provide a system in which resolve this question. We and others have previously suggested that the modular organization in embryonic striatal grafts may reflect an admixture of heterogeneous tissue types (Wictorin et al., 1989c; Graybiel et al., 1989; Liu et al., 1990b). Many striatal markers are concentrated in the AChE-rich patch regions (P regions) of the grafts rather than in the tissue (NP regions) surrounding the AChE-rich patches. Thus, the P regions may represent striatal tissue, whereas the AChE-poor NP zones may represent non-striatal and/or immature striatal tissue (Graybiel et al., 1989; Liu et al., 1990). It has also been shown that the nigrostriatal fibers of the adult host are capable of reinnervating embryonic striatal grafts (Pritzel et al., 1986; Wictorin et al., 1988), and that they form patches of TH-positive fibers that are spatially aligned with AChE-rich P regions (Graybiel et al., 1987a; Wictorin et al., 1989c; Liu et al., 1990). This spatial alignment suggests that the TH-containing fibers may influence the

development of neurons in the P regions of the grafts.

In the present study, briefly summarized elsewhere (Liu et al., 1991a), we tested this possibility by transplanting embryonic striatal primordia into the ibotenate-damaged striatum of adult host rats in which nigrostriatal inputs had been previously removed by nigral 6-OHDA lesions. In this way, we determined with certainty that the TH-positive fibers in striatal grafts are derived from the nigrostriatal afferents of the host. We then tested whether the ingrowing TH-positive fibers are necessary for inducing or maintaining subpopulations of grafted cells to form P regions and whether their absence affected the development of neurochemical phenotypes of the grafted neurons.

METHODS

Denervation of dopaminergic afferents of the host striatum

Twenty five Sprague-Dawley rats were used in the present study. Unilateral dopaminergic denervation of the right striatum of hosts (n=19) was performed 29-32 days before grafting. The denervation of host striatum was done by injecting 4 µl 6-OHDA HBr (2µg/µl, calculated as free base, dissolved in 0.1 mg ascorbic acid/ml in saline) over 4 min at the following coordinates: A=-4.4 mm from bregma, L=-0.9 mm from midline line and V=7.8 mm from the dura matter with the nose bar set at -2.3 mm below the interaural line. The rats were tested with methylamphetamine (2.5 mg/kg)-induced rotation in rotometer bowls 12 days after the 6-OHDA lesions to select rats with large lesions. Only rats showing over 300 turns in a 90 min period were chosen for grafting (n=11).

Embryonic striatal transplantation

One week before grafting, 17 host rats (including 6 normal rats without 6-OHDA lesions) received unilateral intrastriatal injections of 0.5 µl of 0.06 M ibotenic acid dissolved in 0.1 M phosphate buffer (PB, pH 7.4) over 3 min at each of 2 sites: A=0.0 mm, L=-3.0 mm, V=5.0 mm and A=1.2 mm, L=-2.6 mm, V=5.0 mm. Donor tissue was dissected from E15 lateral ganglionic eminence (crown rump length =13-15 mm). The procedure for making cell-suspensions for grafting has been reported elsewhere (Graybiel et al., 1989; Liu et al., 1990b). Four microliters of the cell-suspensions (36 striatal primordia/90 µl glucose-saline) were injected over 8 min into the degenerated striatum at the following site: A=0.8 mm, L=-2.8 mm and V=4.5 mm. After the injection the

needle was left in place for 6 min before being slowly retracted. The survival times for the grafted animals were 3.6-6 months.

Immunocytochemistry and histochemistry

The grafted rats were deeply anaesthetized and perfused through the heart with 4% paraformaldehyde in 0.1 M PB containing either 5% sucrose and 0.9% saline or 15% saturated picric acid (pH 7.4). After removing the brains, they were kept in fresh fixative at 4°C for 2-4 hr, then were stored in 20% sucrose in 0.1 M phosphate buffered-saline. Brain tissue was sectioned in the coronal plane at 30 μm on a freezing microtome. Immunostaining was performed with peroxidase-antiperoxidase immunocytochemistry as described previously (Sternberg, 1979; Graybiel, 1984a; Graybiel and Chesselet, 1984; Liu et al., 1990b). The concentrations of primary antisera were as follows: 1:1,000 for rabbit polyclonal anti-calbindin-D_{28K} antiserum (gift of Dr. P.C. Emson); 1:1,000 for rabbit polyclonal anti-met-enkephalin (gift of Dr. R.E. Elde); 1:20,000 for mouse monoclonal anti-dopamine- and adenosine 3':5'-monophosphate-regulated phosphoprotein (DARPP-32, gift of Dr. E.L. Gustafson); and 1:2,000-2,500 for mouse polyclonal anti-ChAT (provided by Dr. R.W. Baughman). A double bridge procedure was routinely followed. For immunostaining controls, selected sections were incubated without primary antisera. No staining was found in the controls. Acetylcholinesterase histochemistry was processed according to a modified Geneser-Jensen and Blackstad method (Geneser-Jensen and Blackstad, 1971; Graybiel and Ragsdale, 1978).

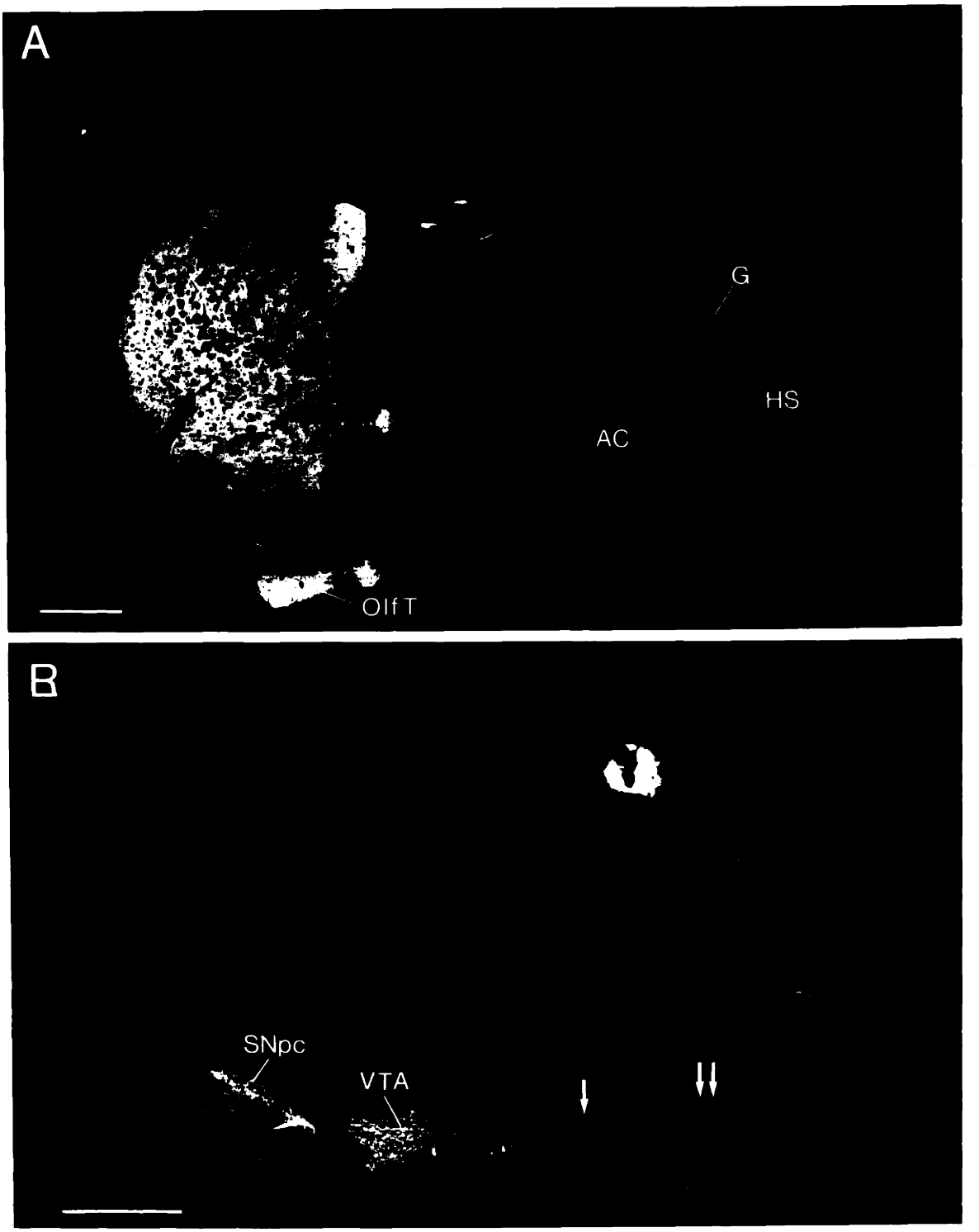
A
G
HS
AC
OlfT
B
SNpc
VTA

Figure 5-1. Reverse contrast photographs illustrating the extent of 6-OHDA lesion as demonstrated by TH immunostaining in the striatum (A) and in the midbrain levels (B) of case V18. A: No TH immunostaining is present in the graft (G) or the host striatum (HS). B: No TH-positive neurons are present in the substantia nigra ipsilateral to the lesion (double arrows). Few TH-positive neurons (arrow) in the ventral tegmental area (VTA) survive the lesion. Note that TH immunostaining in the nucleus accumbens and olfactory tubercle (OlfT) ipsilateral to the graft is also nearly eliminated by the lesion. The white hole at the top right of panel B is a pin hole marking the side of 6-OHDA lesions. AC, anterior commissure; SNpc, substantia nigra pars compacta. Scale bars for A and B indicate 1 mm.

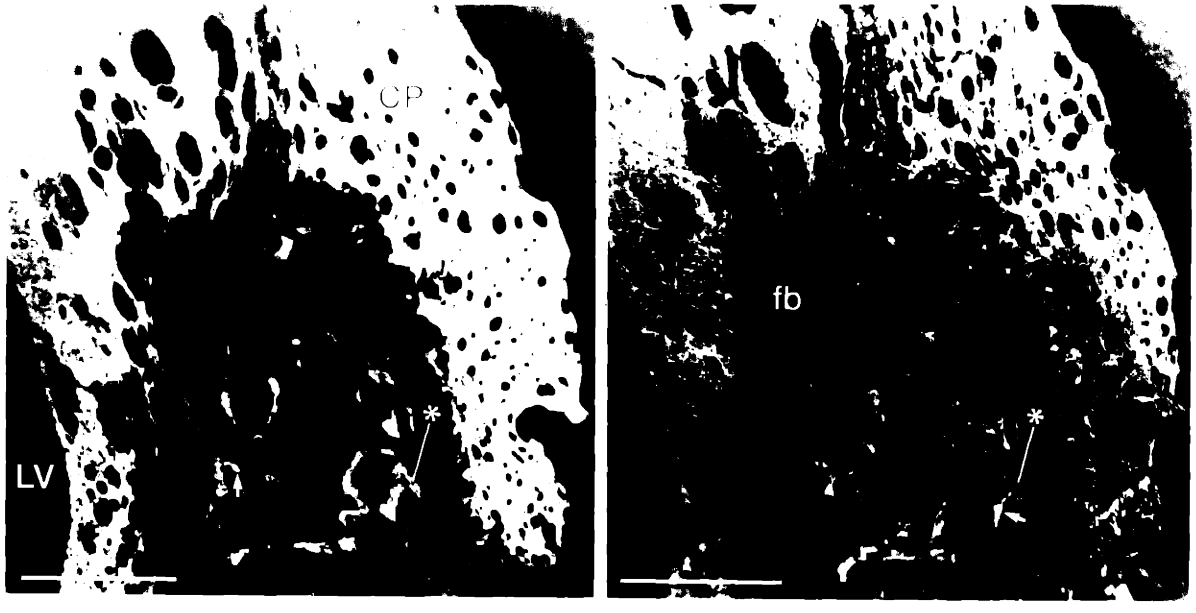
CP
LV
fb

Figure 5-2. Reverse contrast photomicrographs showing adjacent sections stained for AChE (A) and ChAT-like immunoreactivity (B) in a graft implanted into the denervated striatum of case AG-78. The overall AChE staining pattern in the denervated graft is less prominent than that in the control grafts. Small patches with enhanced AChE activity (e.g., see asterisk) are still present in the denervated graft. The arrow indicates an AChE-positive neuron associated with an AChE-rich P region. ChAT immunostaining in the adjacent section demonstrates a comparable staining pattern in the graft (B). Small ChAT-rich patches were distributed unevenly in the denervated graft with several ChAT-immunoreactive neurons associated with the patches (e.g., see arrows). The asterisks in A and B indicate a corresponding AChE-rich and ChAT-rich P zone. LV, lateral ventricle; CP, caudoputamen of the host; fb, fiber bundles. Scale bars for A and B are 500 μm.

RESULTS

Extent of 6-OHDA lesions as assessed with TH immunohistochemistry

The 6-OHDA injection sites were centered in the medial forebrain bundle at nigral levels, and the lesions resulted in the disappearance of nearly all the TH-positive neurons in the substantia nigra pars compacta, ventral tegmental area and retrorubral area, save in some brains where a few TH-positive neurons persisted in the medial part of the ventral tegmental area (Fig. 5-1B). Accordingly, few TH-immunoreactive fibers were present in the grafts and in the host caudoputamen, nucleus accumbens and olfactory tubercle (Fig. 5-1A). There were, however, a few TH-immunoreactive neurons scattered in the denervated grafts, as there are in control grafts implanted into the host striatum without 6-OHDA lesions (Liu et al., 1990b).

Patterns of AChE staining and ChAT immunostaining

Characteristic patches of high AChE activity embedded in AChE-poor surrounds was present in all the control grafts as previously documented (Sanberg et al., 1986; Walker et al., 1987; Isacson et al., 1987; Graybiel et al., 1989; Wictorin et al., 1989c; Liu et al., 1990b). A similar modular organization was also present in the denervated grafts. The 6-OHDA treatment, however, resulted in perceptible changes in the AChE staining pattern of the grafts. In a majority of the denervated grafts (n=7), the AChE-rich P regions tended to be less crisp than those in the control grafts (Fig. 5-2A). The sizes of the AChE-rich P zones tended to be smaller than those in the control grafts, and the

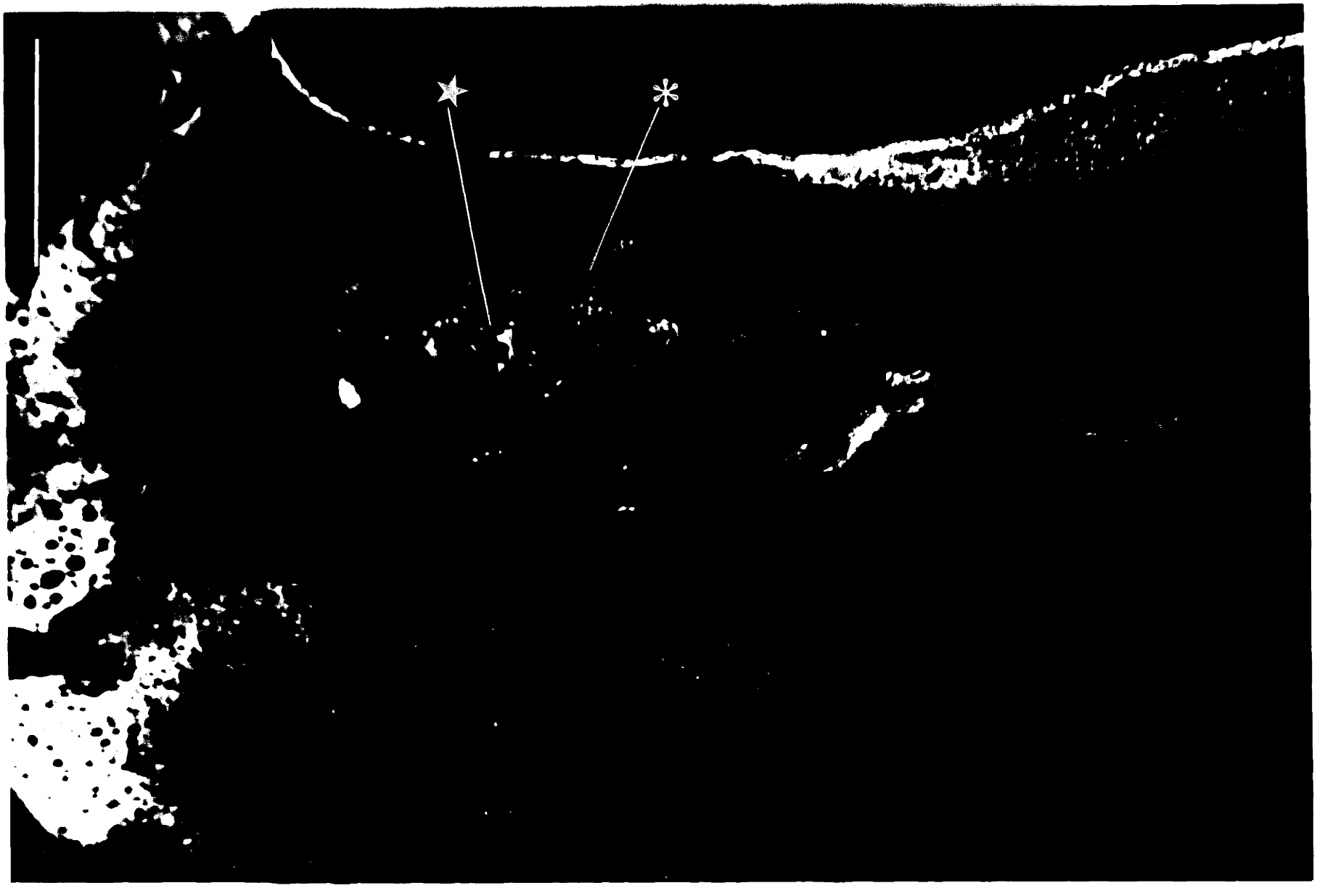

Figure 5-3. Reverse contrast photomicrograph illustrating the calbindin immunostaining pattern in the denervated graft (case V18). Heterogeneous calbindin-like immunoreactivity is distributed throughout the denervated graft. Patches of medium-sized calbindin-immunoreactive neurons (e.g., see asterisk) can be distinguished from the surrounding larger multipolar calbindin-positive neurons with well stained dendrites (e.g., see star). Scale bar indicate 500 μm.

AChE staining intensity also was weaker in the denervated grafts.

A few medium and large ChAT-immunoreactive neurons were present in the denervated and the control grafts. Optimal ChAT immunostaining, obtained in a few denervated brains (n=3), showed that at least some ChAT-positive patches were associated with few large ChAT-positive neurons (Fig. 5-2B). A few medium-sized bipolar ChAT-immunoreactive neurons were also present outside the ChAT-positive patches in the denervated grafts, as previously described for grafts in host striatum retaining normal dopaminergic innervation (Liu et al., 1990b).

Pattern of calbindin immunostaining

As described in a previous report (Graybiel et al., 1989), two populations of calbindin-immunoreactive neurons with different phenotypes were present in the control grafts. Patches of medium-sized calbindin-positive neurons that resemble those in the host striatum were distributed throughout the control grafts. Outside these calbindin-positive patches, there were many medium to large multipolar calbindin-immunoreactive neurons that did not resemble their counterparts in the host striatum. The removal of TH-containing afferents of striatal grafts did not appear to change the immunostaining pattern of calbindin-like immunoreactivity in the grafts (Fig. 5-3). There were clusters of medium-sized neurons immunoreactive for calbindin that closely corresponded to AChE-rich P regions in adjoining sections, and large calbindin-positive neurons with prominent dendrites appeared in regions corresponding to NP regions.

Figure 5-4. Reverse contrast photomicrograph showing the immunostaining pattern of DARPP-32 in the denervated graft of case V18. Several clusters of DARPP-32-immunoreactive neurons are distributed inhomogeneously in the denervated graft (e.g., see asterisk). Scale bar is 500 μm.

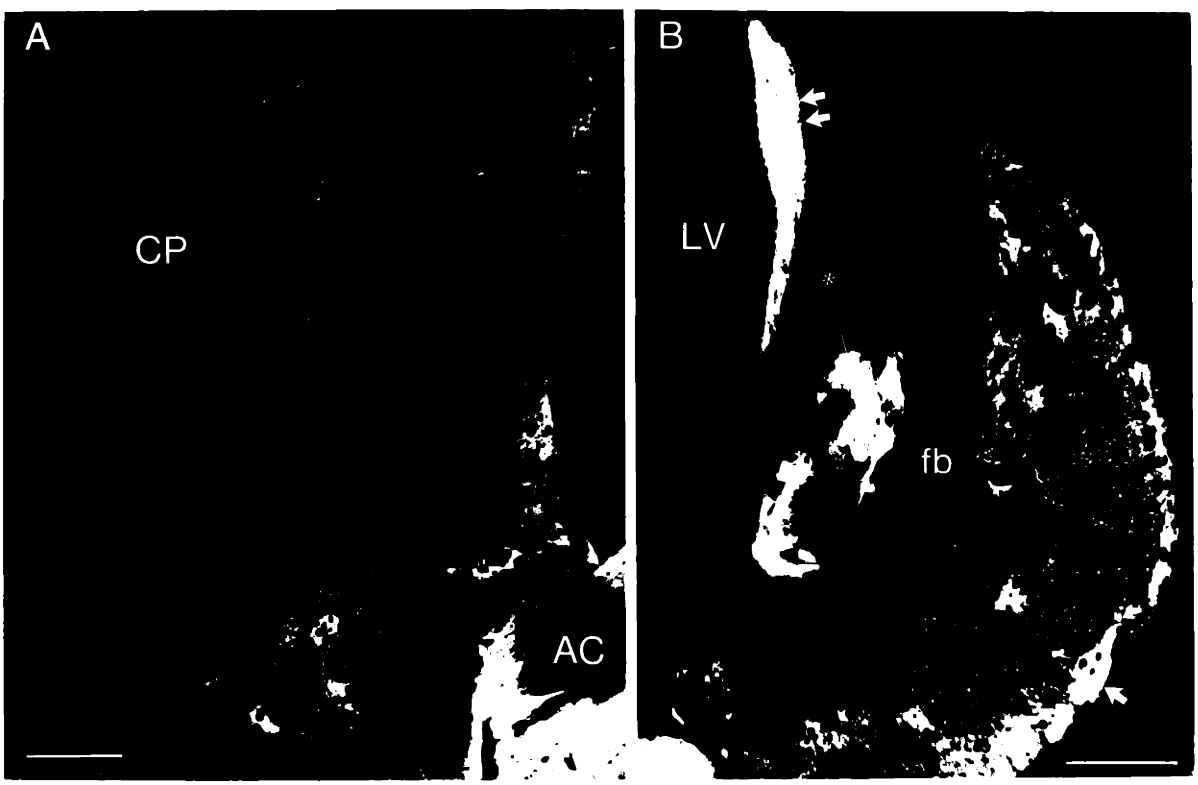
A
CP
AC
B
LV
fb

Figure 5-5. Reverse contrast photographs illustrating the met-enkephalin immunostaining patterns in the normal striatum (A) and a striatal graft placed in the contralateral denervated striatum (B) of case V18. Patches containing high met-enkephalin-like immunoreactivity are distributed unevenly in the denervated graft (e.g., see asterisk). A heterogeneous up-regulation of met-enkephalin-like immunoreactivity is also present in the denervated host striatum ipsilateral to the graft, especially in the region (double arrows) adjacent to the lateral ventricle (LV) and a rim along the ventrolateral striatum (arrow). No such increased met-enkephalin-like immunoreactivity is observed in the contralateral normal striatum except that a few met-enkephalin-rich patches are present in the medial and ventral striatum. LV, lateral ventricle; AC, anterior commissure; CP, caudoputamen; fb, fiber bundles. Scale bars for A and B indicate 500 μm.

Pattern of dopamine- and adenosine 3':5'-monophosphate-regulated phosphoprotein (DARPP-32) immunostaining

DARPP-32-like immunoreactivity was distributed heterogeneously in the control grafts as previously documented by Wictorin et al. (1989c). The destruction of TH-containing nigrostriatal afferents prior to grafting did not perceptibly alter the distribution of DARPP-32-like immunoreactivity in the grafts. Distinct clusters of medium-sized neurons immunoreactive for DARPP-32 were present in the denervated grafts as well as the control grafts (Fig. 5-4). These DARPP-32-positive neurons were very similar to those in the host striatum. Close spatial alignments of DARPP-32-positive patches and patches of medium-sized calbindin-positive neurons in adjacent sections were also observed in both the denervated and the control grafts. A few medium-sized DARPP-32-immunoreactive neurons were scattered outside DARPP-32-positive patches.

Pattern of met-enkephalin immunostaining

Met-enkephalin-like immunoreactivity was distributed unevenly in the normal striatum with a few patches containing met-enkephalin-rich neuropil predominantly in the ventral and medial striatum (Fig. 5-5A). Patches of medium-sized met-enkephalin-immunoreactive neurons with phenotype similar to those in the normal striatum were present throughout the control grafts as previously described (Graybiel et al., 1989). A few of these met-enkephalin-positive patches had higher immunostaining intensity than others. Otherwise, the staining intensity of met-enkephalin-positive patches in the control grafts was similar to that of the regions outside the met-enkephalin-rich patches in the

contralateral normal striatum.

The denervation of the host striatum resulted in a much enhanced heterogeneity in the distribution of met-enkephalin immunostaining in the host striatum. The highest met-enkephalin-like immunoreactivity occurring primarily in the medial part of host striatum adjacent to the lateral ventricle (Fig. 5-5B), as in normal animals (Voorn et al., 1987). Within the denervated grafts, patches of medium-sized met-enkephalin-positive neurons were present. However, the immunostaining intensity of many of these met-enkephalin-positive patches was greatly increased compared to that of the contralateral normal striatum (Figs. 5-5A, 5-5B). The increase of met-enkephalin immunostaining resulted mainly from an increased staining of the neuropil in the met-enkephalin-positive patches. No substantial increase of met-enkephalin immunostaining was observed in regions outside the patches, although some small to medium-sized weakly stained met-enkephalin-immunoreactive cells were present in the NP regions. The met-enkephalin-positive patches in both the denervated and the control grafts were closely aligned with AChE-rich P regions and DARPP-32-positive patches visible in adjoining section.

DISCUSSION

TH-positive fibers of P zones originate from host mesostriatal system

Our findings demonstrate that the selective removal of TH-containing afferents innervating the host striatum prior to introducing embryonic cell suspension grafts results in elimination of all or nearly all the TH-positive patches in the embryonic striatal grafts (see also Wictorin et al., 1989c). This result establishes that the TH-positive fibers innervating the P regions of striatal grafts are derived from the midbrain dopamine-containing cell groups of the host. This finding is in accord with evidence from retrograde tract-tracing studies that striatal grafts can receive innervation by nigrostriatal afferents from the host (Pritzel et al. 1986; Wictorin et al., 1988). A few TH-positive neurons were still scattered in the grafts. Our results suggest that these neurons, although supporting local TH-positive processes, do not contribute in a major way to the TH-positive fiber plexus of P zones.

TH-containing fibers from the host striatum are probably not required for induction or maintenance of the modular organization of striatal grafts

It has been shown that TH-positive fibers appear in striatal grafts before the first appearance of clusters of DARPP-32-positive neurons representing P regions (Labandeira-Garcia et al., 1991). These initial TH-positive fibers are not distributed in a patchy pattern in the grafts. Although subsequent sprouting of fine TH-positive fibers from these initial coarse TH-positive fibers was observed to occur in DARPP-32-positive patches, the initial ingrowing TH-containing fibers from the host striatum may attract a

subpopulation of grafted cells and stimulate them to form P regions in the grafts. With the complete or nearly complete removal of TH-positive fibers in the grafts, however, the modular organization of the grafts, as characterized by the occurrence of patches containing AChE-positive neuropil, medium-sized met-enkephalin-positive, calbindin-positive and DARPP-32 positive neurons, was still present.

This finding strongly suggests that the ingrowing TH-positive fibers from the host striatum are not required for the process either of inducing or maintaining a subpopulation of grafted cells to form P regions in striatal grafts. Target-selectivity has been documented in the dopamine-containing nigrostriatal fibers *in vitro* and *in vivo*. They preferentially innervate the striatal tissue over other types of tissue when given choices both in tissue culture and in intracranial graft condition (Hemmendinger et al., 1981; Denis-Donini et al., 1983; Björklund et al., 1983; Won et al., 1989). If the modular organization in the grafts reflects an admixture of striatal and non-striatal tissue, as we and others previously suggested (Wictorin et al., 1989c; Graybiel et al., 1989), then the fact that ingrowing TH-positive fibers from the host striatum selectively innervate P regions in striatal grafts probably indicates that the TH-containing afferents are attracted to P zone cells rather than the reverse. In fact that TH-containing fibers can be detected in the grafts before clusters of DARPP-32-positive cells does not argue against this possibility. The P regions could have started to form before the expression of DARPP-32 by the neurons of the P zones, and therefore before the invasion of TH-positive afferents. Other cellular mechanisms such as preferential adhesion among striatal cells and repulsion between striatal and non-striatal cells may underlie the formation of P

zones in the grafts.

Expression of cholinergic markers in denervated striatal grafts

It is well established that functional interactions exist between the dopaminergic and cholinergic systems of the mature striatum (for review, see Lehmann and Langer, 1983). Electron microscopic studies have shown close appositions between the TH-containing terminals and ChAT-immunoreactive dendrites and perikarya (Kubota et al., 1987; Chang, 1988; Pickel and Chan, 1990). Furthermore, recent *in situ* hybridization studies have documented that dopamine D2 receptor mRNA is expressed in large striatal neurons, which are the cholinergic interneurons (Brené et al., 1990; Le Moine et al., 1990; Weiner et al., 1991). Our results indicate that removal of incoming TH-containing afferents to striatal grafts does not profoundly change the differentiation process of cholinergic neurons in striatal grafts, because large ChAT-positive neurons characteristic of striatal neurons were still present in the grafts. For technical reasons, we had only limited material in which ChAT-positive neuropil in the grafts could be analyzed. In these limited samples, we could not determine whether the patches of ChAT-positive neuropil in denervated grafts were similar to those found in control grafts innervated by TH-positive fibers. The development of ChAT-positive neurons in the dopamine-depleted developing striatum is unknown, but Brené et al. (1990) have reported that the removal of nigrostriatal afferents of the young adult striatum by 6-OHDA lesions does not alter the level of striatal ChAT mRNA.

Despite this apparent independence of cholinergic neuronal differentiation in the

denervated striatal grafts, the pattern of AChE staining in the grafts (and of ChAT-positive neuropil) was not altogether normal. It has been reported that about 12% of striatal AChE activity is present in the dopaminergic nigrostriatal axons and terminals (Lehmann and Fibiger, 1978). Therefore, the less crisp AChE staining pattern in the denervated grafts may have resulted from removal of AChE activity associated with nigrostriatal afferents. This would not rule out the possibility of postsynaptic changes of AChE activity induced by the destruction of presynaptic TH-containing dopaminergic inputs. AChE in the striatum is associated with neurons (Henderson, 1989) so that second order anterograde effects could also play a part in changes of AChE expression. During normal development, destruction of dopaminergic inputs to the developing striatum in the perinatal period does not profoundly alter the AChE staining pattern in the postnatal striatum (Snyder-Keller, 1991; Liu et al., unpublished observations). Interestingly, however, there are subtle differences in AChE distribution (Liu et al., unpublished observations).

The cholinergic neurons of the striatum are among the earliest born cells in striatal neurogenesis (Semba et al., 1988; Phelps et al., 1989). The majority of them are generated at E12 to E15. However, in contrast to the early expression of DARPP-32 by medium-sized striatal neurons (Foster et al., 1987), ChAT-like immunoreactivity in large striatal neurons in the developing rat striatum is not detectable until E18 (see figures in Armstrong et al., 1987), at which time many TH- and dopamine-containing fibers are already present in the striatal anlage (Specht et al., 1981; Moon Edley and Herkenham, 1984; Voorn et al., 1988). This developmental time-lag of ChAT expression suggests that

the induction of ChAT-like immunoreactivity may be triggered by signals other than those from early-arriving nigrostriatal afferents. It should be noted, however, that a few TH-immunoreactive fibers associated with the scattered TH-positive neurons in the grafts could be sufficient to induce the expression of ChAT-like immunoreactivity, even though these scattered TH-positive cells are not particular associated with the P zones. Interestingly, it has been shown that ChAT activity is increased in striatal tissue co-cultured with ventral mesencephalon (Kessler, 1986).

Expression of DARPP-32 in denervated striatal grafts

One of the most clear-cut findings in the present study is that the expression of DARPP-32 by the grafted neurons in the P regions was not affected by the denervation. Distinct clusters of DARPP-32-immunoreactive neurons still appeared in the denervated grafts, and these were comparable to DARPP-32-positive P zone cell clusters found in grafts maintaining intact dopamine-containing afferents. This result is in good accord with other recent studies of striatal grafts that also demonstrated DARPP-32-immunoreactive neurons in striatal grafts implanted into the dopamine-depleted host striatum (Onteniente et al., 1990; Labandeira-Garcia et al., 1991). These findings suggest that the expression of DARPP-32, a phosphoprotein thought to be associated with dopamine D1 (and/or D5) receptor subtypes (Walaas and Greengard, 1984; Sunahara et al., 1991), is probably not regulated in embryonic striatal grafts by TH-containing afferents from the host striatum.

This striatum situation for striatal grafts is compatible with *in vivo* and *in vitro*

DARPP-32 expression in the developing and mature striatum. The immunoreactivity and biochemical activity of DARPP-32 in the adult rat striatum is not altered by the removal of dopaminergic input in the neonatal period or at adulthood (Luthman et al., 1990; Raisman-Vozari et al., 1990). Furthermore, chronic injections of dopamine D1 receptor antagonist, SCH23390, into adult rats does not change the level of DARPP-32 mRNA (Grebb et al.1990). Clinical study has also documented that DARPP-32 levels in the dopamine deficient striatum of patients with Parkinson's disease are not altered (Raisman-Vozari et al., 1990). Cell culture study has shown that coculturing with mesencephalic cells does not change DARPP-32 levels in striatal cultures (Ehrlich et al., 1990).

All these different lines of evidence suggest that the development and regulation of striatal DARPP-32 are probably independent of the nigrostriatal dopaminergic innervation. It should be emphasized, however, that dopamine-containing nigrostriatal afferents may play a role in the induction of striatal DARPP-32 expression during development. The ontogeny of DARPP-32 expression in striatal grafts has been reported to be delayed about 8 days in grafts placed in the host striatum previously treated with 6-OHDA lesions (Onteniente et al., 1990). Moreover, a few TH- and dopamine-containing nigrostriatal fibers have been shown to invade the striatal primordium as early as E14 (Specht et al., 1981; Moon Edley and Herkenham, 1984; Voorn et al., 1988). As the grafted tissue used in the present study was derived from E15 striatal primordia, we cannot rule out the possibility that such early arriving TH- and dopamine-containing fibers in the donor striatal primordia had pre-conditioning effects on the expression of

DARPP-32 in the grafts. Finally, as mentioned above for the ChAT-positive system of the grafts, TH-immunoreactive fibers from the scattered TH-positive neurons in the denervated grafts could be capable of triggering the expression of DARPP-32 in the grafts. This argument also applies to the calbindin system discussed below.

Expression of calbindin in denervated striatal grafts

It is known that calbindin is compartmentally expressed in the medium-sized neurons of the striatal matrix throughout development and at adulthood (Gerfen et al., 1985; Liu and Graybiel, 1991b). We have previously shown that striatal grafts contain two different populations of calbindin-positive neurons (Graybiel et al., 1989). Clusters of medium-sized calbindin-positive neurons resembling mature calbindin-positive striatal neurons correspond closely to the AChE-rich P regions. By contrast, calbindin-positive neurons in the AChE-poor NP regions have a non-striatal phenotype. Our results clearly demonstrated that the destruction of TH-containing afferents of striatal grafts did not influence the expression of calbindin-like immunoreactivity either by the medium-size neurons of P regions or by the large multipolar neurons of NP regions. This result is compatible with the recent demonstration that denervation of the striatum by perinatal 6-OHDA lesions does not change the pattern of calbindin expression in the developing striatum (Snyder-Keller, 1991).

Expression of met-enkephalin in denervated striatal grafts

Striking effects of dopamine-containing nigrostriatal afferents on the regulation

of striatal neuropeptide expression have been shown in the normal mature striatum (for review, see Graybiel, 1990). For the enkephalinergic system of the striatum, depletion of dopaminergic inputs signalling either by 6-OHDA lesions or by pharmacological blockade with dopamine D2 receptor-selective antagonists results in significant increases of enkephalin levels and of preproenkephalin and proenkephalin mRNAs (Hong et al., 1978; Voorn et al., 1987; Romano et al., 1987; Normand et al., 1987, 1988; Morris et al., 1988; Gerfen et al., 1991). It has therefore been suggested that dopamine-containing nigrostriatal afferents normally exert a tonic inhibitory effect on the enkephalinergic system of the adult striatum.

Our findings demonstrate that the denervation of striatal grafts also results in enhanced met-enkephalin immunostaining in the neuropil of many P zones of the grafts. This suggests that the met-enkephalin-positive neurons in the P regions are under the control of TH-containing afferents from the host striatum, and that the effects of the control are at least qualitatively comparable in that met-enkephalin-like immunoreactivity is enhanced in each striatum by removal of the TH-containing afferents. As the P regions almost certainly represent the striatal tissue in striatal grafts, this region-specific regulation by TH-containing afferents of the enkephalinergic system in the grafts further supports our previous suggestion that the P regions of striatal grafts are the principle zones in which functional integration between the graft and host occurs in the reconstructed striatal circuits (Liu et al., 1990b, 1991b).

This reconstituted system for regulation of enkephalin levels in striatal grafts may be critically important in contributing to the value of intrastriatal grafts in restoring

behavioral defects induced by striatal degeneration. Enkephalin is a principle coexisting neuropeptide in the GABAergic striatopallidal pathway. This pathway, in turn, controls the subthalamic nucleus, whose activity is a critical modulator of activity in the pallidothalamic "release circuit" of the basal ganglia. Reconstituting normal enkephalinergic regulation in striatal grafts could thus help insure normal release function of pallidal outflow pathways.

Chapter 6

Induction of modular patterns of Fos-like immunoreactivity by cocaine in embryonic striatal grafts

ABSTRACT

Cocaine, a catecholamine agonist, has been shown to produce a transient induction of the immediate-early gene c-*fos* and its protein product Fos in the striatum of normal rats. In the present study we report that the expression of Fos can be induced by cocaine challenge in intrastriatal grafts derived from cell suspensions of embryonic striatal primordia. Fos-like immunoreactivity in the nuclei of grafted neurons was detected 2 hr after the injection of 25 or 50 mg/kg cocaine into the host rats. Neurons with Fos-immunoreactive nuclei tended to form clusters in the striatal grafts. The Fos-rich clusters were aligned with acetylcholinesterase (AChE)-rich and tyrosine hydroxylase (TH)-rich patches demonstrated in adjoining sections. The induction of Fos-like immunoreactivity by cocaine is substantially reduced by pretreatment of dopamine D1 antagonist, SCH23390. This suggests that the Fos induction is specific to the regulation of dopamine D1 receptor subtype. Previous studies have shown that presynaptic and postsynaptic cellular markers of the dopaminergic system in the striatum, including immunostaining for TH and dopamine- and adenosine 3':5'-monophosphate-regulated

This chapter is modified from the paper, "Liu, F.-C., S.B. Dunnett, H.A. Robertson, and A.M. Graybiel (1991) Intrastriatal grafts derived from fetal striatal primordia. III. Induction of modular patterns of Fos-like immunoreactivity by cocaine", now in press in Exp. Brain. Res. with permission from the authors.

phosphoprotein (DARPP-32), and binding for high affinity dopamine uptake sites and for dopamine D1 and D2 receptor sites, are all concentrated in the AChE-rich patch regions (P regions) of such embryonic striatal grafts. The preferential expression of Fos in neurons of the P regions of the grafts thus implies that the induction of Fos was cell-type specific in being concentrated in the parts of the grafts that express striatal phenotype and that are innervated by catecholamine-containing fibers. This specificity strongly suggests that the activation of Fos expression in neurons of the P regions of the grafts reflects dopaminergic interactions between the grafts and host nigrostriatal fibers. We conclude that the cellular messenger systems and transcriptional activation mechanisms responsive to dopaminergic stimulation by the host can be activated in the embryonic striatal grafts, and that the grafts are thus functionally integrated into the host brain at the level of cellular signaling systems.

INTRODUCTION

Embryonic striatal transplantation, in which embryonic striatal primordia are implanted into the excitotoxin-damaged striatum, has been studied by several laboratories as a potential model for neuronal replacement therapy for Huntington's disease (for review see Björklund et al., 1987). Such striatal transplants, introduced into adult host rats as cell suspensions, have been shown to survive and to differentiate, and the grafted neurons develop the capacity to express a variety of neurotransmitter-associated substances and to establish selective connections with the host brain (Deckel et al.,, 1983; Isacson et al., 1984; McAllister et al., 1985; Deckel et al., 1986, 1988; Sanberg et al., 1986, 1989; Pritzel et al., 1986; Isacson et al., 1987; Walker et al., 1987; Clarke et al., 1988; Roberts and DiFiglia, 1988; Giordano et al., 1988; Wictorin et al., 1988, 1989a, 1989b, 1989c, 1990a, 1990b; Wictorin and Björklund, 1989; Graybiel et al., 1989; Xu et al., 1989; Sirinathsinghji et al., 1990; Mayer et al., 1990; Liu et al., 1990a, 1990b). Some behavioral recovery has also been demonstrated in animals implanted with such striatal grafts, indicating that the grafts are functionally active (Deckel et al., 1983, 1986, 1988; Sanberg et al., 1986, 1989; Isacson et al., 1986; Giordano et al., 1988; Dunnett et al., 1988).

A fundamental question posed by such grafting experiments is whether the grafts are functionally integrated into the host brain at the level of molecular signaling systems typical of the normal striatum. A promising test of such integration has been suggested by recent studies demonstrating that the immediate-early gene c-*fos* can be transiently induced in some subpopulations of striatal neurons by dopamine agonists (Young et al.,

1989; Johnson and Robertson, 1989; Robertson et al., 1989; Mueller et al., 1989; Graybiel et al., 1990; Moratalla et al., 1990). The induction is dependent on dopamine regulation, because it can be blocked by dopamine antagonists. Cellular constituents of the dopaminergic system, including high affinity dopamine uptake sites and dopamine D1 and D2 receptor binding sites, are present in embryonic striatal grafts (Isacson et al., 1987; Deckel et al., 1988; Mayer et al., 1990; Liu et al., 1990b), and such grafts become innervated by tyrosine hydroxylase (TH)-immunoreactive fibers most probably representing dopamine-containing fibers from the host brain (Isacson et al., 1987; Graybiel et al., 1987a; Clarke et al., 1988; Wictorin et al., 1989b, 1989c; Zhou and Buchwald, 1989; Liu et al., 1990b). As a first approach toward studying the signaling capacity of these reconstituted dopaminergic elements, we tested whether expression of the protein product of the c-*fos* gene, Fos, can be induced in striatal grafts by cocaine treatment of the hosts.

METHODS

The detailed procedure for embryonic striatal grafting has been described elsewhere (Graybiel et al., 1989; Liu et al., 1990b). Hosts (n=11) and donors were Sprague-Dawley rats, as were non-operated animals injected with cocaine (n=2). The grafted rats represent a subset of the animals used in another grafting experiment briefly reported elsewhere (Liu et al., 1990a). Hosts received intrastriatal injections of ca. 2 µl of 10 µg/µl ibotenic acid (Sigma) in the right caudoputamen. Seven to eight days after the initial surgery, single-cell suspensions were prepared from embryonic day 14-16 striatal primordia, and 3 µl of cell-suspension (equivalent to about 1 striatal primordium) were injected into the center of the caudoputamen on the excitotoxin-treated or the intact side.

In the first group of grafted rats (n=6) whose survival times were 13.5-16.5 month following grafting, five of them and the non-operated rats were injected intraperitoneally with 50 mg/kg of cocaine (Sigma), and the sixth grafted rat was injected with saline as a control. In normal rats, the cocaine treatment (25 or 50 mg/kg) results in intense transient activation of c-*fos* in the caudoputamen and expression of Fos-like immunoreactivity in medium-sized striatal neurons peaking at ca. 2 hours post-treatment (Graybiel et al., 1990). The second groups of grafted rats (n=4; survival times 2-6 months after grafting) served as subjects for dopamine D1 receptor blockade experiment. They were injected intraperitoneally with (a) 25 mg/kg of cocaine (n=1), or (b) with a sequential combination of 0.5 mg/kg of SCH23390 30 min before 25 mg/kg of cocaine (n=2), or (c) with the same dose of SCH23390 only (n=1).

Two hours after the cocaine or saline injections or two and half hours after the SCH23390 injections, the animals were deeply anaesthetized with sodium pentobarbital and were perfused transcardially with ice-cold 4% paraformaldehyde in 0.1 M phosphate buffer (PB) (pH 7.4). Brains were cryoprotected with 20% glycerol in PB at 4°C for 24-48 hr and were cut at 20-30 μm in the coronal plane. Adjoining sections from each brain were processed in sequential triplet series for acetylcholinesterase (AChE) activity, for Fos-like immunoreactivity (Graybiel et al., 1990) and for TH-like immunoreactivity.

Immunostaining was carried out by the avidin-biotin-peroxidase method (Vector Labs). Sections were pretreated with 1% H_2O_2 in 0.01 M phosphate-buffered saline containing 0.2% Triton X-100 (PBS-TX) for 10 min followed by 5% normal rabbit serum (NRbS) (for Fos) or normal goat serum (NGS) (for TH) in PBS-TX for 30 min with several intervening rinses in PBS-TX. Sections were incubated in 1:2,000 sheep polyclonal anti-Fos antiserum (OA-11-823, Cambridge Research Biochemicals, Cambridge, U.K.) or 1:240 rabbit polyclonal anti-TH antiserum (Eugene Tech, New Jersey, U.S.A.) containing 1% TX-100, 1 % normal rat serum, 1 % normal secondary serum (NRbS for Fos; NGS for TH) and 0.01 % thimerosal in PBS at 4°C for 24-48 hr. Sections were then incubated in 1:500 biotinylated rabbit anti-sheep IgG or biotinylated goat anti-rabbit IgG in PBS containing 1% TX-100 and normal secondary serum at room temperature for 1 hr, rinsed several times in PBS-TX and incubated in avidin-biotin complex (6 μl A and 6 μl B/ml) in PBS containing 1% TX-100 and normal secondary serum at room temperature for 1 hr. Sections were developed in 0.05% 3,3'diaminobenzidine (Sigma) containing 0.2% ßD(+) glucose, 0.04% NH_4Cl in 0.1 M

PB by adding glucose oxidase (Sigma) to a final concentration of 0.0004%. A few Fos-immunostained sections were counterstained for Nissl substance. AChE histochemistry was processed according to a modified Geneser-Jensen and Blackstad method (Geneser-Jensen and Blackstad, 1971; Graybiel and Ragsdale, 1978).

Controls for the specificity of the immunostaining with anti-Fos antiserum were carried out by incubating sections in the presence of the peptide to which the antibody was raised (OP-11-3210, Cambridge Research Biochemicals) and by incubating sections without the primary antiserum. Our use of the terms Fos-like immunoreactive and Fos-positive refer strictly to staining detectable with the OA-11-823 anti-Fos antiserum.

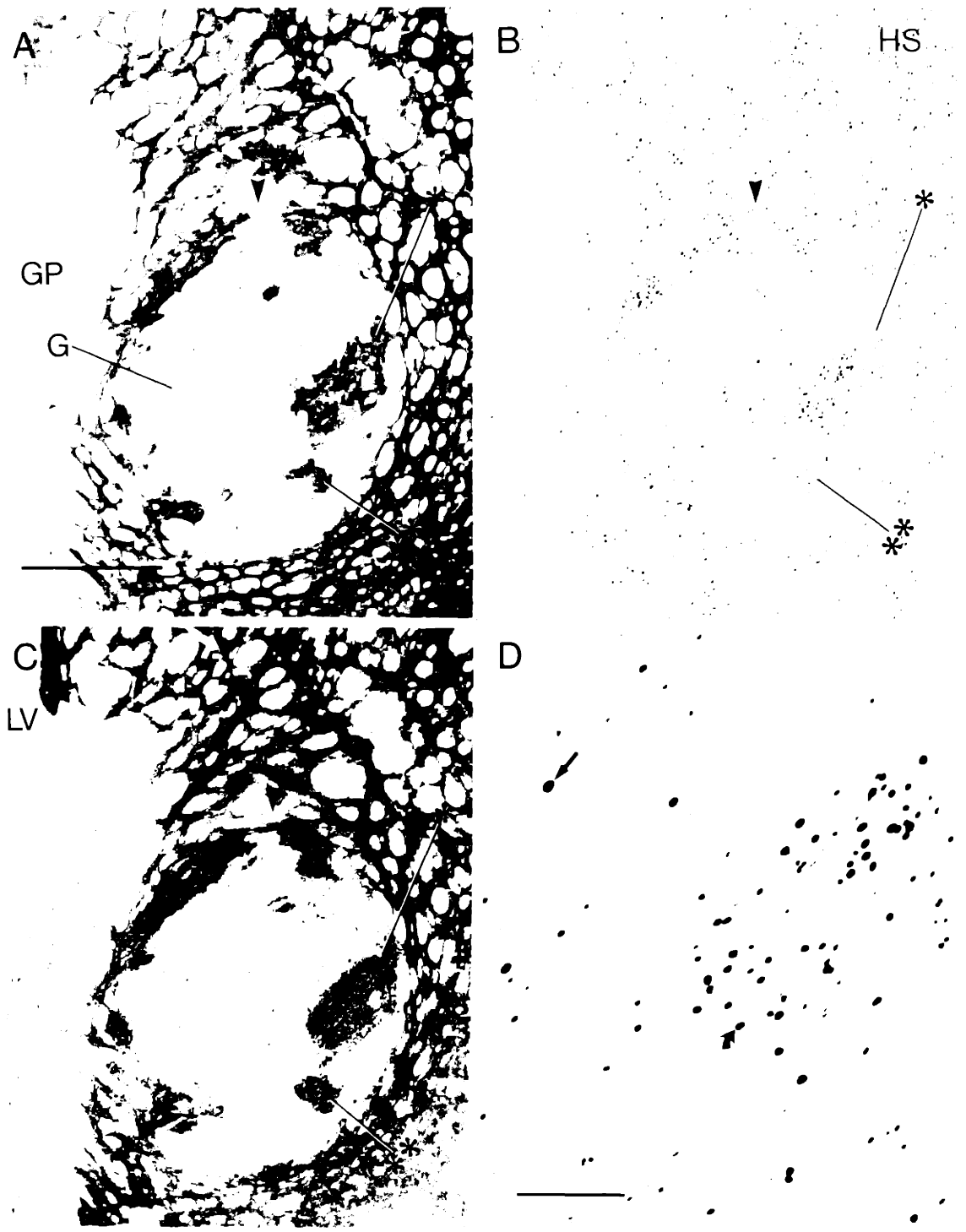
A
GP
G
B
HS
C
LV
D

Figure 6-1: Lightfield photomicrographs of serial sections showing the distribution of AChE staining (A), Fos-like immunostaining (B) and TH-like immunostaining (C) in an embryonic striatal graft (G) placed in the excitotoxin-damaged host striatum (HS) of case RSG4-33 which was treated with 50 mg/kg cocaine. The top of the graft is marked by an arrowhead in each photograph. Each stain has a heterogeneous pattern of distribution in the graft. The patch regions (P regions) of the grafts are identified by their high AChE activity (A) and high TH-like immunoreactivity (C). These P zones have been shown to have a striatal phenotype, unlike the AChE-poor, TH-poor non-patch (NP) regions in which they are embedded. The Fos-immunoreactive neurons tend to form clusters corresponding to AChE-rich and TH-rich P regions. One example of such correspondence is indicated by the single asterisk. A few P regions contain only few Fos-immunoreactive neurons (double asterisks). The arrow in B indicates one of the scattered Fos-immunoreactive neurons lying outside the P regions. LV, lateral ventricle; GP, globus pallidus of the host. D: High magnification lightfield photomicrograph illustrating the region indicated by the single asterisk in Fig. 6-1B, showing Fos-immunoreactive nuclei (e.g., at curved arrow) within a Fos-rich cluster. Some Fos-immunoreactive nuclei were more darkly immunostained than the others. The straight arrow indicates a Fos-immunoreactive nucleus lying outside of the Fos-rich clusters. Photographs of A, B, and C were taken at the same magnification. Scale bar for A-C, shown in A, indicates 500 μm. Scale bar in D, indicates 100 μm.

RESULTS

In all host rats, the grafts survived and were located in the caudoputamen. They varied in size, but all had AChE-rich, TH-rich zones embedded in fields of low AChE- and TH-staining, as described previously (see Figs. 6-1A, C; Graybiel et al., 1989; Liu et al., 1990b). Grafts were larger in the excitotoxin-treated than in the intact host striata.

In each of the animals treated with 25 mg/kg or 50 mg/kg of cocaine, nuclear Fos-like immunoreactivity could be detected in cells of the striatum. In the animals with embryonic striatal grafts, Fos-immunoreactive cells appeared in the grafts as well as in the host striatum. In the saline-treated rat, few Fos-immunoreactive cells were present either in the graft or in the host striatum. Sections incubated in anti-Fos antiserum preabsorbed with Fos peptide or without primary antiserum showed no Fos-like immunostaining. Judging by the appearance of the Fos-positive cells viewed in immunostained sections counterstained for Nissl substance, and by the medium-size of the Fos-immunoreactive nuclei (ca. 8-13 μm in diameter), the Fos-positive cells in the grafts, like those in the host and cocaine-treated normal striatum, were neurons.

There were striking differences in the distributions of Fos-immunoreactive neurons in the grafts and in the host and non-operated caudoputamen of the cocaine-treated animals. In the hosts and non-operated rats, Fos-immunoreactive neurons were distributed relatively homogeneously in the dorsal and medial caudoputamen, as described previously (Graybiel et al., 1990). By contrast, Fos-immunoreactive neurons in the grafts tended to be aggregated in clusters, and there were large regions of the grafts in which a few Fos-immunoreactive neurons were present outside the clusters (Fig.

6-1B).

The clusters of Fos-immunoreactive neurons in the grafts were systematically aligned with AChE-rich and TH-rich patches visible in the adjacent sections. An example of this correspondence is shown in the three serial sections illustrated in Fig. 6-1. One large (ca. 250 by 500 μm) AChE-positive, TH-positive patch and several small AChE/TH-positive patches are visible in the sections flanking the one stained for Fos-like immunoreactivity. Most of the Fos-immunoreactive nuclei in this middle section lie within the large AChE/TH-positive patch, and many of the more scattered Fos-positive nuclei lie in correspondence with the smaller patches.

Fos-immunoreactive neurons were widely dispersed inside some of the patches defined with respect to the adjacent AChE-stained and TH-stained sections through the grafts. For other patches, the Fos-immunoreactive neurons had more limited distributions corresponding only to parts of the AChE-positive, TH-positive patches. Within individual clusters of nuclei expressing Fos-like immunoreactivity, the intensity of Fos-immunostaining varied; some Fos-immunoreactive nuclei were more darkly stained than others (Fig. 6-1D). Such variations in immunostaining also occurred for the Fos-positive nuclei in the host striatum and in the striatum of non-operated rats treated with cocaine. Some AChE/TH-rich patches contained few Fos-immunoreactive neurons (see Figs. 6-1A-1C), but even in regions of the graft in which Fos-immunoreactive neurons were not numerous enough to form clearly defined patches, most of the Fos-immunoreactive neurons could be shown by serial-section comparisons to be preferentially located in the AChE-rich, TH-rich parts of the grafts.

The induction of Fos-like immunoreactivity was greatly reduced by pretreatment of dopamine D1 receptor antagonist, SCH23390. The D1 blockade resulted in disappearance of patches of Fos-positive neurons, and only a few Fos-positive neurons were still present in the grafts and the medial part of host striatum (Fig. 6-2). Injection of SCH23390 alone did not induce Fos-like immunoreactivity in the graft and host striatum except that background levels of few Fos-positive cells were present in the graft and host striatum.

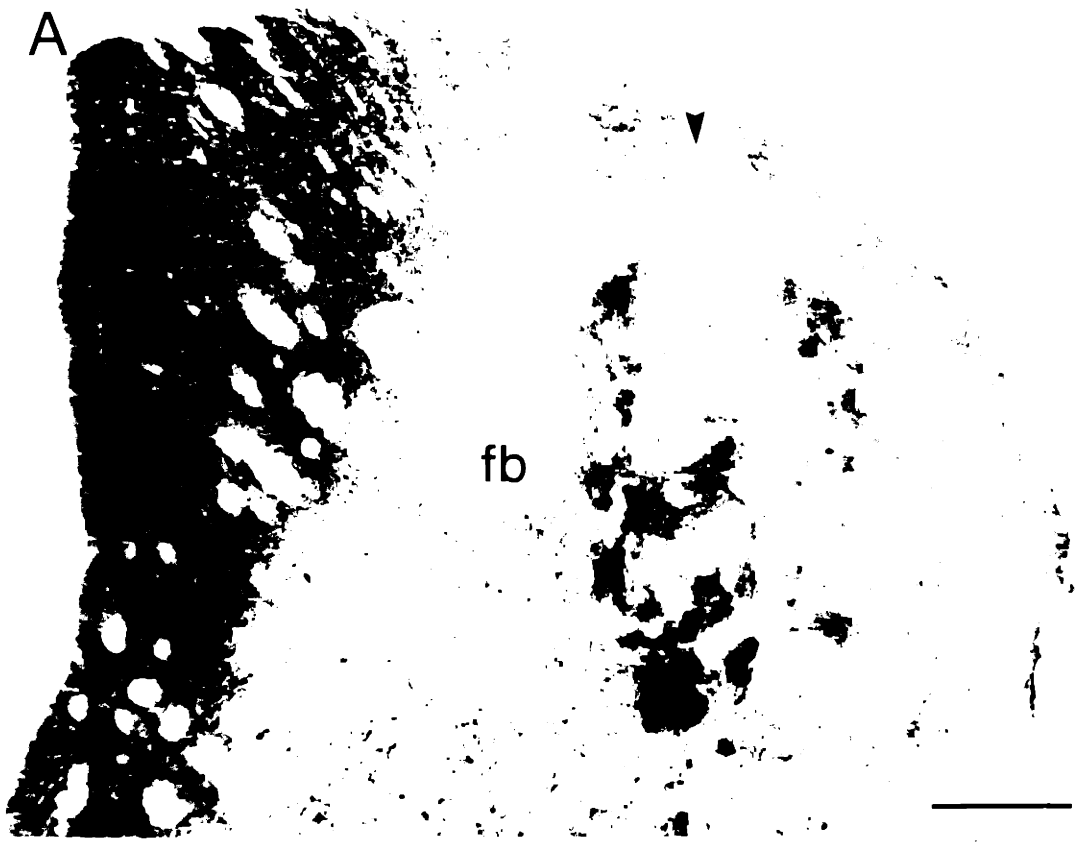
A
fb


B
HS
LV

Figure 6-2: Lightfield photomicrographs of adjacent sections illustrating TH-like immunostaining (A) and Fos-like immunostaining (B) in a striatal graft implanted into a host rat (case RSG7-38) which was pretreated with SCH23390 (0.5 mg/kg) 30 min prior to the injection of cocaine (25 mg/kg). The arrowheads indicate the dorsal margin of the graft in each panel. The D1-selective blockade substantially decreased Fos-like immunoreactivity induced by cocaine (B). No patches of Fos-positive neurons are found in the graft despite the presence of several TH-positive patches in the adjoining section through the graft (A). A few Fos-positive neurons were still present in the grafts (eg., see arrows) and the medial host striatum (HS) adjacent to the lateral ventricle. The curved arrow in B marks the boundary between the striatum and the overlying neocortex. LV, lateral ventricle; fb, fiber bundles. Scale bar indicates 500 μm.

DISCUSSION

These experiments demonstrate that constitutive expression of Fos-like immunoreactivity is low in embryonic striatal grafts implanted into adult host striatum, as it is in the normal mature striatum, and that expression of Fos-like immunoreactivity can be induced in the grafts, as in the normal striatum, by acute administration of cocaine. Our observations further point to marked cell-type specificity of Fos expression within the grafts: the Fos-immunoreactive cells were neurons, and these were concentrated in clusters corresponding to the regions of the grafts expressing high AChE activity and dense TH-like immunoreactivity.

The clustering of the Fos-positive neurons was a key finding. We have previously suggested that the modular organization typical of striatal grafts derived from E15 striatal primordia reflects an admixture of tissue types in such grafts, and that, in particular, the AChE-rich, TH-rich patches (termed P regions) contain tissue with striatal phenotype, whereas the AChE-poor surrounds (non-patch or NP regions) resemble nonstriatal tissue and/or immature striatal tissue (Graybiel et al., 1989; Liu et al., 1990b). We have also demonstrated that neurons in both the P regions and the NP regions of the grafts are indeed derived from donor tissue. Donor neurons pulse-labeled with [^{3}H]thymidine are found in the P and NP regions of embryonic striatal grafts, but not in adjacent host tissue (Graybiel et al., 1989); and conversely, [^{3}H]thymidine labeled neurons of host rats exposed embryonically to [^{3}H]thymidine are almost completely confined to host tissue, including that surrounding embryonic striatal grafts derived from unlabeled donor tissue (Liu et al., 1990a). Thus, the P regions are unlikely to be isolated islands of host striatal

tissue embedded in a sea of donor tissue. They are donor-cell derived and appear to be the main sites in the grafts in which striatal phenotypy is reconstituted. Accordingly, the findings reported here suggest that the activation of Fos expression by cocaine treatment was highly selective for the parts of the grafts resembling striatum. The recent abstract by Cenci et al. (1990) suggests that amphetamine, another indirect dopamine agonist, can also induce Fos in clusters of neurons that correspond to AChE-rich P regions.

It is primarily the P regions that are innervated by TH-immunoreactive fibers (Isacson et al., 1987; Graybiel et al., 1987a; Clarke et al., 1988; Wictorin et al., 1989c; Zhou and Buchwald 1989; Liu et al., 1990b), and it is in the P regions that many of the markers for postsynaptic dopamine-stimulated neurons of the striatum are present (Wictorin et al., 1989c; Liu et al., 1990b). The fact that the dopamine agonist, cocaine, induces Fos expression in neurons with similarly limited P-zone distributions suggests that the induction is largely specific to the parts of the grafts innervated by dopamine fibers and expressing dopamine receptor binding sites.

There were some P regions in which few Fos-positive neurons were present. In normal rats, the induction of Fos expression by cocaine is widespread, but it is more concentrated in the medial and dorsal caudoputamen at caudal levels, as is the induction of c-*fos* (Graybiel et al., 1990). It is conceivable that the P regions containing few Fos-positive neurons consisted of striatal tissue with a relatively low capacity for expression of Fos in response to cocaine challenge.

Cocaine blocks uptake of dopamine and also produces release of catecholamine, but is not thought to activate dopamine receptors directly (Ritz et al., 1987). Thus, it is

likely that the cocaine-induced activation of Fos expression in the striatal grafts resulted from activation of dopamine receptors by dopamine released from the TH-positive fibers innervating the P regions of the grafts. These TH-positive fibers almost certainly derive predominantly from the substantia nigra of the host, as destruction of ascending dopamine-containing nigrostriatal afferents of the host with 6-hydroxydopamine results in the disappearance of TH-rich patches in the grafts despite retention of scattered TH-positive neurons in the grafts (Wictorin et al., 1989c; Liu et al., unpublished observations). Evidence from retrograde tract-tracing studies also suggests that nigrostriatal fibers of the host are capable of reinnervating striatal grafts (Pritzel et al., 1986; Wictorin et al., 1988).

In the normal caudoputamen, cocaine-induced activation of Fos expression can be blocked by the D1 antagonist SCH23390, and the D2-selective antagonist YM-09151 also reduces Fos expression (Graybiel et al., 1990). The result of our D1 blockade experiment suggests that the dopamine receptor selectivity of Fos induction in striatal grafts is similar to that in normal mature striatum because blocking with SCH23390 significantly reduced Fos-like immunoreactivity in the grafts as well as in the host striatum. It is known that SCH23390 also binds to serotoninergic receptor sites (Bischoff et al., 1986), we cannot rule out the possibility that serotoninergic system is involved in the Fos induction in the grafts. Nevertheless, Controls in normal rats suggest that serotonin blockade does not eliminate the Fos response to cocaine (Graybiel et al., 1990), and in striatal grafts, serotonin-positive fibers have been demonstrated to be homogeneously distributed (Wictorin et al., 1988). Thus, the induction of clusters of Fos-

like immunoreactivity in neurons in striatal grafts cannot be fully accounted for by the activation of such evenly distributed serotonin-containing afferents. We did not test D2 receptor selectivity given that D2 antagonist YM-09151 itself would induce Fos expression in the normal striatum (Graybiel., 1990). Interestingly, haloperidol, a D2 receptor antagonist, has been shown to be capable of inducing Fos-like immunoreactivity in embryonic striatal grafts (Dragnow et al., 1990).

It has been documented that dopamine D1 and D2 receptor binding sites, like TH-positive fibers, are mainly confined to the P regions (Isacson et al., 1987; Liu et al., 1990b). The spatial restriction of Fos induction to the P regions thus probably reflects the concentration in these zones of both host-derived dopamine-containing fibers and of donor-derived neurons expressing dopamine receptors. Low concentrations of these fibers and receptor binding sites occur in the NP regions, and this sparseness may account for the weak induction of Fos-like immunoreactivity there.

The immunocytochemical control experiments suggest that the nuclear Fos-like immunostaining induced by cocaine reflected the presence of Fos or other nuclear antigens containing similar peptide sequences (including Fos-related antigens). In normal rats, *in situ* hybridization experiments have demonstrated that the activation of Fos-like immunoreactivity in the striatum is associated with induction of the c-*fos* gene (Graybiel et al., 1990; Moratalla et al., 1990). Interestingly, cocaine administration also induces *jun* B in the striatum, but little c-*jun* at least as detectable by *in situ* hybridization (Moratalla et al., 1990). Thus the program of genomic activation initiated in the striatum by cocaine appears to be specific to some but not other of the immediate-early genes whose

products as known to act in dymeric association as transcription factors.

The functional consequences of this nuclear response to cocaine are not known, but transcription factors of the Fos and Jun families are known to be capable of influencing the expression of other genes, including genes encoding neurotransmitters such as enkephalin, which is present in neurons of the normal striatum and in many neurons of the P regions of embryonic striatal transplants (Sonnenberg et al., 1989; Graybiel et al., 1989; Sheng and Greenberg, 1990). The preferential activation of Fos in the P zones of the grafts does suggest that genomic responses modulated by Fos activation in the grafts may be specific to neurons linking the grafts to the basal ganglia of the host. The P zones of embryonic striatal grafts contain most of the neurons that project to the globus pallidus, a main projection target of the normal striatum (Wictorin et al., 1989b, 1989c). That this linkage is functional is suggested by evidence that striatal grafts can reduce the metabolic hyperactivity induced in the globus pallidus by excitotoxin-induced lesions of the striatum (Isacson et al., 1984) and can partially restore gamma-aminobutyric acid (GABA) release in the host, including stimulation-induced GABA release in methamphetamine-treated rats bearing striatal lesions (Sirinathsinghji et al., 1988).

The novel conclusions of the present study are that embryonic striatal grafts are subject to regulation at the level of gene transcription by catecholamine-containing afferents from the host brain, and that this regulation is exerted mainly in the P regions containing tissue of striatal phenotype. The findings strongly support the suggestion that the P regions are principal zones of information processing in the basal ganglia circuits

reconstructed by embryonic striatal grafting (Liu et al., 1990b). More generally, our observations strengthen the view that embryonic striatal grafts represent neural systems in which the cellular messenger systems and target genes characteristic of normal striatal signaling processings can be generated and functionally integrated into the damaged striatum of adult hosts. Targeted manipulation of gene transcription in such striatal transplants should thus be a promising avenue for influencing graft-host interactions.

Chapter 7

Transient calbindin-D_{28K}-positive systems in the ganglionic eminence and the developing striatum

ABSTRACT

The expression of calbindin-D_{28K} (calbindin), a calcium binding protein, was studied by immunohistochemistry in the ganglionic eminence and developing striatum of prenatal and postnatal rats. We report here that in addition to a steadily increasing expression of calbindin-like immunoreactivity in medium-sized striatal matrix neurons during development (Liu and Graybiel, 1991b), three transient calbindin-positive systems occur in the ganglionic eminence and developing striatum.

First, by embryonic day (E) 18, calbindin-immunoreactive cells begin to appear in the ventricular zone of the ganglionic eminence, and by E20 an extensive array of fine radial calbindin-immunoreactive processes can be traced from the ventricular epithelium, in which many calbindin-immunoreactive cells are now present across the dorsal striatum. Both the calbindin-positive cells in the ganglionic eminence and the radial calbindin-immunoreactive processes are concentrated dorsally and rostrally, and follow steep dorsoventral and rostrocaudal gradients of decreasing calbindin expression. This calbindin-immunoreactive system peaks at P0-P3 and disappears by P15.

Second, a population of calbindin-immunoreactive cells appears transiently in the dorsal and lateral striatum from E20 to P15. These calbindin-immunoreactive cells do

This chapter is modified from the paper, "Liu, F.-C. and A.M. Graybiel (1991a) Transient calbindin$_{28K}$-positive systems in the ganglionic eminence and the developing striatum", now in submission.

not have the phenotype of the common medium-sized neurons of the striatum. They lie scattered among the calbindin-immunoreactive radial processes, and early on may be associated with them.

Third, a system of transient calbindin-positive neuropil patches develops among the array of elongated calbindin-immunoreactive processes, in the dorsal and lateral striatum. These calbindin-immunoreactive patches, about 75-150 μm wide, become visible at about P0, become very prominent at P3, and then fade and disappear by P15. Serial-section analysis showed that these transient calbindin-positive patches lie in spatial register with tyrosine hydroxylase-positive "dopamine islands", the hallmarks of the developing striosomal system of the caudoputamen. The transient calbindin-positive patches were frequently associated with small groups of transient calbindin-immunoreactive cells.

The close spatiotemporal distributions of these three developmentally regulated calbindin-positive systems suggests that there may be interesting interactions among them during phases of cell proliferation and migration in the striatum, and during the early development of striatal compartments.

INTRODUCTION

Calcium ions act as the targets of second messenger systems in neurons and as first and second messengers themselves (Rubin et al., 1985). They participate in critical biochemical events in mature neurons ranging from signal transduction, neurotransmitter synthesis and release, ion channel opening, and activation of kinases, proteases and other enzymes (for review, see Evered and Whelan, 1986; Hidaka et al., 1988). Calcium ions also play important roles in the biochemical mechanisms underlying neuronal development such as migration, outgrowth of neuronal growth cone and differentiation (Walaas and Nairn, 1985; Takeichi, 1988; Kater et al., 1988). The regulation of intracellular calcium levels is thus critical for normal cellular function in the nervous system, and indeed, prolonged increases in Ca^{2+} have been implicated in cell death in the nervous system (Mayer and Westbrook, 1987; Choi, 1988).

One set of candidate molecules for regulation of intracellular Ca^{2+} levels is the superfamily of calcium binding proteins, including calmodulin, oncomodulin, parvalbumin, S-100 proteins, troponin C and calretinin (for review, see Welsh, 1988; Roger, 1989). Many of these calcium binding proteins are expressed in regionally specific distributions in the brain and spinal cord at maturity and during ontogeny, suggesting that they function in relation to regional specifications in neurotransmission and development.

Among these calcium binding proteins, calbindin-D_{28K} (calbindin) had become the focus of special study in the basal ganglia because of two unique properties. First, its expression distinguishes the common medium-sized spiny neurons, the main cell type in the striatum, from other striatal neurons, which do not express calbindin (DiFiglia et al.,

1989). Second, the expression of calbindin distinguishes between neurons in the two main neurochemical compartments of the striatum, the striosomes and the matrix (Graybiel and Ragsdale, 1983): calbindin is constitutively expressed by medium-sized neurons in most of the striatal matrix, but it is expressed by very few striosomal neurons (Gerfen et al., 1985). These patterns are striking because both medium-sized spiny neurons as a population, and extrastriosomal matrix neurons as a subgroup--the two categories distinguished by high calbindin expression in the mature striatum--have been reported to degenerate disproportionately in Huntington's disease (Seto-Ohshima et al., 1988). As noted by DiFiglia and colleagues (1989), the predominantly cytosolic location of calbindin in medium-sized striatal neurons favors the possibility that calbindin could serve to buffer surges of intracellular calcium in normal neurons of this type triggered by glutamatergic corticostriatal fibers acting on NMDA receptors, and this function might be deficient in Huntington's disease (Baimbridge et al., 1982; Seto-Oshima et al., 1988; Iacopino and Christakos, 1990). Excitotoxin-induced death of medium-sized striatal neurons has been documented *in vitro* and is central to some current theories regarding the massive neuronal death that occurs in Huntington's disease (Freese et al., 1988; DiFiglia, 1990). The potential protective role of calbindin against the excitotoxicity has been directly demonstrated in cultured hippocampal neurons by Mattson et al. (1991).

In the study reported here, we set out to determine the development of calbindin expression in the striatum during the perinatal period when, according to our preliminary observations (Liu et al., 1989), medium-sized striatal neurons in large numbers begin to express calbindin and when, according to studies with a large number of neurochemical

markers, the striosome-matrix compartmentation of the striatum becomes identifiable (for review, see e.g. Graybiel, 1984a, 1984b; Foster et al., 1987; Newman-Gage and Graybiel, 1988). This is also a time of substantial cell death in the striatum (Fentress et al., 1981; Fishell and van der Kooy, 1987). We found, to our surprise, that the expression of calbindin during this period is not simply characterized by a gradual appearance of calbindin in medium-sized neurons of the striatal matrix, although, as the second paper of this series documents, such accumulations do occur (Liu and Graybiel, 1991b). There are, in addition, three extensive but transient calbindin-positive systems including (a) a subset of cells of the germinal epithelium of the ganglionic eminence and radial fibers extending from this germinal zone into the striatum, (b) a population of aspiny cells in the caudoputamen, and (c) patches of calbindin-positive neuropil corresponding to dopamine islands, which mark the sets of future striosomes.

METHODS

Embryos and pups from 9 time-pregnant Sprague-Dawley rats (Taconic Farm) were used for brain tissue harvesting. The day of sperm positivity was counted as embryonic day (E) 1 and the day of birth as postnatal day (P) 0. Prenatal specimens were obtained from pregnant rats deeply anaesthetized by an intraperitoneal injection of sodium pentobarbital (Nembutal), and brain tissue was obtained by immersion fixation of heads of embryonic day (E) 13 embryos (n=3) or by perfusing embryos (E14, n=3; E15, n=3; E16, n=4; E18, n=4; E20, n=5) through the transverse sinus or the heart. For all cases the fixative was ice-cold 4% paraformaldehyde containing 5% sucrose in 0.1 M phosphate-buffered saline (PBS) (pH 7.4). For postnatal materials, P0 (n=7), P3 (n=12), P7 (n=6) and P15 (n=3) rat pups and adult rats (n=2) were anaesthetized by cooling on ice (P0 and P3) or by intraperitoneal injection of sodium pentobarbital (P7, P15), and were then perfused transcardially with the same fixative. Heads (E13-E18) or brains (E20-P15) were postfixed in the same fixative at 4°C for 2-12 hr, and then cryoprotected at 4°C for 24-36 hr in 20% sucrose in PBS. Brains or whole heads were cut on a freezing microtome at 40 μm (E13-E20) or 20-30 μm (P0-adult) in the coronal plane. The adult brain tissue (n=4) was obtained from another study (Graybiel et al., 1990).

Immunostaining was performed by peroxidase-antiperoxidase (Sternberger, 1979) or avidin-biotin-peroxidase method (Hsu et al., 1981; Vector Labs). Free-floating sections were pretreated with 3% H_2O_2 and 10% methanol in 0.1 M Tris buffer saline (TBS) (pH 7.4), then rinsed sequentially in 25%, 40%, 25% and 10% ethanol diluted in

TBS. Sections were incubated in 3.3%-5% normal goat serum (NGS) in TBS for 30-60 min, and washed in TBS several times before being placed into primary antisera. The concentrations of primary antisera were as follows: 1:1,000-1:4,000, 1:500 and 1:800, respectively, for rabbit polyclonal anti-calbindin-D_{28K} antisera kindly donated by Drs. P.C. Emson, C.R. Gerfen, S. Christakos; 1:240-500 for rabbit polyclonal anti-tyrosine hydroxylase (TH) antiserum (Eugene Tech, New Jersey); 1:20,000 for mouse monoclonal anti-dopamine- and adenosine 3':5'-monophosphate-regulated phosphoprotein (DARPP-32, antibody kindly provided by Dr. E. L. Gustafson); 1:1 for mouse monoclonal anti-synaptic vesicle-associated protein (SV48, antibody kindly provided by Dr. W.D. Matthew); 1:500 for mouse monoclonal anti-alpha subunit of calcium/calmodulin-dependent protein kinase type II (CCPK II) (6G9, antibody kindly provided by Dr. M.B. Kennedy). All primary antisera were diluted with TBS containing 1% NGS and 1% normal rat serum (NRS) with or without 0.2% Triton X-100. Sections were incubated in primary antisera at 4°C for 24-48 hr. For peroxidase-antiperoxidase immunocytochemistry, sections were washed several times in TBS and incubated in 1:50 goat anti-rabbit IgG (Antibodies Incorporated) containing 1% NGS and 1% NRS in TBS for 1-2 hr and 1:30 or 1:50 rabbit peroxidase-antiperoxidase (Sternberger-Meyer) containing 1% NGS and 1% NRS in TBS for 1-2 hr, with several intervening rinses in TBS. For older tissue (P0, P3 and P7), a double-bridge procedure was followed. Sections were developed in 0.05% diaminobenzidine (DAB) in 0.1 M phosphate buffer (PB) by adding H_2O_2 to a final concentration of 0.0024%. For avidin-biotin-peroxidase complex immunocytochemistry, sections were rinsed in the same buffer, incubated in

1:500 biotinlyated goat anti-rabbit IgG (Vector Labs) containing 1% NGS and 1% NRS in TBS for 1-2 hr, rinsed several times in TBS, and incubated in avidin-biotin complex (6µl A and 6µl B/ml) (Vector Labs) in TBS for 1-2 hr. Sections were developed in 0.05% DAB containing 0.2% ßD(+) glucose and 0.04% NH_4Cl in 0.1 M PB by adding glucose oxidase (Sigma) to a final concentration of 0.0004%. Alternating sets of serial sections from P0, P3 and P7 brains were processed for calbindin and TH immunostaining.

Immunostaining controls for the calbindin immunohistochemistry were performed by incubating selected sections without primary antibodies (sections from all prenatal and postnatal brains) or (sections from E20, P0, and P3 brains) in calbindin antiserum (1:4,000; from Dr. P.C. Emson) preabsorbed with calbindin-D_{28K} protein purified from rat kidney (3.6×10^{-4}M; generously provided by Dr. S. Christakos). A series of antibody dilution tests was also carried out with calbindin antiserum (Dr. P.C. Emson) using ABC immunocytochemistry (E20, P0, P3 brains). The dilutions were 1:1,000, 1:2,000, 1:4,000, 1:8,000, 1:12,000; 1:20,000 and 1:40,000. As the complete series of pre- and postnatal calbindin immunostaining were done with the antiserum provided by Dr. Emson, the data were analyzed primarily according to the immunostaining patterns obtained by this antiserum. Some sections of prenatal brains were stained with cresylecht violet to demonstrate cytoarchitecture.

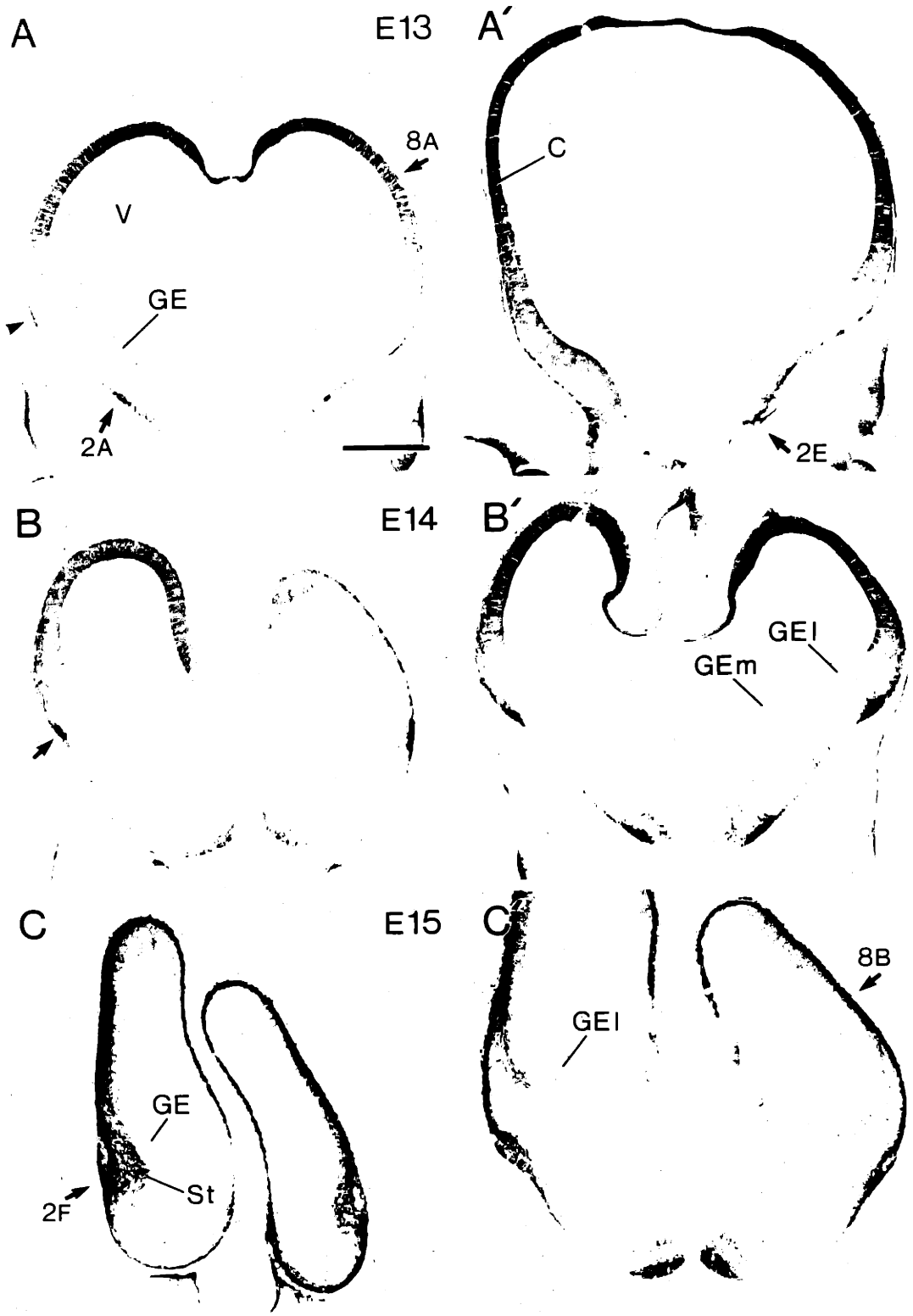
A
E13
A´
8A
C
V
GE
2A
2E
B
E14
B´
GEl
GEm
C
E15
C´
8B
GEl
GE
St
2F

Figure 7-1. Photomicrographs of calbindin immunostaining in coronal sections through the telencephalon of E13 (A, A'), E14 (B, B') and E15 (C, C') rat brains at rostral (A, B, C) and caudal (A', B', C') levels. Regions shown at higher magnification in other figures are indicated by corresponding Figure numbers (8A, 2E, 2F, 8B). A, A': E13, there is a distinct dorsomedial-to-ventrolateral gradient of calbindin immunostaining in the cortical primordium (C). Ventrally, two groups of calbindin-immunoreactive cells are present. One lies in the lateral cortical primordia (arrowhead, presumably pyriform cortical primordium); the second (arrow) is at the base of ganglionic eminence (GE) (see also Fig. 7-2A). The ganglionic eminence itself has very little immunostaining. At caudal levels (A'), a group of large calbindin-positive cells with ramified dendrites (arrow) appears ventrally (presumably in the hypothalamic primordium, see also Fig. 7-2E). B, B': E14, a cleft divides the ganglionic eminence into medial (GEm) and lateral (GEl) bulges. The calbindin-positive pyriform cortical anlage (arrow) now appears lateral to the GEl. The mediolateral gradient of calbindin expression is still evident in the cortical primordium. C, C': Calbindin expression appears throughout the mediolateral extent of the cortical primordium (see Fig. 7-8A), and many calbindin-immunoreactive fibers appear in the intermediate zone of cortical primordium. Laterally, they extend ventrally away from the cortical primordium and appear just under the GEl (C'). The striatal anlage (St) now appears beneath the ganglionic eminence (C). In this region, many calbindin-positive cells are intermingled with calbindin-immunoreactive fibers that appear to emerge from the cortical primordium above (see also Fig. 2F). V, lateral ventricle; Scale bar (for all photographs), 500 μm.

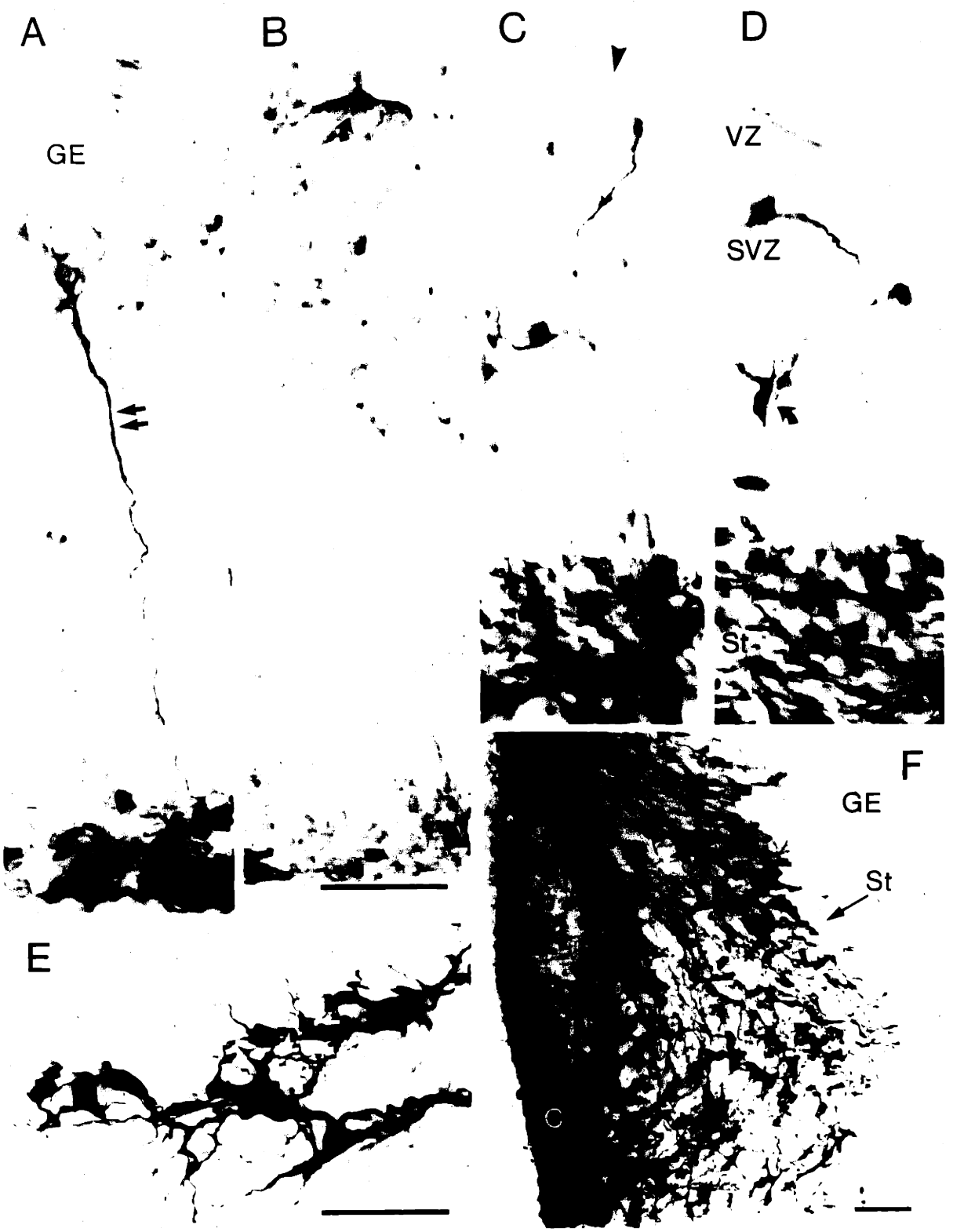
A
B
C
D
GE
VZ
SVZ
St
F
GE
St
E
C

Figure 7-2. Photomicrographs in A-D illustrate calbindin-immunoreactive fibers and cells in the ganglionic eminence (GE). The ventricular zone is shown at the top in each photograph; scale bar for A-D, shown in B, indicate 50 μm. A: High magnification view of the zone indicated by arrow in Fig. 7-1A to show a single calbindin-positive fiber (double arrows) stretching across the E13 ganglionic eminence. Note its swollen end in GE. B: A rare calbindin-immunoreactive cell (curved arrow) appearing in the subventricular zone in the E14 lateral ganglionic eminence. C: A bifurcated calbindin-positive fiber can be traced from the ventricular zone (arrowhead) of the E15 lateral ganglionic eminence toward the striatal anlage that lies below. D: Two curving calbindin-positive fibers in the E15 lateral ganglionic eminence in which a calbindin-immunoreactive cell (curved arrow) is also present. E: Calbindin-positive cells in the region indicated by arrow in Fig. 7-1A' (scale bar, 50μm). These calbindin-positive cells have large perikarya (ca. 15 μm) and thick highly ramified processes. F: High magnification view of the zone indicated by arrow in Fig. 7-1C (E15 embryo). Note the numerous calbindin-positive cells intermingled with calbindin-immunoreactive fibers. This zone lies just ventral to the ganglionic eminence, where the developing striatal anlage merges with the cortical primordium and its underlying white matter. VZ, ventricular zone; SVZ, subventricular zone; St, striatal anlage; C, cortical anlage.

RESULTS

Patterns of calbindin-like immunoreactivity in early telencephalic development (E13-E15)

By E13, calbindin-like immunoreactivity was already distributed in the ventricular zone of the telencephalon along pronounced mediolateral, dorsoventral and caudorostral gradients (Figs. 7-1A, A', B, B'). The highest levels of calbindin expression were in the mediodorsal part of the ventricular zone, where the entire epithelium was intensely stained. Dorsolaterally, calbindin-immunoreactive cells in the ventricular zone were piled up in rows perpendicular to the ventricular surface, and a few tangentially orientated calbindin-immunoreactive cells began to form a thin layer (plexiform primordium or preplate, Uylings et al. 1990). Farther ventrally in the ventricular zone, calbindin-like immunoreactivity was very weak.

In the germinal zone of the ganglionic eminence (GE) at E13 and E14 only a few sporadic cells (Fig. 7-2B) and fibers (Fig. 7-2A) were as strongly immunostained as cells in more dorsal part of the ventricular zone. By El4 the medial and lateral ridges of the GE had formed, and some chains of weakly calbindin-positive cells were found stretching from the ventricular surface toward the base of the lateral GE. These rare calbindin-positive columns were not obviously associated with other calbindin-immunoreactive elements. The lateral GE had perceptible more diffuse immunostaining than the medial GE, but both were very pale. Just lateral to the developing lateral GE, intensely immunoreactive cells began to appear in the developing cortical plate, and as early as E13 the ventral part of the preplate had swollen to form a prominent group of calbindin-

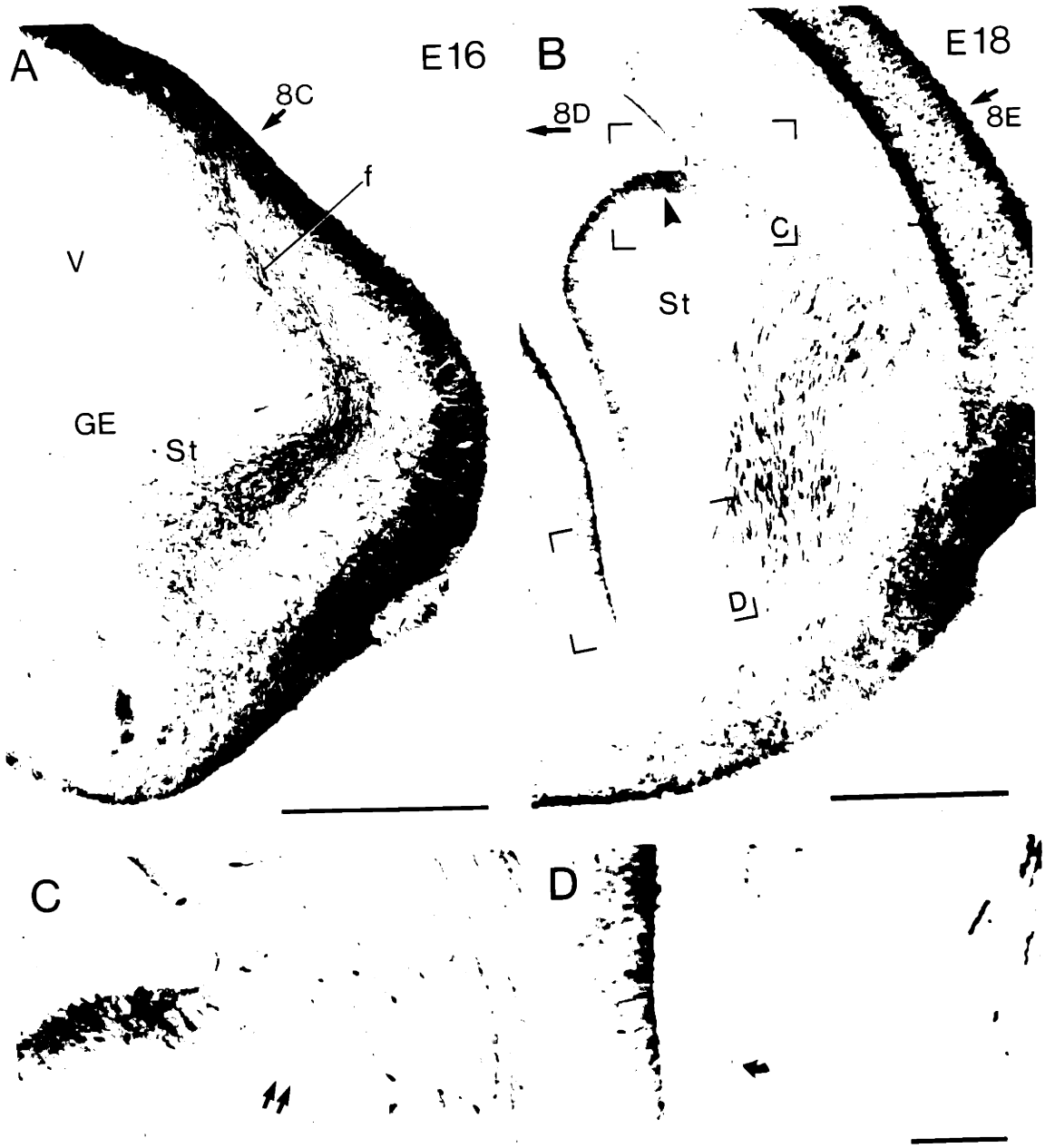
A
E16
8C
f
V
GE
St
B
E18
8D
8E
C
St
D
C
D

Figure 7-3. A and B: calbindin-like immunoreactivity in the E16 (A) and E18 (B) telencephalon. Cortical regions shown at higher magnification are indicated by Figure numbers (8C, 8E, and for medial cortex out of field of view, 8D). Brackets in B show positions of higher magnification photomicrographs shown in C and D. Very little calbindin-like immunoreactivity is detectable in the germinal epithelium of the ganglionic eminence (GE) at E16, but by E18, there is a distinct dorsoventral gradient of calbindin expression in the ganglionic eminence. Calbindin expression has begun to emerge in a group of cells (arrowhead) in the dorsal part of germinal epithelium of the GE (B, C). Some weakly-stained fine calbindin-immunoreactive processes appear to stretch from this calbindin-positive zone across the junction between the cortical primordium and the GE (see arrows in C). Decreasing levels of calbindin-like immunoreactivity appear in the ventral part of the germinal epithelium of the GE, to the foot of the lateral ventricle. A second gradient of ventricular zone expression appears along the ventricular wall of the septal primordium (B, D). Note that many calbindin-positive fibers (f) now extend from the dorsolateral cortical primordium through the base of the striatal anlage (St). By E18 (B), these fibers come to form distinct fascicles. Scale bars for A and B, 500 μm, for C and D, 100 μm.

positive cells (Fig. 7-1A, A', B, B'). This group probably corresponds to the anlage of the pyriform cortex. Ventral to the medial GE, two other prominent groups of calbindin-positive cells piled up (Fig. 7-1B'). The medial group lay near the base of the third ventricle, apparently in the hypothalamic primordium. Some of the cells associated with this group were extremely large and highly ramified (Figs. 7-1A', 7-2E). Such calbindin-positive giant cells were found as early as E13.

Starting from E15, many tangentially oriented calbindin-immunoreactive fibers appeared in the intermediate zone of the cortical primordium, and increasing numbers of calbindin-immunoreactive fibers could be traced from the lateral cortical anlage toward the growing striatal anlage (Figs. 7-1C, C'). When these fibers reached the striatal anlage associated with the lateral GE, they became intermingled with a group of fusiform calbindin-immunoreactive cells that were present there (Fig. 7-2F). A number of the calbindin-immunoreactive fibers appeared to turn at acute angles to invade the subventricular zone of the lateral GE (Fig. 7-2C, 7-2D). Some but not all these fibers emerged from cell bodies in this region. Other calbindin-immunoreactive fibers extended as far as the medial GE (Fig. 7-1C'). Calbindin-immunoreactive fibers were continuously present in the striatal anlage from E16 on (Fig. 7-3A), and began to form fiber fascicles at E16-E18 (See below and Fig. 7-3B).

Emergence of calbindin expression in the ganglionic eminence and development of transient calbindin-immunoreactive radial processes in the striatal anlage

A sharp increase in expression of calbindin-like immunoreactivity in the

ventricular zone of the GE began after El5. At El6 (Fig. 7-3A), most of the GE still had very little calbindin, but a transition to heightened expression began to appear at the dorsal margin of the lateral GE. In the following days a wave of calbindin expression spread from this dorsal zone farther ventrally along the ventricular and subventricular zones of the GE, maintaining strong dorsoventral and rostrocaudal gradients in the GE as described below. Ventrally, at the foot of the lateral ventricle, a second transient wave of calbindin expression developed in the germinal epithelium lining the medial side of the lateral ventricle. A striking dorsoventral gradient of calbindin-like immunoreactivity was present in the ventricular zone of GE at E18 (Fig. 7-3B). By this time,lateral and medial bulges could no longer be distinguished, but in the dorsal part of the ventricular zone of the GE, throughout its anteroposterior extent, intensely calbindin-immunoreactive cells appeared singly and in vertically aligned pairs, or, rarely, in multicellular radial columns (Fig. 7-3C). The dorsal cells of this calbindin-immunoreactive population were associated with weakly stained calbindin-immunoreactive processes that extended from the ventricular zone through the subventricular zone, across the striatal anlage, and beyond it into the deep white matter separating the developing striatum from the cortical primordium (Figs. 7-3B, 7-3C). These calbindin-immunoreactive fibers gave the impression of forming a sharp border between the pallial epithelium and white matter above, and the ganglionic eminence and striatal anlage below. Along more ventral parts of the ventricular zone of the GE, there were progressively fewer calbindin-positive cells, and they were progressively more restricted to the superficial part of the ventricular zone. Very little calbindin-like

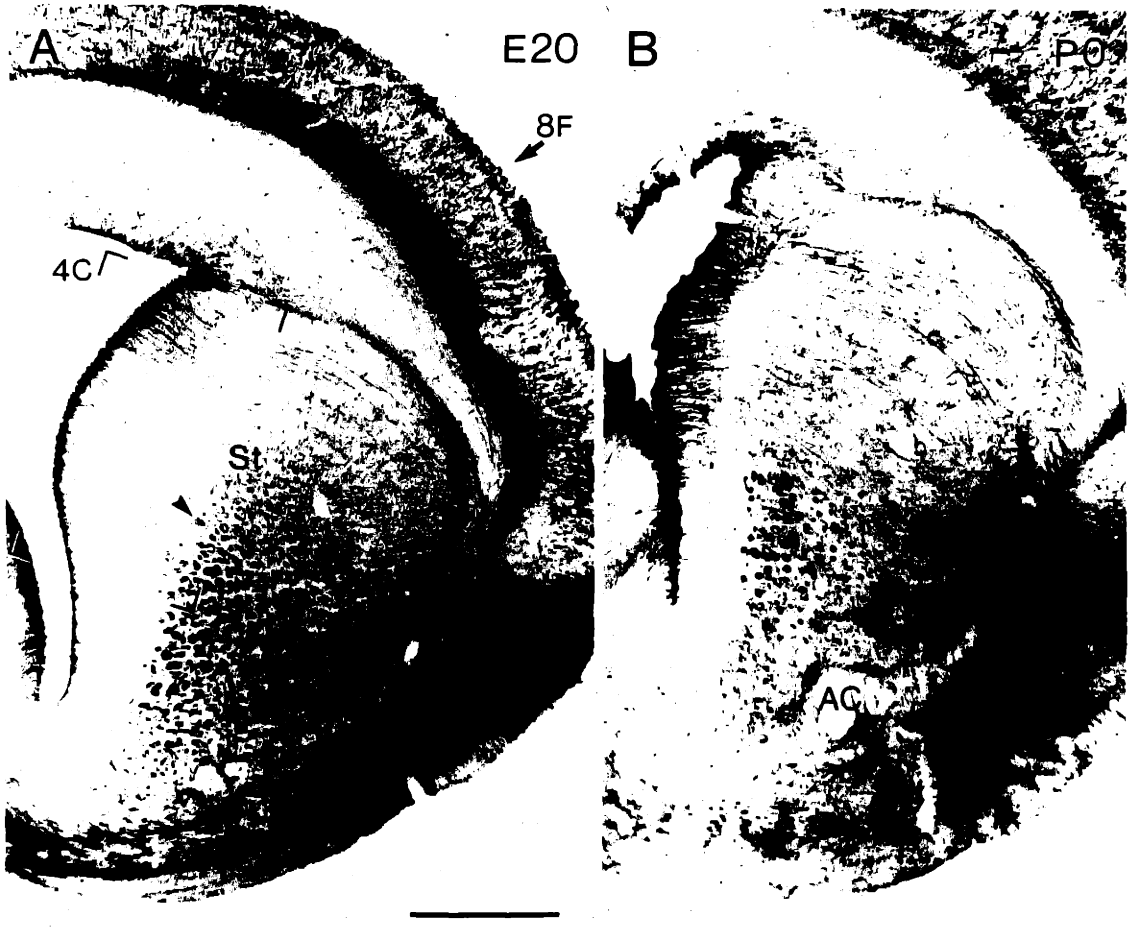
A
E20
B
P0
8F
4C
St
AC

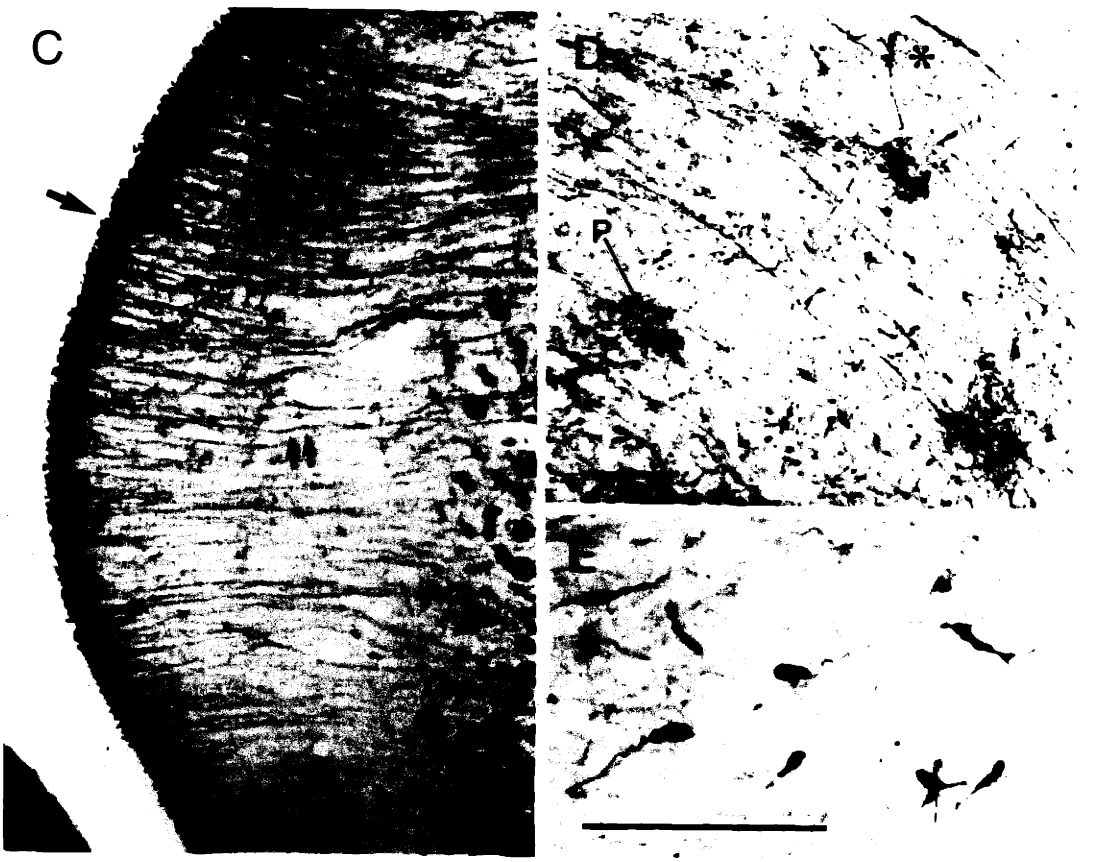
C
D
P
E

Figure 7-4. Calbindin immunostaining patterns in E20 (A) and P0 (B) telencephalon. There is a pronounced dorsoventral gradient calbindin expression in the ventricular and subventricular zones of the ganglionic eminence. Dorsally, many radial calbindin-immunoreactive processes stretch from the ventricular zone into the dorsal part of developing striatum (St), some reaching as far as the external capsule. These processes are fully developed by P0, at which time they have invaded the striatum more ventral parts of the caudoputamen as well. There is also more extensive calbindin expression in the dorsal ganglionic eminence. C: high magnification view of the region bracketed in A, illustrating calbindin-immunoreactive processes (example at double arrows) in the dorsal germinal epithelium (arrow) in which numerous calbindin-positive cells are also present. D: In the P0 caudoputamen, patches of calbindin-positive neuropil (example at P) are present dorsally in addition to the radial calbindin-positive processes (see also B). The calbindin-immunoreactive radial processes arch through the calbindin-positive patches. See also photomontage in Fig. 7-5; asterisks in D and in Fig. 7-5 mark corresponding locations. Calbindin-positive cells are frequently associated with the patches. The morphology of these fusiform and multipolar calbindin-positive cells in the dorsal caudoputamen is illustrated in E. Note that by E20, numerous calbindin-immunoreactive bundles appear in the ventral striatum (see matched arrowheads in A and C). AC, anterior commissure. Scale bars for A and B, 500 μm, for C-E, 100 μm.

immunoreactivity was present in the ventral third to one-half the ventricular zone (Fig. 7-3D).

By E20 (Fig. 7-4A), there was intense calbindin-like immunoreactivity in the ventricular zone of the GE and a strong development of radially organized calbindin-immunoreactive processes stretching away from the epithelium into the striatal anlage. The dorsoventral gradient in calbindin expression in the germinal zone was still prominent. In the dorsal part of the ventricular zone, there were layers of intensely calbindin-immunoreactive cells, but both the numbers and staining intensity of the epithelial cells and their depth distribution in the epithelium decreased ventrally. There was also a pronounced rostrocaudal gradient in calbindin expression in the ventricular zone. Rostrally the calbindin-positive cells were more piled up within the zone, and extended farther ventrally than calbindin-positive cells at caudal levels.

The long calbindin-immunoreactive processes emerging from the ventricular zone were also best developed dorsally and rostrally. They appeared through most of the height of the rostral striatal anlage, but farther caudally they were restricted primarily to its dorsal half. In these dorsal regions, the immunostained processes formed parallel arcs stretching through the subventricular zone and across the dorsal striatal anlage, bending in parallel with the curving dorsal surface of the striatum (Fig. 7-4A). Some of these calbindin-immunoreactive processes could be traced from the ventricular epithelium as far as the external capsule (Fig. 7-4C). The dorsal-to-ventral and rostral-to-caudal decline in the number of such calbindin-immunoreactive processes paralleled the decline in staining of cells in the ventricular zone. The calbindin-immunoreactive processes were


VZ
SVZ
St
a
b
a
b

Figure 7-5. A montage of photomicrographs from a P0 brain illustrating transient calbindin-immunoreactive processes arching across the dorsal caudoputamen, and showing the spatial relationships of these processes and the transient calbindin-positive cells of the dorsal caudoputamen. The montage is oriented dorsal-up, medial-left and follows the curve of the processes. The upper and lower parts of the montage overlap as indicated by fiducial marks (line segments). Many calbindin-positive processes stretch from the ventricular zone (VZ), which is intensely immunoreactive for calbindin, across the subventricular zone (SVZ) and dorsal striatum (St) to the external capsule (just beyond the right hand end of the montage). Note that some of the processes are packed together closely to form fasciculi (example at double arrowheads). Many of the calbindin-positive processes can be followed continuously from the germinal epithelium into the caudoputamen proper. Two examples are indicated by fascicles a/a' and b/b'. Many transient calbindin-immunoreactive cells are scattered among this array of elongated calbindin-immunoreactive processes. Some of them appear to be directly on the calbindin-positive processes (examples at double curved arrows). The asterisk indicates denotes corresponding site illustrated in Fig. 7-4D. Scale bar, 100 μm.

best stained in sections treated with Triton X-100. Without Triton X-100 treatment, they tended to have vague outlines, could not be traced well in continuity, and had a reduced spatial extent.

The calbindin-immunoreactive radial processes were fully developed at P0. As shown in Fig. 7-4B, they formed dense parallel arrays and fascicles emerging from the ventricular epithelium, where there were numerous cells immunoreactive for calbindin, and some could be traced through the full width of the caudoputamen. The calbindin-positive germinal cells and radial processes were still most prominent in the rostral and dorsal caudoputamen, and gradually decreased in number and in staining intensity of immunoreactivity caudally and ventrally. Even at levels where the processes were numerous, they did not appear in the ventral part of the caudoputamen in which a lattice-work of calbindin-immunoreactive medium sized striatal neurons was forming (Liu and Graybiel, 1991b).

The calbindin-positive radial processes were still very prominent at P3 (Fig. 7-6A), and some occurred far enough ventrally to pass through the calbindin-positive band located at the ventrolateral edge of the rostral caudoputamen. At mid-striatal levels, however, only a few weakly stained calbindin-immunoreactive processes remained, and they disappeared altogether in the caudal caudoputamen. The immunostaining for calbindin in the ventricular epithelium also progressively decreased from rostral to caudal and dorsal to ventral.

Transient appearance of calbindin-immunoreactive cells and calbindin-positive patches in the perinatal striatum

As the development of the calbindin-positive GE cells and radial processes was reaching its peak, the two other transient systems of calbindin-immunoreactive elements in the striatal anlage appeared for the first time. The first of these was a set of calbindin-immunoreactive cells first detected at E20 primarily in the lateral striatal anlage (Fig. 7-4A) and found as late as P15. At E20, some of these cells seemed to be associated with the radial calbindin-positive processes described above (Fig. 7-5). By P0, many calbindin-immunoreactive cells were scattered in the rostrodorsal caudoputamen and in the dorsal and lateral parts of the middle and caudal caudoputamen (Figs. 7-4B, 7-5). Some cells were small to medium-sized cells (diameter, ca. 6-12 μm) whereas others had larger perikarya (diameter, ca. 13-18 μm) with ramified immunoreactive dendrites lacking detectable spines (Fig. 7-4E). Few such larger cells were found in the ventral part of the caudoputamen. These calbindin-positive cells were scattering between and alongside the calbindin-immunoreactive radial processes, and some of the calbindin-positive cells were attached to the processes (Figs. 7-4D, 7-5). We could not, however, find a consistent relationship between the orientations of the dendrites of calbindin-immunoreactive cells and the processes. These cells were prominent dorsally until P3, and then gradually disappeared.

The second transient calbindin-immunoreactive system was made up of calbindin-immunoreactive patches ca. 75 to 150 μm wide dispersed in the same regions as the calbindin-immunoreactive cells (Fig. 7-4B). The patches were first visible at P0,


A
B
P3
AC
C

Figure 7-6. Serial sections through the P3 striatum showing the immunostaining patterns for calbindin (A, C) and TH (B). The calbindin-immunostained sections A and C were processed identically except that section A was pretreated with TX-100 while section C was processed without TX-100. The transient calbindin-immunoreactive patches (example at asterisk) and processes in the caudoputamen are evident in the section treated with TX-100 (A), but these transient calbindin-positive patches and processes are only very weakly stained in section processed without TX-100 (C, see corresponding asterisk). The transient calbindin-positive patches visible in A are aligned with TH-positive dopamine islands in the adjoining section (B). Note that the strong calbindin-positive patchwork in the ventrolateral striatum (double asterisks in C) is part of the developing permanent calbindin-positive mosaic system described in the accompanying report (Liu and Graybiel, 1991b). AC, anterior commissure. Scale bar, 500 μm

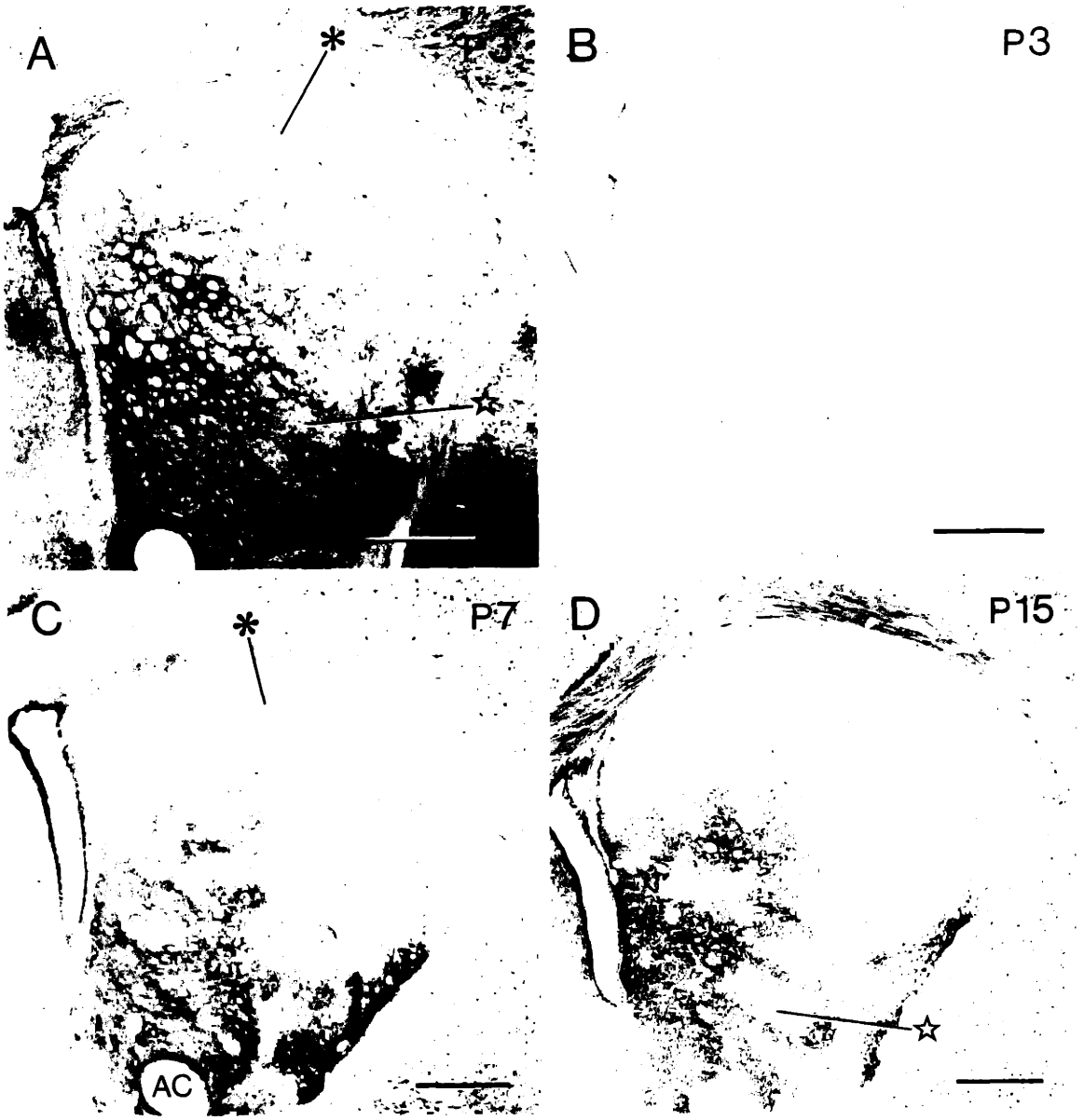
A
B
P3
C
P7
AC
D
P15

Figure 7-7. A & B: A pair of sections through the P3 caudoputamen demonstrating the specificity of the calbindin immunostaining obtained with the calbindin antiserum provided by Dr. P.C. Emson. The section in A was incubated with this antiserum at 1:4,000. Asterisk in A indicates a transient calbindin-positive patch. The section B was incubated with the same 1:4,000 calbindin antiserum preabsorbed with calbindin protein purified from the rat kidney (Dr. S. Christakos). The preabsorption procedure almost completely eliminates the immunostaining in the striatum and the neocortex. C & D: Disappearance of the transient calbindin-positive systems in the P7 (C) and P15 (D) striatum. In the P7 brain (C), a few transient calbindin-positive processes, cells and patches are only faintly stained, even with the standard staining protocol including TX-100 pretreatment (a faintly stained patch is marked by the asterisk). By P15, these transient calbindin-positive systems have disappeared except for a few transient calbindin-immunoreactive cells. The developing permanent calbindin-positive mosaic system appears in the ventral part of striatum. A typical calbindin-poor zone in this mosaic is indicated by the star (see Liu and Graybiel, 1991b). AC, anterior commissure. Scale bars for A, B, C, D, 500 μm.

peaked at P3 and disappeared after P15. They appeared to be made up largely of a fine-fibered calbindin-immunoreactive neuropil, but many of the scattered calbindin-immunoreactive cells were also associated with these patches (Fig. 7-4D). Some of the calbindin-immunoreactive radial processes ran through the calbindin-immunoreactive patches. Both the scattered calbindin-immunoreactive cells and the calbindin-immunoreactive patches were prominent in the dorsal and lateral parts of caudoputamen at P3. The calbindin-positive patches were clearly set off from the now intensely immunostained permanent calbindin-positive mosaic of medium sized striatal cells developing ventrally (Figs. 7-6, 7-7, and see Liu and Graybiel, 1991b). Altogether, the transient calbindin-positive patches formed a dorsolateral system that was roughly co-distributed with the region containing the transient calbindin-positive cells.

It was necessary to treat sections with Triton X-100 to obtain clear staining of the calbindin-immunoreactive patches (Fig. 7-6A). Without Triton X-100 treatment, the calbindin-immunoreactive patches were at most weakly stained (Fig. 7-6C) and in some sections not visible at all.

Correspondence of transient calbindin-positive patches and dopamine islands

The system of calbindin-positive patches was strongly reminiscent of the "dopamine island system" of the developing caudoputamen even in the detail of including rim of calbindin-immunoreactivity along the dorsolateral margin of the caudoputamen (Figs. 7-6, 7-7). To compare the locations of the calbindin-immunoreactive patches and dopamine islands directly, we studied serially aligned pairs and triplets of sections

consecutively stained for calbindin-like immunoreactivity and for TH-like immunoreactivity (P0, n=7; P3, n=12; P7, n=6; P15, n=3) or, in P3 and P7 cases (n=1 for each age), for three other markers of dopamine islands (DARPP-32, SV48 and CCPK II immunoreactivity) (Foster et al., 1987; Newman-Gage and Graybiel, 1988). In the P0 brain, the structure of the patches changed too rapidly in adjoining sections to allow secure comparisons, but serial-section analysis was possible beginning at P3. The calbindin-immunoreactive patches were closely aligned with TH-positive patches in adjacent sections, and there were few TH-positive patches that lacked corresponding calbindin-immunoreactive patches (Figs. 7-6A, 7-6B). Similar alignments were found for the calbindin patches and islands stained for DARPP-32, SV48 and CCPK II (data not shown).

TH-positive dopamine islands were still visible at P7, and continued alignment of the calbindin-positive patches and dorsal islands was confirmed. By P15, however, TH-like immunoreactivity in the extra-islandic matrix had greatly increased so much that only rarely could matches be attempted between the nearly faded calbindin-immunoreactive patches and the island system.

Postnatal decline of the transient calbindin-positive systems of the striatum

The scattered calbindin-immunoreactive cells and patches lingered slightly longer than the calbindin-immunoreactive GE cells and radial processes. A few calbindin-immunoreactive cells and weak calbindin-immunoreactive patches were still present in the rostrodorsal caudoputamen and the dorsal and lateral parts of the middle and caudal

caudoputamen at P7 and P15 (Figs. 7-7C, 7-7D), but they were not detected in the mature caudoputamen. By P7, only a few calbindin-immunoreactive processes remained in the most rostral part of the caudoputamen. Calbindin-like immunostaining was also dramatically reduced in the ventricular epithelium by P7, even far rostrally. No calbindin-immunoreactive processes could be detected in any part of the caudoputamen by P15 (Fig. 7-7D). Some of the cells of the ependyma were still stained, however, in regions adjoining calbindin-positive parts of the striatum.

Changing patterns of calbindin-like immunoreactivity in the fiber bundles of the caudoputamen

During the time that the transient calbindin-positive processes, cells and patches emerged in and then disappeared from the developing caudoputamen, a marked change in calbindin expression was apparent in the fiber fascicles that penetrated the striatum from its lateral side and then organized to form the dispersed fiber bundles typical of the mature rodent caudoputamen (see Figs. 7-3A, 7-3B, 7-4A, 7-4B). As the striatal anlage increased in size, intensely calbindin-immunoreactive fibers sweeping between the developing cortical plate and the deepest part of the corona radiata became incorporated in the lateral striatum, and by E20, these calbindin-immunoreactive fascicles aggregated to form calbindin-immunoreactive bundles squeezed into the medial and ventral part of developing striatum (Figs. 7-4A, 7-4C). The most dorsal of these calbindin-immunoreactive bundles, seen in cross-section, consisted of calbindin-immunoreactive rings around calbindin-poor centers. The more ventral bundles contained calbindin-

immunoreactive fibers throughout. At P0 (Fig. 7-4B), the calbindin-positive bundles were mainly confined to the ventral part of the caudoputamen, and they could be detected in this ventral position at rostral levels at P3 and P7 before disappearing by P15. By contrast, at P15 many weakly stained small calbindin-immunoreactive bundles began to appear in the dorsal and lateral caudoputamen (Fig. 7-7D). They were not found in the mature caudoputamen.

Immunohistochemical controls

Controls for the specificity of immunostaining suggested that calbindin-like immunoreactivity observed in the GE and in the striatum reflected authentic calbindin-D_{28K} or a closely related antigen. Sections incubated without primary antiserum had no immunostaining. The preabsorption control sections, taken from a P3 brain to show the effects on each of the three transient calbindin-positive systems (Fig. 7-7B), showed that immunostaining in the striatum and in the GE was virtually abolished by the addition of calbindin-D_{28K} protein, as was nearly all staining in the developing cortex (see also below). Interestingly, calbindin-immunoreactive neurons were still present in the basal forebrain, though compared to basal forebrain neurons in non-control sections processed at the same time, these neurons were weakly stained. Finally, the intensity of calbindin immunostaining in all regions decreased as the concentration of primary antiserum decreased.

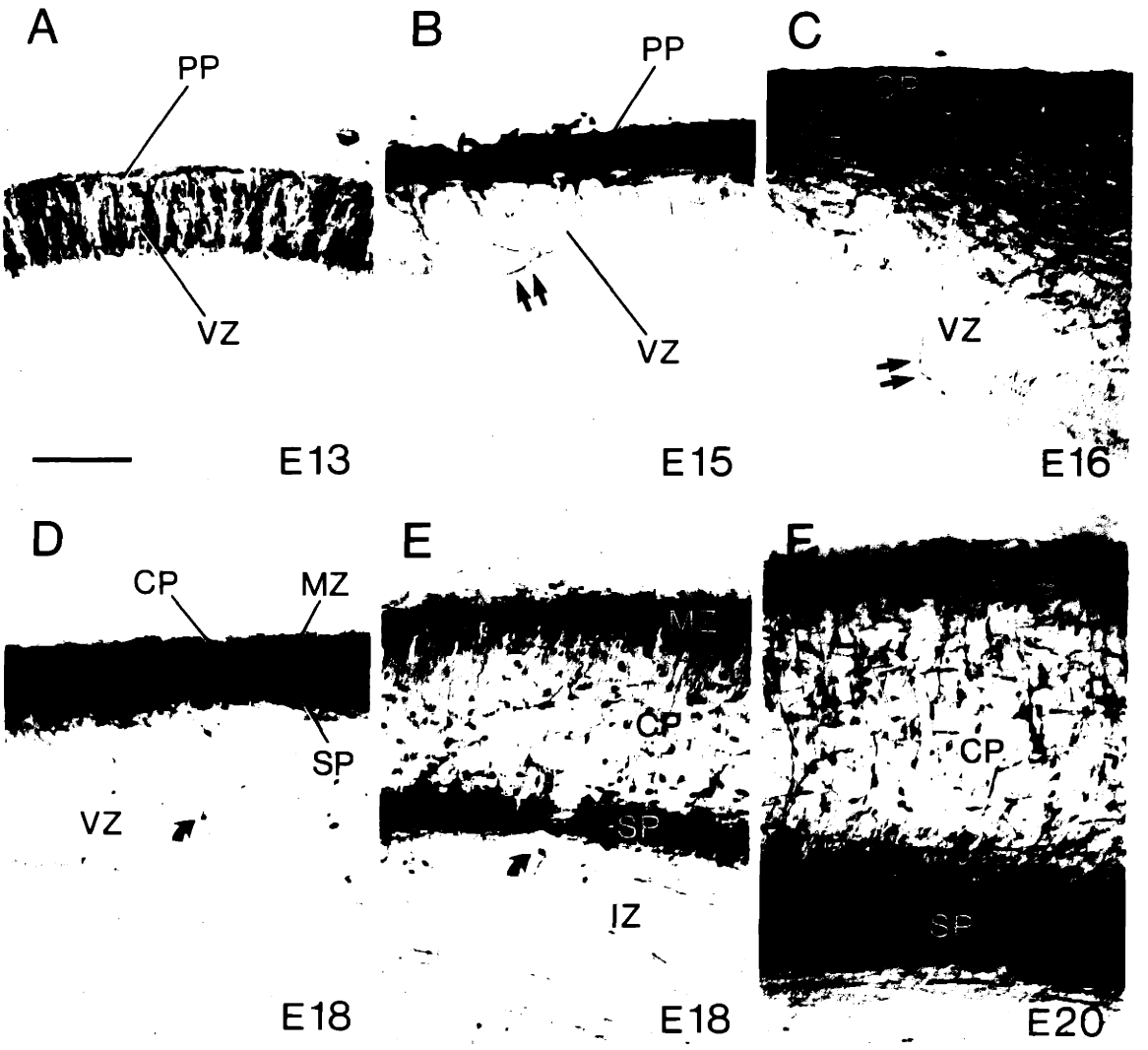
A
PP
VZ
E13
B
PP
VZ
E15
C
CP
VZ
E16
D
CP
MZ
SP
VZ
E18
E
MZ
CP
SP
IZ
E18
F
CP
SP
E20

Figure 7-8. A series of photomicrographs of the developing neocortex, taken at the same magnification to illustrate the sequential division of a single calbindin-positive cortical anlage into calbindin-positive cortical subplate and marginal zones. The zones illustrated are from the regions indicated by arrows in Figs. 7-1A, 7-1C', 7-3A, 7-3B and 7-4A. A: At E13, the dorsal and dorsolateral part of the ventricular zone (VZ) is immunoreactive for calbindin, and many calbindin-positive cells are stacked up in vertical arrays within the ventricular zone. The cortical preplate (PP) consists of a layer of one or two tangentially oriented calbindin-positive cells. B: By E15, the ventricular zone has lost calbindin-like immunoreactivity except that a few calbindin-positive fibers remain (examples at double arrows). The calbindin-positive preplate contains many calbindin-positive cells and these are intermingled with highly calbindin-immunoreactive fibers. C: By E16, an intermediate zone (IZ) containing calbindin-positive fibers appears beneath the cortical plate (CP). A few calbindin-immunoreactive fibers (double arrows) are still present in the ventricular zone. D and E: Views of the dorsomedial (D) and dorsolateral (E) parts of the cortical anlage at E18. The division of a single calbindin-positive cortical preplate into the calbindin-positive subplate (SP) and calbindin-positive marginal zones (MZ) has just started in the dorsomedial part of cortical anlage (photograph shows a region medial to position of the arrow in Fig. 7-3B, and was rotated 90° clockwise to permit comparison with other panels). A few calbindin-positive cells (curved arrow) are present in the ventricular zone. In the same section, a clear separation of the calbindin-positive subplate and calbindin-positive marginal zones has occurred in the dorsolateral part of the cortical anlage, and many fusiform calbindin-positive cells are scattered in

between. A few calbindin-positive cells (example at curved arrow) appear below the SP. F: By E20, the separation between the calbindin-positive subplate and calbindin-positive marginal zones is even greater, and many calbindin-positive cells with radially oriented processes are visible. Scale bar for A-E, 100 μm.

Developmental segregation of the calbindin-positive cortical subplate and calbindin-positive marginal zones from a single calbindin-positive cortical primordium

The wave of calbindin expression documented here for the ventricular zone of the striatum commenced as an earlier wave of calbindin expression in the ventricular zone of the cortex subsided (see above and Fig. 7-1). During the E13-E20 period, however, there was intense calbindin-like immunoreactivity in the developing cortical anlage, as documented in Fig. 7-8, and this calbindin expression appeared in transient patterns.

The expression of calbindin-like immunoreactivity in the cortical anlage started at E13 with a single-cell thick plexiform plate containing tangential orientated calbindin-immunoreactive cells (Fig. 7-8A). As this plexiform plate gradually expanded, more calbindin-immunoreactive cells appeared, and by E15 (Fig. 7-8B) most if not all of the cells in this plate appeared immunostained. At E16, the calbindin-positive plexiform plate remained as a single layer dorsally (Fig. 7-8C), but in the ventrolateral cortical anlage it began to split into two layers packed with numerous calbindin-immunoreactive cells and separated by a layer with far fewer calbindin-positive cells (Fig. 7-3A).

This separation-process followed a ventrolateral to dorsomedial gradient that was very obvious at E18. In fact, the only region lacking the split was the dorsomedial cortical anlage, where the two layers were still fused (Figs. 7-3A, 7-8D). The outer and inner layers of calbindin-immunoreactive cells appeared to intermingle with calbindin-immunoreactive fibers that appear to emerge from the cortical primordium above (see also Fig. 7-2F). V, lateral ventricle; Scale bar (for all photographs), 500 μm.correspond to the marginal zone and the subplate, respectively (Fig. 7-8E). Many fusiform calbindin-

immunoreactive cells were distributed between these two layers. They did not seem to have a single (for example radial) orientation. The distance between the two calbindin-positive layers increased as the cortical anlage became increased in size, but by E20 the intensity of calbindin immunostaining in the subplate and marginal zones had decreased, and it continued to decrease with age. A few calbindin-immunoreactive cells were present in these two zones in the neocortex of adult rats, along with other calbindin-positive cortical cells.

DISCUSSION

Transient calbindin-immunoreactive processes related to the germinal epithelium extend through the developing striatum

Our findings establish that a transient wave of calbindin expression occurs in the ventricular zone of the ganglionic eminence, and that this wave of calbindin expression is correlated temporally and spatially with the transient appearance of calbindin-positive radial processes stretching from the ventricular zone through the subventricular zone and into the striatal anlage. Both the calbindin-positive cells in the ventricular zone and the calbindin-immunoreactive radial processes had appeared by E18, both diminished postnatally after peaking at P0-P3, and both disappeared by P15. Both systems followed similar, pronounced spatial gradients of expression strongly favoring the dorsolateral and rostral parts of the ganglionic eminence and the striatal anlage, respectively, throughout the period in which the two systems could be identified.

The concurrent appearance and disappearance of the calbindin-positive cells in these dorsolateral and rostral positions suggests that the epithelial and radial elements may be related. In fact, many of the calbindin-positive processes appeared to extend from calbindin-immunoreactive cells of the germinal epithelium, including some that could be traced in continuity from the ventricular zone all the way across the dorsal caudoputamen. In the region of densest expression of calbindin-like immunoreactivity, the entire ventricular zone was intensely immunostained, and no unstained cells could be detected. Interestingly, previous studies have demonstrated biochemical specialization of this dorsal part of the germinal zone of the ganglionic eminence (see below and

Graybiel and Ragsdale, 1980; Ragsdale and Graybiel, 1983; Mendez-Otero et al., 1988; see also Layer and Sporns, 1987; Puells et al., 1987; Johnston and van der Kooy, 1989).

The morphology of the elongated calbindin-immunoreactive processes resembles that of two other well-known cell types: radial glial cells, which are known to guide neuronal migrations (Rakic, 1971, 1972, 1988), and tanycytes, another type of processing-bearing cell associated with the ventricular system (Rafols, 1986). However, the radially oriented fibers of both of these cell types are thought to extend from cell bodies in the ventricular zone to the pial surface, whereas the longest calbindin-positive processes we observed could be traced from the ventricular zone only as far as the external capsule. Preliminary observations of an ongoing study (Liu and Graybiel, unpublished observations) suggest that calbindin-positive processes are a subset of radial processes expressing Rat.401-like immunoreactivity. The Rat.401 antigen, nestin, is an intermediate filament protein expressed by neuronal and glial precursor cells and by radial glia (Hockfield and McKay, 1985; Frederiksen and McKay, 1988; Lendahl et al., 1990). One interesting possibility is that the calbindin-positive processes we describe here could serve a developmental role in neuronal migration in the striatum, or in communication between the ventricle or adjoining germinal epithelium and the striatal primordium.

The dorsorostral-to-ventrocaudal gradient of expression of calbindin-like immunoreactivity in the ventricular zone was particularly striking. Dorsoventral differences in immunostaining in the ventricular zone have been observed by Mendez-Otero et al. (1988) with the JONES and D1.1 monoclonal anti-ganglioside antibodies in the El8 rat brain. Both stain the dorsal part of the ganglionic eminence, but apparently

not the ventral part. Both the JONES and D1.1 antibodies are thought to mark ganglioside molecules important in cell adhesion patterns during development, possibly in relation to migrations guided by radial glia. Interestingly, an inverse gradient, with staining most intense ventrally, has been identified in the ganglionic eminence of the embryonic human (Graybiel and Ragsdale, 1980) and cat (Ragsdale and Graybiel, 1983, in preparation) with butyrylcholinesterase histochemistry. Such dorsoventral differences might relate to differential expression of antigen in parts of the ganglionic eminence derived from the medial (ventromedial) and lateral (dorsolateral) ridges of the ganglionic eminence described in the classical literature. If so, the staining patterns could reflect forebrain lineage restriction boundaries analogous to those observed in the hindbrain (Lumsden and Keynes, 1989; Wilkinson and Krumlauf, 1990). We could not test this possibility in the present study, however, because the visible cleft between the medial and lateral ridges, striking at E14 and E15, became obscured before calbindin was strongly expressed in the ganglionic eminence.

There was a clear complementarity between the dorsal and rostral distribution of the transient calbindin-immunoreactive radial processes and ventral location of the growing lattice-work of calbindin-positive medium sized neurons. The only exception was that some calbindin-immunoreactive processes did pass through a calbindin-positive "lateral band system" (see Liu and Graybiel, 199lb) that lay in the ventrolateral part of the rostral striatum. By contrast, the system of calbindin-positive radial processes and the scattered transient calbindin-positive cells had corresponding distributions in the dorsal part of the developing caudoputamen, and early on some of the cells seemed to

be associated with the processes. The calbindin-positive processes could serve as radial guides for the transient calbindin-positive cells, or be among the processes with such a guidance function. An interesting possibility is that the scattered calbindin-positive cells could represent mature products of earlier elongated calbindin-positive precursors. This would be consistent with our observation that some of the calbindin-positive processes, but not the calbindin-positive cells, are Rat.401-positive (Liu and Graybiel, unpublished observations).

A transient population of calbindin-immunoreactive cells in the developing striatum

Our findings demonstrate that there is a transient population of calbindin-positive cells in the developing striatum visible from E20-P15. Some of these calbindin-immunoreactive cells had quite large perikarya with ramified dendrites, and in general these dorsally located cells appeared to be aspiny and otherwise phenotypically distinct from neurons in the calbindin-positive mosaic described in the second report of this series (Liu and Graybiel, 1991b). The transient calbindin-positive cells have a unique distribution in the developing striatum. They are widely scattered and, throughout the time that they can be detected, predominate in the dorsal and lateral striatum. This dorsolateral zone includes the region in which little calbindin-like immunoreactivity is expressed in the mature striatum, and, as noted above, largely corresponds to the region penetrated by transient calbindin-immunoreactive radial processes. Calbindin-positive cells with similar phenotypes were only very rarely identified farther ventrally, but it is conceivable that the increasing immunoreactivity of the medium-cell mosaic hid others

from view.

It is not clear what accounts for the disappearance the transient calbindin-immunoreactive cells during the course of striatal development. They may be selectively removed during the period of neuronal death in the first postnatal week (Fentress et al., 1981; Fishell et al., 1987), or may undergo a transition of neurochemical phenotype, or may be cells migrating through the striatum during development. Interestingly, the phenotype of the larger of these calbindin-immunoreactive cells is similar to that of calbindin-positive cells found in the adjoining developing neocortex, and in some sections the transient calbindin-positive cells seemed to be piled up along the lateral edge of the caudoputamen. Another open question is whether the transient calbindin-positive cells play any functional role in striatal development. A number of these cells were associated with the transient system of calbindin-positive patches in the dorsolateral striatum, and they may have contributed to the calbindin-positive neuropil of the patches.

Transient calbindin-immunoreactive patches aligned with dopamine islands in the developing striatum

A surprising finding in the present study is that there is a transient system of calbindin-positive patches in the striatum corresponding to dopamine islands. The calbindin-positive patches were primarily located in the dorsal and lateral caudoputamen, and visible from P0 to P15. The close correspondence between these transient calbindin-immunoreactive patches and dopamine islands was clear from serial-section comparisons with all four of the immunocytochemical markers of the islandic system that we used

(antisera to TH, DARPP-32, SV48 and CCPK II) (Foster et al., 1987; Newman-Gage and Graybiel, 1988). It was necessary to treat tissue sections with Triton X-100 in order to demonstrate the transient calbindin-immunoreactive patches clearly. The patches were mainly made of fine fibers, and antibody penetration may have been a problem without Triton X-100 pretreatment.

Dopamine islands have been shown unequivocally to mark the sites of developing striosomes in the striatum (Graybiel, 1984a; Moon Edley and Herkenham, 1984; Murrin and Ferrer, 1984; van der Kooy, 1984). Calbindin-like immunoreactivity is selectively expressed in neurons and neuropil of the matrix compartment of the mature rat's striatum (Gerfen et al., 1985), but there is a substantial dorsolateral zone in which very little calbindin is present. Thus on two counts the transient calbindin-positive patchwork is inconsistent with the later pattern of expression of calbindin: the transient calbindin-positive patches are at the sites of future striosomes, not future matrix, and they are best developed dorsolaterally, where calbindin expression will be lowest and TH-positive dopamine islands are most intensely stained. At the same time that the transient system of calbindin-immunoreactive patches is developing dorsally, however, calbindin expression develops ventrally in a steadily increasing proportion of medium-sized neurons of the matrix (Liu and Graybiel, 1991b). Thus, calbindin-immunoreactive systems in the developing striatum can be divided into two systems with respect to the neurochemical compartmentation of the striatum. One is a transient calbindin-positive system located in developing striosomes, and the other one is a permanent calbindin-positive system located in the matrix.

Our observations leave unsettled the questions of where the calbindin-immunoreactive fibers of the patches originate and why the patches disappear later on. The immunohistochemical findings suggest two possible origins. First, some of the transient calbindin-immunoreactive cells scattered through the dorsolateral caudoputamen were associated with these patches, so that at least part of the neuropil of the patches may be contributed by these calbindin-immunoreactive cells. Consistent with this idea is the coordinate time of disappearance of the calbindin-immunoreactive cells and patches, around P15. The slightly earlier appearance of the transient calbindin-positive cells (E20 as opposed to P0) would also fit if the cells, once in dopamine island locations, then generated processes. They might, however, simply have more antigen in the cell body than in coexisting processes.

A second possibility is that the source of the calbindin-immunoreactive neuropil in the patches is extrinsic to the striatum; for example, they could derive from calbindin-immunoreactive cells of the developing neocortex. We observed calbindin-immunoreactive cells in the developing cortical plate and, apparently, the immediately adjoining subplate. In the mature rat, neurons in the deep layers of neocortex project predominantly to the striosomal (patch) compartment of the striatum (Gerfen, 1989). Moreover, in the ferret, subplate neurons have been shown to project to subcortical regions earlier than do neurons in the deep cortical layers (McConnell et al., 1989). Later in development, neurons of the subplate are thought to undergo programmed cell death (Luskin and Shatz, 1985; Chun and Shatz, 1989). If the calbindin-immunoreactive neuropil in the dopamine islands is derived from axons of calbindin-immunoreactive

subplate neurons, a disappearance of the calbindin-positive patches would be predicted: as calbindin-immunoreactive subplate neurons die during development, so would the calbindin-immunoreactive patches disappear. Apparently, however, calbindin-immunoreactive subplate neurons are not projection neurons at least in the ferret (Antonini and Shatz, 1990).

Cortical subplate and marginal zones share the property of intense calbindin immunostaining

Our findings demonstrate that a single-cell layer of calbindin-immunoreactive cells appears in the cortical plexiform plate as early as E13, and that, at about E16, this single calbindin-positive plexiform plate begins to split into two calbindin-positive zones which become the subplate and marginal zones. This developmental separation is in good accord with the developmental sequence observed by Luskin and Shatz (1985) with [^{3}H]thymidine neuronography in the cat's visual cortex. These authors proposed that cells in the cortical subplate and marginal zones are transient cells first co-generated in a single zone, that they appear earlier than other cells of the cortex, and that the original single zone is subsequently separated into two zones by the insertion of later born cells constituting the cortical plate. Our results suggest that the early-forming cells share the property of calbindin immunoreactivity, that this chemospecificity is retained during an extended period of cortical development that culminates finally in a major wave of cell-death in the calbindin-positive cell populations in the marginal and subplate zones. Moreover, we have shown that this developmental sequence of calbindin expression in

the cortical anlage is preceded by a period of intense calbindin expression in the underlying ventricular zone. Thus, our observations suggest collectively that in both the developing cortex and the developing striatum, there are consecutive waves of transient calbindin expression in precursor cells of their germinal epithelia and in progeny of these epithelia.

Chapter 8

Heterogenous development of calbindin-D_{28K} expression in the developing striatum

ABSTRACT

In the present study, we analyzed the ontogenetic expression of calbindin-D_{28K} (calbindin), a calcium binding protein selectively expressed in medium-sized neurons of the striatal matrix compartment in large parts of the mature rat's caudoputamen. We used tyrosine hydroxylase (TH)-immunostaining of dopamine islands as a marker for future striosomal loci so that the compartmental location of medium-sized neurons expressing calbindin-like immunoreactivity could be assessed.

From their first appearance at embryonic day (E) 20, medium-sized striatal neurons expressing calbindin-like immunoreactivity had highly heterogeneous distributions. They first formed a latticework of patches and bands in a ventral region of the caudoputamen. By postnatal day (P) 7, this early calbindin-positive lattice had evolved into a mosaic in which circumscript pockets of low calbindin-like immunoreactivity appeared in more extensive calbindin-rich surrounds. With further development, the mosaic gradually encroached on all but the dorsolateral caudoputamen, a district that is calbindin-poor at adulthood. Quantitative analysis of the sizes of calbindin-poor zones of the mosaic across different developmental ages indicated that

This chapter is modified from the paper, "Liu, F.-C. and A.M. Graybiel (1991b) Heterogeneous development of calbindin-D_{28K} expression in the developing striatum", now in submission.

the average size of the calbindin-poor zones at mid-striatal levels decreased from P3 to P15, and then increased from P15 to adulthood. A special lateral branch of the striatal calbindin system was also identified, distinct from the rest of the calbindin-positive mosaic in several developmental characteristics.

Dopamine islands with the most intense TH-like immunoreactivity were nearly all dorsal to the developing calbindin system, but many more weakly stained dopamine islands were present ventrally. These invariably lay in calbindin-poor zones. Most dopamine islands only filled parts of the corresponding calbindin-poor zones, however, and there were some calbindin-poor zones for which TH-positive dopamine islands could not be detected. Thus during development, the extrastriosomal matrix of the striatum could be divided into calbindin-rich and calbindin-poor zones. Moreover, in the calbindin-rich regions, there were patches of especially intense calbindin expression and zones of weaker expression.

These results suggest three main conclusions. First, the expression of calbindin-like immunoreactivity in medium-sized striatal neurons is consistently restricted to the extrastriosomal matrix during development. Second, there is neurochemical heterogeneity in the striatal matrix during the prolonged developmental period in which the early calbindin-positive lattice expands to form the calbindin-positive matrix of the mature striatum. Third, calbindin expression in the matrix, although eventually distributed in strictly complementary fashion to striosomes, does not originate as a system complementary to dopamine islands. The prolonged disparity between the border of dopamine islands and calbindin poor zones, and the different spatiotemporal schedules

of development of the islands and the calbindin gaps suggest instead that the final match between the borders of striosomes and surrounding matrix result from dynamic process occurring early in postnatal development.

INTRODUCTION

The striatum is organized into at least two histochemically identifiable subdivisions, the striosomes and extrastriosomal matrix. The striosomal compartment is embedded in the complementary matrix, which surrounds it in a mosaic way so that the striosomes form three-dimensional labyrinthine networks infiltrating the much larger striatal matrix (Graybiel and Ragsdale, 1978; Groves et al., 1988; Desban et al., 1989).

Compartmentalization in the striatum has been characterized not only by expression of different neurotransmitter-related compounds and biochemical substances in each compartment (for reviews, see Graybiel and Ragsdale, 1983; Gerfen, 1987; Graybiel, 1989, 1990), but also by the different patterns of connectivity of these compartments with other regions of the brain (Ragsdale and Graybiel, 1981, 1988a, 1988b, 1990; Herkenham and Pert, 1981; Gerfen, 1984, 1985, 1989; Donoghue and Herkenham, 1986; Gerfen et al., 1987b, 1990; Jiménez-Castellanos and Graybiel, 1987, 1989; Langer and Graybiel, 1989; Giménez-Amaya and Graybiel, 1990, 1991), and their different developmental schedules (Graybiel and Hickey, 1982; Graybiel, 1984a; Fishell and van der Kooy, 1987a, 1989; van der Kooy and Fishell, 1987; Voorn et al., 1988), and their different genomic responsiveness to dopaminergic drug treatments (Graybiel et al., 1990; Paul et al., 1990; Grimes et al., 1990). These different lines of anatomical evidence suggest that the striosomes and matrix may differ in their contributions to the functions carried out by the striatum.

With respect to the development of striatal compartmentalization, striosomes have been recognized as ontogenic units (Graybiel and Hickey, 1982; Graybiel, 1984a; van der

Kooy and Fishell, 1987; Fishell et al., 1990). Tyrosine hydroxylase (TH), dopamine, high affinity dopamine uptake sites, dopamine D1 and D2 receptor sites, dopamine- and adenosine 3':5'-monophosphate-regulated phosphoprotein (DARPP-32), μ opiate receptors, acetylcholinesterase, high affinity choline uptake sites, muscarinic M1 and M2 receptor sites, synaptic vesicle-associated protein recognized by SV48 antibody, calcium/calmodulin-dependent protein kinase type II and tachykinin have been shown in anatomical studies to be preferentially expressed in patchy distributions during prenatal and early postnatal periods, and a number of these patch systems have been identified as representing future striosomes in the developing striatum (Olson et al., 1972; Tennyson et al., 1972; Butcher and Hodge, 1976; Kent et al., 1982; Graybiel, 1984a; Moon Edley and Herkenham, 1984; Murrin and Ferrer, 1984; van der Kooy, 1984; Foster et al., 1987; Lowenstein et al., 1987, 1989; Newman-Gage and Graybiel, 1988; Voorn et al., 1988; Murrin and Zeng, 1989; Happe and Murrin, 1989; Nastuk and Graybiel, 1989; Boylan et al., 1990; Zahm et al., 1990). It is also known that striosomes and matrix do not develop at the same rate (Foster et al., 1987; Fishell and van der Kooy, 1987a, 1989; Newman-Gage and Graybiel, 1988), and that these two compartments can be dissociated in development by chemically-induced lesions of the nigrostriatal system in newborn rats (Gerfen et al., 1987a) and also by expression of the mutant gene *weaver* (Graybiel et al., 1990).

In contrast to striosomal development, very little is known about the development of the matrix compartment, because there have been no selective markers for the immature matrix comparable to those available for identifying immature striosomes. In

an attempt to study developmental events in the matrix, we analyzed the ontogeny of expression of calbindin-D_{28K} (calbindin), a calcium binding protein that is selectively and apparently constitutively expressed in medium-sized neurons of the matrix in the mature caudoputamen (Bambridge et al., 1982; Gerfen et al., 1985). We found calbindin-positive systems of two sorts in the developing striatum. First, as reported in the companion paper, there are transient calbindin-positive systems in the ganglionic eminence and striatal anlage (Liu and Graybiel, 1991a). We report here on a second, progressively increasing calbindin-positive system made up of medium-sized striatal neurons. We demonstrate that during development, as at adulthood, calbindin in the medium-sized neuronal population is selectively expressed in populations of striatal matrix neurons. However, during development, calbindin-positive neurons have heterogenous distributions within the matrix that are not complementary to the boundaries of the developing striosomal system and that contrast with the relatively homogenous distribution of calbindin-positive matrix neurons at adulthood. These developmental patterns suggest that dynamic mechanisms generate striosome-matrix complementarity in the striatum, and that there also are early developmental events that establish a compartmental architecture of the matrix itself. Some of these findings have been reported in abstract form elsewhere (Liu et al., 1989).

METHODS

Most of the brain tissue analyzed in this study was used also for study of the transient calbindin systems in the striatum (accompanying report, Liu and Graybiel, 1991a). The details of experimental procedures were described in the accompanying report (Liu and Graybiel, 1991a). In brief, brain tissue was obtained from Sprague-Dawley rats (Taconic Farm) at embryonic days (E) 18 (n=4) and E20 (n=5), and at postnatal days (P) 0 (n=7), P3 (n=12), P7 (n=6), P15 (n=3). The day of sperm positivity was defined as E1, the day of birth as P0. Brain tissue from additional adult rats (n=2) was also prepared and sections of adult brains (n=4) prepared for another study (Graybiel et al., 1990) were also analyzed. All brains were fixed by transcardial perfusion with fixative contained 4% paraformaldehyde, 5% sucrose and 0.1 M phosphate-buffered saline (PBS) (pH 7.4, 4°C). Heads or brains were postfixed in fresh fixative (2-12 hr) and cryoprotected (24-36 hr, 20% sucrose in 0.1 M PBS) at 4°C, and cut into coronal 40 μm frozen sections (E18 and E20 tissue) or 20-30 μm sections (postnatal tissue).

Free-floating sections were processed for calbindin and TH immunostaining by avidin-biotin or peroxidase-antiperoxidase immunocytochemistry as described in the accompanying paper (Liu and Graybiel, 1991a). Polyclonal rabbit anti-calbindin D_{28K} antisera were generously provided by Drs. P.C. Emson, C.R. Gerfen and S. Christakos and were diluted 1:1,000-4,000, 1:500 and 1:800, respectively. Rabbit anti-TH antiserum (Eugene Tech.) was diluted 1:240-500. Series of sections from brains at each age were incubated in primary antiserum containing 0.2% Triton X-100, and other series from the

same brains were incubated without Triton X-100. Alternating sections from E20, P0, P3, P7 and P15 brains were processed for calbindin and TH immunocytochemistry. The immunostaining controls for calbindin and TH were described in the accompanying paper (Liu and Graybiel, 1991a), and included incubation with the calbindin-D_{28K} antiserum from Dr. P.C. Emson in the presence of calbindin-D_{28K} protein (3.6×10^{-4}M) purified from rat kidney and generously supplied by Dr. S. Christakos. The complete series of pre- and postnatal calbindin immunostaining was also performed with the Emson antiserum.

Quantitative analysis of the areas of calbindin-poor zones in the developing striatum

A computer-assisted measurement of calbindin-poor zones in the developing striatum was performed with the aid of a BIOCOM image-analysis system (Ulis, France). The borders of calbindin-poor zones in sections from P0, P3, P7, P15 and adult striatum were first drawn with the aid of a projector, and the contours of calbindin-poor zones were then traced to enter them into the BIOCOM system for quantitative analysis. We attempted to chart sections from matched anteroposterior levels through the striatum by using cues from the anatomy. We chose two levels for analysis, approximately at the middle (e.g., see Figs. 8-4B, 8-5B, 8-6B, 8-7B) and mid-caudal parts of the striatum (e.g., see Figs. 8-2C, 8-4C, 8-5C, 8-6C, 8-7C). The measurements at the middle level could not be made at P0 because calbindin-poor zones could not be definitively defined at this level. No measurements were made anteriorly, for this was the last site invaded by the calbindin-positive mosaic.

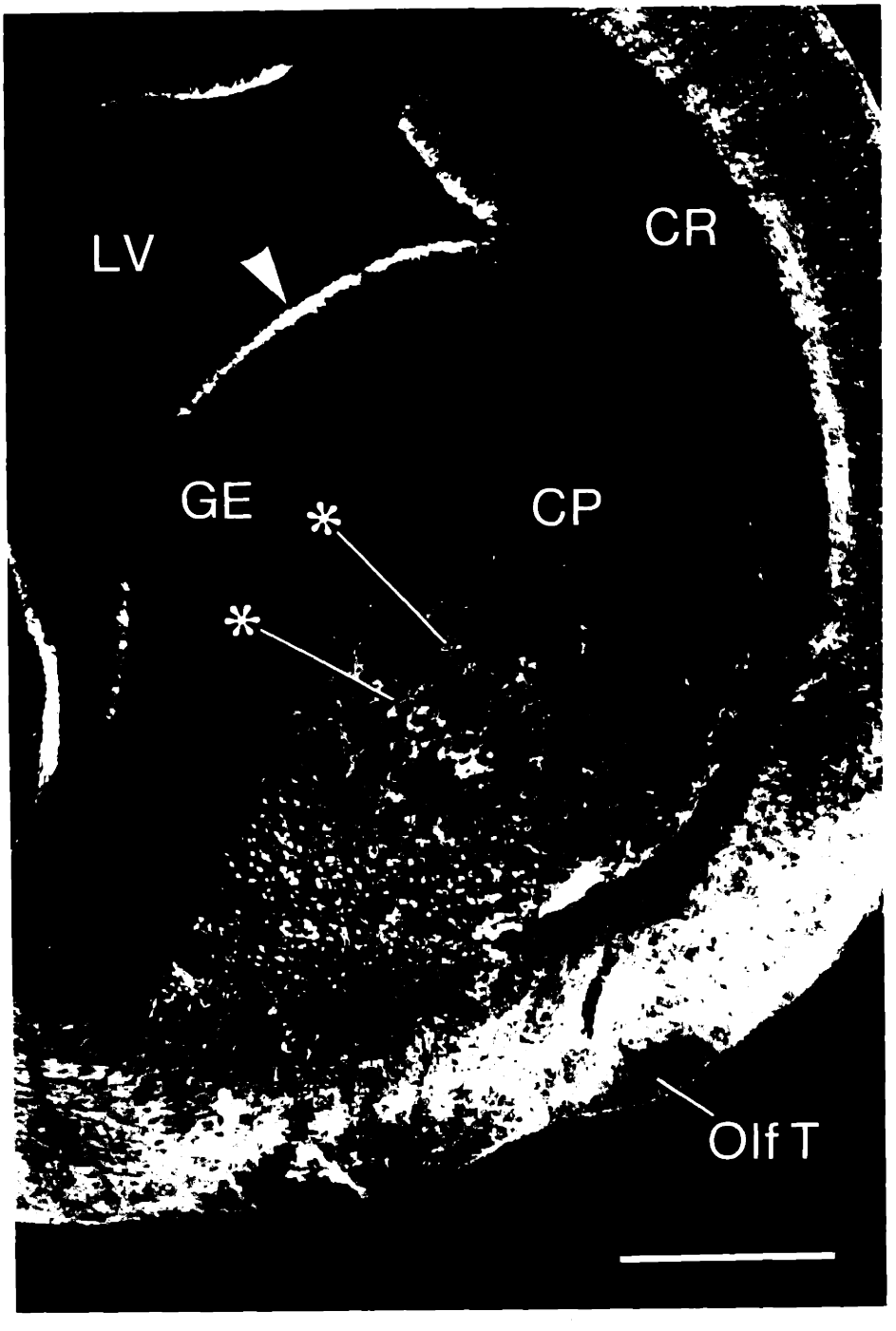
LV
CR
GE
CP
*
*
Olf T

Figure 8-1. Reverse contrast photograph of coronal section through the striatum of an E20 rat stained for calbindin-like immunoreactivity. A calbindin-positive lattice-work consisting of a few calbindin-immunoreactive strands (examples at asterisks) has started to emerge in the caudoputamen (CP). Intense calbindin-like immunoreactivity is present in the dorsal ventricular zone (arrowhead). CR, corona radiata; GE, ganglionic eminence; LV, lateral ventricle; Olf T, lateral olfactory tract. Scale bar, 500 μm.

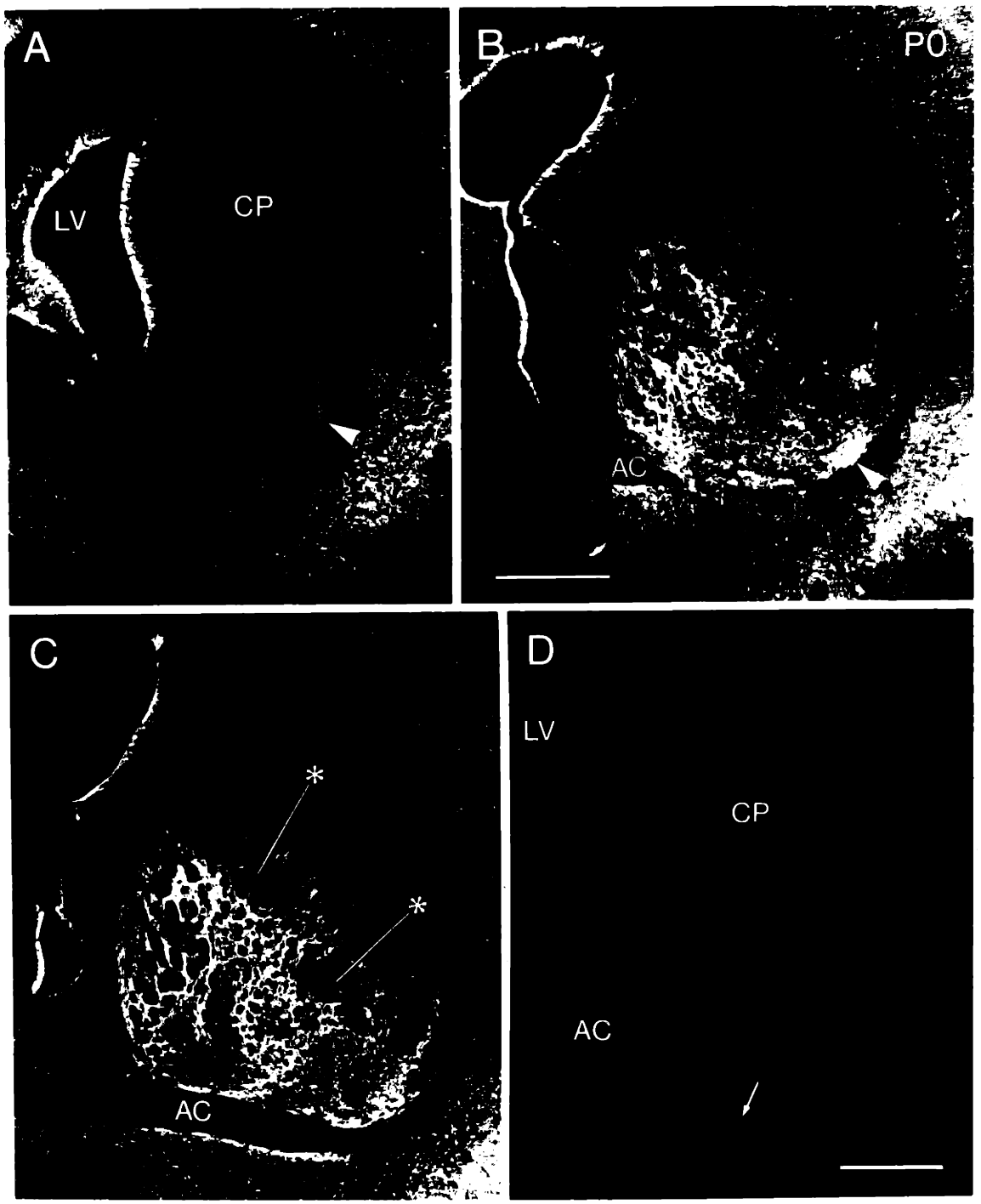
A
LV
CP
B
P0
AC
C
AC
D
LV
CP
AC

Figure 8-2. A, B & C: Reverse contrast photographs of coronal sections stained for calbindin-like immunoreactivity taken from the rostral (A), middle (B) and caudal (C) striatum of a P0 rat. The expression of calbindin-like immunoreactivity in the medium-sized neurons of the caudoputamen follows caudal-to-rostral and ventral-to-dorsal gradients. In contrast to the rostral striatum, which at P0 contains a few medium-sized calbindin-positive neurons, the middle and caudal parts of the striatum contain a lattice-work of calbindin-immunoreactive neurons and neuropil. There are calbindin-poor zones embedded in calbindin-rich matrix (examples at asterisks in C). Even at caudal levels, the dorsolateral caudoputamen does not contain much calbindin-like immunoreactivity, but many scattered multipolar calbindin-immunoreactive neurons appear in this region. At the rostral pole of the striatum (A), a thin layer of calbindin-positive small to medium-sized neurons is present ventrolaterally (arrowhead). This thin layer extends caudally to form a small strong calbindin-positive lateral band (arrowhead in B). D shows a control section from a P0 brain processed with calbindin antiserum (Dr. P.C. Emson) preabsorbed with calbindin protein (Dr. S. Christakos). Immunostaining was abolished in the caudoputamen, but staining in the basal forebrain (arrow) was not completely eliminated. CP, caudoputamen; LV, lateral ventricle; AC, anterior commissure. Scale bars in B and D indicate 500 μm. A-C were taken at the same magnification, D at slightly higher magnification.

Figure 8-3. Lightfield photomicrograph illustrating calbindin-immunoreactive neurons in the calbindin-positive lattice-work of a P3 rat. The calbindin-positive neurons are small to medium-sized, have round or oval cell bodies and lack well stained dendrites. They are tightly packed together. Scale bar, 50 μm.

RESULTS

Calbindin immunostaining of medium-sized striatal neurons was first clearly detectable in large numbers of cells at E20 and increased steadily to adulthood. The distributions of these calbindin-immunoreactive neurons appeared similar, if not identical, in sections treated with the three different calbindin antisera, and in sections processed with or without Triton X-100. Absorption controls for the specificity of the immunostaining, carried out with the Emson antiserum, showed almost complete abolition of staining in the striatum (Fig. 8-2D). The serial dilution controls yielded a progressive decline in immunostaining intensity. Analysis of the patterns of calbindin immunostaining was carried out primarily on sections stained with the calbindin antiserum from Dr. Emson, as staining with this antiserum was crisp and consistent. Most of the calbindin-immunostained tissue illustrated in the present report is taken from series of sections processed without Triton X-100, because the addition of this detergent enhanced calbindin immunostaining of the neuropil so as to obscure staining of perikarya. As reported in the preceding paper (Liu and Graybiel, 1991a), processing with Triton X-100 resulted in additional clear staining of transient calbindin-positive cells of the ganglionic eminence, radial processes extending from the germinal zone into the striatal anlage, and calbindin-positive populations of multipolar neurons and neuropil patches in the perinatal caudoputamen. These transient system will not be discussed in the present account.

Early appearance of calbindin-positive medium-sized neurons in the striatal anlage

Groups of medium-sized calbindin-immunoreactive neurons appeared in the caudal and medial parts of the striatal anlage by E20 (Fig. 8-1). These cells had already begun to form a loosely arranged lattice of calbindin-positive strands. At the same time, a small but prominent calbindin-positive band packed with small to medium-sized calbindin-immunoreactive neurons appeared at the ventrolateral edge of the striatal anlage. Each of these zones of early calbindin immunostaining could be recognized at subsequent developmental stages.

Development of calbindin-positive lattice-works in the caudoputamen

P0 striatum

Calbindin-poor zones and calbindin-rich zones in the P0 caudoputamen formed a clear lattice-work that consisted of many small to medium-sized calbindin-immunoreactive neurons and associated neuropil grouped together and interspersed with groups of calbindin-poor cells (Fig. 8-2). This lattice was prominent in the ventromedial caudoputamen at caudal and middle transverse levels, but faded anteriorly. The calbindin-immunoreactive neurons of the lattice had oval or rounded perikarya (diameter, ca. 6-12 μm), and very few had well-stained dendrites (Fig. 8-3). In the caudal part of the caudoputamen (Fig. 8-2C), the calbindin-positive zones were considerably larger than the calbindin-poor zones, so that the lattice-pattern began to give way to one in which calbindin-poor pockets appeared in a calbindin-rich surrounding field. There was also a gradient in the intensity of calbindin immunostaining ranging from higher

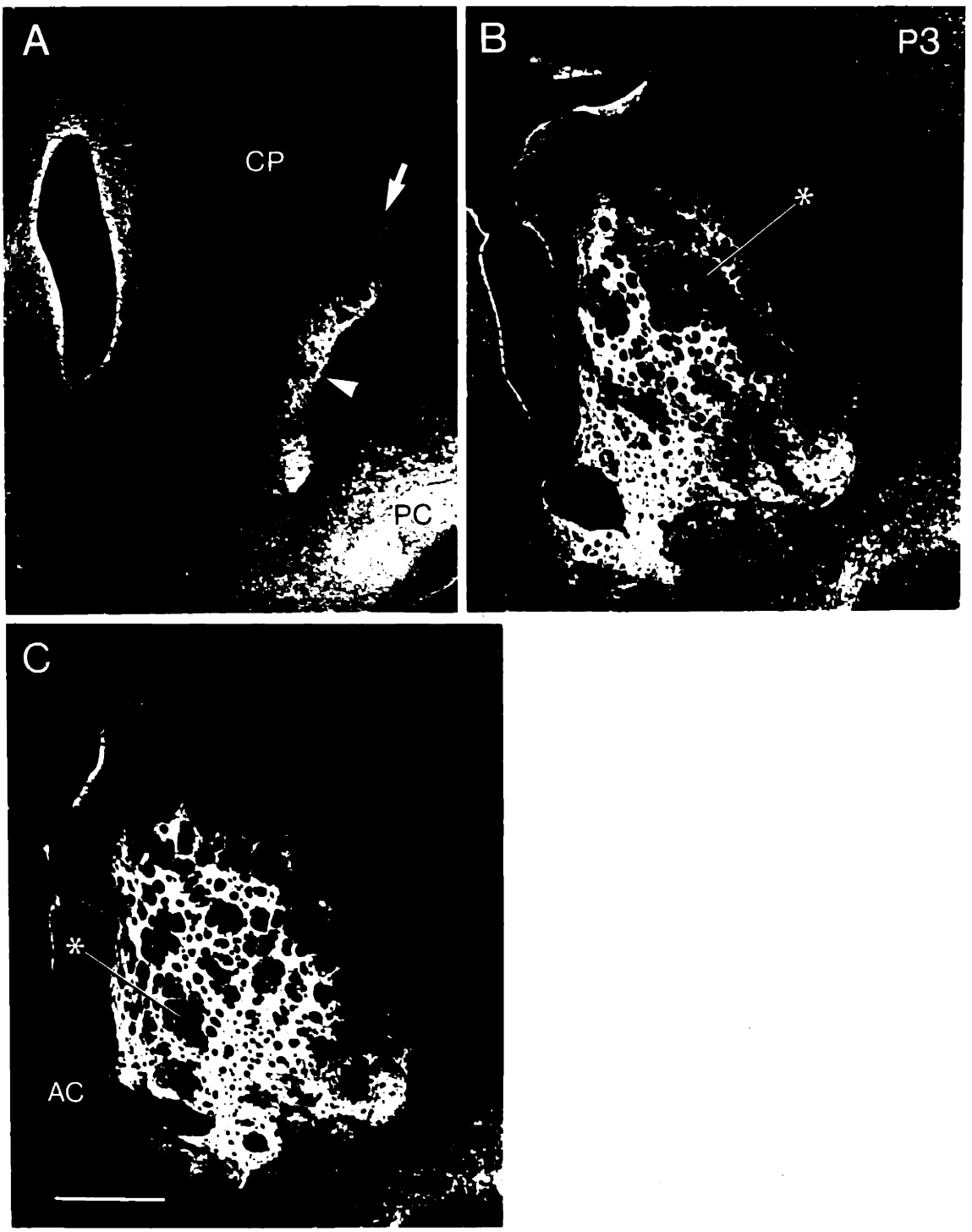
A
CP
PC
B
P3
*
C
*
AC

Figure. 8-4. A, B & C: Calbindin-immunostaining in the striatum of a P3 rat shown in reverse contrast photographs of coronal sections at rostral (A), middle (B) and caudal (C) levels. In the rostral striatum (A), there is a prominent band of calbindin-immunoreactive neurons and neuropil extending along the lateral edge of the ventral part of the caudoputamen (arrowhead). An isolated group of calbindin-positive neurons lies just dorsal to this band (arrow). More regions in the middle (B) and caudal (C) striatum express calbindin-like immunoreactivity than in the P0 brain (cf. Fig. 8-2). They start to fill in the lattice-work to form a pattern of calbindin-rich fields with calbindin-poor gaps (examples at asterisks). The so-called core subdivision (lateral part) of the nucleus accumbens, but not its medial "shell" subdivision, is calbindin-immunoreactive (B). CP, caudoputamen; AC, anterior commissure; PC, pyriform cortex. Scale bar for A-C, 500 μm.

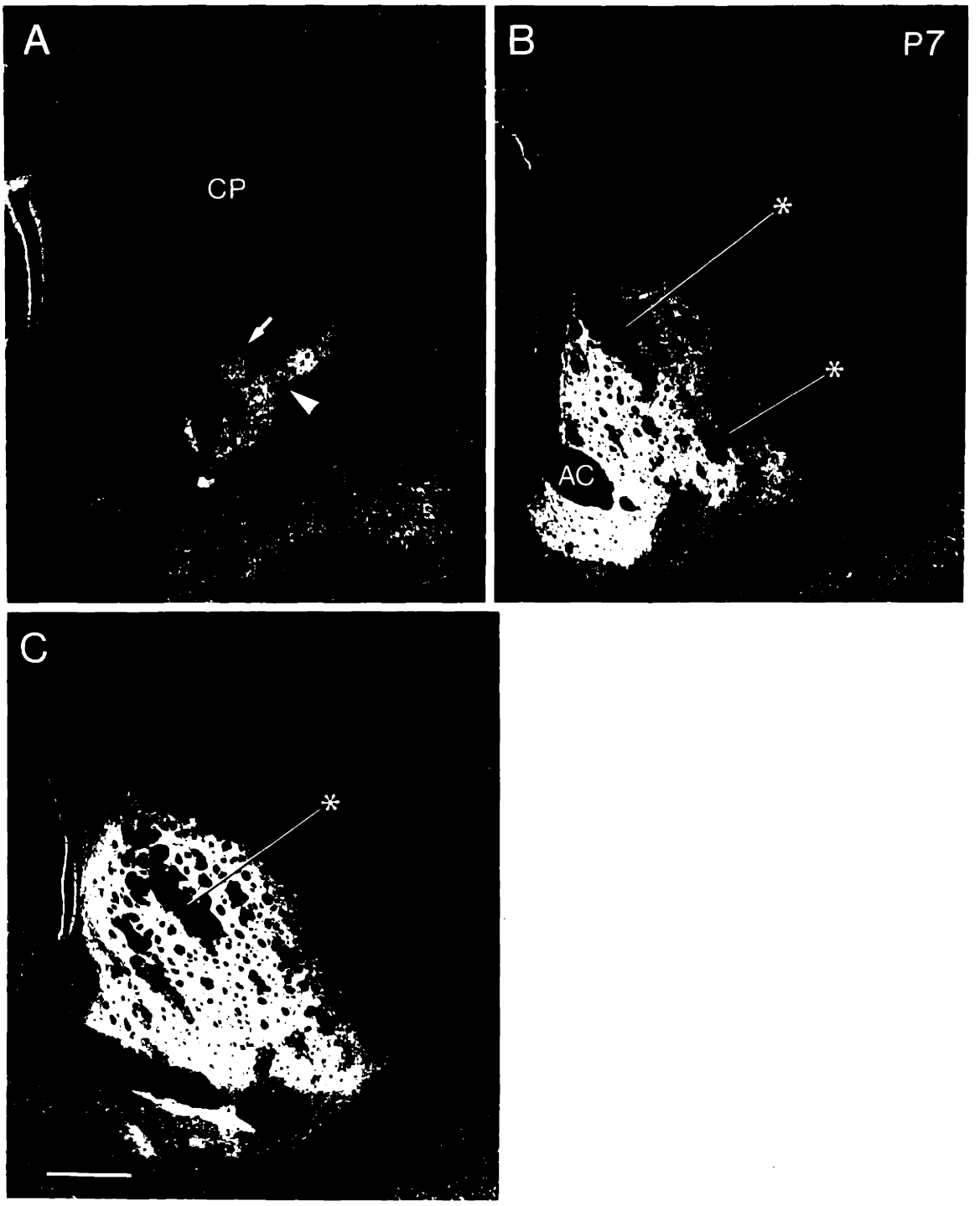
A
CP
B
P7
*
*
AC
C
*

Figure 8-5. A, B & C: Coronal sections through the striatum of a P7 rat, stained for calbindin-like immunoreactivity and photographed in reverse contrast. In the rostral striatum (A), the calbindin-positive lateral band is still present in the ventrolateral caudoputamen (arrowhead), but it has begun to grow medially directed branches (arrow). A very weak calbindin-positive mosaic appears in the medial caudoputamen at these rostral levels. In the middle (B) and caudal (C) parts of the striatum, zones of low calbindin-like immunoreactivity (see asterisks) are embedded in calbindin-rich surrounds to form a heterogenous mosaic-pattern throughout all except the dorsolateral part of the caudoputamen. CP, caudoputamen; AC, anterior commissure. Scale bar for A-C, 500 μm.

levels in the caudal and ventromedial caudoputamen to lower levels in the rostral and dorsolateral caudoputamen. A distinct zone of especially intensely immunostained neurons appeared ventrolaterally at mid-striatal levels, and at rostral levels there was a thin zone in the ventrolateral part of the caudoputamen, adjacent to the pyriform cortex, that contained small to medium-sized calbindin-immunoreactive cells with rounded perikarya (Fig. 8-2A).

P3 striatum

The distribution of small to medium-sized calbindin-immunoreactive neurons followed a sharp caudomedial to rostrodorsal gradient in the P3 caudoputamen (Fig. 8-4). Compared to the patterns at P0, more regions in the middle and caudal caudoputamen had become filled with calbindin-immunoreactive neurons so that the calbindin-poor zones took on more clearly the appearance of lacunae (Figs. 8-4B, 8-4C). The calbindin-rich zones of the mosaic themselves were unevenly immunostained (see below). Calbindin-like immunoreactivity was strongly expressed in the lateral ("core") subdivision of the nucleus accumbens by P3. The staining pattern in this region was similar to that of the adjoining parts of the caudoputamen except that there were few calbindin-poor gaps.

Rostrally, the band of calbindin-immunoreactive neurons along the ventrolateral edge of the caudoputamen had grown relative to the thin calbindin-positive zone present there at birth (Fig. 8-4A). The calbindin-immunoreactive neurons in this band had phenotypes similar to those of the calbindin-immunoreactive neurons in the middle and

caudal caudoputamen, but individual calbindin-immunoreactive perikarya were more clearly visible in this band than elsewhere in the calbindin mosaic, apparently because of their intense staining and lower packing density. The band was distinguished from the rest of the striatal calbindin-positive mosaic as a "lateral band system" (see Figs. 8-4A, 8-5A, 8-6A, 8-7A). A few very weakly-stained calbindin-positive patches also appeared in more medial parts of the rostral caudoputamen, probably representing the rostral tips of the calbindin mosaic found at more caudal levels.

P7 striatum

With more of the caudoputamen expressing calbindin-like immunoreactivity, and with progressive filling-in of the calbindin lattice, a mosaic pattern emerged by P7 in which circumscript zones of low calbindin-like immunoreactivity were embedded in calbindin-rich surrounds throughout the middle and caudal caudoputamen (Figs. 8-5B, 8-5C). Meanwhile, part of the calbindin-positive lateral band system extended to caudal striatal levels, where it fused with the more medial calbindin-positive mosaic. The dorsolateral caudoputamen still lacked extensive immunostaining even at middle and caudal levels, and much of the rostral caudoputamen remained calbindin-poor.

At rostral levels, the calbindin-positive lateral band system had enlarged medially, and a few calbindin-poor pockets now appeared within it (Fig. 8-5A). A weak calbindin-positive mosaic also began to emerge in the medial half of the rostral caudoputamen.

P15 striatum

By P15, the pattern of calbindin immunostaining at middle and caudal striatal

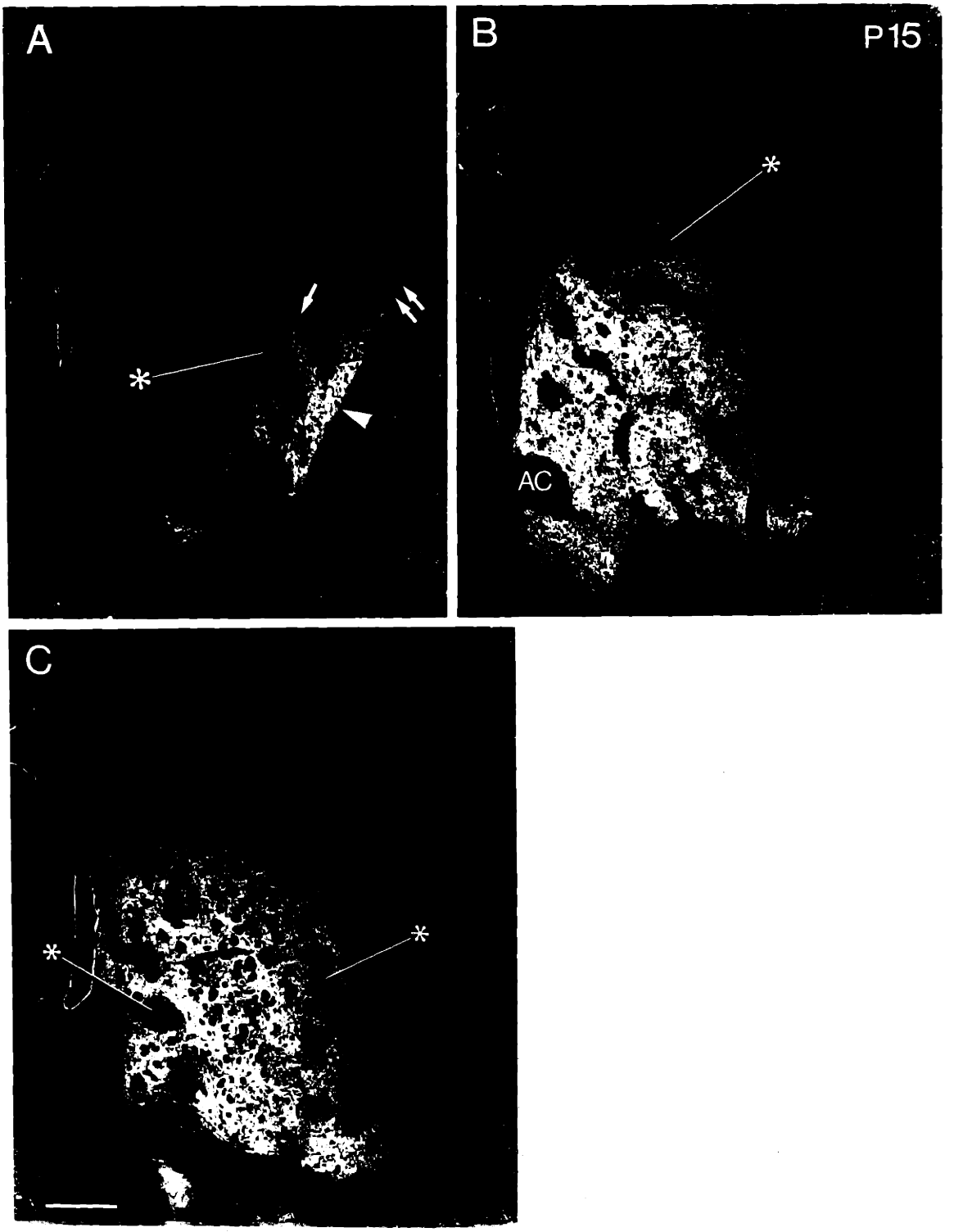
A
B
P15
AC
C

Figure 8-6. A, B & C: Coronal sections through the rostral (A), middle (B) and caudal (C) striatum of a P15 rat, stained for calbindin-like immunoreactivity and shown in reverse contrast photographs. The calbindin-positive lateral band system of the rostral striatum (see arrowhead in A) has more branches stretching medially and dorsally than at earlier ages. The medial branches (arrow) have begun to interweave with the weak calbindin-positive mosaic developing in the medial caudoputamen. The dorsal branch (double arrows) still grows along the lateral edge of the caudoputamen. The distribution of calbindin-like immunoreactivity in the middle (B) and caudal (C) striatum has almost achieved an adult status in which a mosaic pattern appears throughout the caudoputamen except for its dorsolateral and lateral parts (compare with Figs. 8-7B, 8-7C). The asterisks in A-C indicate calbindin-poor zones embedded in calbindin-rich surrounds. AC, anterior commissure. Scale bar for A-C, 500 μm.

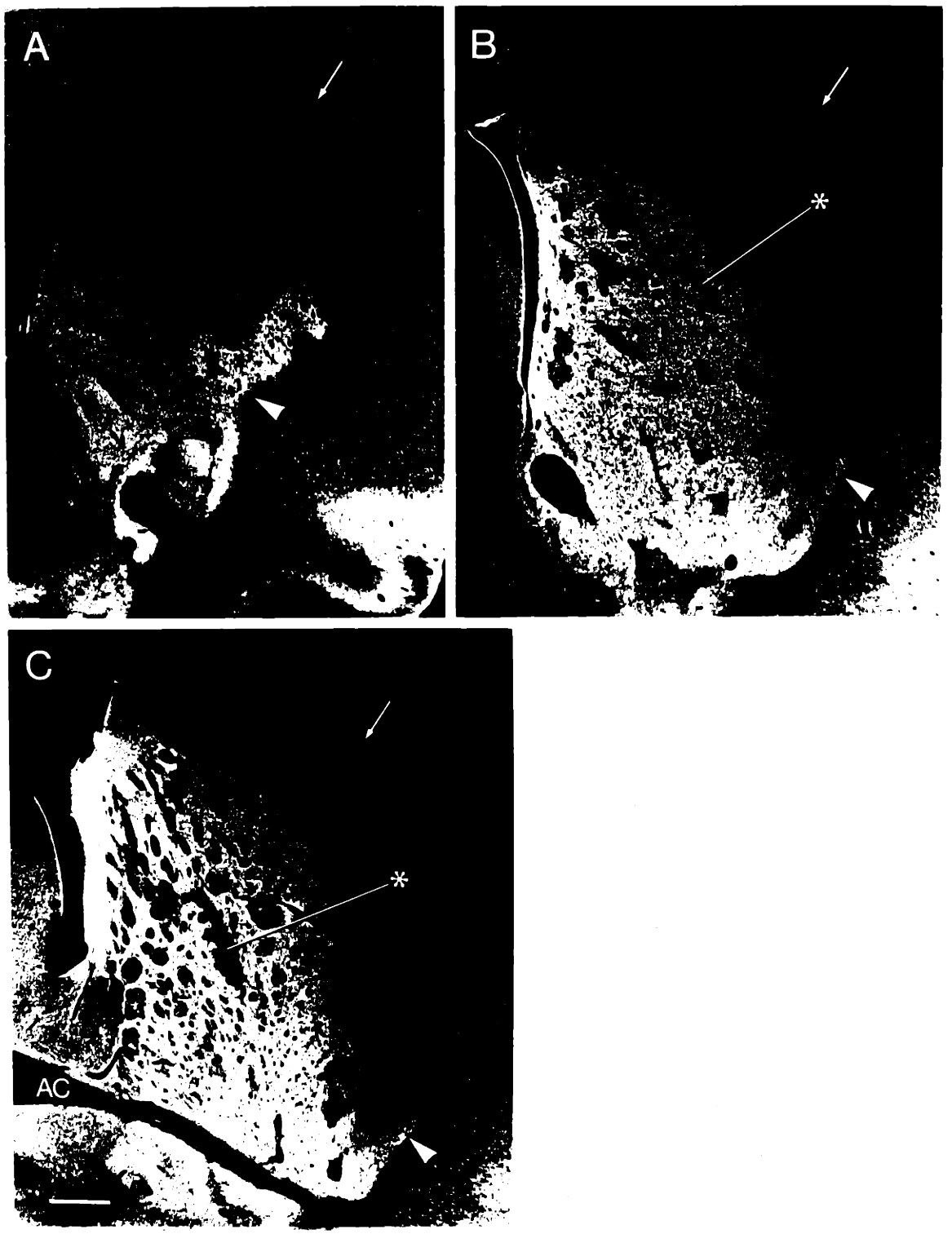
A
B
C
AC

Figure 8-7. A, B & C: Calbindin-like immunoreactivity in the striatum of an adult rat, shown in reverse contrast photographs of coronal sections. A prominent calbindin-positive mosaic appears throughout the rostral (A), middle (B) and caudal (C) caudoputamen except dorsolaterally and laterally, where little calbindin-like immunoreactivity is expressed. The arrows in A-C point to the dorsolateral margin of the caudoputamen. Examples of the calbindin-poor zones of the mosaic are indicated by asterisks. The calbindin-positive lateral band system in the rostral caudoputamen (arrowhead) can be clearly identified on the basis of its intense immunostaining (A). The intensely immunostained lateral band system (arrowheads) is still visible at the ventrolateral margin of caudoputamen. Immunostaining along the ependymal lining of the lateral ventricle is an artifact. AC, anterior commissure. Scale bar for A-C, 500 μm.

levels was quite similar to that of adult rats (Figs. 8-6B, 8-6C; see also Figs. 8-7B, 8-7C). In these regions, a prominent mosaic of calbindin immunostaining with crisp calbindin-poor gaps appeared throughout all except dorsolateral part of the caudoputamen. Rostrally, the calbindin-positive lateral band system extended farther dorsally, and its branches penetrated more deeply into the caudoputamen than in the P7 brains. The lateral and medial calbindin-positive zones now merged to form a ventral intensely calbindin-positive mosaic extending across the full width of the caudoputamen (Fig. 8-6A).

Mature striatum

A nearly homogeneous distribution of calbindin-positive neurons, interrupted by patches of low calbindin immunostaining known to correspond to striosomes (patches) (Gerfen et al., 1985), appeared in all except the dorsolateral and lateral parts of the caudoputamen (Fig. 8-7). The calbindin-positive lateral band system could readily be distinguished from the rest of calbindin mosaic in the rostral caudoputamen (Fig. 8-7A) by virtue of its stronger immunostaining, and because the calbindin-immunoreactive perikarya and processes were more sharply etched in the lateral band than in the other calbindin-positive regions.

Comparison of the distributions of TH-positive dopamine islands and calbindin-poor zones in the caudoputamen

The distributions of dopamine islands and calbindin-poor zones were compared

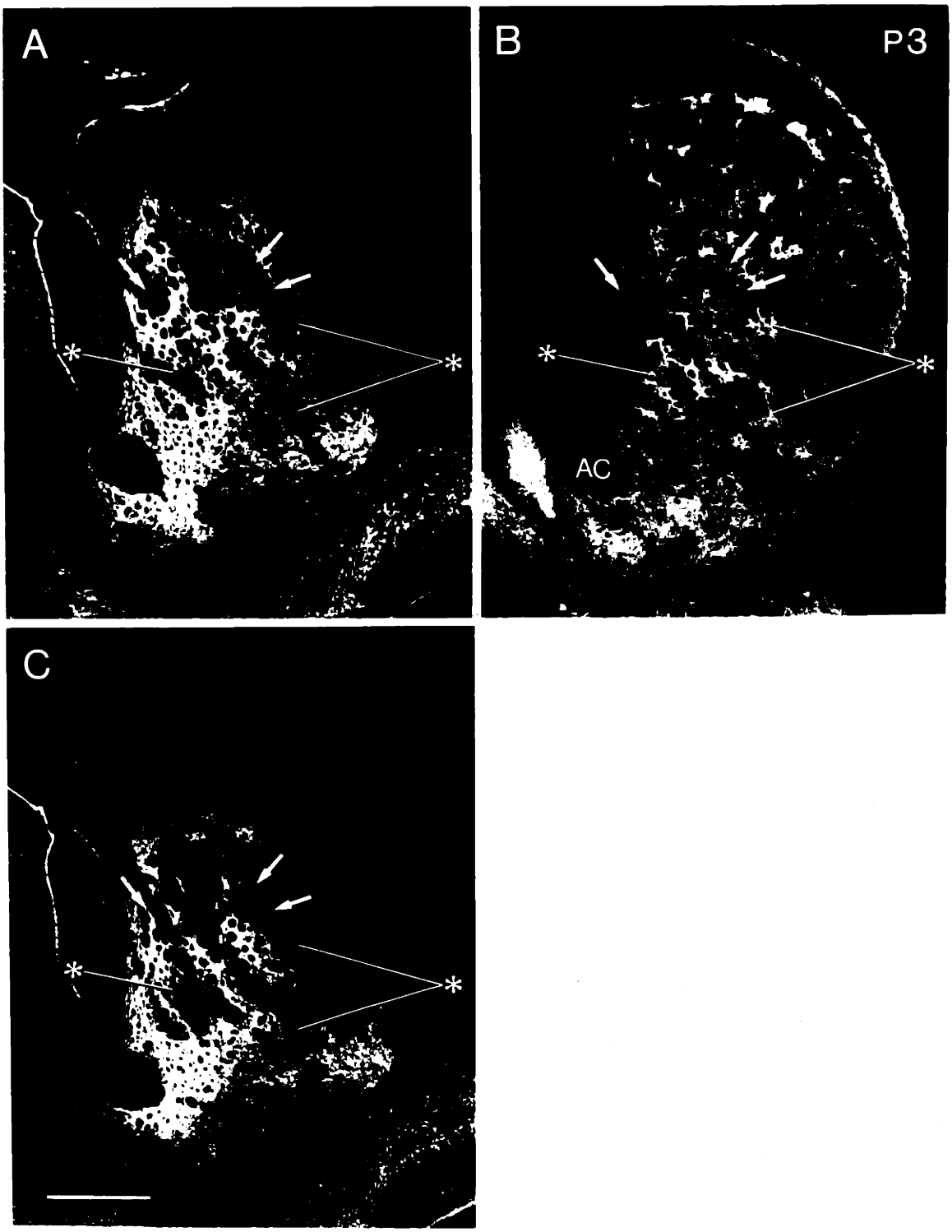
A
B
P3
AC
C

Figure 8-8. A, B & C: A triplet of serially adjoining sections through the P3 caudoputamen, stained for calbindin-like immunoreactivity (A, C) and TH-like immunoreactivity (B) and shown in reverse contrast photographs to illustrate relationship between the dopamine island system (B) and the growing calbindin mosaic. Dorsal TH-positive dopamine islands are not in regions containing the calbindin mosaic. The dopamine islands in the ventral caudoputamen (examples at asterisks in B) are in the calbindin mosaic, but are all located within the limits of the calbindin-poor zones (see accompanying sites marked by asterisks in A and C). Note that the calbindin-poor zones are larger than the corresponding TH-positive patches (see asterisks). Note also that some calbindin-poor zones do not have TH-positive correspondents (examples at arrows). AC, anterior commissure. Scale bar for A-C, 500 μm.

in the P0, P3, P7 and P15 caudoputamen in sets of serial sections stained alternately for calbindin-like and TH-like immunoreactivity. Strongly TH-immunostained patches appeared mainly in the dorsolateral caudoputamen, the regions in which the calbindin-positive mosaic was least developed, but there were also moderately to weakly-stained TH-positive patches in the ventromedial caudoputamen, which made the TH-calbindin comparisons possible (Fig. 8-8). With increasing age, the islands became obscured by the development of strong TH immunostaining in the neuropil around them. Most of our observations, therefore, were made before P15. A further constraint was the small size of the dopamine islands (e.g., ca. 20 μm to 210 μm diameter in the P3 caudoputamen illustrated in Fig. 8-8), which made it imperative to analyze runs of at least three sections. We analyzed both calbindin-TH-calbindin and TH-calbindin-TH triplets. Few successful triplets were obtained in the P0 material, because the TH-positive islands usually disappeared from one section to the next.

Nearly all TH-positive patches found in the striatal zones containing the calbindin-positive mosaic were located in the calbindin-poor parts of the mosaic (Fig. 8-8). This spatial correspondence held for each age at which we could observe the TH-positive and calbindin-poor zones in triplets of sections (P3, P7 and occasional samples at P0 and P15). Thus, given that the dopamine islands represent forerunners of striosomes, the evidence clearly suggested calbindin is expressed in medium-sized neurons of the striatal matrix compartment throughout postnatal development.

Remarkably, many of the corresponding calbindin-poor zones and TH-positive patches had strikingly different sizes and shapes despite their spatial alignment. The TH-

positive patches were nearly always considerably smaller than calbindin-poor zones whether analyzed in Triton X-100 treated sections or in sections processed without Triton X-100, and they had more angular profiles than did the calbindin-poor zones. As a result of these differences, many calbindin-poor zones of the developing striatum could be divided into subfields of two types: parts that were TH-rich and other parts that TH-poor. Some TH-positive islands formed concentric subfields within the corresponding calbindin-poor zones, but others were eccentric so that part of the TH-positive patch was in contact with the calbindin-rich surround. In the TH-poor subfields of the calbindin gaps, only the weaker "diffuse" TH-positive fiber system appeared; this system grew stronger with increasing age.

Some calbindin-poor zones lacked corresponding TH-positive patches even in triplets of sections in which correspondences could be seen elsewhere. These calbindin-poor zones thus seemed independent of the dopamine island system altogether. There was also no clear relation between TH and calbindin in the developing lateral band system in the rostral caudoputamen. Although a strong TH-positive streak extended along the dorsolateral margin of the caudoputamen, no prominent TH-positive band was found ventrally.

Highly calbindin-immunoreactive patches in the calbindin-rich matrix

Within the calbindin-rich matrix in the P3 brains, there were some small patches expressing particularly high levels of calbindin-like immunoreactivity relative to that in

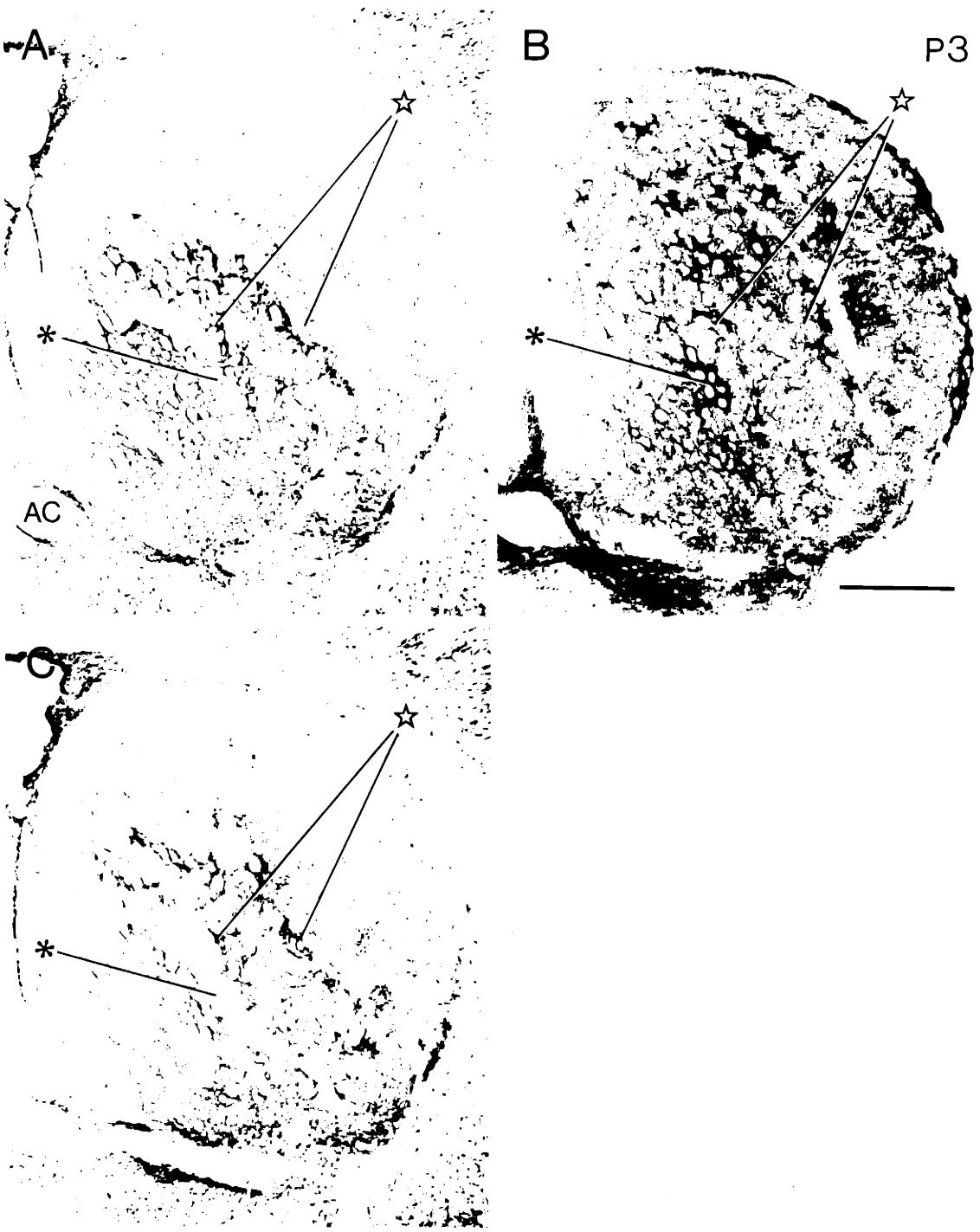
A
B
P3
AC
C

Figure 8-9. A, B & C: Lightfield photographs of serially adjoining coronal sections through the P3 caudoputamen stained for calbindin-like immunoreactivity (A, C) and TH-like immunoreactivity (B) to illustrate the heterogeneous expression of calbindin-like immunoreactivity in the calbindin-rich matrix. Small patches and bands of medium-sized neurons expressing high levels of calbindin-like immunoreactivity relative to their surrounds (examples at stars) appear in the calbindin-rich matrix. They are not aligned with TH-positive patches in adjacent sections; the TH-positive dopamine islands lie inside calbindin-poor zones (see asterisks). This triplet of sections and that in Fig. 8-8 illustrate the necessity of having "sandwiches" of sections to take into account of displacement of the patches and gaps through the distance covered by the three coronal sections (ca. 75 μm and 60 μm in Figs. 8-9 and 8-8, respectively). Even in such triplets, the calbindin-rich patches are never aligned with dopamine islands, indicating that they are patches in the striatal matrix. AC, anterior commissure. Scale bar for A-C, 500 μm.

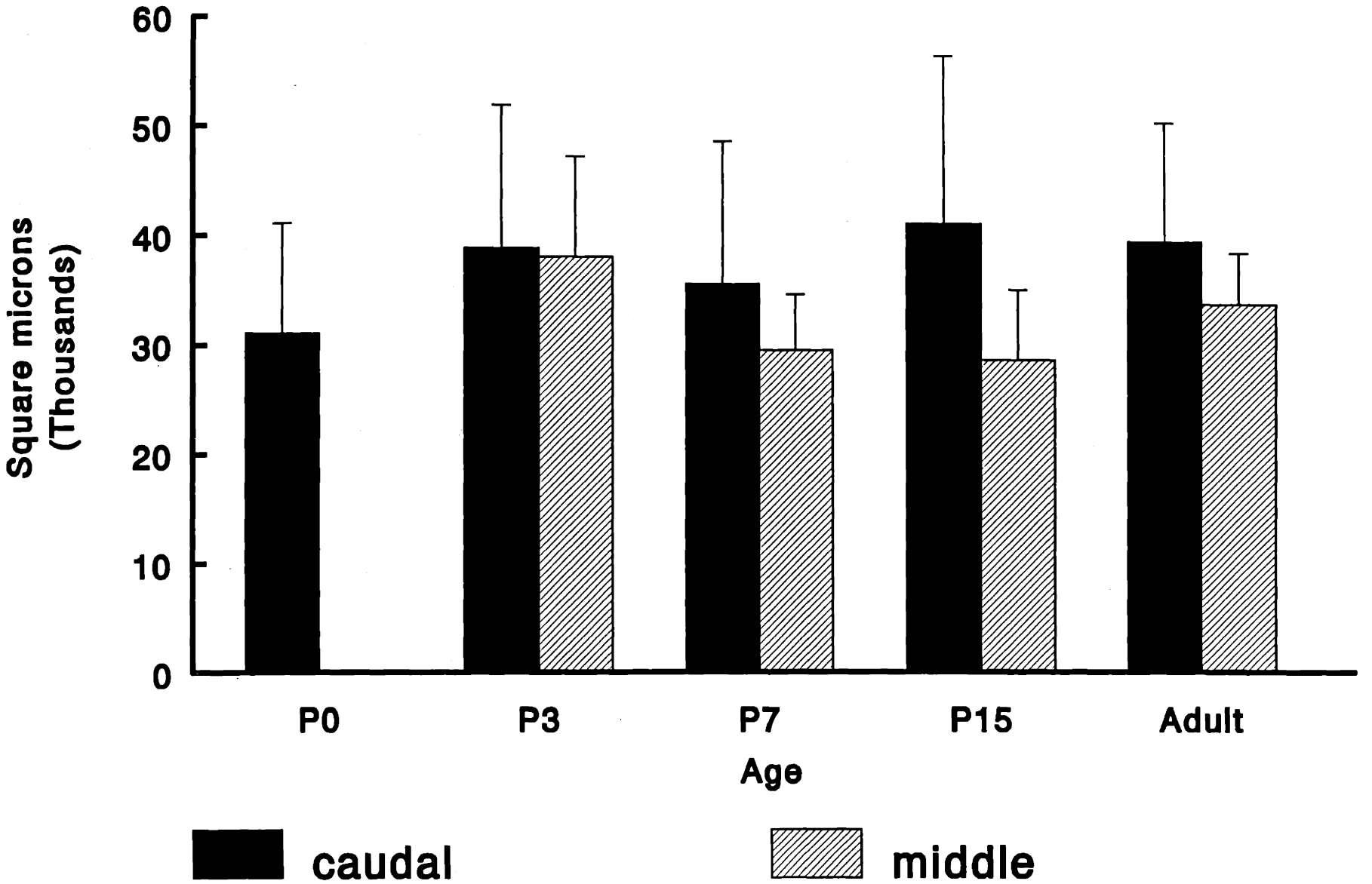
60
50
40
30
20
10
0
Square microns
(Thousands)
P0
P3
P7
P15
Adult
Age
caudal
middle

Figure 8-10. A bar graph illustrating the results of quantitative analysis of the calbindin-poor zones in the developing striatum. No statistical difference was found in the average sizes of calbindin-poor zones in the caudal levels of striatum from P0 to adulthood (black bars). At mid-striatal levels (hatched bars), the average sizes of the calbindin-poor zones decreased from P3 to P15, and then increased to adulthood. Statistical analysis by t-test (2-tailed) showed that the differences between P3 and P7 ($p \leq 0.01$), P3 and P15 ($p \leq 0.01$), P7 and adult ($p \leq 0.05$) and P15 and adult striatum ($p \leq 0.01$) were significant. There are no statistically significant differences between the average sizes of calbindin-poor zones in the middle and caudal striatum within each age group except in P15 striatum ($p \leq 0.01$).

Table 1

Age	Sections	N(CPZ)	CPZ Area	C−P Area	dl CP Area	Mosaic Area	CPZ/C−P	CPZ Area/N	EqD
P0	mean (8)	(47) 5.88	177984	2670102	1062215	1607887	0.06629	31063	189.68
Caudal	std	1.17	48247	104288	82976	67526	0.01567	10056	30.38
P3	mean (24)	(138) 5.75	221064	3571248	1233481	2337768	0.06287	38912	209.80
Caudal	std	1.90	101364	312056	279056	322052	0.03006	12990	33.56
P7	mean (22)	(140) 6.36	229630	5312257	1560794	3751463	0.04197	35553	203.11
Caudal	std	2.12	114941	845403	632131	587439	0.01833	13023	33.99
P15	mean (19)	(141) 7.42	306296	7612800	2473440	5139361	0.03939	41117	216.50
Caudal	std	2.35	145438	633312	462378	410853	0.01630	15309	39.43
Adult	mean (10)	(118) 11.8	450099	12146268	2049040	10097228	0.03701	39463	209.17
Caudal	std	3.49	154666	1036802	195542	977933	0.01200	10827	28.04
P3	mean (16)	(126) 7.88	293180	3688474	1343412	2345062	0.08066	38091	206.70
Middle	std	1.73	74590	388148	205115	360815	0.02235	9140	24.97
P7	mean (18)	(192) 10.67	315807	5520584	1852173	3668411	0.05725	29511	186.18
Middle	std	2.03	89060	875589	502656	643536	0.01348	5133	15.11
P15	mean (22)	(234) 10.64	302026	7455754	2616446	4839308	0.04010	28631	183.03
Middle	std	2.48	92582	646392	412522	366939	0.01010	6433	19.44
Adult	mean (15)	(261) 17.4	582925	11908718	2181491	9849748	0.04894	33739	198.60
Middle	std	3.07	108313	889181	349970	1248803	0.00814	4676	13.28

Table 1: Summary of quantitative data illustrating: N(CPZ)- the number of calbindin-poor zones; CPZ area- total average areas of calbindin-poor zones (averaged per section for all sections of the sample at a given age and level); C-P area- average total areas of caudoputamen; dl C-P- average total areas of the calbindin-poor dorsolateral caudoputamen; Mosaic area- average area of the calbindin mosaic; CPZ/C-P- ratios of the calbindin-poor zones to total caudoputamen areas; CPZ area/N- average sizes of calbindin-poor zones; and EqD- the equivalent diameters of circles with areas corresponding to those of the average calbindin-poor zones.

their surrounds. These patches of strongly calbindin-immunoreactive medium-sized neurons and neuropil were not aligned with the TH-positive patches in adjoining sections; they were located in the calbindin-rich matrix (Fig. 8-9). They thus were not the transient calbindin-positive patches described in the first report of this series, which correspond to dopamine islands (Liu and Graybiel, 1991a) but, instead, specialized zones in the developing matrix. These highly calbindin-immunoreactive patches were primarily distributed in the regions in which medium-sized neurons had most recently expressed calbindin-like immunoreactivity according to the developmental gradient described above: they tended to be in lateral and dorsal parts of the calbindin-positive mosaic. Some were in the calbindin-rich matrix immediately adjacent to calbindin-poor zones, but others did not have an obvious relation to the calbindin-poor zones.

Quantitative analysis of the areas of calbindin-poor zones

Because the calbindin-poor zones so often were larger than the corresponding dopamine islands, or even failed to have a corresponding TH-positive patches, we attempted to measure the dimensions of the calbindin-poor zones in a series of P0, P3, P7, and P15 brains and in brains from adult rats to see whether the calbindin-poor zones were getting smaller with ages. The analysis was limited to middle and caudal levels of the striatum because the calbindin-positive mosaic had not yet developed in the rostral striatum of the P0-P15 brains. The findings (Fig. 8-10) indicate that the average size of calbindin-poor zones do not differ significantly from P0 to adulthood at caudal levels of the caudoputamen. At mid-anteroposterior levels, however, the average sizes of

calbindin-poor zones gradually decreased from P3 to P15, and then increased from P15 to adulthood. The area of calbindin-rich matrix surrounding the calbindin-poor zones steadily increased with age as did the dorsal and lateral striatum in which low levels of calbindin-like immunoreactivity was expressed (see Table 1.).

DISCUSSION

The observations reported here lead to three main conclusions: First, calbindin-like immunoreactivity, a marker for medium-sized striatal matrix neurons at maturity, is specific to such matrix neurons throughout development. Second, despite the eventual correspondence of calbindin-poor zones and striosomes, this correspondence, as judged by comparing the calbindin-poor zones with TH-positive dopamine islands, known forerunners of striosomes, does not hold throughout development. Both the compartmental boundaries and the regional gradients of development of calbindin-poor zones and dopamine islands differ. Third, the expression of calbindin in the developing calbindin-positive matrix is itself heterogeneous, in contrast to the relatively homogeneous expression of this antigen at maturity. These findings point to a diversity of developmental factors influencing the internal architecture of the striatum, and raise the possibility that boundary formation for the striosomal system is not a singular event, but rather, the result of dynamic adjustments leading to eventual striosome-matrix complementarity.

Calbindin-like immunoreactivity is consistently expressed in the extrastriosomal matrix during development

The distribution of medium-sized calbindin-immunoreactive neurons developed gradually from a lattice with large calbindin-negative gaps into a mosaic in which more circumscript calbindin-poor zones lay embedded in calbindin-rich surrounds. Throughout this prolonged period of maturation, expression of calbindin-like immunoreactivity

followed distinct developmental gradients and was strongest in the ventral and medial parts of the developing caudoputamen. These are regions in which few strongly TH-positive dopamine islands occur, but they contained enough medium to weakly TH-immunostained patches for us to follow the strategy of comparing the developing calbindin mosaic to the dopamine island compartmentation of the striatum.

The results of these comparisons were unequivocal. TH-positive dopamine islands lay within calbindin-poor zones but not in calbindin-rich regions. Given definitive evidence the dopamine islands in the developing striatum are the forerunners of the striosomes of the mature striatum (Graybiel, 1984a; Moon Edley and Herkenham, 1984; Murrin and Ferrer, 1984; van der Kooy, 1984), we conclude that calbindin-like immunoreactivity in the medium-sized cells of the striatum is selectively expressed in the extrastriosomal matrix of the rat's striatum throughout postnatal development.

A special lateral branch of striatal calbindin system was identified at the lateral edge of the developing rostral caudoputamen and this system persisted into adulthood. Here there was some overlap of calbindin expression at diffuse TH-like immunoreactivity, but where clear TH-positive patches occurred they lay inside calbindin-poor parts of the lateral band system. Interestingly, this region is distinguished by especially dense expression of mRNA for proenkephalin (Morris et al., 1988) and by especially enhanced immunostaining for leu-enkephalin (Berendse, personal communication).

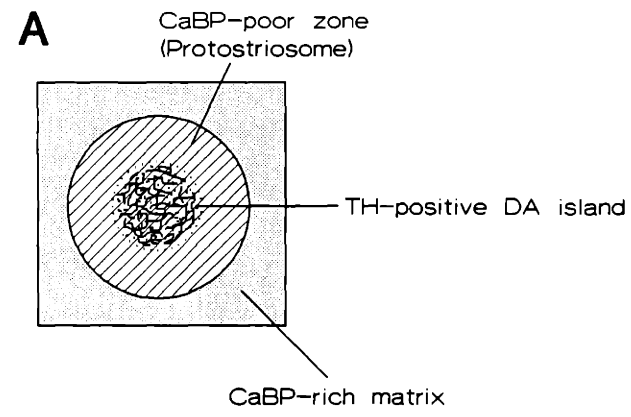
A
CaBP-poor zone
(Protostriosome)
TH-positive DA island
CaBP-rich matrix

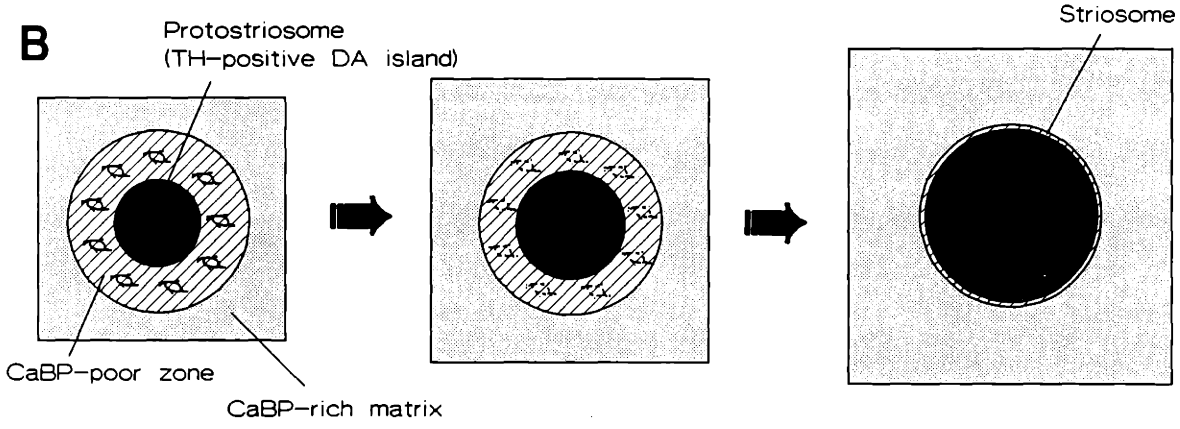
B
Protostriosome
(TH-positive DA island)
Striosome
CaBP-poor zone
CaBP-rich matrix

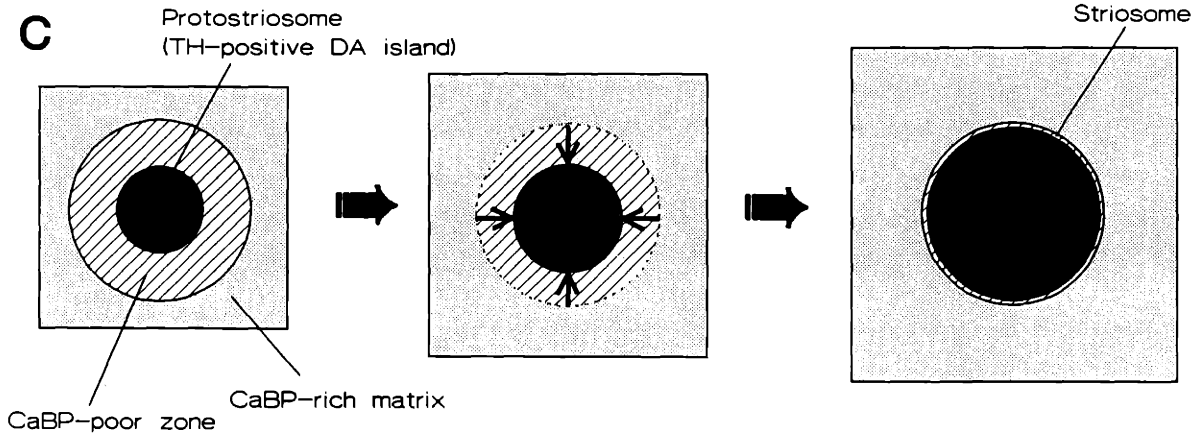
C
Protostriosome
(TH-positive DA island)
Striosome
CaBP-poor zone
CaBP-rich matrix

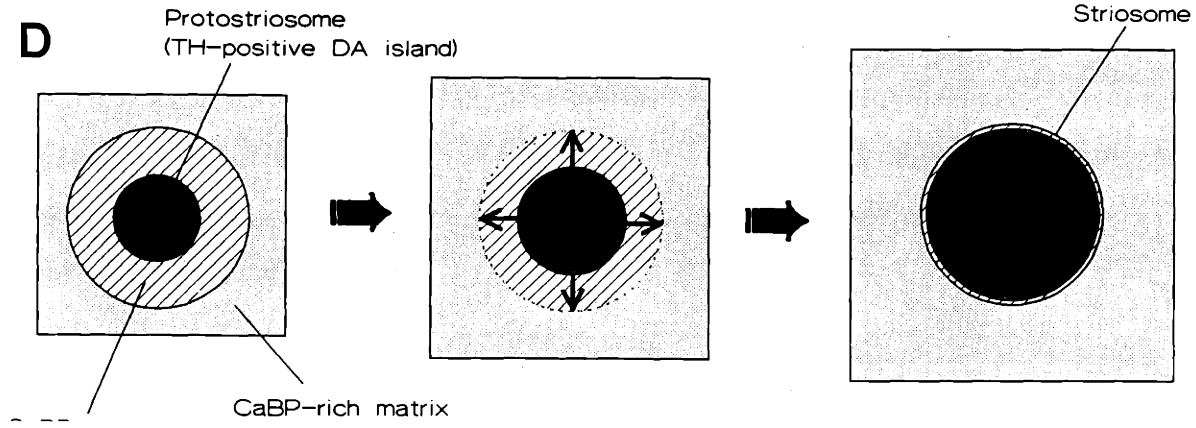
D
Protostriosome
(TH-positive DA island)
Striosome
CaBP-rich matrix

Figure 8-11. A, B, C & D: Schematic drawings illustrating four hypotheses to account for the disparity in size between the TH-positive dopamine islands and the corresponding calbindin-poor zones during striatal development and the possible mechanisms by which the striosomes and calbindin-rich matrix come to reach complementarity. In A, the TH-positive dopamine (DA) island represents only part of the developing striosome (protostriosome). The calbindin-poor zone defines the borders of the protostriosome, and the corresponding TH-positive dopamine island forms a subfield within it. B suggests that cell death occurs disproportionally in the calbindin-poor gaps around dopamine islands, and that as a consequence, the two developing striatal compartments eventually meet each other in a complementary spatial relationship. In C, the closure of the calbindin-poor gap is achieved by its "filling in" by calbindin-positive neurons around the developing striosomes. In D, there is differential expansion ("growing out") of the striosome to a relatively stable border of calbindin expression.

We never detected more than faint calbindin immunostaining in the medium-cell population of the dorsolateral caudoputamen, a region in which calbindin expression is also nearly absent at adulthood. Thus, the expression of calbindin in the medium-sized neurons of the striatum is negatively regulated here as it is in the striosomal system. Despite this negative regulation, transient calbindin-positive processes and multipolar cells appeared in this zone, as in striosomes (see accompanying paper, Liu and Graybiel, 1991a). Thus, the exclusion of calbindin expression from the medium-sized neurons of the striosomes and the dorsolateral gradient did not result from a generalized spatial restriction of expression or failure of immunostaining.

Dopamine islands and calbindin-poor zones are differentially regulated during development

A striking finding of this study is that many of the TH-positive dopamine islands, forerunner of striosomes, were clearly smaller than the corresponding calbindin-poor zones. Yet eventually, the striosomes and calbindin-poor zones precisely match (Gerfen et al., 1985). This suggests that two well-established markers for the mature striosomal system-- one expressed in striosomes and one in the complementary matrix-- follow different developmental programs.

At least two main classes of regulatory events could account for this developmental mismatch (Fig. 8-11). First, the discrepancy could reflect different compartmental regulation of afferent fibers (dopamine islands) and intrinsic striatal cells (Fig. 8-11A). The dopamine islands could, in other words, be smaller than the

developing striosomal cell clusters, and these developing cell clusters (protostriosomes) could precisely match calbindin-poor zones. At first glance, this seems unlikely because of the close spatial correspondence between dopamine islands and patches of μ opiate receptors in the developing rat's striatum (Moon Edley and Herkenham, 1984; Murrin and Ferrer, 1984; van der Kooy, 1984). These matches were mainly noted dorsally, however, where the most intensely fluorescent and TH-immunoreactive dopamine islands are, and our observations were mainly made ventrally, where the calbindin mosaic was developing but dopamine islands were less intensely stained. There are, in fact, dorsoventral differences in dopamine islands, but these would favor ventral TH-positive patches being larger, not smaller, than corresponding cell clusters (Graybiel, 1984a). We have tried to approach this issue directly by using DARPP-32 immunostaining (Foster et al., 1987) as a method to see cell clusters known to match dopamine islands (Liu and Graybiel, unpublished observations). Our findings to date suggest that DARPP-32-positive patches in the P3 and P7 caudoputamen do tend to be more nearly matched in size to corresponding calbindin-poor zones than TH-positive dopamine islands in the same sections. The DARPP-32 cell clusters may not accurately reflect the size of young striosomal cell clusters, however, because DARPP-32 is eventually expressed by both striosomal and matrix cells in the mature striatum. By P3-P7, some of the cells in the DARPP-32-positive patches could be matrix cells that had started to express DARPP-32.

An alternative interpretation of the boundary mismatch between the dopamine islands and developing calbindin-poor zones is that it reflects an early stage of a dynamic maturation process by which cells of the developing striosomes and cells of the

developing matrix eventually achieve the complementary patterns of calbindin expression characteristic of adulthood. At least three types of adjustment could close the gap between protostriosome and matrix (Figs. 8-11B-D).

First (Fig. 8-11B), neuronal death may occur selectively or disproportionally in the calbindin-poor zones around the TH-positive dopamine islands, and as a consequence, the sizes of calbindin-poor zones may be adjusted to the sizes of striosomes with which they are spatially aligned. About 25% of the neurons in the rat's striatum are thought to be lost during the first postnatal week (Fentress et al., 1981; Fishell and van der Kooy, 1987b). It is not known whether neuronal death occurs equally in the striosomal and matrix compartments of the striatum. If cells are lost predominantly in the matrix compartment, the complementary relationship between striosomes and matrix that holds at maturity could readily be achieved during development by a weighing factor applied to the matrix cells around dopamine islands. Unfortunately, because the TH immunostaining of the developing striatum becomes homogeneous before the calbindin-positive matrix completes its development, we could not determine the time at which the calbindin-poor zones came to fit the striosomes precisely. On the other hand, our quantitative measurements did suggest that the calbindin-poor zones shrink during the P3-P15 period (see below). Interestingly, during the first postnatal week boundaries around the developing striosomes have been identified with glycoconjugate markers in the mouse (Steindler et al., 1988); and at maturity, an annular peristriosomal arrangement of a number of transmitter-related markers has been demonstrated (in primates and cats, see e.g., Graybiel and Ragsdale, 1978, 1983; Beach and McGeer, 1984;

Faull et al., 1989). Conceivably, this "annular compartment" (Faull et al., 1989) could have a distinctive developmental course.

A second possibility (Fig. 8-11C) is that neurons in the calbindin-poor zones surrounding TH-positive patches may be immature matrix cells that will "fill in" the zones of discrepancy by expressing calbindin-like immunoreactivity later in the course of striatal development. This hypothesis suggests that the maturation of nearby striosomal and matrix compartments would be under joint control by local regulatory factors. For example, the developmental expression of calbindin in matrix neurons might follow a local outside-in gradient with respect to the TH-positive dopamine islands. This "filling in" hypothesis also suggests that the matrix is developmentally heterogeneous, which is consonant with other evidence (see below).

A third alternative (Fig. 8-11D) is that the gap between the protostriosomes and calbindin-rich matrix is filled in by striosomal cells, not cells of the matrix. The most reasonable possibility here is that there could be differential growth of the perikarya and processes of striosomal cells relative to that occurring in cells of the matrix. There are sufficient neurochemical differences between striosomes and matrix, many undergoing dynamic shifts in the early postnatal period, to suggest that differential maturation could occur in the two compartments. Indeed, over a prolonged period of development striosomes lead the matrix, so that they might be favored competitively at striosome/matrix boundaries.

The different regulatory schemes summarized in Fig. 8-11 are not mutually exclusive. For example (Figs. 8-11A and 8-11B), the early development of dopamine

island afferents could serve to stabilize corresponding striatal cells and their striatonigral connections (see Graybiel and Hickey, 1982; Fishell and van der Kooy, 1987b), and cell death could occur in the calbindin-poor gaps around dopamine islands because of the temporal lag between maturation of the dopamine island and matrix innervations. Similarly, "filling in" by matrix and "growing out" by striosomes (Figs. 8-11C and 8-11D) could occur simultaneously and with mutual interactions.

The results of our quantitative analysis added an unexpected finding by suggesting that the average areas of calbindin-poor zones in the neonatal (P3) and mature caudoputamen are very similar. In fact, traced successively from P0 to P3, P7, P15 and maturity, the sizes of the calbindin-poor zones in the caudal caudoputamen do not change significantly during the course of development. This finding tends to support the possibility that there are relatively stable borders of calbindin expression and that the calbindin-poor zones, rather than the TH-positive dopamine islands, are the better predictors of future striosomal borders (Fig. 8-11A, 8-11D). However, the quantitative results suggest that calbindin-poor zones in mid-striatal levels decrease in average size from P3 to P15, and then increase to mature. These more anterior levels are near the growing front of calbindin-expression and may better reflect dynamic changes occurring in the maturing caudoputamen. The finding of the decrease in size followed by an increase suggests that early in development the calbindin-poor gaps fill in (or are eliminated by cell death) and then expand with the general maturational expansion of the developing striatum. The adjustment of the striosome and matrix borders by selective cell death or by matrix cells filling in the calbindin-poor gaps around the

dopamine islands would, by this account, be counterbalanced by the increasing size of the two striatal compartments. The lack of significant changes in size of calbindin-poor zones at caudal levels should reflect the greater maturity of this region. Interestingly, according to our findings, dynamic interactions at the borders may occur until relatively late in development at all but these most caudal levels, so that activity could play a role in achieving the final matches.

Heterogeneity of calbindin expression in the striatal matrix

Developmental heterogeneity of the matrix near striosomes is suggested by the second hypothesis noted above (Fig. 8-11B). There was also direct evidence for matrix heterogeneity in the differential calbindin immunostaining of different parts of the matrix. In early postnatal brains there were clusters of cells with particularly intense calbindin-like immunoreactivity within the calbindin-rich matrix. These patches were sometimes but not always beside calbindin-poor zones, and they were mainly seen in the newly formed parts of the calbindin-rich lattice-works. Zahm and coworkers (1990) have also reported a form of non-striosomal, but patchy, neurochemical differentiation in the developing rat's caudoputamen. They found patches of cells expressing neurotensin-like immunoreactivity in regions outside substance P-immunoreactive patches that were spatially aligned with TH-positive dopamine islands.

Evidence from recent track-tracing studies suggests that in the mature striatum there is sub-compartmentalization of medium-sized projection neurons in the matrix of the mature striatum both in the cat (Desban et al., 1989; Jiménez-Castellanos and

Graybiel, 1989) and in the primate (Selemon and Goldman-Rakic, 1990; Giménez-Amaya and Graybiel, 1990, 1991). If some clustered sets of efferent neurons reach their targets before other sets, early differentiation of such neurons and therefore expression of antigens characteristic of maturity could be triggered. Afferent fiber projections to the striatal matrix are also distributed in heterogeneous patterns within the matrix (see, e.g., Malach and Graybiel, 1986; Ragsdale and Graybiel, 1988b; Flaherty et al., 1989). Early arrival of subsets of these afferents might also trigger patchy expression of calbindin-like immunoreactivity.

Compartmental expression of calbindin in the striatal matrix and development of the dopamine island/striosome system occur along different spatial gradients during development

It was striking that the compartmental expression of calbindin-like immunoreactivity by medium-sized striatal neurons, despite being clearly correlated with the dopamine island compartmentation of nigrostriatal afferents, occurred mainly in districts in which only weakly or moderately immunostained TH-positive dopamine islands were present. Moreover, the ontogenic ventral-to-dorsal gradients of calbindin expression by the medium-sized striatal neurons were inverse to the developmental gradient of the dopamine island system (Voorn et al., 1988). This evidence suggests that the compartmental expression of calbindin-like immunoreactivity may occur separately from, and even independently of, the compartmental development of the dopamine island system. This conclusion is compatible with the demonstration that the expression

of calbindin-like immunoreactivity in the striatum of young adult and developing rats is not altered by lesions destroying the nigrostriatal dopaminergic fibers at the time of birth or even before dopamine islands start to form (Gerfen et al., 1987a; Snyder-Keller, 1991). The calbindin-positive mosaic also occurs in the weaver mouse despite abnormalities occurring in the dopamine-containing innervation as early as P7 (Graybiel et al., 1990; Roffler-Tarlov et al., 1990).

It has been shown for the rat that patches of dopamine D1 binding sites, which mark striosomal loci, follow a ventral to dorsal developmental gradient in the caudoputamen as does calbindin expression in the matrix (Murrin and Zeng, 1989). The ontogeny of several other neurochemicals in striatal neurons, including glutamic acid decarboxylase and DARPP-32, has similarly been reported to follow ventral to dorsal gradients (Fisher et al., 1987; Foster et al., 1987). However, patches of developmental μ opiate receptors (Murrin and Zeng, 1989) and AChE-rich patches (Butcher and Hodge, 1975; Murrin and Ferrer, 1984; Liu and Graybiel, unpublished observations), also marking striosomal loci, develop along the dorsolateral to medial gradient followed by dopamine islands (Voorn et al., 1988). This suggests that the developmental gradients of neurochemical constituents of striosomes and matrix are not necessarily compartment-specific. Some are shared by striosome and matrix constituents, but others are not.

Relationship of the developing calbindin-positive mosaic to the transient calbindin-positive systems of the striatum

As described in the accompanying paper (Liu and Graybiel, 1991a), transient

calbindin-positive systems were visible in the perinatal striatum as well as in the ganglionic eminence at E18-P15 in sections treated with Triton X-100. These included radially arranged calbindin-positive processes stretching from the germinal epithelium into the developing caudoputamen, patches of calbindin-positive neuropil in register with many of the dorsal dopamine islands, and a scattered population of calbindin-positive neurons with clearly immunostained, ramified dendrites. The transient calbindin-immunoreactive systems in the caudoputamen mostly lay dorsal to the regions in which the calbindin-positive lattice-works and mosaics were developing, but there was some overlap nonetheless. Some radial calbindin-positive processes passed through the lateral band system, a few calbindin-immunoreactive neurons with well-stained dendrites were present in the lateral and dorsal parts of the calbindin-positive medium-cell mosaics, and some transient calbindin patches extended fairly far ventrally. The dense immunostaining in the calbindin lattice-works and mosaics obscured greater overlap, and weak neuropil staining in some calbindin-poor gaps may actually have represented transient calbindin-positive patches. There was no evidence, however, of any systemic link between the transient (more dorsal) and persistent (more ventral) calbindin-immunoreactive systems.

Because calbindin functions in relation to intracellular calcium stress (Mattson et al., 1991), the primary compartmental affiliation of calbindin with neurons of the developing matrix is probably an important indicator of the functional development of the matrix. The transient calbindin-positive patches aligned with dopamine islands appeared to be mainly comprised of fibers (and a few multipolar cells), but not of the medium-sized neurons that were sites of calbindin expression farther ventrally. It should

be noted, however, that the compartmental pattern of expression of calbindin in the developing matrix is not shared by another calcium-related protein, calcium/calmodulin-dependent protein kinase type II, which is concentrated in clusters of medium-sized cells corresponding to dopamine islands during striatal development (Newman-Gage and Graybiel, 1988; Liu and Graybiel, unpublished observations). Therefore, two different calcium-related proteins, presumably serving different intracellular functions (e.g., calcium buffering and protein kinase activity), are expressed in a spatially complementary way in medium-sized neurons of the developing striosome and matrix compartments. Functionally, this suggests that biochemical cascades activated by elevated levels of calcium may differ in the medium-sized cell population of immature striosomes and matrix.

Chapter 9

General discussion

The results of the transplantation studies in the present thesis are summarized as follows:

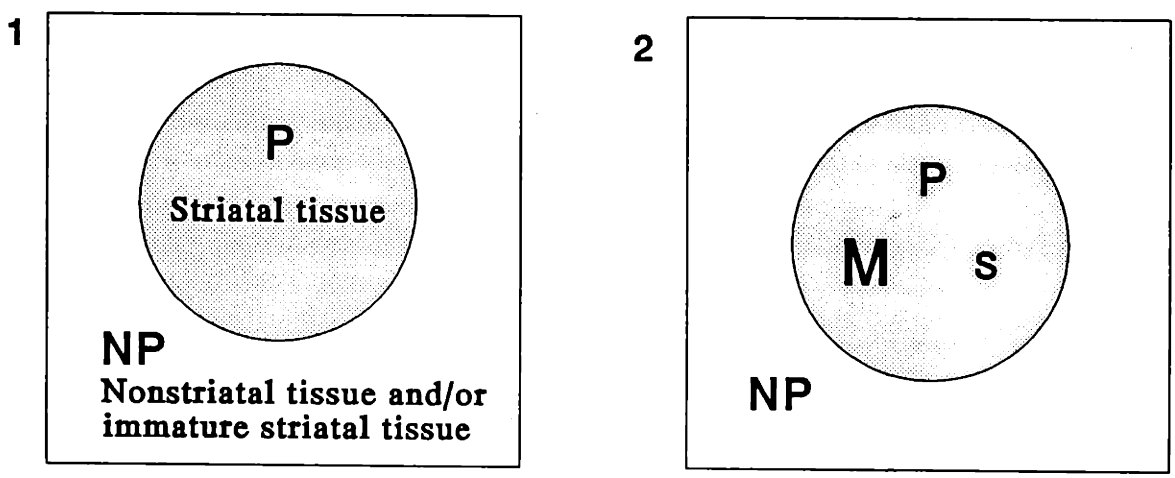

1. The modular organization of embryonic striatal grafts may reflect an admixture of different tissue types. The P regions almost certainly represent striatal tissue, whereas the NP regions may contain non-striatal tissue and/or immature striatal tissue.

2. The P regions of embryonic striatal grafts at least contain the matrix tissue.

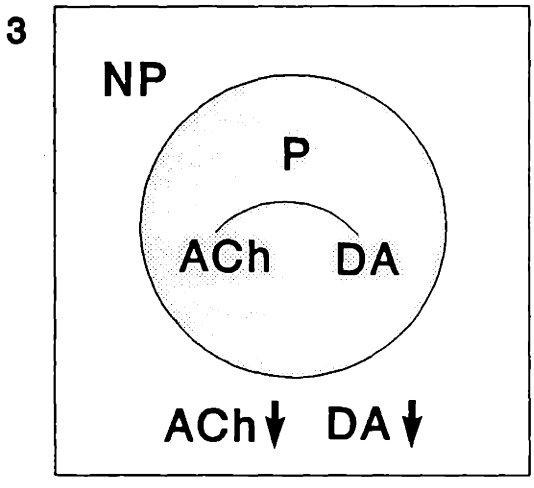

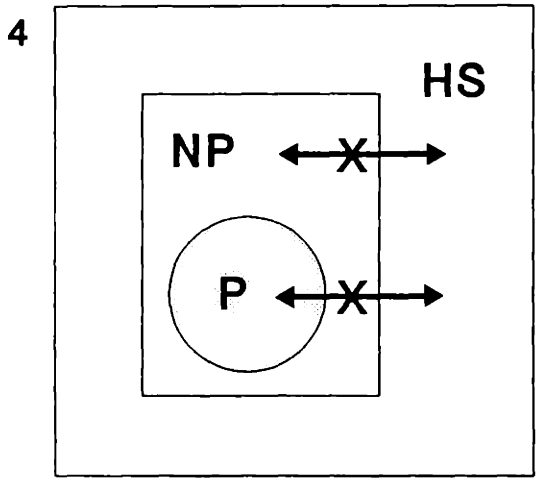

3. There is an anatomical reconstitution of cellular components of cholinergic and dopaminergic systems in the P regions of embryonic striatal grafts.

4. There is no extensive mutual migration between donor neurons and host striatal neurons in striatal graft environment.

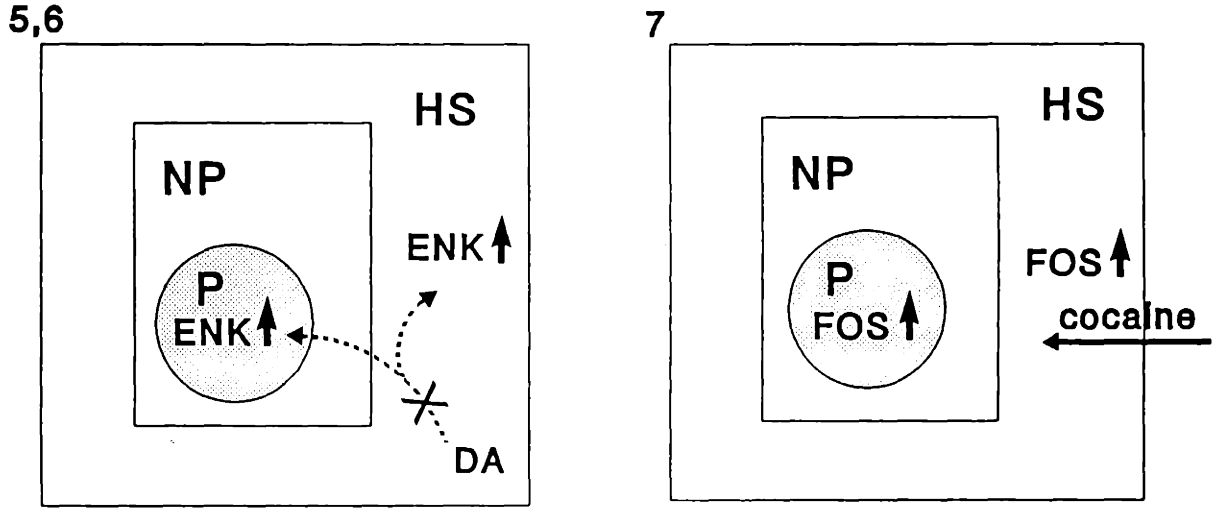

5. The TH-containing afferents from the host striatum are not obligatorily involved in sorting out of subpopulations of grafted cells to from P regions and NP regions.

6. The enkephalin-positive neurons in the P regions of embryonic striatal grafts are likely to be regulated by the TH-containing dopaminergic nigrostriatal afferents from the host.

7. The neurons of P regions are likely to be integrated at the signal-transduction level into the striatal circuits reconstructed by embryonic striatal grafts in the excitotoxin-damaged striatum.

The importance of the P regions in embryonic striatal grafts

The central basis of the work presented in this thesis is that embryonic striatal grafts may contain heterogeneous types of tissues of which only one, comprising the P regions, represents striatal tissue. The thesis demonstrates not only that these are the sites in which striatal neurotransmission elements are reconstituted, but also that these sites are those in which the nigrostriatal pathway is rebuilt. Furthermore, the thesis demonstrates that the neurons of P regions are probably functionally integrated into the dopaminergic nigrostriatal system of the host at a level as fundamental as signal-transduction. The importance of the P regions in striatal grafts is further supported by the recent connectivity studies of striatal grafts (Wictorin et al., 1988, 1989a, 1989b, 1989c, 1990a, 1990b; Wictorin and Björklund, 1989). Wictorin et al. (1989b, 1989c) have shown that the frontal cortex of the host projects to both the P and NP regions of striatal grafts. What is more striking is that there is a strong projection form the P regions of striatal grafts to one of the normal striatal targets, the globus pallidus (Wictorin et al., 1989b, 1989c). Thus, the P regions can process neural information from the cortex, and this information can be modulated by the dopaminergic inputs from the substantia nigra. The neural information can be further forwarded to the globus pallidus, and then be relayed back to the cortex through the thalamus. Therefore, transtriatal circuitry running through the P regions of striatal grafts can be reconstructed in the host brain. Together with the results of the studies in the present thesis, these findings suggest that the P regions of striatal grafts may play a major role in determining the functional integration between embryonic striatal grafts and the host brain.

Why P regions of E15-E16 striatal grafts are smaller than the surrounding NP zones?

If the P regions of striatal grafts is important as discussed above, the amount of the P tissue may critically determine how extensively functional interactions between striatal grafts and host brain can occur. One of the consistent findings in our graft preparations is that the cross-sectional sizes of P regions were almost always smaller than those of NP regions in striatal grafts derived from E15 and E16 striatal primordia. P regions took up ca. 15-23% of the total cross-sectional area of the grafts (Liu and Graybiel, unpublished observations). The main exceptions to this trend were in the caudal sections in which the grafts became smaller. Thus, the P regions appeared to be islands in a sea of NP tissue. Three explanations could account for this phenomenon. First, the dissection of donor tissue may include more progenitor cells of NP regions than progenitor cells of P regions. Second, the cells in NP regions may preferentially survive transplantation over the cells in P regions. Third, the proliferation of neural precursor cells in the donor tissue may continue to occur in the graft milieu. If histogenesis in the P and NP regions occurs disproportionally and/or with different time courses in the graft milieu, more cells could be generated in the NP regions than in the P regions. Proliferation of donor cells has been shown to persist in solid cortical grafts, and moreover, the neurogenesis in such grafts follows a similar time schedule as that occurring in normal cortical development *in vivo* (Jaeger and Lund, 1980; Das and Ross, 1986). Experiments designed to determine whether histogenesis could occur in our cell-suspension striatal grafts are now in progress. Fourth, many neurons in NP regions are larger than those in P regions, and the neuropil density in NP regions could therefore be

higher than that in P regions. Together, these factors could contribute to the larger size of the NP regions.

Interestingly, we have found that the relative proportion of the grafts taken up by P regions was greater in striatal grafts derived from E14 donor tissue (ca. 24%-71%) than in grafts derived from E15-E16 donor tissue (ca. 15%-23%) (Liu and Graybiel, unpublished observations). In fact, in some sections of E14 grafts, smaller NP regions appeared as modules with larger P regions surrounding them. As discussed in Chapters 2 and 7, a population of multipolar calbindin-positive neurons similar to those in the NP regions were transiently present in the junction between the ventral part of lateral ganglionic eminence and the dorsal part of ventrolateral cortical anlage of E15 brain. A much smaller population of similar multipolar calbindin-positive neurons appeared in the same region in the E14 brains. Conceivably, then, the dissection of E15 donor tissue could have included more of this calbindin-positive population than that of E14 donor tissue. The variation in dissection of each striatal primordium, i.e. the amount of the ventral part of lateral ganglionic eminence included in the donor tissue may account for the fact that the proportions of P regions varied from graft to graft.

An interest possibility raised by these observations is that this calbindin-positive population may be derived from cortical cells migrating tangentially from the lateral cortical primordium, and not migrating radially from the ganglionic eminence (Bayer, 1990; Austin and Cepko, 1990). If these multipolar calbindin-positive neurons were derived from the progenitors in the lateral ganglionic eminence, the distribution of P and NP regions should be roughly the same in E14 grafts and in E15-E16 grafts, as the

dissection always included the ventricular zone of lateral ganglionic eminence. It should be noted, however, the differential status of the progenitor cells in the lateral ganglionic eminence may vary in developmental course. Thus, progenitor cells at E14 lateral ganglionic eminence may give rise predominantly to striatal cells, but at E15-E16, more progenitor cells may start to differentiate into non-striatal cells.

Interestingly, the presence of multipolar calbindin-positive neurons in embryonic striatal grafts seems to be donor-age dependent. It has been reported that very few large multipolar calbindin-positive neurons appear in E17-E18 striatal grafts (Roberts and DiFiglia, 1990). Curiously, however, the modular organization as seen with AChE stain is still present in E17 striatal grafts (Sanberg et al., 1986). The modularity of the grafts and the occurrence of the large multipolar calbindin-positive neurons may thus not be rigidly linked.

Embryonic striatal grafting as a paradigm for studying the development and function of the striatal system

One of the initial motives behind the striatal grafting studies of the present thesis was to investigate the development of striatal compartmentation by using embryonic striatal grafting as a model system. Although our results do not support the original suggestion that the modularity of embryonic striatal grafts represents immature striatal compartmentation (Chapter 2), there are still a number of interesting phenomena associated with the striatal grafting system. For example, one can study the relevance of reestablishing striatonigral connections and the full expression of striosomal

organization in striatal grafts (see Chapter 2) by co-grafting striatal and nigral primordia into the host striatum.

More promisingly, with the advance of molecular biological techniques, transplanting embryonic cells derived from specific developing neural primordia of animals in which certain genes have been ablated or replaced with others (e.g. see Rossant, 1990) into the homotopic regions of the host brain may become possible. This strategy will offer a unique approach to target certain molecules of cells in a specific population of the nervous system and then evaluate the functional consequence. For instance, one can graft striatal cells derived from transgenic mice in which the expression of certain genes has been disrupted, and then to study whether the nigrostriatal afferents from the host brain can still preferentially innervate the P regions of striatal grafts (see Chapter 3), or to study which molecules are involved in the induction of Fos by dopamine agonists (see Chapter 6). Thus, the combination of intracerebral grafting and molecular genetic manipulation techniques should provide a new avenue for studying how specifical genetic activation is involved in the development and function of the striatal system.

Embryonic striatal grafting as a neuronal replacement therapy for Huntington's disease: its potential and limitations

It is remarkable that embryonic striatal grafts can develop properly in the exctiotoxin-damaged striatum, and reestablished the connectivity, though not in full extent, with the adult host brain. Moreover, at least dopamine-containing nigrostriatal

afferents from the host can be functionally integrated into striatal circuits rebuilt by striatal grafts. All these different lines of evidence suggest that embryonic striatal transplantation represents a promising therapy for Huntington's disease in the future. However, several important questions should be considered before any initiation of clinical trials.

First, can similar striatal grafting be successfully reproduced in non-human primate experiments as that in the rodent? A pilot study by Isacson et al. (1989) has demonstrated that striatal grafts derived from rat donor tissue can survive in the baboon striatum. Furthermore, Wictorin et al. (1990a) have shown that similar modular pattern of P/NP regions as that in rodent striatal grafts appears in the human forebrain/striatal grafts implanted into the rat host striatum. Evidently, it is important to know how the NP tissue affect the development and function of striatal grafts. If the NP tissue is not beneficial to the grafts, how could the grafting procedure be improved to increase the P tissue in the grafts? Second, can the progressive process of neurodegeneration in Huntington's disease destroy the transplanted cells? As we lack an appropriate animal model of Huntington's disease in reflecting its progressive neuronal death in the striatum, it is not known whether embryonic striatal grafts could survive in the host striatum in which neuronal degeneration continues to occur. Thus, developing a suitable animal model of Huntington's disease is necessary and important not only for understanding the mechanism of the disease, but also for testing experimental therapies. On the contrary, embryonic striatal grafts may have positive effects in protecting the host striatal neurons from degeneration. Such protective function of striatal grafts have recently been shown

in the excitotoxin-damaged adult striatum (Pearlman et al., 1991). Third, the ultimate goal of most graft therapies is to replace the full repertoire of neuronal substrates in the neurodegenerative disorders. As demonstrated in Chapter 2, the P zones of striatal grafts contain primarily striatal matrix tissue. Therefore, an important question is whether the protocol of striatal grafting can be modified to increase the striosomal tissue. Fourth, much of normal striatal function is dependent on the appropriately topographic connections with the other brain regions. Can the normal topography of afferent and efferent connections be reconstructed in striatal grafts? Finally, can the grafts survive for a long time-- as long as the life span of the patient receiving the transplant? Quantitative study has shown that striatal grafts derived from E17-E18 rat donors can survive as long as 16 months without losing substantial numbers of grafted neurons (Roberts and DiFiglia, 1990).

Only with all these questions being explored continuously will it be then possible to develop a truly efficient striatal grafting therapy for Huntington's disease.

REFERENCES

Antonini, A., and C.J. Shatz (1990) Relation between putative transmitter phenotypes and connectivity of subplate neurons during cerebral cortical development. Eur. J. Neurosci. **2**:744-761.

Aguayo, A.J. (1985) Axonal regeneration from injured neurons in the adult mammalian central nervous system. In: Synaptic Plasticity, C.W. Cotman, ed. pp. 457-484, Guilford Press, New York.

Armstrong, D.M., G. Bruce, L.B. Hersh, and F.H. Gage (1987) Development of cholinergic neurons in the septal/diagonal band complex of the rat. Dev. Brain Res. **36**:249-256.

Aquilonius, S.M., and R. Sjöström (1971) Cholinergic and dopaminergic mechanisms in Huntington's chorea. Life Sci. **10**:405-414.

Austin, C.P., and C.L. Cepko (1990) Cellular migration patterns in the developing mouse cerebral cortex. Development **110**:713-732.

Backlund, E.-O., P.-O. Granberg, B. Hamberger et al. (1985) Transplantation of adrenal medulla tissue to striatum in parkinsonism. J. Neurosurg. **62**:169-173.

Baimbridge, K.G., J.J. Miller, and C.O. Parkes (1982) Calcium-binding protein distribution in rat brain. Brain Res. **239**:519-525.

Barbe M.F. and P. Levitt (1991) The early commitment of fetal neurons to the limibic cortex. J. Neurosci. **11**:519-533.

Barbeau, A. (1962) The pathogenesis of Parkinson's disease: a new hypothesis. Can. Med. Ass. J. **87**:802-807.

Bayer, S.A. (1984) Neurogenesis in rat striatum. Int. J. Devel. Neurosci. **2**:163-175.

Bayer, S.A., J. Altman, and R. Russo (1990) Lateral migration of cells in embryonic neocortex. Soc. Neurosci. Abstr. **16**:803.

Beach, T.G., and E.G. McGeer (1984) The distribution of substance P in the primate basal ganglia: an immunohistochemical study of the baboon and human brain. Neuroscience **13**:29-52.

Beal, M.F., N.W. Kowall, D.W. Ellison, M.F. Mazurek, K.J. Swartz, and J.B. Martin (1986) Replication of the neurochemical characteristics on Huntington's disease by quinolinic acid. Nature **321**:168-171.

Beckenstein, J.W., and G.F. Wooten (1989) Hemicholinium-3 binding sites in rat brain: a quantitative autoradiographic study. Brain Res. **481**:97-105.

Beckstead, R.M., G.F. Wooten, and J.M. Trugman (1988) Distribution of D1 and D2 dopamine receptors in the basal ganglia of the cat determined by quantitative autoradiography. J. Comp. Neurol. **268**:131-145.

Berger, B., C. Verney, P. Gaspar, and A. Febvert (1985) Transient expression of tyrosine hydroxylase immunoreactivity in some neurons of the rat neocortex during postnatal development. Devel. Brain Res. **23**:141-144.

Besson, M.-J., A.M. Graybiel, and M. Nastuk (1988a) SCH 23390 ligand binding for striatal D1 dopamine receptors: distribution follows striosomal ordering in cat, monkey and human. Neuroscience **26**:101-119.

Besson, M.-J., A.M. Graybiel, and B. Quinn (1986) Coexistence of dynorphin B-like and substance P-like immunoreactivity in striatal neurons in the cat. Soc. Neurosci. Abstr. **12**:876.

Besson, M.-J., A.M. Graybiel, and B. Quinn (1988b) Patterns of coexistence of neuropeptides and glutamic acid decarboxylase in neurons of the feline striatum. Soc. Neurosci. Abstr. **14**:156.

Bignami, A., L.F. Eng, D. Dahl, and C.T. Uyeda (1972) Localization of the glial fibrillary acidic protein in astrocytes by immunofluorescence. Brain Res. **43**:429-435.

Bischoff, S., M. Heinrich, J.M. Sonntag, and J. Krauss (1986) The D-1 dopamine receptor antagonist SCH23390 also interacts potently with brain serotonin (5-HT2) receptors. Eur. J. Pharmacol. **129**:367-370.

Björklund, A., O. Lindvall, O. Isacson, P. Brundin, K. Wictorin, R. Strecker, D.J. Clarke and S.B. Dunnett (1987) Mechanisms of action of intracerebral neural implants: Studies on nigral and striatal grafts to the lesioned striatum. Trends Neurosci. **10**:509-516.

Björklund, A. and U. Stenevi (1984) Intracerebral neural implants: Neuronal replacement and reconstruction of damaged circuitries. Ann. Rev. Neurosci. **7**:229-308.

Björklund, A., U. Stenevi, R.H. Schmidt, and S.B. Dunnett (1983) Intracerebral grafting of neuronal cell suspensions. II. Survival and growth of nigral cells implanted in different brain sites. Acta Physiol. Scand. Suppl. **522**:11-22.

Bolam, J.P., B.H. Wainer, and A.D. Smith (1984) Characterization of cholinergic neurons in the rat neostriatum. A combination of choline acetyltransferase immunocytochemistry, Golgi-impregnation and electron microscopy. Neuroscience **12**:711-718.

Boylan, M.K., M.S. Levine, N.A. Buchwald and R.S. Fisher (1990) Patterns of tachykinin expression and localization in developing feline neostriatum. J. Comp. Neurol. **293**:151-163.

Boyson, S.J., P. McGonigle, and P.B. Molinoff (1986) Quantitative localization of the D1 and D2 subtypes of dopamine receptors in rat brain. J. Neurosci. **6**:3177-3188.

Brené, S., N. Lindefors, M. Herrera-Marschitz, and H. Persson (1990) Expression of dopamine D2 receptor and choline acetyltransferase mRNA in the dopamine deafferented rat caudate-putamen. Exp. Brain Res. **83**:96-104.

Butcher, L.L. (1983) Acetylcholinesterase histochemistry. In: Handbook of Chemical Neuroanatomy, Vol. I: Method in Chemical Neuroanatomy, A. Björklund and T. Hökfelt eds., pp.1-49, Elsevier, Amsterdam.

Butcher, L.L., and G.K. Hodge (1976) Postnatal development of acetylcholinesterase in the caudate putamen and substantia nigra of rats. Brain Res. **106**:223-240.

Cenci, M.A., R.J. Mandel, P. Kalen, K. Wictorin, and A. Björklund (1990) C-*fos* induction in intrastriatal grafts of fetal nigral and striatal tissue: Functional role of D1 dopamine receptors in graft-host interactions. Soc. Neurosci. Abstr. **16**:469.

Cepko, C. (1988) Immortalization of neural cells via oncogene transduction. Trends Neurosci. **11**:6-8.

Chang, H.T. (1987) Evidence for a monosynaptic relationship between dopaminergic terminals and cholinergic neurons in the rat striatum: a double-labeling immunocytochemical study. Soc. Neurosci. Abstr. **13**:1572.

Choi, D.W. (1988) Calcium mediated neurotoxicity: relatioship to specific channel types and role in ischemic damage. Trends Neurosci. **11**:465-469.

Chun, J.J.M., and C.J. Shatz (1989) Interstitial cells of the adult neocortical white matter are the remnant of the early generated subplate neuron population. J. Comp. Neurol. **282**:555-569.

Chang, H.T. (1988) Dopamine-acetylcholine interaction in the rat striatum: A dual labeling immunocytochemistry. Brain Res.Bull. **21**:295-304.

Chesselet, M.-F. (1984) Presynaptic regulation of neurotransmitter release in the brain: Facts and hypothesis. Neuroscience **12**:347-375.

Clarke, D.J., S.B. Dunnett, O. Isacson, D.J.S. Sirinathsinghji and A. Björklund (1988) Striatal grafts in rats with unilateral neostriatal lesions-I. Ultrastructural evidence of

afferent synaptic inputs from the host nigrostriatal pathway. Neuroscience **24**:791-801.

Coyle, J.T., and R. Schwarcz (1976) Lesions of striatal neurons with kainic acid provides a model for Huntington's chorea. Nature **263**:244-246.

Das, G.P., and D.T. Ross (1986) Neural transplantation: autoradiographic analysis of histogenesis in neocortical transplants. Int. J. Devl. Neurosci. **4**:69-79.

Davies, S.W., and P.J. Roberts (1988) Sparing of cholinergic neurons following quinolinic acid lesions of the rat striatum. Neuroscience **26**:387-393.

Deckel A.W., R.G. Robinson, J.R. Coyle, P.R. Sanberg (1983) Reversal of long-term locomotor abnormalities in the kainic acid model of Huntington's disease by day 18 fetal striatal implants. Eur J Pharmacol **93**:287-288.

Deckel, A.W., T.H. Moran, J.T. Coyle, P.R. Sanberg, and R.G. Robinson (1986) Anatomical predictors of behavioral recovery following fetal striatal transplants. Brain Res. **365**:249-258.

Deckel A.W., T.H. Moran, R.G. Robinson (1988a) Receptor characteristics and recovery of function following kainic acid lesions and fetal transplants of the striatum. I. Cholinergic systems. Brain Res. **474**:27-38.

Deckel A.W., T.H. Moran, R.G. Robinson (1988b) Receptor characteristics and recovery of function following kainic acid lesions and fetal transplants of the striatum. II. Dopaminergic systems. Brain Res. **474**:39-47.

Deckel, A.W., and R.G. Robinson (1987) Receptor characteristics and behavioral consequences of kainic acid lesions and fetal transplants of the striatum. Annals N.Y. Acad. Sci. **495**:556-580.

Denis-Donini, S., J, Glowinski, A. Prochiantz (1983) Specific influence of striatal target neurons on the in vitro outgrowth of mesencephalic dopaminergic neurites: a morphological quantitative study. J. Neurosci. **3**:2292-2299.

Desban, M., C. Gauchy, M.L. Kemel, M.J. Besson, and J. Glowinski (1989) Three-dimensional organization of the striosomal compartment and patchy distribution of striatonigral projections in the matrix of the cat caudate nucleus. Neuroscience **29**:551-566.

DiFiglia, M. (1990) Excitotoxic injury of the neostriatum: a model for Huntington's disease. Trends Neurosci. **13**:286-289.

DiFiglia, M., S. Christakos, and N. Aronin (1989) Ultrastructural localization of

immunoreactive calbindin-D28K in the rat and monkey basal ganglia, including subcelluar distribution with colloidal gold labeling. J. Comp. Neurol. **279**:653-665.

DiFiglia, M., L. Schiff, and A.W. Deckel (1988) Neuronal organization of fetal striatal grafts in kainate- and sham-lesioned rat caudate nucleus: Light- and electron-microscopic observations. J. Neurosci. **8**:1112-1130.

Donoghue, J.P., and M. Herkenham (1986) Neostriatal projections from individual cortical fields conform to histochemically distinct striatal compartments in the rat. Brain Res. **365**:397-403.

Dragunow, M, M. Williams, and R.L.M. Faull (1990) Haloperidol induces Fos and related molecules in intrastriatal grafts derived from fetal striatal primordia. Brain Res. **530**:309-311.

Dunnett, S.B. (1990) Neural transplantation in animal models of dementia. Eur. J. Neurosci. **2**:567-587.

Dunnett, S.B., O. Isacson, D.J.S. Sirinathsinghji, D.J. Clarke, and A. Björklund (1988) Striatal grafts in rats with unilateral neostriatal lesions-III. Recovery from dopamine-dependent motor asymmetry and deficits in skilled paw reaching. Neuroscience **24**:813-820.

Duvoisin, R.C. (1967) Cholinergic-anticholinergic antagonism in Parkinsonism. Archs. Neurol., Paris 17:124-137.

Eckenstein, F., and R.W. Baughman (1984) Two types of cholinergic innervation in cortex, one co-localized with vasoactive intestinal polypeptide. Nature **309**:153-155.

Eckenstein, F., and M.V. Sofroniew (1983) Identification of central cholinergic neurons containing both choline acetyltransferase and acetylcholinesterase and of central neurons containing only acetylcholinesterase. J. Neurosci. **3**:2286-2291.

Eckenstein, F., and H. Thoenen (1983) Cholinergic neurons in the rat cerebral cortex demonstrated by immunohistochemical localization of choline acetyltransferase. Neurosci. Lett. **36**:211-215.

Eghbali, M., C. Santoro, W. Paredes, E. L. Gardner, and R.S. Zukin (1987) Visualization of multiple opioid-receptor types in rat striatum after specific mesencephalic lesions. Proc. Natl. Acad. Sci. USA **84**:6582-6586.

Eisen (1991) Determination of primary motoneuron identity in developing zebrafish embryos. Science **252**:569-572.

Emson, P.C., G. Paxinos, G. Le Gal La Salle, Y. Ben-Ari, and A. Silver (1979) Choline acetyltransferase and acetylcholinesterase containing projections from the basal forebrain to the amygdaloid complex of the rat. Brain Res. **165**:271-282.

Eriksdotter-Nillson, M., H. Björklund, and L. Olson (1986) Laminin immunohistochemistry: A simple method to visualize and quantitate vascular structures in the mammalian brain. J. Neurosci. Meth. **17**:275-286.

Edwards, M.A., M. Yamamoto and V.S.Jr Caviness (1990) Organization of radial glial and related cells in the developing murine CNS. An analysis based upon a new monoclonal antibody marker. Neuroscience **36**:121-144.

Evered, D., and J. Whelan (1986) *Calcium and the cell*, Jonn Wiely & Sons, Chichester, UK.

Fallon, J.H., and S.E. Loughlin (1987) Monoamine innervation of cerebral cortex and a theory of the role of monoamines in cerebral cortex and basal ganglia. In: Cerebral Cortex, Vol. 6, E.G. Jone and A. Peters eds., pp.41-127, Plenum, New York.

Fallon, J.H., K.B. Seroogy, S.E. Loughlin, R.S. Morrison, R.A. Bradshaw, D.J. Knauer, and D.D. Cunningham (1984) Epidermal growth factor immunoreactive material in the central nervous system: Location and development. Science **224**:1107-1109.

Faull, R.L.M., M. Dragunow, and J.W. Villiger (1989) The distribution of neurotensin receptors and acetylcholinesterase in the human caudate nucleus: evidence for the existence of a third neurochemical compartment. Brain Res. **488**:381-386.

Fentress, J.C., B.B. Stanfield and W.M. Cowan (1981) Observations on the development of the striatum in mice and rats. Anat. Embryol. **163**:275-298.

Ferrante, R.J., and N.W. Kowall (1987) TH-like immunoreactivity is distributed in the matrix component of normal human and Huntington's disease striatum. Brain Res. **416**:141-146.

Fishell, G., J. Rossant, and D. van der Kooy (1990) Neuronal lineages in chimeric mouse forebrain are segregated between compartments and in the rostrocaudal and radial planes. Dev. Biol. **141**: 70-83.

Fishell, G., and D. van der Kooy (1987a) Pattern formation in the striatum: developmental changes in the distribution of striatonigral neurons. J. Neurosci. **7**:1969-1978.

Fishell, G. and D. van der Kooy (1987b) Patch striatonigral neurons preferentially survive the period of striatal cell death. Soc. Neurosci. Abstr. **13**:1575.

Fishell, G. and D. van der Kooy (1989) Pattern formation in the striatum: developmental changes in the distribution of striatonigral projections. Dev. Brain Res. **45**:239-255.

Fisher, R.S., M.S. Levine, A.M. Adinolfi, C.D. Hull, and N.A. Buchwald (1987) The morphogenesis of glutamic acid decarboxylase in the neostriatum of the cat: neuronal and ultrastructural localization. Dev. Brain Res. **33**:215-234.

Flaherty, A.W., Graybiel, A.M., M. Sur, and P. Garraghty (1989) Distinctive patterns of projections to striatum from physiologically mapped somatosensory representations in primate cortex. Soc. Neurosci. Abstr. **15**:659.

Foster, G.A., M. Schultzberg, T. Hokfelt, M. Goldstein, H.C.Jr. Hemmings, C.C. Ouimet, S.I. Walaas, P. Greengard and (1987) Development of a dopamine- and cyclic adenosine 3':5'-monophosphate -regulated phosphoprotein (DARPP-32) in the prenatal rat central nervous system, and its relationship to the arrival of presumptive dopaminergic innervation. J. Neurosci. **7**:1994-2018.

Frederiksen, K. and R.D.G. McKay (1988) Proliferation and differentiation of rat neuroepithelial precursor cells in vivo. J. Neurosci. **8**:1144-1151.

Freed, W.J. (1983) Functional brain tissue transplantation: reversal of lesion-induced rotation by intraventricular substantia nigra and adrenal medulla grafts, with a note on intracranial retinal grafts. Biol. Psychiat. **18**:1205-1267.

Freed, W.J., R.E. Breeze, N.L. Rosenberg, S.A. Schneck, T.H. Well, J.N. Barrett, S.T. Grafton, S.C. Huang, D. Eidelberg and D.A. Tottenberg (1990a) Transplantation of human fetal dopamine cells dor Parkinson's disease. Results at 1 year. Arch. Neurol. **10**:1268-1275.

Freed, W.J., M. Poltorak and J.B. Becker (1990b) Intracerebral adrenal medulla grafts: A review. Exp. Neurol. **110**:139-166.

Freese, A., M. DiFiglia, M.F. Beal and J.B. Martin (1988) Characterization and mechanism of glutamate toxicity in primary striatal culture. Soc. Neurosci. Abstr. **14**:422.

Freund, F., J.P. Bolam, A. Björklund, U. Stenevi, S.B. Dunnett, J.F. Powell, and A.D. Smith (1985) Efferent synaptic connections of grafted dopaminergic neurons reinnervating the host neostriatum: a tyrosine hydroxylase immunocytochemical study. J. Neurosci. **5**:603-616.

Freund, F., J.F. Powell, and A.D. Smith (1984) Tyrosine hydroxylase-immunoreactive synaptic buttons in contact with identified striatonigral neurons, with particular reference to dendritic spines. Neuroscience **13**:1189-1215.

Gage, F.H. and A. Björklund (1986) Neural grafting in the aged rat brain. Ann. Rev. Physiol. **48**:447-459.

Gage, F.H., J.A. Wolff, M.B. Rosenberg, L. Xu, J.E. Yee, C. Shults and T. Friedmann (1987) Grafting genetically modified cells to the brain: possibilities for the future. Neuroscience **23**:795-807.

Gale, K., J. Segovia, N.J.K. Tillakarathe, K. Whelan, and A.J. Tobin (1988) Dopaminergic control of striatal GABA synthesis is reflected in the expression of mRNA for striatal glutamic acid decarboxylase. Soc. Neurosci. Abstr. **14**:1066.

Gehlert, D.R., and J.K. Wamsley (1985) Dopamine receptors in rat brain: quantitative autoradiographic localization using [^{3}H] sulpiride. Neurochem. Int. **7**:717-723.

Geneser-Jensen, F.A., and J.W. Blackstad (1971) Distribution of acetylcholinesterase in the hippocampal region of the guinea pig. Z. Zellforsch. Mirkrosk. Anat. **114**:460-481.

Gerfen, C.R. (1984) The neostriatal mosaic: compartmentalization of corticostriatal input and striatonigral output systems. Nature **311**:461-464.

Gerfen, C.R. (1985) The neostriatal mosaic. I. Compartmental organization of projections from the striatum to the substantia nigra in the rat. J. Comp. Neurol. **236**:454-476.

Gerfen, C.R. (1989) The neostriatal mosaic: striatal patch-matrix organization is related to cortical lamination. Science **246**:385-388.

Gerfen, C.R., K.G. Baimbridge, and J.J. Miller (1985) The neostriatal mosaic: Compartmental distribution of calcium binding protein and parvalbumin in the basal ganglia of the rat and monkey. Proc. Natl. Acad. Sci. USA **82**:8780-8784.

Gerfen, C.R., K.G. Baimbridge, and J. Thibault (1987b) The neostriatal mosaic: III. Biochemical and developmantal dissociation of patch-matrix mesostriatal systems. J. Neurosci. **7**:3935-3944.

Gerfen, C.R., T.M. Engber, L.C. Mahan, Z. Susel, T.N. Chase, F.J. Monsma, and D.R. Sibley (1990) D1 and D2 receptor-regulated gene expression of striatonigral and striatopallidal neurons. Science **250**:1429-1432.

Gerfen, C.R., M. Herkenham, and J. Thibault (1987a) The neostriatal mosaic: II. Patch- and matrix-directed mesostriatal dopaminergic and non-dopaminergic systems. J. Neurosci. **7**:3915-3934.

Gerfen, C.R., J.F. McGinty, and W.S. Young III (1991) Dopamine differentially regulate dynorphin, substance P, and enkephalin expression in striatal neurons: *In situ*

hybridization histochemical analysis. J. Neurosci. **11**:1016-1031.

Giménez-Amaya, J.-M., and A.M. Graybiel (1990) Compartmental origins of the striatopallidal projection in the primate. Neuroscience **34**:111-126.

Giménez-Amaya, J.-M., and A.M. Graybiel (1991) Modular organization of projection neurons in the matrix compartment of the primate striatum. J. Neurosci. **11**:779-791.

Giordano M, S.H. Hagenmeyer-Houser, and P.R. Sanberg (1988) Intraparenchymal fetal striatal transplants and recovery in kainic acid lesioned rats. Brain Res. **446**:183-188.

Goetz, C.G., C.W. Olanow, W.C. Koller, R.D. Penn, D. Cahill, R. Morantz, G. Stebbins, C.M. Tanner, H.L. Klawans, K.M. Shannon, C.L. Comella, T. Witt, C. Cox, M. Waxman, and L. Gauger (1989) Multicenter study of autologous adrenal medulla transplantation to the corpus striatum in patients with advanced Parkinson's disease. N. Engl. J. Med. **320**:337-341.

Graybiel, A.M. (1984a) Correspondence between the dopamine islands and striosomes of the mammalian striatum. Neuroscience **13**:1157-1187.

Graybiel, A.M. (1984b) Modular patterning in development of the striatum. In: Cortical integration, F. Reinoso-Suárez and C. Ajmone-Marsan, eds, pp.223-235, Raven, New York.

Graybiel, A.M. (1986) Neuropeptides in the basal ganglia. In: Neuropeptides in Neurologic and Psychiatric Disease, J.B. Martin and J.D. Barchas, eds., pp.135-161, Raven, New York.

Graybiel, A.M. (1989) Dopaminergic and cholinergic systems in the striatum. In: Neural Mechanisms in Disorders of Movement, A. Crossman and M.A. Sambrook, eds. pp. 3-15, Libbey, London.

Graybiel, A.M. (1990) Neurotransmitters and neuromodulators in the basal ganglia. Trend Neurosci. **13**:244-254.

Graybiel, A.M., and M.F. Chesselet (1984a) Compartmental distribution of striatal cell bodies expressing met-enkephalin-like immunoreactivity. Proc. Natl. Acad. Sci. USA **81**:7980-7984.

Graybiel, A.M., and M.F. Chesselet (1984b) Distribution of cell bodies expressing substance P, enkephalin and dynorphin B in kitten and cat striatum. Anat. Rec. **208**:64A.

Graybiel, A.M., S.B. Dunnett, R.W. Baughman, and F.-C. Liu (1987a) Cholinergic neurons and neuropil and tyrosine hydroxylase-positive fibers cluster together in

circumscribed patches in intrastriatal grafts derived from embryonic striatal donor tissue. Neurosci. Suppl. **22**:S265.

Graybiel, A.M., E.C. Hirsch, and Y.A. Agid (1987b) Differences in tyrosine hydroxylase-like immunoreactivity characterize the mesostriatal innervation of striosomes and extrastriosomal matrix at maturity. Proc. Natl. Acad. Sci. USA **84**:303-307.

Graybiel, A.M., and T.L. Hickey (1982) Chemospecificity of ontogenetic units units in the striatum: demonstration by combining [3H] thymidine neuronography and histochemical staining. Proc. Natl. Acad. Sci. USA **79**:198-202.

Graybiel, A.M., F.-C. Liu, and S.B. Dunnett (1989) Intrastriatal grafts derived from fetal striatal primordia. I. Phenotypy and modular organization. J. Neurosci. **9**:3250-3271.

Graybiel, A.M., R. Moratalla, and H.A. Robertson (1990a) Amphetamine and cocaine induce drug-specific activation of the c-*fos* gene in striosome-matrix and limbic subdivisions of the striatum. Proc. Natl. Acad. Sci. USA **87**: 6912-6916.

Graybiel, A.M., and H. Newman-Gage (1987) Ontogeny of dopaminergic and cholinergic systems in the basal ganglia. In: Extrapyramidal disorders in childhood, L. Angelini et al., eds, pp.1-10, Elsevier.

Graybiel, A.M., K. Ohta, and S. Roffler-Tarlov (1990b) Patterns of cell and fiber vulnerability in the mesostriatal system of the mutant mouse weaver. I. Gradients and compartments. J. Neurosci. **10**:720-733.

Graybiel, A.M., V.M. Pickel, T.H. Joh, D.J. Reis, and C.W. Ragsdale (1981) Direct demonstrations of a correspondence between the dopamine islands and acetylcholinesterase patches in the developing striatum. Proc. Natl. Acad. Sci. USA **78**:5871-5875.

Graybiel, A.M., and C.W. Ragsdale (1978) Histochemically distinct compartments in the striatum of human, monkey, and cat demonstrated by acetylthiocholinesterase staining. Proc. Natl. Acad. Sci. USA **75**:5723-5726.

Graybiel, A.M., and C.W. Ragsdale (1979) Fiber connections of the basal ganglia. In: Development and Chemical Specificity of Neurons. Prog. Brain Res. **51**:239-283.

Graybiel, A.M., and C.W. Ragsdale (1980) Clumping of acetylcholinest erase activity in the developing striatum of the human fetus and young infant. Proc. Natl. Acad. Sci. USA **77**:1214-1218.

Graybiel, A.M., and C.W. Ragsdale (1983) Biochemical Anatomy of the Striatum. In: Chemical Neuroanatomy P.C. Emson, ed. pp. 427-504, Raven Press, New York.

Grebb, J.A., J.A. Girault, M. Ehrlich, and P. Greengard (1990) Chronic treatment of rats with SCH-23390 or raclopride does not affect the concentrations of DARPP-32 or its mRNA in dopamine- innervated brain regions. J. Neurochem. **55**:204-207.

Grimes, L.M., X. Ping, H.-K. Jiang, and J.-S. Hong (1990) Striatal patch/matrix distribution of Fos, substance P and dynorphin induced by apomorphine in intact and 6-OHDA-lesions rats. Soc. Neurosci. Abstr. **16**:800.

Groves, P.M. (1983) A theory of the functional organization of the neostriatum and the neostriatal control of voluntary movement. Brain Res. Rev. **5**:109-132.

Groves, P.M, M. Martone, S.J. Young, and D.M. Armstrong (1988) Three-dimensional pattern of enkephalin-like immunoreactivity in the caudate nucleus of the cat. J. Neurosci. **8**:892-900.

Gusella, J.F., N.S. Wexler, P.M. Conneally, S.L. Naylor, M.A. Anderson, R.E. Tanzi, P.C. Watkins, K. Ottina, M.R. Wallace, A.Y. Sakaguchi, A.B. Young, I. Shoulson, E. Bonilla, and J.B. Martin (1983) A polymorphic DNA marker genetically linked to Huntington's disease. Nature **306**:234-238.

Happe, H.K., and L.C. Murrin (1989) Development of cholinergic terminals in rat striatum as visualized by [^{3}H]Hemicholinium-3 autoradiography. Soc. Neurosci. Abstr. **15**:293.

Helm, G.A, M.W. Robertson, G.I. Jallo, N. Simmons, and J.P. Bennett (1991) Development of D1 and D2 dopamine receptors and associated second messenger systems in fetal striatal transplants. Exp. Neurol. **111**:181-189.

Hemmendinger, L.M., B.B. Garber, P.C. Hoffmann, and A. Heller (1981) Target neuron-specific process formation by embryonic mesencephalic dopamine neurons in vitro. Proc. Natl. Acad. Sci. USA **78**:1264-1268.

Henderson, Z. (1989) Acetylcholinesterase on the dendrites of central cholinergic neuorns: An electron microscopic study in the ferret. Neuroscience **28**:95-108.

Herkenham, M., and C.B. Pert (1981) Mosaic distribution of opiate receptors, parafascicular projections and acetylcholinesterase in rat striatum. Nature **291**:415-418.

Herkenham, M., and C.B. Pert (1982) Light microscopic localization of brain opiate receptors: a general autoradiographic method which preserves tissue quality. J. Neurosci. **2**:1129-1149.

Herman, J.P., A. Lupp, N. Abrous, G.Le Moal,M. Hertting, and R. Jackisch (1988a) Intrastriatal dopaminergic grafts restore inhibitory control over striatal cholinergic

neurons. Exp. Brain Res. **73**:236-248.

Herman, J.P., N. Abrous, A. Vigny, J. Dulluc, and M. Le Moal (1988b) Distorted development of intracerebral grafts: long-term maintenance of tyrosine hydroxylase-containing neurons in grafts of cortical tissue. Devel. Brain Res. **40**:81-88.

Hidaka, H., E. Carafoli, A.R. Means, and T. Tanaka (1988) *Calcium protein signaling*, Plenum Press, New York.

Hockfield, S., and R.D.G. McKay (1985) Identification of major cell classes in the developing mammalian nervous system. J. Neurosci. **5**:3310-3328.

Hökfelt, T., R. Mårtensson, A. Björklund, S. Kleinau, and M. Goldstein (1984) Distributional maps of tyrosine-hydroxylase-immunoreactive neurons in the rat brain. In: Handbook of Chemical Neuroanatomy, Vol. II:Classic Transmitters in the CNS, part I, A. Björklund and T. Hökfelt eds., pp.277-379, Elsevier, Amsterdam.

Hong, J.S., H.-Y. T. Ynag, W. Fratta, and E. Costa (1978) Rat striatal methionine-enkephalin content after chronic treatment with cataleptogenic and non-cataleptogenic antischizophrenic drugs. J. Pharmac. Exp. Ther. **205**:141-147.

Hong, J.-S., K. Yoshikawa, T. Kanamastu, and S.L. Sabol (1985) Modulation of striatal enkephalinergic neurons by antipsychotic drugs. Fed. Proc. Fed. Am. Soc. Exp. Biol. **44**:2535-2539.

Horellou P., P. Brundin, P. Kalén, J. Mallet, and A. Björklund (1990) In vivo release of DOPA and dopamine from genetically engineered cells grafted to the denervated rat striatum. Neuron **5**:393-402.

Horvitz H.R., P.W. Sternberg, I.S. Greenwald, W. Fixsen, and H.M. Ellis (1983) Mutations that affect neural cell lineages and cell fates during the development of the nematode Caenorhabditis elegans. In: Molecular Neurobiology, Vol. XLVIII: Cold Spring Harbor Symposia on Quantitative Biology, J.D. Watson and R. McKay eds., pp.453-463, Cold Spring Harbor, New York.

Houser, C.R., G.D. Crawford, R.P. Barber, P.M. Salvaterra, and J.E. Vaughn (1983) Organization and morphological characteristics of cholinergic neurons: an immunocytochemical study with a monoclonal antibody to choline acetyltransferase. Brain Res. **266**:97-119.

Hsu, S.M., L. Raine, and H. Fanger (1981) The use of avidin-biotin-peroxidase complex (ABC) in immunoperoxidase techniques: A comparison between ABC and unlabeled antibody (peroxidase) procedure. J. Histochem. Cytochem. **29**:577-590.

Iacopino, A.M., and S. Christakos (1990) Specific reduction of calcium-binding protein (28-kilodalton calbindin-D) gene expression in aging and neurodegenerative diseases. Proc. Natl. Acad. Sci. USA **87**:4078-4082.

Iacovitti, L., J. Lee, T.H. Joh, and D.J. Reis (1987) Expression of tyrosine hydroxylase in neurons of cultured cerebral cortex: evidence for phenotypic plasticity in neurons of the CNS. J. Neurosci. **7**:1264-1270.

Isacson, O. (1987) Neural grafting in an animal model of Huntington's disease. Doctoral dissertation, Lund, Sweden.

Isacson O., P. Brundin, F.H. Gage, and A. Björklund (1985) Neural grafting in a rat model of Huntington's disease: progressive neurochemical changes after neostriatal ibotenate lesions and striatal tissue grafting. Neuroscience **16**:799-817.

Isacson O., P. Brundin, P.A.T. Kelly, F.H. Gage, and A. Björklund (1984) Functional neuronal replacement by grafted striatal neurons in the ibotenic acid-lesioned rat striatum. Nature **311**:458-460.

Isacson, O., D. Dawbarn, P. Brundin, F.H. Gage, P.C. Emson, and A. Björklund (1987) Neural grafting in a rat model of Huntington's disease:striosomal-like organization of striatal grafts as revealed by immunohistochemistry and receptor autoradiography. Neuroscience **22**:481-497.

Isacson, O., S.B. Dunnett, and A. Björklund (1986) Graft-induced behavioral recovery in an animal model of Huntington's disease. Proc. Natl. Acad. Sci. USA **83**:2728-2732.

Isacson, O., D, Riche, P. Hantraye, M.V. Sofroniew, and M. Maziere (1989) A primate model of Huntington's disease: cross-species implantation of striatal precursor cells to the excitotoxically lesioned baboon caudate-putamen. Exp. Brain Res. **75**:213-220.

Izzo, P.N., and J.P. Bolam (1988) Cholinergic synaptic input to different parts of spiny striatonigral neurons in the rat. J. Comp. Neurol. **269**:219-234.

Jackson, D., M.K. Stachowiak, J.P. Bruno, and M.J. Zigmond (1988) Inhibition of striatal acetylcholine release by endogenous serotonin. Brain Res. **457**:259-266.

Jaeger, C.B., and R.D. Lund (1980) Transplantation of embryonic occipital cortex to the brain of newborn rats. An autoradiographic study of transplant histogenesis. Exp. Brain Res. **40**:265-272.

Javitch, J.A., S.M. Strittmatter, and S.H. Snyder (1985) Differential visualization of dopamine and norepinephrine uptake sites in rat brain using [^{3}H]mazindol autoradiography. J. Neurosci. **5**:1513-1521.

Jiang, H.-K., J.F. McGinty, and J.S. Hong (1990) Differential modulation of striatonigral dynorphin and enkephalin by dopamine receptor subtypes. Brain Res. **507**:57-64.

Jiménez-Castellanos, J., and A.M. Graybiel (1987) Subdivisions of the dopamine-containing A8-A9-A10 complex identified by their differential mesostriatal innervation of striosomes and extrastriosomal matrix. Neuroscience **23**:223-242.

Jiménez-Castellanos, J., and A.M. Graybiel (1989) Compartmental origins of striatal efferent projections in the cat. Neuroscience **32**:297-321.

Johnson K., and H.A. Robertson (1989) The NMDA antagonist MK-801 reverses d-amphetamine-induced activation of the proto-oncogene c-*fos* in rat striatum. Soc. Neurosci. Abstr. **15**:782.

Johnston, J.G., S.R. Boyd, and D. van der Kooy (1987) Compartmentalization of the embryonic striatum after intraocular transplantation. Dev. Brain Res. **33**:310-314.

Johnston, J.G., nd D. van der Kooy (1989) Protooncogene expression identifies a transient columnar organization of the forebrain within the late embryonic ventricular zone. Proc. Natl. Acad. Sci. USA **86**:1066-1070.

Kater, S.B., M.P. Mattson, C.S. Cohan, and J.A. Connor (1988) Calcium regulation of the neuronal growth cone. Trends Neurosci. **11**:315-321.

Kessler, J.A. (1986) Differential regulation of cholinergic and peptidergic development in the rat striatum in culture. Dev. Biol. **113**:77-89.

Kent, J.L., C.B. Pert, and M. Herkenham (1982) Ontogeny of opiate receptors in rat forebrain: visualization by in vitro autoradiography. Dev. Brain Res. **2**:487-504.

Kowall, N.W., R.J. Ferrante, and J.B. Martin (1987) Patterns of cell loss in Huntington's disease. Trends Neurosci. **10**:24-29.

Köhler, C., and R. Schwarcz (1983) Comparison of ibotenic and kainate neurotoxicity in the rat brain: a histological study. Neuroscience **8**:819-835.

Kubota, Y., S. Inagaki, S. Kito, H. Takagi, and A.D. Smith (1986a) Ultrastructural evidence of dopaminergic input to enkephalinergic neurons in rat neostriatum. Brain Res. **367**:374-378.

Kubota, Y., S. Inagaki, and S. Kito (1986b) Innervation of substance P neurons by catecholaminergic terminals in the neostriatum. Brain Res. **375**:163-167.

Kubota, Y., S. Inagaki, S. Kito, and J.Y. Wu (1987a) Dopaminergic axons directly make

synapses with GABAergic neurons in the rat neostriatum. Brain Res. **406**:147-156.

Kubota, Y., S. Inagaki, S. Shimada, S. Kito, F. Eckenstein, and M. Tohyama (1987b) Neostriatal cholinergic neurons receive direct synaptic inputs from dopaminergic axons. Brain Res. **413**:179-184.

Labandeira-Garcia, J.L., K. Wictorin, E.T. Cunninghham Jr., and A. Björklund (1991) Development of intrastriatal grafts and their afferent innervation from the host. Neuroscience **42**:407-426.

Lammers, G.J., A.A.M. Gribnau, and H.J. ten Donkelaar (1980) Neurogenesis in the basal forebrain in the Chinese hamster (Cricetulus griseus). II. Site of neuron origin: Morphogenesis of the ventricular ridges. Anat. Embryol. **158**:193-211.

Lanca A.J., S. Boyd, B.E. Kolb, and D. van der Kooy (1986) The development of a patchy organization of the rat striatum. Dev. Brain Res. **27**:1-10.

Lange, H., G. Thörner, A. Hopf, and K.F. Schröder (1976) Morphometric studies of the neuropathological changes in choreatic diseases. J. Neurol. Sci. **28**:401-425.

Layer, P.G., and O. Sporns (1987) Spatiotemporal relationship of embryonic cholinesterase with cell proliferation in chicken brain and eye. Proc. Natl. Acad. Sci. USA **84**:284-288.

LeDouarin, N.M., and M.-A. Teillet (1974) Experimental analysis of the migration and differentiation of neuroblasts of the autonomic nervous system and of the neuroectodermal mesenchymal derivatives, using a biological cell marking technique. Dev. Biol. **41**:162-184.

Lehmann, J. and H.C. Fibiger (1978) Acetylcholinesterase in the substantia nigra and caudate-putamen of the rat: properities and localization in dopaminergic neurons. J. Neurochem. **30**:615-624.

Lehmann, J., and S.Z. Langer (1983) The striatal cholinergic interneuron: synaptic target of dopaminergic terminals? Neuroscience **10**:1105-1120.

Lehmann, J., and B. Scatton (1982) Characterization of the excitatory amino acid receptor-mediated release of the ^{3}H-acetylcholine from rat striatal slices. Brain Res. **252**:77-90.

Le Moine, C., F. Tison, and B. Bloch (1990) D2 dopaminergic receptor gene expression by cholinergic neurons in the rat striatum. Neurosci. Lett. **117**:248-252.

Lendahl, U., L.B., Zimmerman, and R.D.G. McKay (1990) CNS stem cells express a new

class of intermediate filament protein. Cell **60**:585-595.

Lindvall, O., E.-O. Backlund, L. Farde et al. (1987) Transplantation in Parkinson's disease: two cases of adrenal medulla grafts to the putamen. Ann. Neurol. **22**:457-468.

Lindvall, O., P. Brundin, H. Winder, S. Rehncrona, B. Gustavii, R. Frackowiak, K.L. Leenders, G. Sawle, J.C. Rothwell, C.D. Marsden, and A. Björklund (1990) Grafts of fetal dopamine neurons survive and improve motor function in Parkinson's disease. Science **247**:574-577.

Liu, F.-C., S.B. Dunnett, and A.M. Graybiel (1991) The influence of TH-containing afferents on the development of modular organization in embryonic striatal grafts. Soc. Neurosci. Abstr., in press.

Liu, F.-C., S.B. Dunnett, H.A. Robertson, and A.M. Graybiel (1991) Intrastriatal grafts derived from fetal striatal primordia. III. Induction of modular patterns of Fos-like immunoreactivity by cocaine. Exp. Brain. Res., in press.

Liu, F.-C., and A.M. Graybiel (1991a) Transient calbindin-D_{28K}-positive systems in the ganglionic eminence and the developing striatum. Submitted.

Liu, F.-C., and A.M. Graybiel (1991b) Heterogeneous development of calbindin-D_{28K} expression in the developing striatum. Submitted.

Liu, F.-C., A.M. Graybiel, and S.B. Dunnett (1988) Modular organization of fetal striatal grafts. Soc. Neurosci. Abstr. **14**:763.

Liu, F.-C., A.M. Graybiel, and S.B. Dunnett (1990a) Autoradiographic study of fetal striatal grafts placed in host striatum pulse-labeled with [3H]-thymidine. Soc. Neurosci. Abstr. **16**:1286.

Liu, F.-C., A.M. Graybiel, P.C. Emson, and C.R. Gerfen (1989) Developmental expression of calbindin-28KD in striatum of postnatal rats. Soc. Neurosci. Abstr. **15**:909.

Liu, F.-C., A.M. Graybiel, S.B. Dunnett, and R.W. Baughman (1990b) Intrastriatal grafts derived from fetal striatal primordia: II. Reconstitution of cholinergic and dopaminergic systems. J. Comp. Neurol. **295**:1-14.

Loopuijt, L.D., J.B. Sebens, and J. Korf (1987) A mosaic-like distribution of dopamine receptors in rat neostriatum and its relationship to striosomes. Brain Res. **405**:405-408.

Lowenstein, P.R., P.A. Slesinger, H.S. Singer, L.C. Walker, M.F. Casanova, D.L. Price, and J.T. Coyle (1987) An autoradiographic study of the development of [^{3}H] hemicholinium-3 binding sites in human and baboon basal ganglia: a marker for the

sodium-dependent high-affinity choline uptake system. Dev. Brain Res. **34**:291-297.

Lowenstein, P.R., P.A. Slesinger, H.S. Singer, L.C. Walker, M.F. Casanova, L.S. Raskin, D.L. Price, and J.T. Coyle (1989) Compartment-specific changes in the density of choline and dopamine uptake sites and muscarinic and dopaminergic receptors during the development of the baboon striatum: A quantitative receptor autoradiographic study. J. Comp. Neurol. **288**:428-446.

Lumsden, A., and R. Keynes (1989) Segmental patterns of neuronal development in the chick hindbrain. Nature **337**:424-428.

Luskin, M.B., and C.J. Shatz (1985) Studies of the earliest generated cells of the cat's visual cortex: Cogeneration of subplate and marginal zones. J. Neurosci. **5**:1062-1075.

Luthman, L., E. Lindqvist, D. Young, and R. Cowburn (1990) Neonatal dopamine lesion in the rat results in enhanced adenylate cyclase activity without altering dopamine receptor binding or dopamine- and adenosine 3':5'-monophosphate-regulated phosphoprotein (DARPP-32) immunoreactivity. Exp. Brain Res. **83**:85-95.

Madrazo, I., R. Drucker-Colin, V. Diaz, J. Martinez-Mata, C. Torres, and J.J. Becerril (1987) Open microsurgical autograft of adrenal medulla to the right caudate nucleus in two patients with intractable parkinson's disease. N. Engl. J. Med. **316**:831-834.

Malach, R., and A.M. Graybiel (1986) Mosaic architecture of the somatic sensory-recipient sector of the cat's striatum. J. Neurosci. **6**:3436-3458.

Marchand, R., and L. Lajoie (1986) Histogenesis of the striopallidal system in the rat. Neurogenesis of its neurons. Neuroscience **17**:573-590.

Martin, J.B. (1984) Huntington's disease. New approaches to an old problem. Neurology **34**:1059-1072.

Mattson, M.P., B. Rychilk, C. Chu, and S. Christakos (1991) Evidence for calcium-reducing and excito-protective roles for the calcium binding protein calbindin-D_{28K} in cultured hippocampal neurons. Neuron **6**:41-51.

Mayer E., R.P. Heavens, and D.J.S. Sirinathsinghji (1990) Autoradiographic localization of D1 and D2 dopamine receptors in primordial striatal tissue grafts in rats. Neurosci. lett. **109**: 271-276.

Mayer, M.L., and G.L. Westbrook (1987) Cellular mechanisms underlying excitotoxicity. Trends Neurosci. **10**:59-61.

McAllister, J.P. (1987) Tritiated thymidine identification of embryonic neostriatal

transplants. In: Cell and Tissue Transplantation in the Adult Brain, E. Azmitia and A. Björklund eds., Annals N.Y. Acad. Sci. **495**:745-748.

McAllister, J.P., P.D. Walker, M.C. Zemanick, A.B. Weber, L.I. Kaplan, and M.A. Reynolds (1985) Morphology of embryonic neostriatal cell suspensions transplanted into adult neostriata. Dev. Brain Res. **23**:282-286.

McConnell, S.K. (1988) Fates of visual cortical neurons in the ferret after ischronic and heterochronic transplantation. J. neurosci. **8**:945-974.

McConnell, S.K., A. Ghosh, and C.J. Shatz (1989) Subplate neurons pioneer the first axon pathway from the cerebral cortex. Science **245**: 978-982.

McGeer, P.L., J.E. Boulding, W.C. Gibson, and R.G. Foulkes (1961) Drug-induced extrapyramidal reactions. J. Am. med. Ass. **177**:665-670.

McGeer, P.L., H. Kimura, and E.G. McGeer (1984) Transplantation of new born brain tissue into adult kainic-acid-lesioned neostriatum. In: Neural Transplants, Development and Function J.R. Sladek and D.M. Gash, eds., pp. 361-371, Plenum, New York.

McGeer, P.L., and E.G. McGeer (1976) Duplication of biochemical changes of Huntington's chorea by intrastriatal injections of glutamic and kainic acids. Nature **263**:517-519.

McKay, R.D.G. (1989) The origins of cellular diversity in the mammalian central nervous system. Cell **58**:815-821.

Mendez-Otero, R., B. Schlosshauer, C.J. Barnstable, and M. Constantine-Paton (1988) A developmentally regulated antigen associated with neural cell and process migration. J. Neurosci. **8**:564-579.

Merchant, K.M., L. Bush, J.W. Gibb, and G.R. Hanson (1988) Receptor-specific interactions of the nigro-striatal dopamine projections with striatal neurotensin systems in rat brain. Soc. Neurosci. Abstr. **14**:114-114.

Moon Edley, S., and M. Herkenham (1984) Comparative development of striatal opiate receptors and dopamine revealed by autoradiography and histofluorescence. Brain Res. **305**:27-42.

Moratalla R., H.A. Robertson, P.A. DiZio, and A.M. Graybiel (1990) Parallel induction of *jun* B and c-*fos* evoked in the striatum by psychomotor stimulant drugs cocaine and amphetamine. Soc. Neurosci. Abstr. **16**:953.

Morris, B.J., V. Höllt, and A. Herz (1988) Dopaminergic regulation of striatal

proenkephalin mRNA and prodynorphin mRNA: contrasting effects of D1 and D2 antagonists. Neuroscience **25**:525-532.

Mueller, R.A., L.M. Grimes, H. Criswell, L.S. Carter, W.C. McGimsey, W. Stumpf, and G.R. Breese (1989) D1 dopamine agonist induces c FOS protein in the striatum of 6-OHDA-lesioned rats. Soc. Neurosci. Abstr. **15**:430.

Murrin, L.C., and J.R. Ferrer (1984) Ontogeny of the rat striatum: correspondence of dopamine terminals, opiate receptors and acetylcholinesterase. Neurosci. Lett. **47**:155-160.

Murrin, L.C., and W. Zeng (1989) Dopamine D1 receptor development in the rat striatum: early localization in striosomes. Brain Res. **480**:170-177.

Nastuk, M.A., and A.M. Graybiel (1985) Patterns of muscarinic cholinergic binding in the striatum and their relation to dopamine islands and striosomes. J. Comp. Neurol. **237**:176-194.

Nastuk, M.A., and A.M. Graybiel (1988) Autoradiographic localization and biochemical 2characteristics of M1 and M2 muscarinic binding sites in the striatum of the cat, monkey, and human. J. Neurosci. **8**:1052-1062.

Nastuk, M.A., and A.M. Graybiel (1989) Ontogeny of M1 and M2 muscarinic binding sites in the striatum of the cat: relationships to one another and to striatal compartmentalization. Neuroscience **33**:125-147.

Newman-Gage, H., and A.M. Graybiel (1988) Expression of calcium/calmodulin dependent protein kinase in relation to dopamine islands and synaptic maturation of cat striatum. J. Neuroscience **8**:3360-3375.

Nieto-Sampedro, M., S.R. Whittemore, D.L. Needels, J. Larson, and C.W. Cotman (1984) The survival of brain transplants is enhanced by extracts from injured brain. Proc. Natl. Acad. Sci. USA **81**:6250-6254.

Normand, E., T. Popovici, D. Fellmann, and B. Bloch (1987) Anatomical study of enkephalin gene expression in the rat forebrain following haloperidol treatment. Neurosci. Lett. **83**:232-236.

Normand, E., T. Popovici, B. Onteniente, D. Fellmann, D. Piatier-Tonneau, C. Auffray, and B. Bloch (1988) Dopaminergic neurons in the substantia nigra modulate preproenkephalin A gene expression in rat striatal neurons. Brain Res. **439**:39-46.

O'Dell, S.J., and J.F. Marshall (1988) Transport of [^{3}H]mazindol binding sites in mesostriatal dopamine axons. Brain Res. **460**:402-406.

Olson, L., A. Seiger, and K. Fuxe (1972) Heterogeneity of striatal and limbic dopamine innervation: Highly fluorescent islands in developing and adult rats. Brain Res. **44**:283-288.

Onteniente, B., M. Peschanski, and B. Desfontaines (1990) Phenotypic differentiation of striatal transplanted neurons in relation to dopaminergic host afferents. Soc. Neurosci. Abstr. **16**:974.

Oppenheim, R.W. (1991) Cell death during development of the nervous system. Ann. Rev. Neurosci. **14**:453-501.

Park, J.K., T.H. Joh, and F.F. Ebner (1986) Tyrosine hydroxylase is expressed by neocortical neurons after transplantation. Proc. Natl. Acad. Sci. USA **83**:7495-7498.

Paul, M.L., A.M. Graybiel, and H.A. Robertson (1990) Synergistic activiation of the immediate-early gene c-FOS in striosomes by D1- and D2-selective dopamine agonists. Soc. Neurosci. Abstr. **16**:954.

Pearlman, S.H., M. Levivier, T.J. Collier, J.R. Sladek, D.M. Gash (1991) Striatal implants protect the host striatum against quinolinic acid toxicity. Exp. Brain Res. **84**, 303-310.

Phelps, P.E., D.R. Brady, and J.E. Vaughn (1989) The generation and differentiation of cholinergic neurons in rat caudate-putamen. Dev. Brain Res. **46**:47-60.

Phelps, P.E., C.R. Houser, and J.E. Vaughn (1985) Immunocytochemical localization of choline acetyltransferase within the rat neostriatum: a correlated light and electron microscopic study of cholinergic neurons and synapses. J. Comp. Neurol. **238**:286-307.

Pickel, V.M. and J. Chan (1990) Spiny neurons lacking choline acetyltransferase immunoreactivity are major targets of cholinergic and catecholaminergic terminals in rat striatum. J. Neurosci. Res. **25**:263-280.

Pritzel, M., O. Isacson, P. Brundin, L. Wiklund, and A. Björklund (1986) Afferent and efferent connections of striatal grafts implanted into the ibotenic acid lesioned neostriatum in adult rats. Exp. Brain Res. **65**:112-126.

Puelles, L., J.A., Amat, and M. Martinez-de-la-Torre (1987) Segment-related, mosaic neurogenetic pattern in the forebrain and mesencephalon of early chick embryos: I. Topography of AChE-positive neuroblasts up to stage HH18. J. Comp. Neurol. **266**:247-268.

Purves, D., and J.W. Lichtman (1985) *Principles of Neural Development*, Sinauer Associates, Sunderland, MA.

Rafols, J.A. (1986) Ependymal tanycytes of the ventricular system in vertebrates. In: Astrocytes. Volume 1, S. Fedoroff and A. Vernadakis, eds. pp. 131-148, Academic Press, Orlando.

Ragsdale, C.W., and A.M. Graybiel (1981) The fronto-striatal projection in the cat and monkey and its relationship to inhomogeneities established by acetylcholinesterase histochemistry. Brain Res. **208**:259-266.

Ragsdale, C.W., and A.M. Graybiel (1983) Butyrylcholinesterase in the dorsal and ventral striatum: observations of histochemical distributions in adult, fetal and neonatal cats. Soc. Neurosci. Abstr. **9**:15.

Ragsdale, C.W., and A.M. Graybiel (1988a) Fibers from the basolateral nucleus of the amygdala selectively innervate striosomes in the caudate nucleus of the cat. J. Comp. Neurol. **269**:506-522.

Ragsdale, C.W., and A.M. Graybiel (1988b) Multiple patterns of thalamostriatal innervation in the cat. In: Cellular Thalamic Mechanisms, M. Bentivoglio and R. Spreafico, eds. pp. 261-267, Elsevier, Amsterdam.

Ragsdale, C.W., and A.M. Graybiel (1990) A simple ordering of neocortical areas established by the compartmental organization of their striatal projections. Proc. Natl. Acad. Sci. USA **87**:6196-6199.

Raisman-Vozari, R., J.A. Girault, S. Moussaoui, C. Feuerstein, P. Jenner, C.D. Marsden, and Y. Agid (1990) Lack of change in striatal DARPP-32 levels following nigrostriatal dopaminergic lesions in animals and in parkinsonian syndromes in man. Brain.Res. **507**:45-50.

Rakic, P. (1971) Guidance of neurons migrating to the fetal monkey neocortex. Brain Res. **33**:471-476.

Rakic, P. (1972) Mode of cell migration to the superficial layers of fetal monkey neocortex. J. Comp. Neurol. **145**:61-84.

Rakic, P. (1988) Specification of cerebral cortical areas. Science **241**:170-176.

Rhodes, K.J., J.N. Joyce, D.W. Sapp, and J.F. Marshall (1987) [^{3}H]Hemicholinium-3 binding in rabbit striatum: correspondence with patchy acetylcholinesterase staining and a method for quantifying striatal compartments. Brain Res. **412**:400-404.

Richfield, E.K., A.B. Young, and J.B. Penney (1987) Comparative distribution of dopamine D-1 and D-2 receptors in the basal ganglia of turtles, pigeons, rats, cats, and monkeys. J. Comp. Neurol. **262**:446-463.

Ritz M.C., R.J. Lamb, S.R. Goldberg, and M.J. Kuhar (1987) Cocaine receptors on dopamine transporters are related to self-administration of cocaine. Science **237**: 1219-1223.

Roberts, R.C., and M. DiFiglia (1988) Localization of immunoreactive GABA and enkephalin and NADPH-diaphorase-positive neurons in fetal striatal grafts in the quinolinic-acid-lesioned rat neostriatum. J. Comp. Neurol. **274**:406-421.

Roberts, R.C., and M. DiFiglia (1990) Long-term survival of GABA-, enkephalin-, NADPH-diaphorase- and calbindin-d28k-containing neurons in fetal striatal grafts. Brain Res. **532**:151-159.

Robertson, H.A., M.R. Peterson, K. Murphy, and G.S. Robertson (1989) D_1-dopamine receptor agonists selectively activate striatal c-fos independent of rotational behaviour. Brain Res. **503**:346-349.

Roffler-Tarlov, S., D. Pugatch, and A.M. Graybiel (1990) Patterns of cell and fiber vulnerability in the mesostriatal system of the mutant mouse weaver. II. High affinity uptake sites for dopamine. J. Neurosci. **10**:734-740.

Rogers, J.H. (1989) Calcium binding proteins: The search for functions. Nature **339**:661-662.

Romano, G.J., B.D. Shivers, R.E. Harlan, R.D. Howells, and D.W. Pfaff (1987) Haloperidol increases proenkephalin mRNA levels in the caudate-putamen of the rat: a quantitative study at the cellular level using in situ hybridization. Mol. Brain Res. **2**:33-41.

Rosenberg, M.B., T. Friedmann, R.C. Robertson, M. Tuszynski, J.A. Wolff, X.O. Breakefield, and F.H. Gage (1988) Grafting genetically modified cells to the damaged brain: restorative effects of NGF expression. Science **242**:1575-1578.

Rossant, J. (1990) Manipulating the mouse genome: Implication for neurobiology. Neuron **2**:323-334.

Rubin, R.P., G.B. Weiss, and J.W. Putney (1985) *Calcium in biological systems*, Plenum Press, New York.

Rutherford, A., M. Garcia-Munoz, S.B. Dunnett, and G.W. Arbuthnott (1987) Electrophysiological demonstration of host cortical inputs to striatal grafts. Neurosci. lett. **83**:275-281.

Sanberg, P.R., M.A. Henault, and A.W. Deckel (1986) Locomotor hyperactivity: Effects of multiple striatal transplants in an animal model of Huntington's disease. Pharmacol.

Biochem. Behav. **25**:297-300.

Sanberg, P.R., M.A. Henault, S.H. Hagenmeyer-Houser, M. Giordano, and K.H. Russell (1987) Multiple transplants of fetal striatal tissue in the kainic acid model of Huntington's disease:Behavioral recovery may not be related to acetylcholinesterase. In: Cell and Tissue Transplantation in the Adult Brain., E. Azmitia and A. Bjorklund eds., Annals N.Y. Acad. Sci. **495**:781-785.

Satoh, J., and K. Suzuki (1988) Postnatal development of tyrosine hydroxylase immunoreactive neurons in the mouse CNS. Soc. Neurosci. Abstr. **14**:407.9.

Schnell, L., and M.E. Schwab (1990) Axonal regeneration in the rat spinal cord produced by an antibody against myelin-associated neurite growth inhibitors. Nature **343**:269-272.

Selemon, L.D., and P.S. Goldman-Rakic (1989) Retrograde labeling of striatonigral and striatopallidal neurons in the rhesus monkey. Soc. Neurosci. Abstr. **15**:659.

Semba, K., S.R. Vincent, and H.C. Fibiger (1988) Different times of origin of choline acetyltransferase- and somatostatin-immunoreactive neurons in rat striatum. J. Neurosci. **8**:3937-3944.

Seto-Oshima, A., E. Lawson, L.H. carrasco, C.Q. Mountjoy, and P.C. Emson (1988) Loss of matrix calcium-binding protein-containing neurons in Huntington's disease. Lancet **1** (8597):1252-1255.

Sheng M., and M.E. Greenberg (1990) The regulation and function of c-*fos* and other immediate early genes in the nervous system. Neuron **4**:477-485.

Shinoda, H., A.M. Marini, C. Cosi, and J.P. Schwartz (1989) Brain region and gene specificity of neuropeptide gene expression in cultured astrocytes. Nature **245**:415-417.

Shiosaka, S., K. Takatsuki, M. Sakanaka, S. Inagaki, H. Takagi, E. Senba, Y. Kawai, H. Iida, H. Minagawa, Y. Hara, T. Matsuzaki, and M. Tohyama (1982) Ontogeny of somatostatin-contaning neuron system of the rat: Immunohistochemical analysis. II. Forebrain and diencephalon. J. Comp. Neurol. **204**:211-224.

Sirinathsinghji D.J.S., S.B. Dunnett, O. Isacson, D.J. Clarke, K. Kendrick, and A. Björklund (1988) Striatal grafts in rats with unilateral neostriatal lesions-II. In vivo monitoring of GABA release in globus pallidus and substantia nigra. Neuroscience **24**:803-811.

Sirinathsinghji D.J.S., B.J. Morris, W. Wisden, A. Northrop, S.P. Hunt, and S.B. Dunnett (1990) Gene expression in striatal grafts-I. Cellular localization of neurotransmitter mRNAs. Neuroscience **34**:675-686

Smart, I.H.M., and R.R. Sturrock (1979) Ontogeny of the neostriatum. In: The Neostriatum, I. Divac, R. Oberg and E. Guanila, eds, pp.127-146, Pergamon Press, New York.

Snyder-Keller, A.M. (1991) Development of striatal compartmentalization following pre- and postnatal dopamine depletion. J. Neurosci. **11**:810-821.

Sonnenberg J.L., F.J.III Rauscher, J.I. Morgan, and T. Curran (1989) Regulation of proenkephalin by *fos* and *jun*. Science **246**: 1622-1625

Specht, L., V.M. Pickel, T.H. Joh, and D.J. Reis (1981a) Light-microscopic immunocytochemical localization of tyrosine hydroxylase in prenatal rat brain. I. early ontogeny. J. Comp. Neurol. **199**:233-253.

Specht, L., V.M. Pickel, T.H. Joh, and D.J. Reis (1981b) Light-microscopic immunocytochemical localization of tyrosine hydroxylase in prenatal rat brain. II. late ontogeny. J. Comp. Neurol. **199**:255-276.

Spemann, H., and H. Mangold (1924) Induction von embryonolanlagen durch implantation artfremder organisatoren. Arch. Mikrosk. Anat. Entwicklungsmech. **100**:599-638.

Steindler, D.A., T.F. O'Brien, and N.G.F. Cooper (1988) Glycoconjugate boundaries during early postnatal development of the neostriatal mosaic. J. Comp. Neurol. **267**:357-369.

Sternberger, L.A. (1979) Immunocytochemistry. Wiley, New York.

Stoof, J.C., E.J.S. De Breejen, and A.R. Mulder (1979) GABA modulates the release of dopamine and acetylcholine from rat caudate nucleus slices. Eur. J. Pharmac. **57**:35-42.

Stromberg, I. C.J. Wetmore, T. Ebendal, P. Enfors, H. Persson, and L. Olson (1990) Rescue of basal forebrain cholinergic neurons after implantation of genetically modified cells producing recombinant NGF. J. Neurosci. Res. **25**:405-411.

Sunahara, R.K., H.-C. Guan, B.F. O'Dowd, P. Seeman, L.G. Laurier, G. Ng, S.R. George, J. Torchia, H.H.M. Van Tol, and H.B. Niznik (1991) Cloning of the gene for a human dopamine D_5 receptor with higher affinity for dopamine than D_1. Nature **350**:614-619.

Surmeier, D.J., P. Akins, and S.T. Kitai (1987) Neuronal migration in primary monolayer cultures of rat neostriatum. Soc. Neurosci. Abstr. **13**:1575.

Takeichi, M. (1988) The cadherins: cell-cell adhesion molecules controlling animal

morphogenesis. Development **102**:639-655.

Tashiro, Y., T. Sugimoto, T. Hattori, Y. Uemura, I. Nagatsu, H. Kikuchi, and N. Mizuno (1989) Tyrosine hydroxylase-like immunoreactive neurons in the striatum of the rat. Neurosci. Letts. **97**:6-10.

Tennyson, V.M., R.E. Barrett, G. Cohen, L. Côté, R. Heikkila, and C. Mytilneou (1972) The developing neostriatum of the rabbit: correlation of fluorescence histochemistry, electron microscopy, endogenous dopamine levels, and [^{3}H] dopamine uptake. Brain Res. **46**:251-285.

Uylings, H.B., C.G. Van Eden, J.G. Parnavelas, and A. Kalsbeek (1990) The prenatal and postnatal development of rats cerebral cortex. In: The Cerebral Cortex of the Rat, B. Kolb and R.C. Tees eds., pp. 35-76, MIT press, Cambridge.

van der Kooy, D. (1984) Developmental relationships between opiate receptors and dopamine in the formation of caudate-putamen patches. Dev. Brain Res. **14**:300-303.

van der Kooy, D., and G. Fishell (1987) Neuronal birthdate underlies the development of striatal compartments. Brain Res. **401**:155-161.

van der Kooy, D., G. Fishell, L.A. Krushel, and J.G. Johnston (1987) The development of striatal compartments: From proliferation to patches. In: The Basal Ganglia II, M.B. Carpenter and A. Jayarama, eds, pp.81-98, Plenum, New York.

Vernier, P., J.-F. Julien, P. Rataboul, O. Fourrier, C. Feuerstein and J. Mallet (1988) Similar time course changes in striatal levels of glutamic acid decarboxylase and proenkephalin mRNA following dopaminergic deafferentation in the rat. J. Neurochem. **51**:1375-1380.

Vickroy, T.W., W.R. Roeske, D.R. Gehlert, J.K. Wamsley, and H.I. Yamamura (1985) Quantitative light microscopic autoradiography of [^{3}H]hemicholinium binding sites in the rat central nervous system: a novel biochemical marker for mapping the distribution of cholinergic nerve terminals. Brain Res. **329**:368-373.

Voorn, P., G. Roest, and H.J. Groenewegen (1987) Increase of enkephalin and decrease of substance P immunoreactivity in th dorsal and ventral striatum of the rat after midbrain 6-hydroxydopamine lesions. Brain Res. **412**:391-396.

Voorn, P., A. Kalsbeek, B. Jorritsma-Byham, and H.J. Groenewegen (1988) The pre- and postnatal development of the dopaminergic cell groups in the ventral mesencephalon and the dopaminergic innervation of the striatum of the rat. Neuroscience **25**:857-888.

Walaas, S.I., and P. Greengard (1984) DARPP-32, a dopamine- and adenosine

3':5'-monophosphate-regulated phosphoprotein enriched in dopamine-innervated brain regions I. Regional and cellular distribution in the rat brain. J. Neurosci. **4**:84-98.

Walaas, S.I., and A.C. Nairn (1985) Calcium-regulated protein phosphorylation in mammalian brain. In: Calcium and cell physiology, D. Marmé, ed. pp. 239-264, Springer-Verlag, Heidelberg.

Walaas, S.I., G. Sedvall, and P. Greengard (1989) Dopamine-regulated phosphorylation of synaptic vesicle-associated proteins in rat noestriatum and substantia nigra. Neuroscience **29**:9-19.

Walker, P.D., G.I. Chovanes, and J.P. McAllister (1987) Identifiaction of acetylcholinesterase-reactive neurons and neuropil in neostriatal transplants. J. Comp. Neurol. **259**:1-12.

Weiss, L.T., and M.-F. Chesselet (1989) Regional distribution of preprosomatostatin messenger RNA in the striatum, as revealed by in situ hybridization histochemistry. Mol. Brain Res. **5**:121-130.

Weiner, D.M., A.I. Levey, R.K. Sunahara, H.B. Niznik, B.F. O'Dowd, P. Seeman, and M.R. Brann (1991) D1 and D2 dopamine receptor mRNA in rat brain. Proc. Natl. Acad. Sci. USA **88**:1859-1863.

Welsh, M.J. (1988) Localization of intracellular calcium-binding proteins. In: Calcium-binding proteins. vol.II, Biological functions, M.P. Thompson, ed., pp. 1-19, CRC press, Florida.

Wexler, N.S., E.A. Rose, and D.E. Housman (1991) Molecular approaches to hereditary disease of the nervous system: Huntington's disease as a paradigm. Annu. Rev. Neurosci. **14**:503-529.

Wictorin, K., and A. Björklund (1989) Connectivity of striatal grafts implanted into the ibotenic acid-lesioned striatum-II. Cortical afferents. Neuroscience **30**:297-311.

Wictorin, K., P. Brundin, P., B. Gustavii, O. Lindvall, and A. Björklund (1990a) Reformation of long axon pathways in adult rat central nervous system by human forebrain neuroblast. Nature **347**:556-558.

Wictorin K, D.J. Clarke, J.P. Bolam, and A. Björklund (1990b) Fetal striatal neurons grafted into the ibotenate lesioned adult striatum: efferent projections and synaptic contacts in the host globus pallidus. Neuroscience **37**:301-315

Wictorin K, D.J. Clarke, J.P. Bolam, and A. Björklund (1989a) Host corticostriatal fibers establish synaptic connections with grafted striatal neurons in the ibotenic acid lesioned

striatum. Eur. J. Neurosci. **1**:189-195

Wictorin, K., O. Isacson, W. Fischer, F. Nothias, M. Peschanski, and A. Björklund (1988) Connectivity of striatal grafts implanted into the ibotenic acid-lesioned striatum-I. Subcortical afferents. Neuroscience **27**:547-562.

Wictorin K., C. Quimet, and A. Björklund (1989c) Intrinsic organization and connectivity of intrastriatal striatal transplants as revealed by DARPP-32 immunohistochemistry: specificity of connections with the lesioned host brain. Eur. J. Neurosci. **1**: 690-701

Wictorin, K., R.B. Simerly, O. Isacson, L.W. Swanson, C. Quimet, and A. Björklund (1989b) Connectivity of striatal grafts implanted into the ibotenic acid lesioned striatum-III. Efferent projecting graft neurons and their relations to host afferents within the grafts. Neuroscience **30**:313-330.

Wilkinson, D.G., and R. Krumlauf (1990) Molecular approaches to the segmentation of the hindbrain. Trends Neurosci. **13**:335-339.

Whetsell, W.O., M.S. Ecob-Johnston, and W.J. Nicklas (1979) Studies of kainate-induced caudate lesions in organotypic tissue culture. Adv. Neurol. **23**:645-654.

Wolff, J.A., L.J. Fisher, L. Xu, H.A., Jinnah, P.J. Langlais, P.M. Iuvone, K.L. O'Malley, M.B. Rosenberg, S. Shimohama, T. Friedmann, and F.H. Gage (1989) Grafting fibroblasts genetically modified to produce L-dopa in a rat model of Parkinson disease. Proc. Natl. Acad. Sci. USA **86**:9011-9014.

Won, L., A. Heller, and P.C. Hoffmann (1989) Selective association of dopamine axons with their striatal target cells in vitro. Devel. Brain Res. **74**:93-100.

Xu, Z.C., C.J. Wilson, and P.C. Emson (1989) Restoration of the corticostriatal projection in rat neostriatal grafts: Electron microscopic analysis. Neuroscience **29**:539-550.

Yamada, T., M. Placzek, H. Tanaka, J. Dodd, and T.M. Jessell (1991) Control of cell pattern in the developing nervous system: Polarizing activity of the floor plate and notochord. Cell **64**:635-647.

Young, S.T., L.J. Porrino, and M.J. Iadarola (1989) Induction of c-*fos* by direct and indirect dopamine agonists. Soc. Neurosci. Abstr. **15**: 1091.

Young, W.S.III., T.I. Bonner, and M.R. Brann (1986) Mesencephalic dopamine neurons regulate the expression of neuropeptide mRNAs in the rat forebrain. Proc. Natl. Acad. Sci. USA **83**:9827-9831.

Zahm, D.S., K.W. Eggerman, R.F. Sprung, D.E. Wesche, and E. Payne (1990) Postnatal development of striatal neurotensin immunoreactivity in relation to clusters of substance P immunoreactive neurons and the "dopamine islands" in the rat. J. Comp. Neurol. **296**:403-414.

Zhou, F.C., and N. Buchwald (1989) Connectivities of the striatal grafts in adult rat brain: a rich afference and scant striatonigral efference. Brain Res. **504**: 15-30.

ACKNOWLEDGEMENTS

It is my great pleasure to thank the following people for their supports during the preparation of this dissertation:

My thesis advisor: Dr. Ann M. Graybiel.

Our collaborators: Dr. Stephen B. Dunnett and Dr. Robert W. Baughman.

The members in my thesis committee: Dr. Fred H. Gage, Dr. Arthur D. Lander and Dr. Mriganka Sur.

The staff in Dr. Graybiel's laboratory: Henry F. Hall, Glenn Holm, Diane Major, Amelia Rosales and Celia Shneider.

The academic administrator in the department: Jan Ellertsen.

Funding for my graduate study was provided by the Upham Fund, Germeshausen Fund, Cerebral Palsy Research Fund and by Markey fellowship.